uOttawa

L'Université canadienne
Canada's university

FACULTÉ DES ÉTUDES SUPÉRIEURES ET POSTOCTORALES

uOttawa

L'Université canadienne
Canada's university

FACULTY OF GRADUATE AND POSDOCTORAL STUDIES

Michael Huh

AUTEUR DE LA THÈSE / AUTHOR OF THESIS

Ph.D. (Cellular and Molecular Medicine)

GRADE / DEGREE

Department of Cellular and Molecular Medicine

FACULTÉ, ÉCOLE, DÉPARTEMENT / FACULTY, SCHOOL, DEPARTMENT

Functional Studies in Rb Regulation of Skeletal Myogenic Program

TITRE DE LA THÈSE / TITLE OF THESIS

Michael Rudnicki

DIRECTEUR (DIRECTRICE) DE LA THÈSE / THESIS SUPERVISOR

CO-DIRECTEUR (CO-DIRECTRICE) DE LA THÈSE / THESIS CO-SUPERVISOR

EXAMINATEURS (EXAMINATRICES) DE LA THÈSE / THESIS EXAMINERS

Robert Korneluk

Alan Mears

Gustavo Leone

Luc Sabourin

Gary W. Slater

Le Doyen de la Faculté des études supérieures et postdoctorales / Dean of the Faculty of Graduate and Postdoctoral Studies

Functional Studies in Rb Regulation of Skeletal Myogenic Program

Michael S. Huh

Thesis submitted to the
Faculty of Graduate and Postdoctoral Studies
in partial fulfillment of the requirements
for a Ph.D. degree in
Cellular and Molecular Medicine

Department of Cellular and Molecular Medicine
Faculty of Medicine
University of Ottawa

Your file Votre référence
ISBN: 978-0-494-49359-5
Our file Notre référence
ISBN: 978-0-494-49359-5

Reproduction Authorizations

Permission to reproduce manuscript in Chapter 2:

Reproduction Authorizations

Permission to reproduce manuscript in Appendix A:

Reproduction Authorizations

Permission to reproduce manuscript in Appendix B:

Abstract

The molecular orchestration of skeletal muscle differentiation is a concerted process involving muscle specific transcription factors and components of the cell cycle machinery. The functional capacity of the master myogenic transcription factors MyoD and Myf5 are directly coupled to cell cycle regulatory molecules. MyoD activation powerfully induces differentiation and cell cycle withdrawal in G1. Transit through the G1 restriction point is regulated by the retinoblastoma (Rb) protein. Therefore, skeletal muscle differentiation was assessed in the absence of Rb by histology, immunohistochemistry, and molecular techniques. Rb null myoblasts displayed profound deficiencies in their ability to exit the cell cycle, inhibit apoptosis, and fuse into terminally differentiated myotubes. Global expression analysis revealed a much higher number of deregulated genes in fully differentiated Rb^- myotubes than in proliferating Rb^- myoblasts. Specifically, the loss of Rb in myotubes resulted in upregulation of cell cycle genes and the downregulation of muscle structural genes and glycolytic enzymes. Finally, ChIP-RDA genomic location analysis identified E2F7 and Myf5 as direct targets of Rb complexes. These data present a transcriptional model in which Rb potentiates the activity of MyoD by repressing Myf5, thereby promoting the progression of skeletal muscle differentiation.

Contents

List of Tables

Chapter 3. Rb Dependent Repression and Activation of Opposing Transcriptional Networks in Skeletal Muscle Differentiation

List of Figures

List of Abbreviations

bHLH	basic helix-loop-helix
ChIP	chromatin immunoprecipitation
ChIP-RDA	chromatin immunoprecipitation – representational difference analysis
DAPI	4',6-diamidino-2-phenylindole
dblKO	double-knockout (*MyoD*$^{-/-}$;*Myf5*$^{-/-}$)
DMEM	Dulbecco's modified Eagle's medium
DNA	deoxyribonucleic acid
EGFP	enhanced green-fluorescent protein
FACS	fluorescence-activated cell sorting
FGF	fibroblast growth factor
FITC	fluorescein (isothiocyanate)
FKHR	FoxO1
Fluc	firefly luciferase
GAPDH	glyceraldyde-3-phosphate dehydrogenase
$GL^{+/-}$	glycine-leucine +/-
HGF	hepatocyte growth factor
MRF	myogenic regulatory factor
MyHC	myosin heavy chain
NH_2-	amino-
PBS	phosphate-buffered saline
PCR	polymerase chain reaction
PFA	paraformaldehyde

$Q^{+/-}$	glutamine +/-
RDA	representational difference analysis
RIPA	radioimmunoprecipitation assay
Rluc	Renilla luciferase
RMS	rhabdomyosarcoma (alveolar, aRMS; embryonal, eRMS)
RNA	ribonucleic acid
RT	reverse-transcription
SDS-PAGE	sodium dodecyl sulfate-polyacrylamide gel electrophoresis
Sp	*Splotch* (*Pax3*-null)
SP cells	side-population cells
UTR	untranslated region

Chapter 1

General Introduction

1. Introduction

Molecular mechanisms that govern cellular division are among the most fundamental of biological processes. The ability to replicate and propagate genetic information is of essential function for the perpetuation of cellular based organisms. Hence the most basic constituents of the cell cycle machinery are conserved across all species. Moreover, mechanisms that inhibit cell division are also in place to maintain proper cellular function. Diseases such as cancer display uninhibited cell proliferation and are poorly differentiated derivatives of their tissue of origin. Thus the study of tumour cells has given us an awareness of putative mechanisms that couple cell cycle arrest and cellular differentiation. The retinoblastoma (Rb) tumour suppressor is critical with respects to both these functions. However, our present understanding of how Rb couples cell cycle arrest to differentiation is rudimentary. Skeletal muscle provides a well defined and physiologically relevant system in which to study Rb's function. Thus functional studies into Rb's role in skeletal muscle differentiation will likely provide future avenues of therapies for diseases such as cancer.

1.1 The Retinoblastoma Family

The retinoblastoma (*Rb*) gene has been discovered in virtually all metazoan and plant species that are used in experimental research. To date an *Rb* gene or *Rb like* gene has been found in humans, mice, rat, fish, worms, chicken, dogs, frogs, flies, arabidopsis, maize, and tobacco (Friend et al. 1986; Clarke et al. 1992; Destree et al. 1992; Jacks et al. 1992; Lee et al. 1992; Roy et al. 1993; Boehmelt et al. 1994; Dunaief et al. 1994; Grafi et al. 1996; Ach et al. 1997a; Ach et al. 1997b; Lu and Horvitz 1998; Brunelli and

Thorgaard 1999; Nakagami et al. 1999; Rotchell et al. 2001). The presence of Rb in these multicellular organisms suggests that the *Rb* gene is an evolutionary characteristic of more complex multicellular organisms. This being said, an ortholog of *Rb* has been identified in as primitive an organism as the unicellular alga Chlamydomonas (Umen and Goodenough 2001). Furthermore, a functional counterpart of Rb has also been characterized in yeast (Costanzo et al. 2004).

In mammals, the retinoblastoma family of proteins consists of three members (Rb, p107, p130). Collectively, the Rb family plays a central role in regulating transcriptional networks involved in cell cycle progression and cellular differentiation (Cobrinik 2005; Nguyen and McCance 2005; Zhu 2005; Wikenheiser-Brokamp 2006). Within a historical context, the cloning of *Rb* was of significant note, in that it was the first tumour suppressor gene discovered (Friend et al. 1986). The conceptual framework for the classic tumour suppressor gene was elucidated by the seminal publication by Alfred Knudson (Knudson 1971). Knudson determined that patients with bilateral retinoblastoma had inherited one 'hit' in the hypothetical tumour suppressor gene, thus a shorter latency period as compared to patients with unilateral retinoblastoma that required two successive hits. Knudson's 'two hit' hypothesis for retinoblastoma was validated in the following years by the cloning and functional analysis of the retinoblastoma gene. Disease causing mutations in *Rb* leads to the formation of retinoblastoma, osteosarcoma, and small cell lung carcinoma in humans (Goodrich and Lee 1993). In humans and mice, Rb is the only family member to have distinct tumour suppressor capabilities. Heterozygous *Rb* mutant mice develop pituitary and thyroid tumours (Hu et al. 1994). Mutations are very rarely associated with p107 and p130 in human tumours.

Furthermore, specific inactivation of p107 and p130 alone has never been unequivocally demonstrated as a causative event in tumour formation (Cobrinik et al. 1996; LeCouter et al. 1998a; LeCouter et al. 1998b). However, compound ablation of *Rb* and either of its family members creates a more severe tumour phenotype in mice (Dannenberg and te Riele 2006).

As with many other families of genes, there are unique and redundant aspects to each protein's function. Rb, p107 and p130 all share a highly homologous structural motif known as the 'pocket domain' (Figure 1). Hence, they are commonly described as the "pocket proteins" (Claudio et al. 2002). The importance of this motif is most evident by the observation that the vast majority of mutations are found in the exons encoding the small pocket domain of Rb (Goodrich 2003). The small pocket domain is a bipartite motif composed of the A and B domains, separated by an intervening linker sequence of amino acids. In its native conformation, the pocket domain serves as the interface for the majority of the pocket proteins' function. Arguably the most basic role of the pocket proteins is to properly regulate transcription of target genes. Through its interaction with transcription factors such as the E2Fs, the Rb family is believed to regulate the proper induction of genes involved in a large number of cellular processes (Cam and Dynlacht 2003; Frolov and Dyson 2004). The pocket domain is the region with the highest degree of homology between all three family members. The integrity of this domain is critical for most of Rb's active functions. Activity of Rb proteins are regulated by phosphorylation on serine and threonine residues by cyclin-cdk complexes (Buchkovich et al. 1989; Chen et al. 1989; DeCaprio et al. 1989; Mihara et al. 1989; Lees et al. 1991; Hu et al. 1992). Rb has been reported to interact with more than 100 protein

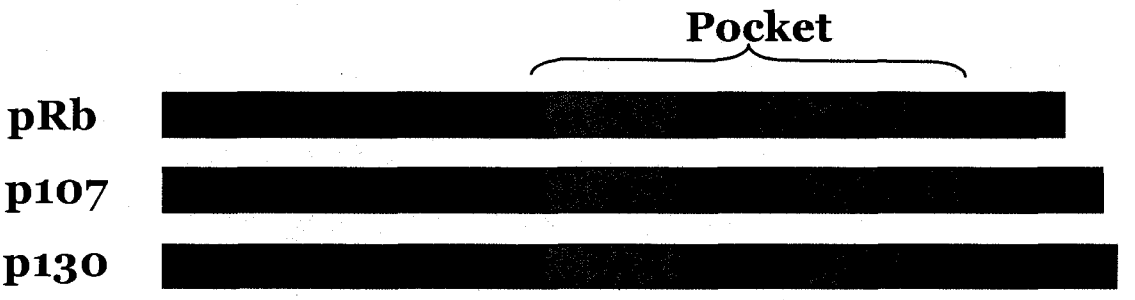

Figure 1. **Schematic representation of the Rb family of pocket proteins.** The relative position and organization of A and B pocket domains are denoted by the orange regions.

(Morris and Dyson 2001). However, the best characterized and perhaps the most significant binding partners are the E2F family of transcription factors. Rb-E2F interactions regulate the transcription of E2F target genes in proliferating and growth arrested cells (Cam et al. 2004; Balciunaite et al. 2005). Specifically, phosphorylation of Rb family members results in the dissociation of Rb from E2F, thus activating the transcription of E2F target genes. Therefore cell cycle dependent phosphorylation of Rb family members triggers the G1/S transition through the activation of E2F target genes (Figure 2).

Among the family members, p107 and p130 are the most homologous in amino acid identity. Hence, functional compensation between family members in many respects parallels this degree of similarity. Indeed, targeted deletion of p107 or p130 in a mixed 129/SV and C57/B6 genetic background does not result in any developmental or post-natal abnormalities. However, compound p107 and p130 mutant mice have defects in endochondral ossification and do not come to term as a result (Cobrinik et al. 1996). Rb is unique among its family members in that it cannot be fully compensated for by both p107 and p130 during mouse development (Clarke et al. 1992; Jacks et al. 1992; Lee et al. 1992). Structurally, the spacer region of p107 and p130 are highly similar and possess the ability to bind to cyclinA-cdk2 and cyclinE-cdk2 complexes (Ewen et al. 1992; Faha et al. 1992; Lees et al. 1992; Cobrinik et al. 1993; Hannon et al. 1993; Li et al. 1993; Mayol et al. 1993). Unlike p107 and p130, Rb's spacer does not bind to cyclinE-cdk2 or cyclinA-cdk2 complexes. Outside of the pocket, p107 and p130 are also highly homologous in the amino terminal portion that is suggested to function as a cdk inhibitor (Woo et al. 1997; Castano et al. 1998). Due to their biochemical properties, Rb proteins

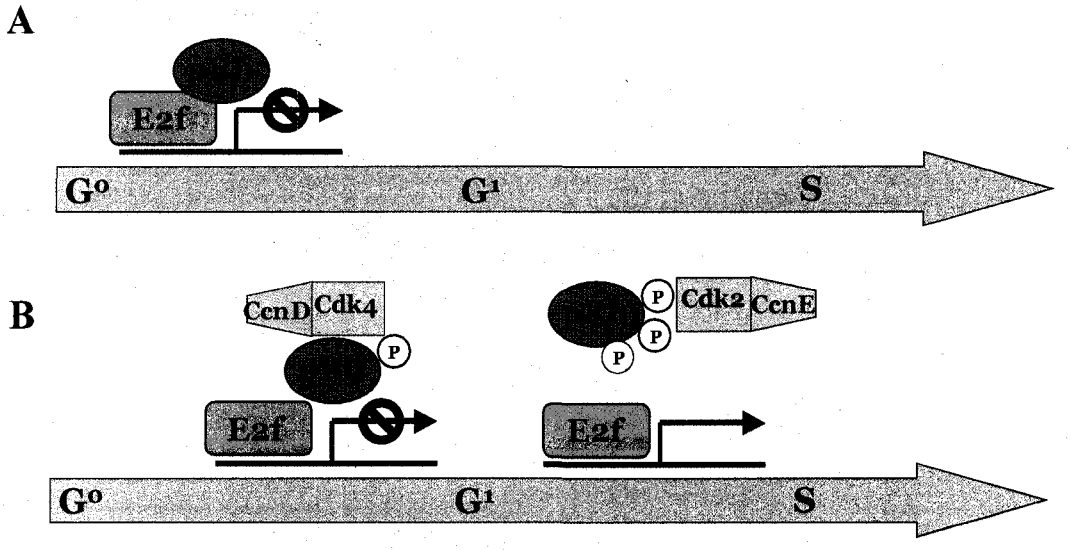

Figure 2. **Model of Rb mediated E2F target gene regulation.** (A) Inhibition of E2F target gene transcription by active pRb. (B) Activation of E2F target gene by the dissociation of hyperphosphorylated pRb from E2F by cyclin/cdk complexes.

dynamically modify their function according to the signals of the cellular environment. Changes in cellular environment occur throughout the progression of the cell cycle (G0, G1, S, G2, M), cellular transformation, cell lineage commitment, cell senescence, cell stress response, and the progression towards terminal differentiation (Du and Pogoriler 2006). A living snap shot of these states represent distinct and often radically different portraits. Hence, the activity and gene target preference of the pocket proteins are significantly influenced by the cellular environment. This is no better illustrated by the tissue specific nature of tumours that develop in humans and mice due to the loss of Rb. In these respects, Rb provides irreplaceable functions in specific cell types that cannot be compensated by p107 and p130.

1.2 Transcriptional Regulation by Rb Complexes

The mechanistic details of Rb dependent transcriptional regulation is the result of a considerable body of research in this area. Tumour suppression and cell cycle inhibition appears to be a logical and somewhat synonymous pairing. The first experimental insight into Rb's ability to inhibit cell cycle emerged through two compelling lines of evidence. The first major observation was that overexpression of Rb was able to G1 arrest some tumour cell lines (Huang et al. 1988). A converging observation was also made through the study of DNA viral oncoproteins. Viral oncoproteins have the capacity to induce neoplastic transformation when expressed in normal cells. Importantly, proteins such as E1A, SV40 Large T antigen, and E7 target and inhibit the activity of Rb (DeCaprio et al. 1988; Whyte et al. 1988; Munger et al. 1989). These lines of evidence provided the experimental support for Rb's function as a

cell cycle inhibitory protein. A transcriptional basis for Rb's effect on cell cycle was established upon the discovery that Rb complexed with E2F1 transcription factor (Helin et al. 1992; Kaelin et al. 1992; Nevins 1992). The significance of this interaction lies in the ability of E2Fs to activate target genes required for the transition from G1 through to S phase (Hurford et al. 1997; Rayman et al. 2002; Ren et al. 2002; Wells et al. 2002; Dimova et al. 2003). This seminal discovery proved to be the foundation for the development of a multi-faceted model of transcriptional control.

Protein-protein interactions are central to Rb mediated transcriptional regulation. Rb can be viewed as a versatile adapter of a larger protein complex. Therefore Rb in itself does not have the ability to bind DNA and alter transcription (Ross et al. 2001). The C-terminal large pocket domain is most critical for the vast majority of Rb-protein interactions (Goodrich 2003). Identification of Rb binding proteins has been important in unraveling the mechanisms behind Rb mediated transcriptional regulation. The E2F transcription factors were the first physiological protein partners of Rb to be characterized. Currently, there are 8 known members of the E2F family (E2F1-8). The E2F family is functionally subdivided into two groups. The activator E2Fs are comprised of E2F1, E2F2, and E2F3a. The repressor E2Fs consists of E2F3b, E2F4, E2F5, E2F6 and the most recently discovered E2F7 and E2F8. Under physiological conditions, Rb has been shown to complex with E2F1, E2F2, E2F3, and E2F4. Rb-E2F complexes are present during specific stages of the cell cycle, namely G0 and early G1 (Figure 2). Therefore it is believed that Rb is required to repress E2F target genes during this period, thus impeding the transition from G1 to S phase. The Rb-E2F interaction has provided a useful foundation for testing different concepts of Rb mediated gene repression.

There are two prevailing mechanistic models of Rb inhibition of E2F target genes. Rb has been demonstrated to physically interfere with the transcriptional activating domain of E2F factors. In E2F1, the Rb binding region physically overlaps with the transactivating domain (Flemington et al. 1993; Helin et al. 1993). Indeed, in vitro transcription assays have demonstrated that Rb-E2F interaction precludes the formation of pre-initiation complexes onto the promoter (Ross et al. 1999). More recently, an alternative model has taken prominence in the field of Rb transcription regulation. This concept is based on the idea that Rb alters the local chromatin structure, thus affecting transcription of nearby genes. Rb complexes have been shown to alter the chromatin structure by histone modification and nucleosomal remodeling. Covalent modifications of histones have been demonstrated to correlate to the expression levels of nearby genes. The protruding N-terminal tails of histone H3 and H4 are frequently targeted by histone modifying enzymes. Moiety linkages such as acetylation are associated with transcriptional activation. While methylation at specific residues can either be associated with activation or repression of transcription (Jenuwein and Allis 2001). Therefore, the discovery that Rb physically interacts and recruits these histone modifying enzymes were of major significance.

The acetylation status of histones are maintained by the enzymatic activities of two groups of proteins. These histone modifying enzymes are categorized as histone acetyl transferases (HATs) and histone deacetylases (HDACs). HDAC activity contributes to a repressive chromatin structure by removing acetyl groups from histones. Indeed, the repressive properties of Rb complexes can largely be attributed to the HDAC component. The A and B pocket domains of Rb which is minimally required for Rb

mediated transcriptional repression (Chow and Dean 1996; Chow et al. 1996), is critical for Rb's interaction with HDACs 1-3. Indeed, repression of transcription was demonstrated to be directly related to the deacetylation of the target promoter (Brehm et al. 1998; Ferreira et al. 1998; Luo et al. 1998; Magnaghi-Jaulin et al. 1998). Deacetylation by Rb recruited HDACs at E2F promoters are counter balanced by activator E2Fs. E2Fs have been shown to recruit HATs such as CREB-binding protein (CBP), p300 and P/CAF (Trouche and Kouzarides 1996; Martinez-Balbas et al. 2000; Marzio et al. 2000; Morris et al. 2000). Histone acetylation/deacetylation thus appears to play a major role in the dynamic regulation of E2F target promoters through the course of the cell cycle.

Histone methylation is another form of covalent modification that affects gene transcription. Methyl groups are neutral in charge, and therefore do not exert their effects on chromatin electrostatically. However, methylation is considered to be a more stable modification than acetylation. Due to this notion, the discovery that the *cyclinE* promoter was subject to such modification came as a surprise. Moreover, the histone methylation of the *cyclinE* promoter was absolutely dependent on Rb-SUV39H1 complex (Nielsen et al. 2001). This novel insight contributed yet another mechanistic mode of action for Rb mediated transcriptional regulation. These results suggest a sequential model of histone modification by Rb. Since H3-K9 acetylation and methylation are mutually exclusive modifications (Rea et al. 2000), it is plausible that Rb mediated histone deacetylation facilitates the eventual methylation. Rb has also been co-purified with DNMT1, a DNA methyltransferase enzyme (Robertson et al. 2000). Methylation on DNA is also considered a mark of repressive chromatin. More specifically, methylation of cytosines

of CpG dinucleotides serve as docking sites for methyl-CpG binding proteins (MBDs) (Meehan et al. 1989; Lewis et al. 1992). Interestingly, MBDs are able to recruit histone deacetylase activity and nucleosome remodeling complexes (Jones et al. 1998; Ng et al. 1999; Wade et al. 1999).

Chromatin structure can also be altered in a non-covalent manner by large nucleosomal remodeling protein complexes. It is hypothesized that ATPase driven helicases loosen the physical contact between the DNA and core histones, allowing for the repositioning of the nucleosomes. This is believed to accommodate or hinder the access of transcriptional machinery at the promoter of genes. BRG1 and hBRM are the human homologs to the yeast chromatin remodeling SWI2/SNF2 ATPase-heliase. Rb has been shown to interact with BRG1 and hBRM to inhibit *cyclinA* transcription. Interestingly, the BRG1 induced cell cycle arrest is a direct result of *p21* induction (Kang et al. 2004). Therefore, the increase in p21 in turn reduces the levels of cdk activity thus activating Rb and ensuing cell cycle arrest. Taken together, Rb mediated transcriptional control involves multiple layers of chromatin modifying activities.

1.3 Mouse Models of Rb Dependent Muscle Differentiation

Mouse models provide a powerful tool in which gene functionality can be assessed in an in vivo mammalian context. Mouse genetics have allowed us to glean unanticipated insights into the function of Rb. In humans, the inheritance of a mutated allele of *Rb* almost always leads to childhood retinoblastoma and osteosarcoma. This neoplastic phenotype is invariably associated with the inactivation of the wildtype *Rb* allele. The study of Rb function in humans is limited due to the developmental lethality

of Rb loss in the embryo. As a result, Rb deficiency in humans can only be ascertained in the context of the tumour tissue, that develop through the amplification of a limited founder population of cells. Therefore, mouse models have been tremendously important in understanding the physiological function of critical gene products. Studies of Rb gene inactivation in the mouse have garnered a wealth of data from a developmental and disease ontology perspective. Whole knockouts of *Rb* in mice lead to embryonic lethality generally by E. 14.5 (Clarke et al. 1992; Jacks et al. 1992; Lee et al. 1992). These initial studies experimentally demonstrated that Rb was indeed critical for the development of neural and haematopoietic systems. In hindsight, these pilot studies just scratched the surface of uncovering Rb's function. Our current concept of Rb biology has much evolved since those early knockout studies. This is due to our increasingly more sophisticated means to dissect out the specifics of Rb function. We now identify the function of Rb in a cell context specific manner. Although Rb is expressed in virtually all cell types, its actions are not equivalent across all cell types. An example of this would be to compare the phenotypes of Rb loss specifically in brain and muscle development. Conditional knockout of Rb in the developing telencephalon does not effect differentiation of the neuroblasts, but compromises their cell cycle arrest (Ferguson et al. 2002). Surprisingly, the developmental defect in Rb deficient telencephalic neurons was that of improper migration (Ferguson et al. 2005). In comparison, skeletal muscle specific deficiency of Rb causes poor terminal differentiation, apoptosis, and ectopic DNA synthesis (Zacksenhaus et al. 1996).

Studying Rb deficiency in skeletal muscle was problematic due to the embryonic lethality prior to full skeletal muscle development. Cell culture models of muscle

differentiation in part helped to address this problem. Rb's role in muscle differentiation was first explored through the use of cultured Rb deficient mouse cells (Schneider et al. 1994; Novitch et al. 1996). Although quite artificial, these studies provided us with our first insight into the function of Rb in muscle differentiation. The cell culture model was then superseded by an in vivo partial rescue model. The study by Zacksenhaus et al generated a transgenic line of mice expressing an *Rb* minigene. The *Rb* minigene when crossed into an *Rb* null background rescued the embryonic lethal phenotype by expressing low levels of Rb. This was the first in vivo example of Rb's role in muscle differentiation. Several more mouse models have since provided additional insight into the importance of Rb in skeletal muscle differentiation. More recently, it has been demonstrated that much of the developmental abnormalities of whole *Rb* knockouts can be circumvented by nurturing the embryo through a wildtype placenta (Wu et al. 2003). However, even in the presence of a wildtype placenta, the skeletal muscle still remained poorly developed in the absence of Rb (de Bruin et al. 2003).

Mouse models have also been an important tool in genetically delineating discreet functions of Rb. Compound mutant mouse models have allowed us to separate some of the relevant pathways that interact with Rb. The straight elimination of Rb results in ectopic DNA synthesis, apoptosis, and deficits in cellular differentiation. Much of the cell cycle defects can be attributed to Rb's interaction with the E2F transcription factors. Indeed, Rb's interaction with E2Fs leads to the repression of E2F target genes. Aberrant induction of E2F targets usually leads to ectopic DNA synthesis and the progression of the cell cycle (Johnson et al. 1993). As a corollary to this function, the combined loss of E2Fs 1-3 in mouse embryonic fibroblasts inhibits S-phase progression and mitosis (Wu et

al. 2001). These Rb-E2F interactions have been genetically validated by the study of compound Rb and E2F 1-3 mice (Tsai et al. 1998; Ziebold et al. 2001; Saavedra et al. 2002). Despite partial rescue of the cell cycle deficits in the CNS and PNS, muscle differentiation was still impaired. These results clearly demonstrate a genetic separation between cell cycle inhibition and cellular differentiation with respects to Rb function. Conversely, Rb compound mutations have also been shown to rescue differentiation specific defects. The inhibitor of differentiation (Id) family of proteins are important molecular regulators of differentiation (Ruzinova and Benezra 2003). Id proteins act in a dominant negative manner by sequestering E proteins that are required by bHLH transcription factors. Furthermore, Id proteins are also capable of binding to the Rb family of pocket proteins. Lasorella et al demonstrated a genetic link between Id2 and Rb dependent cellular differentiation (Lasorella et al. 2000). Compound ablation of *Rb* and *Id2* was able to rescue the neural and haematopoietic defects associated with Rb loss. The partial rescue *Rb:Id2* compound mutant embryos came to term but died due to skeletal muscle defects. Cellular context in this case, appears to be quite important in rescuing differentiation deficits by *Id2* ablation. Rb has also been implicated as an upstream effector of ras signaling (Lee et al. 1999). Takahashi et al demonstrated that N-*ras* ablation can rescue the skeletal muscle differentiation defect in an *Rb* null background (Takahashi et al. 2003). Despite proper skeletal muscle differentiation, *Rb*:N-*ras* compound mutants still displayed aberrant cell cycle and apoptosis. In summary, mouse models of Rb deficiency have provided valuable insight into the different aspects of Rb function. Furthermore, mouse models have provided the means to investigate key genetic interactions in a complex in vivo system.

1.4 Myogenic Transcription Factors

(Chapters 1.4 & 1.5; excerpts from Birth Defects Research: Part C, 75(3):180-192)

Skeletal muscle specific gene regulation in the embryonic somite requires a family of bHLH transcription factors known as the Myogenic Regulatory Factors (MRFs)(Parker et al. 2003). The members of the family include Myf5, Mrf4 (Myf6), MyoD, and myogenin. Moreover, the paired-box homeodomain transcription factors Pax3 and Pax7 play an important role in the specification of myogenic progenitors. Mouse knockout models have been important in understanding functional relationships in the context of embryonic muscle development. Analysis of compound mutant mice has allowed researchers to assess functional redundancy amongst family members. Additionally, the application of this approach was instrumental in understanding the functional hierarchy of myogenic transcription factors in the developing somite.

The bHLH MRFs represent an excellent point of focus for examining the molecular biology of skeletal muscle development. The MRFs are specifically expressed in skeletal muscle tissues and potently induces myogenic conversion when expressed in non-myogenic cell types. Gene targeting experiments has provided valuable insight regarding their biological duties. *Myf5* and *MyoD* were the first two MRFs that were genetically targeted for ablation (Braun et al. 1992; Rudnicki et al. 1992). All told, the muscle phenotypes for both knockout mice were relatively subtle. *MyoD*-null mice were born viable and fertile with no apparent gross muscle defects. However, one phenotypic observation strongly suggested of Myf5 and MyoD's compensatory nature. Northern expression analysis on newborn *MyoD* mutant skeletal muscles revealed abnormally

elevated levels of *Myf5* RNA. Subsequent studies of compound *Myf5*$^{-/-}$:*MyoD*$^{-/-}$ mice clearly demonstrated their redundant functions. Mice without Myf5 and MyoD were completely devoid of skeletal muscle (Rudnicki et al. 1993). Thus defining the essential requirement for Myf5 or MyoD in the context of skeletal muscle development.

The identification of somitic domains that initially or exclusively express *Myf5* or *MyoD* by β-Gal marking has additionally been valuable in deducing their developmental role. Kablar and colleagues demonstrated an epaxial and hypaxial division of labor by characterizing a *MyoD-LacZ* transgene in *Myf5*$^{-/-}$ and *MyoD*$^{-/-}$ embryos (Kablar et al. 1997). Migrating hypaxial limb precursors were developmentally delayed by 2.5 days in *MyoD*$^{-/-}$ embryos. While *Myf5*$^{-/-}$ embryos displayed no delay in limb muscle development, but delayed development in the epaxial musculature. These methods were also the means to examine Myf5 and MyoD's function in myogenic lineage determination and migration.

Functional elimination of Myf5 was achieved by insertion of the *LacZ* coding sequence into the *Myf5* locus (*Myf5*$^{a2-/-}$) (Tajbakhsh et al. 1996). *LacZ* expressing DML derived cells in *Myf5*$^{a2-/-}$ embryos were mislocalized and expressed non-myogenic markers such as the dermal marker *dermo-1* and cartilage marker *scleraxis*. Tajbakhsh and colleagues thus demonstrated that Myf5 is largely responsible for myogenic lineage restriction and localization in the DML. A similar type of phenomenon was observed in MyoD dependent limb muscle precursors in *Myf5*$^{-/-}$:*MyoD*$^{-/-}$ embryos. *MyoD-LacZ* expressing mesenchymal progenitors in the limb differentiated into cartilage rather than muscle (Kablar et al. 1999). Taken together, Myf5 and MyoD are important regulators of

myogenic lineage commitment in epaxial and hypaxial progenitors in a normal biological setting.

Knockout studies of *myogenin* and *MRF4* have proven to be equally informative in assessing their developmental function. The skeletal muscle of *myogenin* mutant neonates were poorly differentiated, sparse, and unorganized (Hasty et al. 1993; Nabeshima et al. 1993). The residual myotubes lacked sarcomeric Z lines as assessed by electron microscopy (Nabeshima et al. 1993). Interestingly, there were many mononucleated cells that were presumably undifferentiated myoblasts. In support of this notion, it was shown that *MyoD-LacZ* was appropriately expressed in the *myogenin*-null embryo (Venuti et al. 1995). Furthermore, $MyoD^{-/-}$:$myogenin^{-/-}$ and $Myf5^{-/-}$:$myogenin^{-/-}$ mice analysis revealed muscle phenotypes similar to that of *myogenin*-null alone (Rawls et al. 1995). These lines of evidence clearly place myogenin downstream of Myf5 and MyoD in the process of differentiation. The function of MRF4 has been more difficult to assess through targeted disruption studies due to the close proximity of the *MRF4* and *Myf5* genes (*MRF4* is 8kb upstream of *Myf5* transcriptional start site) (Olson et al. 1996). Due to the expansive and complex regulatory sequences at this locus, gene-targeting constructs must be carefully designed. Multiple allelic variants of *MRF4* and *Myf5* targeted disruptions result in variable phenotypes (Braun and Arnold 1995; Patapoutian et al. 1995; Zhang et al. 1995; Kaul et al. 2000; Kassar-Duchossoy et al. 2004). The severity of the muscle and rib defect phenotype directly correlates to the extent in which the neighboring gene's endogenous expression has been disrupted. Not surprisingly, the severe *MRF4* allele phenocopies the severe *Myf5* allele (Olson et al. 1996). Kassar-Duchossoy and colleagues demonstrated that the $Myf5^{nLacZ/nLacZ}$:$MyoD^{-/-}$ embryo is in

essence a triple MRF knockout (*MRF4*, *Myf5*, *MyoD*) (Kassar-Duchossoy et al. 2004). The $Myf5^{nLacZ/nLacZ}$:$MyoD^{-/-}$ mutant had no skeletal muscle, phenocopying the original compound *Myf5:MyoD* mutant described by Rudnicki et al. *Myf5* knockout alleles that do not disrupt *MRF4* expression [$Myf5^{GFP\text{-}P/GFP\text{-}P}$ and $Myf5^{lox\text{-}P/loxP}$ (Kassar-Duchossoy et al. 2004), $Myf\text{-}5^{FGF\text{-}ki/FGF\text{-}ki}$ and $Myf\text{-}5^{\Delta loxP/\Delta loxP}$ (Kaul et al. 2000)] results in viable mice. Furthermore, $Myf5^{lox\text{-}P/loxP}$ embryos were capable of inducing early epaxial myotome formation and the proper induction of *MyoD* expression (Kassar-Duchossoy et al. 2004). Finally, correct expression of *MRF4* in $Myf5^{GFP\text{-}P/GFP\text{-}P}$:$MyoD^{-/-}$ embryos was sufficient for the formation of myosin heavy chain (MHC; marker of terminal differentiation) positive skeletal muscle. Therefore, MRF4 is a myogenic determination factor acting upstream of MyoD.

1.5 Myogenic Pax Transcription Factors

Pax3 and Pax7 are highly homologous paired-box transcription factors necessary for the specification of embryonic and adult MPCs (Seale et al. 2000; Relaix et al. 2005). *Pax3* expression can first be detected in the presomitic mesoderm prior to the formation of the epithelial somite (Goulding et al. 1994; Williams and Ordahl 1994). At the onset of dorsal ventral somite compartmentalization, *Pax3* is expressed throughout the entire epithelial dermomyotome. Expression of *Pax3* is subsequently down regulated in the DML and becomes regionalized to the hypaxial VLL domain (Goulding et al. 1994; Tajbakhsh et al. 1997). The developmental role of Pax3 has been analyzed mainly in the Pax3 deficient *Splotch* (*Sp*) mice and in mice with targeted disruptions of the *Pax3* locus. Mice that are Pax3 deficient lack limb musculature and have poorly developed epaxial

and hypaxial trunk musculature (Bober et al. 1994; Goulding et al. 1994; Daston et al. 1996; Tremblay et al. 1998). The limb muscle progenitors in a *Sp* embryo undergo apoptosis and are incapable of migrating into the developing limb buds (Borycki et al. 1999a). However, the *Sp* limb progenitors do appear to have an intrinsic ability to activate the myogenic program when placed in an inductive environment (Daston et al. 1996).

Pax3 has been demonstrated to directly target genes required for cell migration. The receptor tyrosine kinase c-met and its ligand hepatocyte growth factor (HGF) are required for the migration of limb muscle progenitors (Bladt et al. 1995). Migrating limb muscle precursors express *c-met*, however targeted disruption of *c-met* or *HGF* results in the absence of limb muscles. Importantly, the regulation of *c-met* expression is Pax3 dependent (Epstein et al. 1996). The absence of Pax3 function also results in the down regulation of *Lbx1* in limb muscle progenitors (Mennerich et al. 1998). Similar to the *c-met/HGF* mutants, *Lbx1*-null limb muscle progenitors fail to migrate properly.

The myogenic regulatory network involved in Pax3 dependent myogenesis mirrors that of an evolutionarily conserved developmental pathway elucidated in the drosophila (Heanue et al. 1999). Regulation of drosophila eye development involves the gene products eyeless (Pax6 homolog), daschund, eyes absent, and sine oculis that function in a synergistic fashion. Heanue et al. have proposed that an analogous pathway is utilized in vertebrate muscle development. The vertebrate homolog of fly *daschund*, *Daschund2* (*Dach2*) was demonstrated to be expressed in the myogenic compartment in the developing somite along with *Pax3*. Moreover, the vertebrate components of this pathway namely Dach2, Eya2 and Six1 are capable of synergistically activating the

myogenic program along with Pax3. This specific regulatory network has also been demonstrated to be important in the myogenic differentiation of P19 embryonic carcinoma cells (Ridgeway and Skerjanc 2001). Pax3 is also an upstream activator of the MyoD dependent differentiation pathway. Compound *Myf5*$^{-/-}$*:Sp* embryos were incapable of inducing MyoD dependent myogenesis in the limbs and trunk (Tajbakhsh et al. 1997). In retrospect, the *Myf5*$^{-/-}$*:Sp* embryos were also deficient in the expression of *MRF4*. Therefore, MyoD is downstream of Pax3, Myf5, and MRF4 in a myogenic developmental hierarchy.

Unlike Pax3, Pax7 deficiency does not affect embryonic myogenesis (Seale et al. 2000). The *Pax7* expression domain does partially overlap that of *Pax3* during the early epithelial dermomyotome stage (Jostes et al. 1990). Pax7 is also capable of substituting for most of Pax3's function (Borycki et al. 1999b; Relaix et al. 2004). However, Pax7 is primarily involved in the specification and maintenance of satellite cells (Seale et al. 2000). In a recent publication by Relaix et al., a somitically derived mitotically active population of myogenic progenitors were found to co-express *Pax3* and *Pax7* (Relaix et al. 2005). These *Pax3/Pax7* expressing progenitors significantly contribute to the growth of late embryonic and fetal skeletal muscle and are the progenitors of satellite cells. Pax3 and Pax7 are essential for the maintenance and myogenic specification of these progenitors. Compound ablation of *Pax3:Pax7* results in severe muscle growth deficiencies (Relaix et al. 2005).

The growth and regenerative capacity of the post-natal skeletal muscle depends primarily on satellite cells (Holterman and Rudnicki 2005). Satellite cells are the committed resident stem cell population of the skeletal muscle. The maintenance and

functionality of this population during adulthood is critically dependent on the transcription factor Pax7 (Seale et al. 2000). Pax7 is highly expressed in quiescent and activated satellite cells and is believed to play a role in myogenic specification and cell survival. Indeed, ectopic expression of Pax7 in skeletal muscle resident non-myogenic $CD45^{+}Sca1^{+}$ cells, sets off the myogenic program resulting in myoblast conversion (Seale et al. 2004). The Pax7 gene product is also found endogenously as four different alternatively spliced isoforms (Holland et al. 1999). Based on functional studies on Pax3 isoforms, it is believed that Pax7 isoforms also confer unique DNA binding properties (Vogan et al. 1996). Furthermore, Pax7 expression is abruptly down-regulated upon induction of the differentiation program. Taken together, Pax7 function correlates to maintaining a stem cell-like state in adult myogenic cells.

In summary, myogenic transcription factors interact in a developmental hierarchy with partially overlapping functions. Myogenic transcriptional activation results in a cascade of gene induction events that ultimately result in a physiologically functional myotube. When the balance of signaling cascade is disrupted embryonic development is abnormal resulting in disease and sometimes cancer.

1.6 Molecular Integration of the Cell Cycle and Myogenic Differentiation

Induction of myogenic differentiation is invariably accompanied by terminal cell cycle exit. The tight association between muscle differentiation and cell cycle exit is rooted at the molecular level. The molecular cogs of the cell cycle machinery physically interact with and influence the activity of myogenic transcription factors. The activity of the myogenic transcription factor MyoD in turn can induce the transcription of cell cycle

inhibitors. The bi-directionality of these interactions is suggestive of a tightly coupled regulation of these two processes.

Retinoblastoma (Rb) and its family members p107 and p130 regulate the G1/S cell cycle transition (Dannenberg et al. 2000; Sage et al. 2000). The activity of Rb proteins is modulated by the cyclical associations with cyclin dependent kinase (cdk) complexes. As the cell cycle progresses towards the G1/S boundary, Rb proteins progressively become phosphorylated by cyclin-cdk complexes. Hyperphosphorylation of Rb proteins thus results in the dissociation from, and activation of E2F and their target genes. Timely and ordered phosphorylation events are thus paramount for properly regulating the progression of the cell cycle. Cell cycle dependent phosphorylation is mediated by cyclin-cdk complexes. The assembly and activation of these complexes follow an orderly sequence during active cell division. Following mitosis, and entering G1 phase, cyclinD-cdk4/6 complexes assemble to initiate G1 progression. As the cell cycle progresses towards the G1/S phase transition, active cyclinE-cdk2 complexes assemble. The activity of cyclinE-cdk2 complexes promotes progression past the G1 restriction point, at which an irreversible decision to complete cell division has been made. CyclinA-cdk2 complexes assemble during S phase and finally cyclinB-cdc2 complexes form during the G2/M transition of the cell cycle.

The myogenic transcription factors MyoD and Myf5 are important regulators of myogenic specification and differentiation. The abundance and activity level of both transcription factors are responsive to the modulations of the cell cycle (Figure 3). Studies in synchronized C2C12 myoblasts have shown that MyoD and Myf5 proteins are at their maximum level at different points in the cell cycle. The levels of MyoD protein

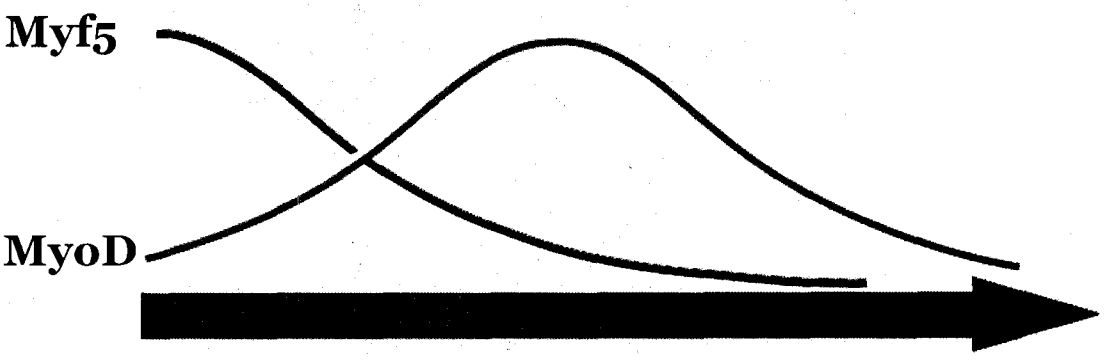

Figure 3. **Cell cycle dependent modulation of Myf5 and MyoD protein levels.**

are the lowest at G0 and hit their peak at mid G1 of the cell cycle. While Myf5 levels are at their peak at G0 and G2, and lowest at mid G1. Thus, the levels of Myf5 and MyoD are in opposite phases during G0 and mid G1. Interestingly, the G0 expression pattern of Myf5 and MyoD appear to mimic that of quiescent satellite cells (resident adult muscle stem cells). Moreover, the mid G1 pattern resembles that of a differentiated state.

The cyclical turnover of MyoD and Myf5 proteins are linked to the activity of cdk complexes. The cell cycle dependent fluctuations of MyoD protein levels are regulated by cdk phosphorylation events. Cyclin D1 overexpression studies first demonstrated a link between cyclin-cdk activity and inhibition of MyoD induction of muscle promoters (Skapek et al. 1996). Subsequently, it was shown that MyoD protein was targeted by a proteasome pathway through cdk1 and cdk2 dependent phosphorylation of serine 200 (Song et al. 1998; Kitzmann et al. 1999; Tintignac et al. 2000). Similarily, Myf5 protein is also degraded through cell cycle dependent phosphorylation events. Myf5 degradation is accomplished through two different phosphorylation sites. The degradation of Myf5 at mitosis requires a residue within its bHLH domain (R93) while another site is responsible for its steady state degradation (S158) (Lindon et al. 2000). The instability of MyoD and Myf5 throughout the cell cycle counteracts their potential for target gene induction. The stability and activity is thus critically important for MyoD induced cell cycle arrest and myogenic induction. Upon low serum conditions, cdk inhibitors act to stabilize MyoD protein levels for the subsequent differentiation program (Figure 4). Indeed, it has been demonstrated that the cdk inhibitor p57 blocks cyclinE-cdk2 phosphorylation of MyoD, thus stabilizing it. Furthermore, activated MyoD in turn can induce the expression of cdk inhibitor *p21*, differentiation specific *cyclinD3*, and *Rb*

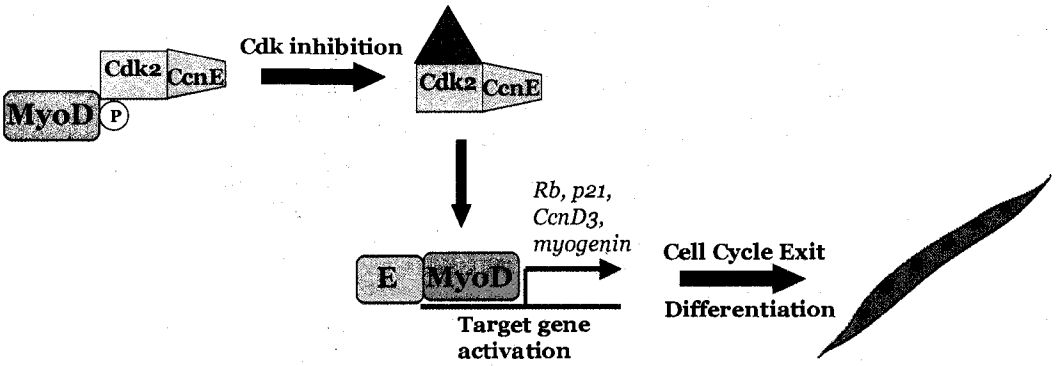

Figure 4. **Cell cycle dependent mechanistic model of MyoD activation by cdk inhibition.**

(Martelli et al. 1994; Guo et al. 1995; Cenciarelli et al. 1999). The induction of *p21* thus further inhibits cdk phosphorylation and the induction of *cyclinD3* and *Rb* contributes to terminal cell cycle exit and differentiation. Additionally, MyoD stabilization also serves to directly inhibit the activity of cyclinD-cdk4 complexes (Zhang et al. 1999). The inactivation of cdk4 inhibits its ability to phosphorylate Rb, thus activating Rb. Therefore Rb activation may doubly serve to arrest the cell cycle and promote differentiation.

1.7 Hypothesis and Specific Aims

1.7.1 Skeletal Muscle Specific Deletion of Rb

Myogenic conversion and gene induction requires the activity of both MyoD and Rb. Therefore, we postulated a critical function for Rb during the physiological progression of myogenic differentiation. To this end, we utilized a *LoxP-Cre* conditional deletion of *Rb* in skeletal myoblasts and myotubes. The in vivo and in vitro implications were assessed through gross morphological, histological, immunocytochemical and molecular techniques.

1.7.2 Identifying Rb Targets in Skeletal Muscle

Rb complexes regulate target genes in conjunction with cell specific transcriptional regulatory co-factors. Uncovering the nature of Rb targets will provide novel insight with respects to Rb's physiological functions in skeletal muscle. Affymetrix global expression profiling of Rb deleted and wildtype primary myoblast cultures were analyzed. Additionally, physical binding targets of Rb complexes were

cloned through the combined use of chromatin immunoprecipitations and representational difference analysis (ChIP-RDA).

Chapter 2

Rb is Required for Progression through Myogenic Differentiation but not Maintenance of Terminal Differentiation

Purpose

To delineate the requirement for Rb in the progression and maintenance of skeletal muscle differentiation, in vivo and in cultured adult primary myoblasts.

Submission Information

Submitted: 1 March 2004
Accepted: 27 July 2004
Published: 13 September 2004

Contribution of Co-Authors

Michael Huh did all of the experimental work and analysis with the exception of Figure 10 C.

Anthony Scimè provided Figure 10 C.

Maura Parker provided a single line of $Rb^{f/f}$ primary myoblasts.

Robin J. Parks provided the Ad-Lac-Z and Ad-Cre viruses.

Revised Manuscript 200403004

Rb is Required for Progression through Myogenic Differentiation but not Maintenance of Terminal Differentiation

Michael S. Huh[1], Maura H. Parker[1,2], Anthony Scimè[1], Robin Parks[1], and Michael A. Rudnicki[1,2,3]

1. Ottawa Health Research Institute
   Molecular Medicine Program
   501 Smyth Road,
   Ottawa, Ontario
   Canada, K1H 8L6
   Tel: 613-739-6740
   Fax: 613-737-8803

2. McMaster University
   Medical Sciences Program
   Hamilton, Ontario
   Canada

3. Correspondence should be addressed to M.A.R.
   E-mail: mrudnicki@ohri.ca

Accepted July 26, 2004

Running Title: Rb is not required for maintenance of differentiation

Key words: pRb, Cre, primary myoblasts, proliferation, differentiation, MyoD, Myogenin

Summary

To investigate the requirement for pRb in myogenic differentiation, a floxed *Rb* allele was deleted in either proliferating myoblasts, or following differentiation. *Myf5-Cre* mice, lacking pRb in myoblasts, died immediately at birth and exhibited high numbers of apoptotic nuclei and an almost complete absence of myofibers. By contrast, *MCK-Cre* mice, lacking pRb in differentiated fibers, were viable, and exhibited a normal muscle phenotype and ability to regenerate. Induction of differentiation of Rb-deficient primary myoblasts resulted in high rates of apoptosis and a total inability to form multinucleated myotubes. Upon induction of differentiation Rb-deficient myoblasts up regulated myogenin, an immediate early marker of differentiation, but failed to down regulate Pax7 and exhibited growth in low serum conditions. Primary myoblasts in which *Rb* was deleted following expression of *MCK-Cre* after differentiation formed normal multinucleated myotubes that did not enter S-phase in response to serum stimulation. Therefore, Rb plays a crucial role in the switch from proliferation to differentiation rather than maintenance of the terminally differentiated state.

Introduction

The development of skeletal muscle in mammals provides a powerful system with which to study the molecular regulation of the genesis, growth and differentiation of stem cells during embryonic and regenerative myogenesis (Parker et al., 2003). Importantly, the activity of the bHLH transcription factor family of myogenic regulatory factors (MRFs) is tightly coupled to cell-cycle control and the study of this regulation has provided important insights into the cellular mechanisms that regulate cell growth versus differentiation or apoptosis (Puri and Sartorelli, 2000; Walsh and Perlman, 1997; Yee et al., 1998).

The myogenic regulatory factors (MRFs) are subject to regulation that acts to couple MRF activity to the cell cycle. Hypophosphorylated pRb was suggested to bind MyoD and this association to be required for MyoD-mediated activation of E-box containing muscle-specific promoters (Gu et al., 1993). However, direct binding between pRb and MyoD has been ruled out by *in vivo* and *in vitro* assays (Zhang et al., 1999a; Zhang et al., 1999b). Therefore, pRb likely potentiates MyoD activity via an indirect mechanism not involving binding of Rb to MyoD.

Proliferating myoblasts express Id, activated Cdk4, low levels of hyperphosphorylated Rb, and free E2Fs as well as E2Fs complexed largely with p107. Activated Cdks and Id both act to stimulate cell cycle progression. By contrast, myotubes express high levels of p21 and hypophosphorylated pRb. Despite the abundance of hypophosphorylated pRb, p130-E2F4 complexes are the predominant E2F complexes in the myotube (Corbeil et al., 1995). Terminal differentiation and protection against apoptosis is maintained by Cdk inhibitors (p21, p27 etc.), and high expression of

hypophosphorylated pRb (Ho et al., 2004; Jiang et al., 2000; Peschiaroli et al., 2002). Together, these data suggest that during myogenic differentiation pRb plays a role distinct from the conventional repression of E2F transcriptional activity.

Newborn mice lacking pRb exhibit multiple deficits including severe deficiencies in the formation of skeletal muscle (de Bruin et al., 2003; Wu et al., 2003; Zacksenhaus et al., 1996). Studies using MyoD-converted pRb-deficient embryonic fibroblasts have suggested that *Rb* is essential for both MyoD and MEF2 transcriptional activity, as well as maintaining the terminally differentiated state (Novitch et al., 1996; Novitch et al., 1999; Schneider et al., 1994). Although pRb-deficient fibroblasts transfected with MyoD become myogenic and express early muscle markers, such as myogenin, expression of late markers, such as myosin heavy chain is reduced. In addition, serum restimulation of these differentiated pRb-deficient myoblasts results in bromodeoxyuridine (BrdU) incorporation and thus, S-phase entry and DNA synthesis. However, these cells are unable to enter mitosis. Moreover, forced expression of MyoD in a variety of $Rb^{-/-}$ fibroblastic cells results in apoptosis that appears to be p21 dependent (Peschiaroli et al., 2002). In the absence of N-*ras*, pRb-deficient embryos exhibit normal muscle differentiation without apoptosis suggesting a role for signaling downstream of N-*ras* in provoking cell death in $Rb^{-/-}$ muscle (Takahashi et al., 2003).

Rb plays a key role in controlling cell cycle progression through the G1 restriction point for entry into S-phase (Stevaux and Dyson, 2002). During myogenic differentiation, proliferating myoblasts must also exit the cell cycle from G1 phase, prior to the restriction point (R) (Perry and Rudnick, 2000). Therefore, it can be hypothesized that

pRb plays an analogous role in myoblasts by regulating the switch from proliferation to differentiation.

To investigate the requirement for pRb in myogenic differentiation, we examined the proliferation and differentiation potential of primary myoblasts in which a floxed *Rb* allele was deleted either before or after differentiation. Our experiments unequivocally establish that pRb is required for progression of the differentiation program and not for maintenance of the differentiated state.

Results

Rbf/f:Myf5-Cre Mice Die at Birth with Severe Muscle Deficits

To investigate the requirement for pRb in myogenesis, mice carrying a floxed *Rb* allele (Marino et al., 2000) were interbred with *Myf5-Cre* knock in mice (Tallquist et al., 2000), or *MCK-Cre* transgenic mice (Wang et al., 1999). The *Myf5-Cre* allele faithfully recapitulates the expression pattern of the endogenous *Myf5* gene and is uniformly expressed in all proliferating myoblasts (Tallquist et al., 2000). By contrast, the *MCK-Cre* transgene is not expressed in myoblasts but is upregulated in differentiated multinucleated skeletal myotubes (Andrechek et al., 2002; Wang et al., 1999).

$Rb^{f/f}$ males were crossed with $Rb^{f/wt}$*:Myf5-Cre* females to generate $Rb^{f/f}$*:Myf5-Cre* progeny. Notably, no viable $Rb^{f/f}$*:Myf5-Cre* mice were identified after genotyping over 95 offspring. Examination of newborn litters revealed the expected Mendelian proportion of $Rb^{f/f}$*:Myf5-Cre* pups. However, the newborn pups lacking pRb in myoblasts were motionless, became cyanotic and failed to survive. Therefore, we concluded that $Rb^{f/f}$*:Myf5-Cre* mice exhibited a phenotype similar to other *Rb* knockout mouse models (de Bruin et al., 2003; Lasorella et al., 2000).

Histological examination of skeletal muscle revealed the presence of severe differentiation deficits (Fig. 1, A-F). Hind limb muscles exhibited a dramatic reduction in mass with a complete absence of mature fibers as compared to littermate controls (n = 3 independent animals; Fig. 1, compare A with B). In addition, the morphology of the residual muscle fibers in the $Rb^{f/f}$*:Myf5-Cre* mice was short and irregular in shape (Fig. 1 D). Moreover, the typically long and orderly parallel arrangement of the fibers seen in the

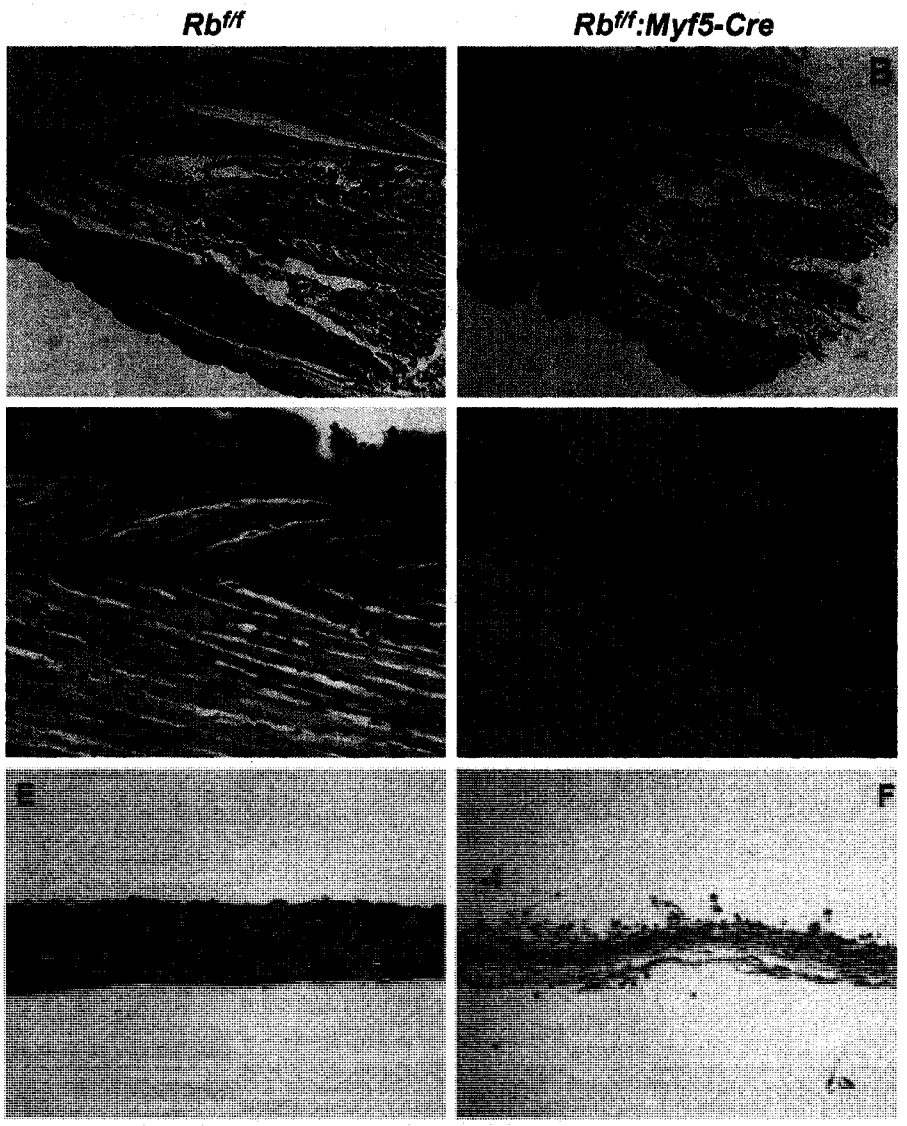

Figure 1. **Severely impaired myogenesis in P0 Rbf/f:Myf5-Cre mice.** Hematoxylin and eosin staining of paraffin-embedded longitudinal sections through the hind limb of control (A and C) and Rbf/f:Myf5-Cre (B and D) mice. Hematoxylin and eosin staining of cross sections through diaphragm of control (E) and Rbf/f:Myf5-Cre (F) mice. Original magnifications in A and D, 50x; B, C, E, and F 400x.

wild-type controls was absent in the *Rb$^{f/f}$:Myf5-Cre* muscle (Fig. 1, compare C with 1D). These results confirm the well-established requirement for pRb in myogenesis.

The severe deficit in muscle tissue development lead us to question whether the residual muscle fibers were undergoing appropriate differentiation. Therefore, immuno-fluorescent staining of the terminal differentiation marker, myosin heavy chain (MHC), and of Desmin, a marker for myoblasts and newly formed fibers was performed (Fig. 2, A-H). Desmin expression was significantly diminished in both hind limb and intercostal muscles in the *Rb$^{f/f}$:Myf5-Cre* in comparison to the level of staining in the control sections (n = 3 independent animals; compare Fig. 2, compare A and C with E and G). Interestingly, MHC expression was considerably diminished in limb musculature but was less affected in intercostal muscles (Fig. 2, F and H). Taken together, the histological and immuno-fluorescent analysis support the notion that *Rb$^{f/f}$:Myf5-Cre* pups die at birth due to severe deficiencies in skeletal muscle that impede ventilation leading to rapid cyanosis and death.

Rb$^{f/f}$:MCK-Cre Mice are Viable and Apparently Normal

Genetic crosses between *Rb$^{f/wt}$* and *Rb$^{f/wt}$:MCK-Cre* mice resulted in completely viable and healthy *Rb$^{f/f}$:MCK-Cre* mice in the expected mendelian ratio. *Rb$^{f/f}$:MCK-Cre* mice were similar to wild-type littermates in size from birth to late adulthood and appeared normally in all respects. Skeletal muscle specific expression of the *MCK-Cre* transgene was tested by crossing *MCK-Cre* mice with the *R26R3* Cre inducible LacZ reporter line of mice. Single fibers isolated from *R26R3:MCK-Cre* mice displayed robust X-Gal staining confirming the proper expression of the *MCK-Cre* transgene (Fig. 3 H).

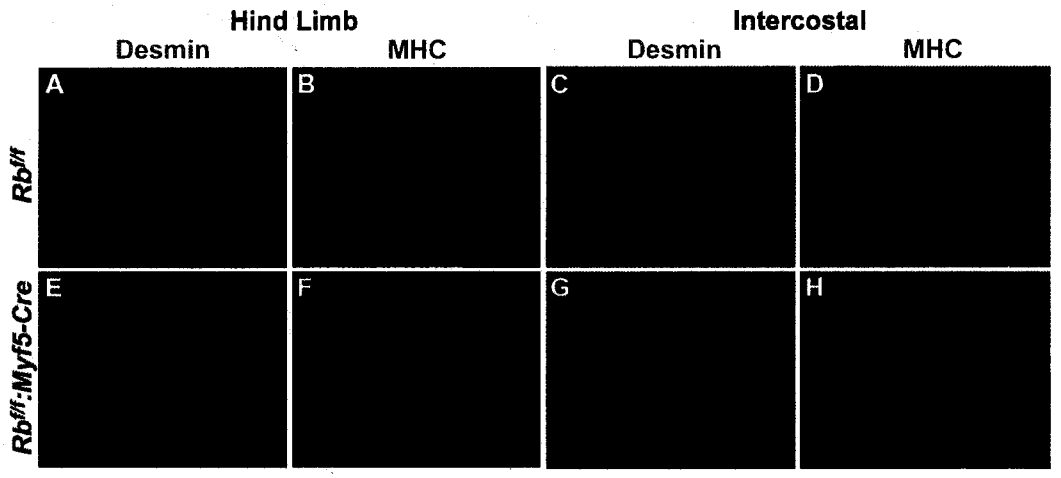

Figure 2. **Abnormal skeletal muscle differentiation in P0 Rbf/f:Myf5-Cre mice.** Immunofluorescent staining of longitudinal sections through the hind limb of control (A and B) and Rbf/f:Myf5-Cre (E and F) mice with antibodies to desmin and myosin heavy chain (MHC). Immunofluorescent staining of intercostal muscles of control (C and D) and Rbf/f:Myf5-Cre (G and H) mice with antibodies to desmin and MHC. Original magnifications of A-H, 200x.

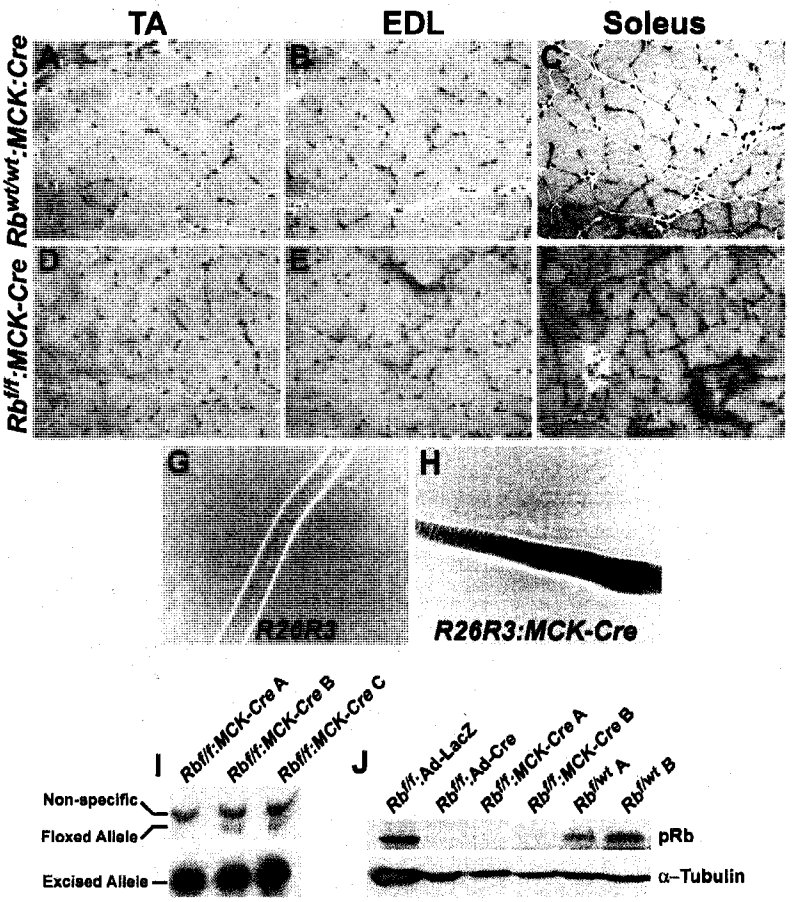

Figure 3. **Rbf/f:MCK-Cre mice have normal skeletal muscle.** Hematoxylin and eosin staining of frozen cross sections of control muscles (A-C) and Rbf/f:MCK-Cre muscles (D-F). TA, tibialis anterior; EDL, extensor digitorum longus. Phase-contrast micrograph of X-Gal-stained single muscle fibers of R26R3 control (G) and R26R3:MCK-Cre (H) mice. (I) 32P end-labelled PCR genotype analysis of the floxed Rb locus revealed between 98-99% excision. 32P end-labelled PCR was performed on DNA samples extracted from a pool of 20 single fibers from three independent mice (Rbf/f:MCK-Cre A, Rbf/f:MCK-Cre B, and Rbf/f:MCK-Cre C). (J) pRb immunoblot analysis of single fiber protein extracts reveals virtually no detectable pRb. a-Tubulin protein levels were used as loading controls. Protein was extracted from a pool of 200 single fibers from Rbf/f:MCK-Cre A and Rbf/f:MCK-Cre B mice, and from Rbf/wt A and Rbf/wt B littermate controls. Protein extracts from Ad-LacZ and Ad-Cre infected Rbf/f primary myoblasts were used as positive and negative controls respectively. Original magnifications of A-H, 200x.

To quantitatively assess the efficiency of *Rb* gene deletion in $Rb^{f/f}$*:MCK-Cre* mice, we utilized densitometry to calculate the Rb^{flox}:$Rb^{excised}$ allele ratios. The allele ratios were used to determine the percentage of unexcised Rb^{flox} allele from pooled single muscle fiber preps (n = 3 independent animals). As expected, we detected low levels of unexcised Rb^{flox} allele likely due to the presence of satellite cells on the muscle fibers (~1-2% Rb^{flox} remaining in $Rb^{f/f}$*:MCK-Cre* fibers; Fig. 3 I). Additionally, protein levels of pRb were examined by western blot analysis of pooled single fibers from $Rb^{f/f}$*:MCK-Cre* and $Rb^{f/wt}$ littermate controls (200 fibers per animal). Levels of pRb were readily detectable in the control fibers but below the limit of detection in the $Rb^{f/f}$*:MCK-Cre* fibers (Fig. 3 J). The extremely low levels of pRb in the $Rb^{f/f}$*:MCK-Cre* fibers precluded any possibility of comparing fold differences by this method. Our histological analysis of the hind limb skeletal muscle revealed no gross abnormalities in the skeletal muscle fibers of $Rb^{f/f}$*:MCK-Cre* mice in comparison to littermate controls (n = 3 independent animals; Fig. 3, compare A-C with D-F). The fiber caliber of $Rb^{f/f}$*:MCK-Cre* and littermate controls (n = 3) were on average similar (unpublished data). The apparently normal skeletal muscle phenotype prompted us to examine the regenerative capacity of the $Rb^{f/f}$*:MCK-Cre* skeletal muscle using cobra venom derived cardiotoxin. Following cardiotoxin induced injury into the tibialis anterior muscle, $Rb^{f/f}$*:MCK-Cre* mice demonstrated no deficit in the regeneration of the damaged muscle tissue (n = 3 independent animals; unpublished data). Taken together, these data suggest that pRb is not required for the maintenance or regeneration of differentiated skeletal muscle.

Rb-Deficient Primary Myoblasts Exhibit Altered Cell Cycle Kinetics

To investigate the cellular basis for the muscle deficits in newborn $Rb^{f/f}$*:Myf5-Cre* mice, primary myoblasts were isolated from $Rb^{f/f}$ adult muscle. To generate null mutations in *Rb*, primary myoblasts isolated from $Rb^{f/f}$ mice were infected with Cre expressing adenovirus (Ad-Cre; Anton and Graham, 1995). Myoblasts were infected with Lac-Z expressing adenovirus (Ad-Lac-Z) as a control.

Adenoviral infection and expression of Cre resulted in the complete excision of the floxed region of *Rb* as assessed by ^{32}P end-labeled PCR genotyping and western blot analysis (Fig. 4, A and B). Our method of ^{32}P end-labeled PCR was capable of detecting an Rb^{flox}:$Rb^{excised}$ allele ratio as low as 10^{-4} when amplified from 20 ng of total DNA (unpublished data). Moreover, pRb protein was below the level of detection by western blot analysis in Ad-Cre infected $Rb^{f/f}$ myoblasts (n=3 independent isolates and more than 3 infections per isolate). Additionally, pRb protein was undetectable by immuno-fluorescence in the nuclei of the Ad-Cre infected myoblasts after 2 days in differentiation media (DM), when pRb is normally expressed at high levels (n = 3; Fig. 4 C). Ad-Cre infected myoblasts appeared to be smaller and more compact than the control infected cells . Our visual assessment was validated by flow cytometry analysis that confirmed the actual decrease in average size of pRb-deficient myoblasts relative to controls (unpublished data).

Cells with null mutations in *Rb* display altered cell cycle kinetics consistent with a role for pRb as an important G1/S checkpoint regulator (Classon et al., 2000; Herrera et al., 1996). Therefore, we examined the growth characteristics of pRb-deficient primary myoblasts. We observed increased growth kinetics with a 2.5 fold decrease in the average

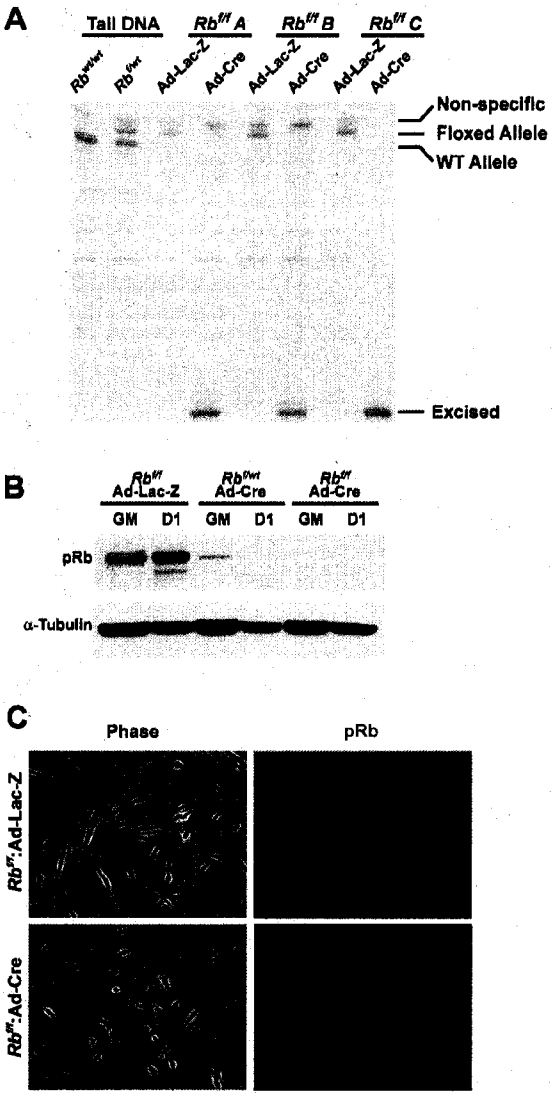

Figure 4. **Adenoviral delivery of Cre recombinase into Rb floxed primary myoblasts completely eliminates pRb expression.** (A) 32P end-labelled PCR genotype analysis of floxed Rb locus revealed complete excision. Primers flanking the LoxP sites in the Rb locus were used to amplify DNA samples from Ad-Lac-Z control infected and Ad-Cre infected Rb flox homozygous (f/f) primary myoblasts from 3 independent isolates (Rbf/f A, Rbf/f B, and Rbf/f C). (B) Immunoblot detection of pRb from control and Ad-Cre infected primary myoblast protein extracts indicated a complete absence of pRb. Whole cell protein extract was harvested from primary myoblasts in growth media (GM) and 1 d in DM (D1). (C) Immunofluorescent staining of control and Ad-Cre infected Rbf/f primary myoblasts. Infected primary myoblasts were PFA fixed after 2 d in DM and stained with antibody to pRb.

doubling time (n > 6). The myoblasts exhibited a 17% reduction in the G0/G1 population (~60% compared with ~50% for control and $Rb^{f/f}$:Ad-Cre, respectively) and a 30% increase in S phase populations (~20% compared with ~30% for control and $Rb^{f/f}$:Ad-Cre, respectively) of an asynchronously dividing pool of cells. Despite the compact morphology and altered cell cycle characteristics, pRb null primary myoblasts under sub-confluent growth conditions showed no obvious evidence of senescence or cell death after a high number of passages (n = 3, > 15 passages). Taken together, these data indicate that pRb-deficient myoblasts exhibit a relatively subtle phenotype associated with an enhanced proliferative potential. Therefore, these data suggest that the perinatal death of pups was not due to proliferation deficiencies of the myogenic progenitors.

Rb-Deficient Primary Myoblasts are Incapable of Differentiation

Primary myoblasts can be quickly and efficiently induced to exit the cell cycle and initiate the differentiation program by exposure to low serum conditions. To investigate the differentiation potential of primary myoblasts lacking pRb, Ad-Cre infected $Rb^{f/f}$ myoblasts were exposed to low serum conditions using standard procedures (Sabourin et al., 1999). We observed a rapid loss of cell viability (Fig. 5) together with an inability of the remaining cells to form multinucleated myotubes (see Fig. 6, compare C with F).

Detection of nuclear fragmentation by TUNEL revealed apoptotic nuclei beginning to accumulate at six hours following serum reduction (Fig. 5, A-F). TUNEL staining was detected in a markedly higher numbers of pRb-deficient myoblasts by 6 hours in low serum media (6.7 ± 2.4% compare with 22.3 ± 1.52% for control and

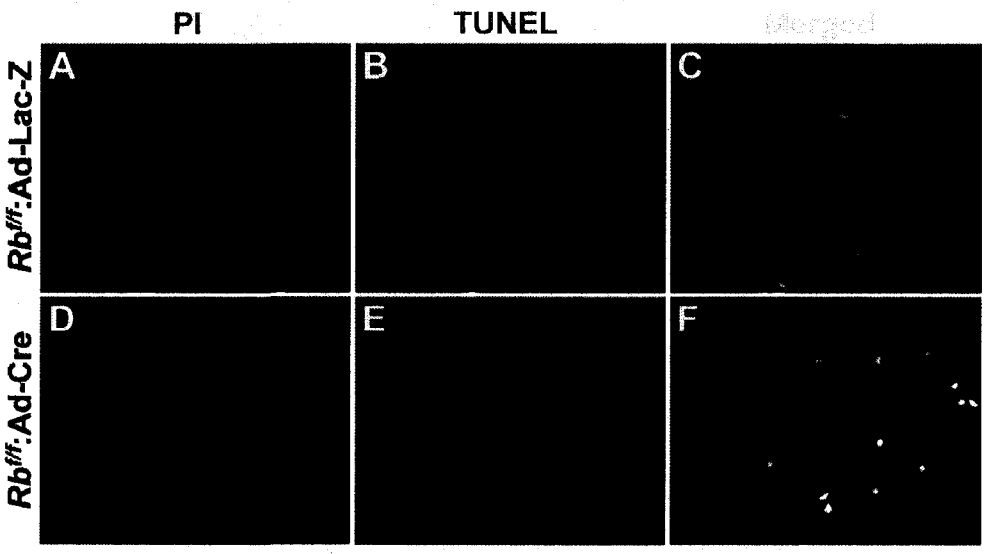

Figure 5. **pRb null primary myoblasts exhibit high rates of apoptosis in response to serum withdrawal.** Apoptotic cell death was assessed by fluorescein-conjugated TUNEL analysis after 6 h in DM on control (A-C) and Ad-Cre infected (D-F) Rbf/f primary myoblasts. Primary myoblasts were counterstained with Propidium Iodide (PI).

Rb$^{f/f}$:Ad-Cre, respectively). The elevated levels of apoptosis gradually diminished the total cell numbers in direct relation to the length of time under low serum conditions (n = 3 independent isolations and infections; ~25% compared to ~85% cell death in controls and *Rb*$^{f/f}$:Ad-Cre, respectively, after 5 d in low serum).

Interestingly, the small number of cells that did survive the low serum conditions appeared incapable of differentiation. The surviving pRb-deficient primary cells were adherent and formed elongated mononuclear myocytes that failed to fuse with closely neighboring myocytes to form multinucleated myotubes (Fig. 4 C, bottom left).

We conducted immunofluorescent staining experiments to examine the cellular expression and localization patterns of MyoD, myogenin, and myosin heavy chain (MHC) (n = 3 independent isolations and infections; Fig. 6, A-L). MyoD is expressed in proliferating myoblasts and is down regulated during differentiation. Myogenin is not expressed in proliferating myoblasts and is upregulated in mononuclear cells as an early response gene during induction of differentiation. Lastly, MHC is up regulated relatively late in the differentiation program and is typically detected in multinucleated myotubes (Sabourin et al., 1999).

Under growth conditions, MyoD was localized to the nuclear compartment and similarly expressed in almost all of the pRb-deficient and wild type primary myoblasts (Fig. 6, A and D). In addition, high levels of MyoD were detected in the nuclei of the pRb-deficient and wild type myoblasts by day 1 of differentiation (Fig. 6, B and E). After differentiation, MyoD protein was down regulated to low levels in virtually all nuclei of wild type multinucleated myotubes (Fig. 6 C). By contrast, ~36% of the pRb-deficient *Rb*$^{f/f}$:Ad-Cre myocytes continued to express high levels of MyoD (Fig. 6 F). By Western

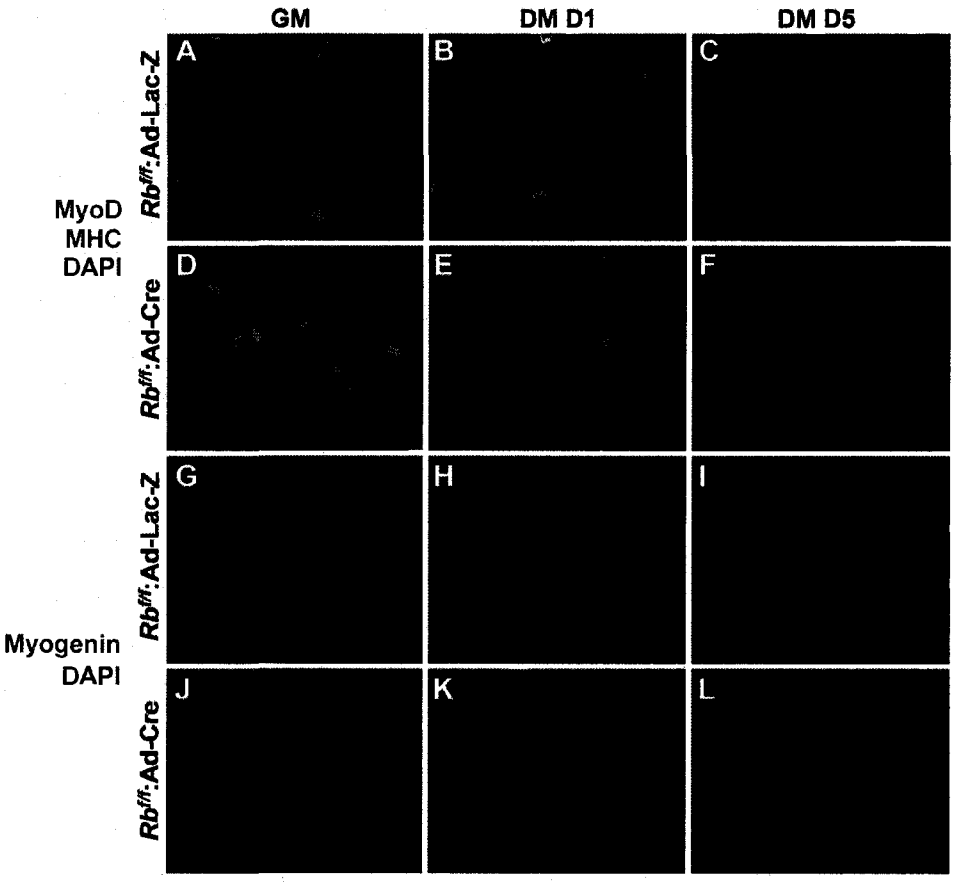

Figure 6. **pRb null primary myoblasts are incapable of forming terminally differentiated multinucleated myotubes.** Double immunofluorescent staining of control (A-C) and Ad-Cre infected (D-F) Rbf/f primary myoblasts with antibodies to MyoD (FITC) and MHC (rhodamine). Immunofluorescent staining of control (G-I) and Ad-Cre infected (J-L) Rbf/f myoblasts with antibody to myogenin (rhodamine). Nuclei were counterstained with DAPI. Infected primary myoblasts were PFA fixed and stained at the indicated time points; GM, growth; DM D1, differentiation day1; DM D5, differentiation day 5.

blot analysis, both wild type and mutant myoblasts expressed similar levels of MyoD in subconfluent growth conditions (Fig. 7 C). However, by day 3 and day 5 of differentiation mutant cells failed to down regulate MyoD (n = 3; Fig. 7 C).

Myogenin was expressed at typically low levels in subconfluent cultures of wild type and *Rb* mutant primary myoblasts. Up regulation of Myogenin expression occurred after one day of differentiation in both wild type and pRb-deficient cells to about equal levels (Fig. 6, G, H, J, and K). However, by day 5 of differentiation myogenin protein was detectable in only 17% of wild type nuclei where as ~50% of Rb-deficient cells exhibited robust nuclear expression (Fig. 6, I and L). By Western blot analysis, myogenin was not detectable in both wild type and mutant myoblasts in growth conditions (Fig. 7 C). However, by day 3 and day 5 of differentiation mutant cells failed to down regulate myogenin (n = 3; Fig. 7 C). Therefore, pRb-deficient myoblasts entered the differentiation program as evidenced by up regulation of myogenin, an immediate early marker of commitment for differentiation (Bergstrom et al., 2002).

After one day of differentiation, cytoplasmic MHC expression was detected by immuno-fluorescence in newly formed wild type myotubes whereas little expression was detected in mutant cells (Fig. 6, compare B with E). By 5 days of differentiation, robust cytoplasmic MHC staining was evident in wild type multinucleated myotubes (Fig. 6 C). By contrast, the pRb-deficient cells were incapable of completing the differentiation program as evidenced by the absence of multinucleated myotubes expressing MHC (Fig. 6 F). Western blot analysis confirmed the very low level expression of MHC in $Rb^{f/f}$:Ad-Cre derived cells (Fig. 7 C). Taken together, these data suggest that the perinatal death of

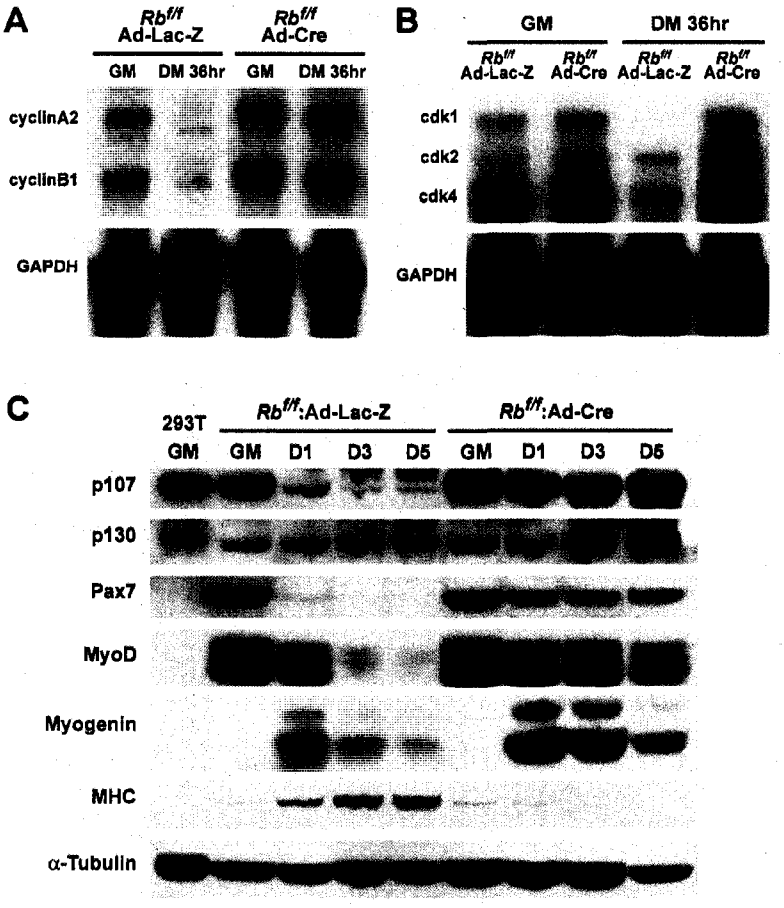

Figure 7. **Absence of terminal differentiation in pRb null primary myoblasts correlates with an inability to down regulate markers of proliferation and early markers of myogenic differentiation.** (A) RNase protection assay for cyclinA2 and cyclinB1 mRNA in control and Ad-Cre infected Rbf/f primary myoblasts. (B) RNase protection assay for cdk1, cdk2, and cdk4 mRNA in control and Ad-Cre infected Rbf/f myoblasts. GAPDH mRNA levels were used as loading controls. Total RNA was harvested from infected myoblasts at the indicated time points (A and B). GM, growth; DM 36hr, differentiation 36 h. (A and B) White lines indicate that intervening lanes have been spliced out. (C) Immunoblot differentiation time course analysis of p107, p130, Pax7, MyoD, Myogenin, and MHC in control and Ad-Cre infected Rbf/f myoblasts. a-Tubulin protein levels were used as loading controls. Whole cell protein extract was harvested at the indicated time points. GM, growth; D1, differentiation day 1; D3, differentiation day 3; D5, differentiation day 5. Protein extract from 293T cells were used as a nonmyogenic control.

$Rb^{f/f}$:Myf5-Cre mice is due to an intrinsic defect in differentiation of the myogenic progenitors.

Pax7 is typically expressed at high levels in proliferating myoblasts and is rapidly down regulated upon induction of differentiation (Seale et al., 2000). Western blot analysis revealed that pRb-deficient primary myoblasts exposed to differentiation medium fail to down regulate Pax7 (Fig. 7 C). Taken together, these data suggest that the low numbers of pRb null myoblasts that survive are capable of initiating differentiation, but subsequently fail to properly regulate the progression of the myogenic program required for the completion of myogenic differentiation.

Primary Myoblasts Lacking pRb Fail to Arrest Upon Induction of Differentiation

To elucidate the cell cycle and differentiation phenotype of the Ad-Cre infected *$Rb^{f/f}$* myoblasts, we performed a series of RNA and protein expression analysis for cell cycle and differentiation markers. RNA expression levels for *cyclins* and *cdks* were analyzed under growth conditions and serum withdrawal differentiation conditions (n = 3). By RNase protection, pRb-deficient primary myoblasts fail to down regulate *cyclinA2*, *cyclinB1*, *cdk1*, *cdk2*, and *cdk4* mRNAs in response to serum withdrawal (Fig. 7, A and B).

Mutant pRb-deficient cells displayed increased levels of p107 protein under growth conditions in comparison to the wild type cells (Fig. 7 C). In addition, mutant cells after differentiation continued to express high levels of p107 protein relative to wild type myotubes (n = 3; Fig. 7 C). However, the levels and pattern of p130 expression appeared normal (n = 3; Fig. 7 C). Therefore, pRb-deficient primary myoblasts display a

similar cell-cycle phenotype as MyoD-transfected pRb-deficient fibroblasts (Novitch et al., 1996; Novitch et al., 1999; Schneider et al., 1994).

To investigate whether pRb-deficient myoblasts were appropriately withdrawing from the cell cycle upon induction of differentiation, we performed BrdU incorporation experiments on newly differentiated cultures. Wild type cells displayed no incorporation of BrdU in cultures exposed for one hour to BrdU after 4 days of differentiation (Fig. 8 A). In contrast, ~25% of $Rb^{f/f}$:Ad-Cre myoblasts present after 4 days exposure to differentiation medium incorporated BrdU (Fig. 8 C). In addition, $Rb^{f/f}$:Ad-Cre myocytes also resumed cell division and exhibited about a 50% increase in total cell numbers after re-exposure to growth medium for 24 h (Fig. 8 D). These data are consistent with the hypothesis that Rb-deficient myoblasts display an intrinsic failure of the G1 restriction point necessary for the switch to terminal myogenic differentiation.

Primary Myoblasts from *$Rb^{f/f}$:MCK-Cre* Mice Exhibit Normal Differentiation

To investigate whether pRb is required to maintain the terminally differentiated state, primary myoblasts were derived from *$Rb^{f/f}$:MCK-Cre* mice and their growth and differentiation characteristics examined. The *MCK-Cre* transgene has been used extensively to efficiently and completely excise floxed alleles in terminally differentiated cardiac and skeletal muscle (Andrechek et al., 2002; Kim et al., 2001; Norris et al., 2003; Wang et al., 1999; Zisman et al., 2000). We verified the efficiency of *Rb* gene deletion in the *$Rb^{f/f}$:MCK-Cre* by quantitating the allele ratios by ^{32}P end-labeled PCR (100% Rb^{flox} allele present during growth vs. < 1% Rb^{flox} allele remaining by day 5 of differentiation; Fig. 9 A). In addition, Rb protein levels were undetectable by western blot analysis in all

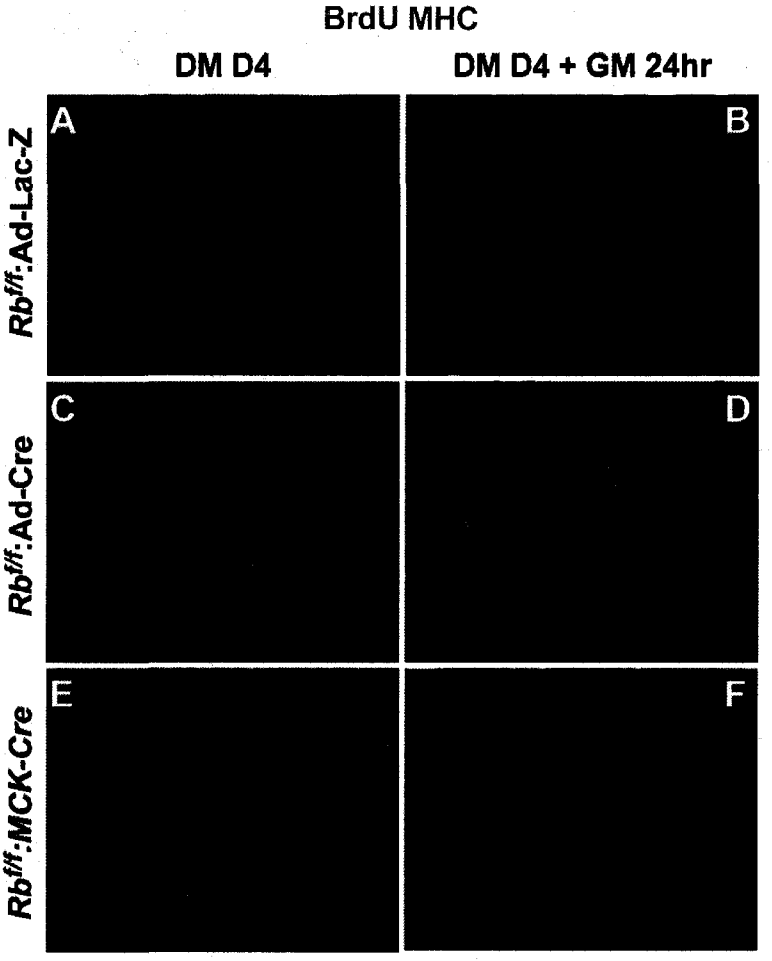

Figure 8. **Serum restimulation is unable to induce DNA synthesis in terminally differentiated Rbf/f:MCK-Cre myotubes.** Double immunoflourescent staining for BrdU (FITC) and MHC (rhodamine) in Rbf/f:Ad-Lac-Z infected (A and B), Rbf/f:Ad-Cre infected (C and D), and Rbf/f:MCK-Cre (E and F) primary myoblasts. Primary myoblasts were cultured in DM for 4 d and were either BrdU pulsed for 1 h before fixation (DM D4) or restimulated with BrdU-supplemented growth media for 24 h before fixation (DM D4+GM 24 hr).

3 isolates of *Rb$^{f/f}$:MCK-Cre* myoblasts by day 5 of differentiation (Fig. 9 B). Finally, we did not detect pRb positive nuclei in multinucleated MHC expressing *Rb$^{f/f}$:MCK-Cre* myotubes by day 5 of differentiation (Fig. 9 C).

Rb$^{f/f}$:MCK-Cre primary myoblasts were indistinguishable from wild type primary myoblasts in appearance, expression of myoblast-specific (Pax7, Myf5) and cell-cycle regulators (*cyclinA2*, *cyclinB1*, *cdk1*, *cdk2*, and *cdk4*), and growth rate of (unpublished data). Importantly, of *Rb$^{f/f}$:MCK-Cre* primary myoblasts were fully capable of differentiating into robust multinucleated MHC-expressing myotubes that were apparently normal (n = 3 independent isolates; Fig. 9 C).

The levels of pRb over four days of differentiation was examined by Western blot to determine the temporal kinetics of pRb elimination by the *MCK-Cre* transgene (n = 3; Fig. 10 B). Levels of pRb in wild type and mutant cells were similar in growth media and after 2 d in DM (Fig. 10, compare A with B). However, *MCK-Cre* mediated deletion of the *Rb$^{f/f}$* allele resulted in the complete ablation of pRb after 4 d of differentiation (Fig. 10, compare A with B). Interestingly, this late stage elimination of pRb did not result in the up regulation of p107 as observed in *Rb$^{f/f}$*:Ad-Cre cultures (compare Fig. 10 B with Fig. 7 C). Consistent with the normal differentiation of *Rb$^{f/f}$:MCK-Cre* primary myoblasts, MyoD and myogenin levels were subject to normal modulation (Fig. 10 B). Thus, functional pRb is critically involved in the cascade of regulatory events required for progression through myogenic differentiation, but pRb is not required for the maintenance of the terminally differentiated state.

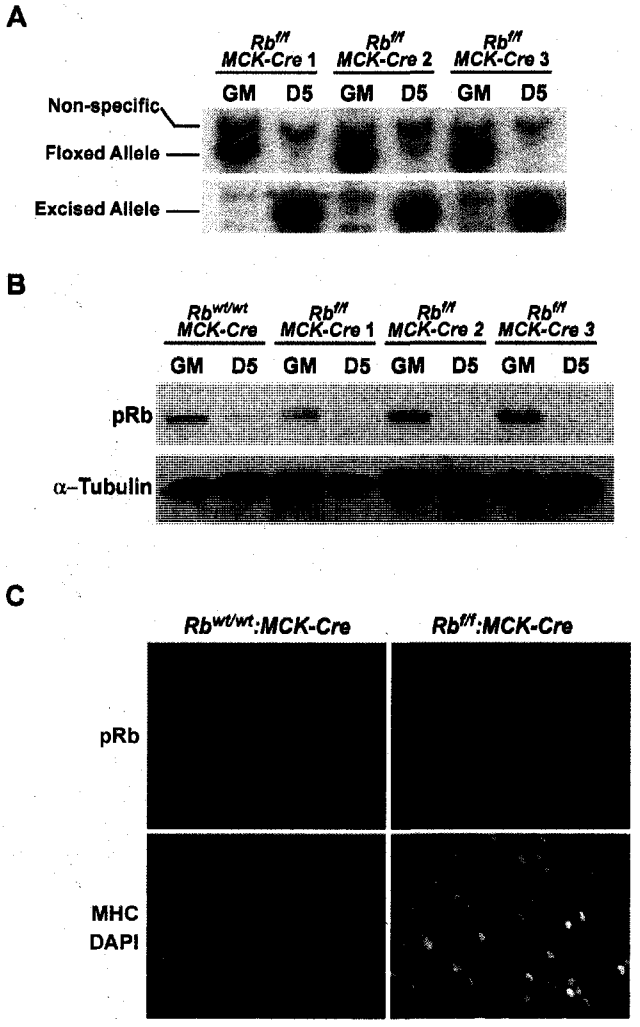

Figure 9. **MCK-Cre transgene efficiently eliminates pRb expression in Rbf/f:MCK-Cre differentiated primary myotubes.** (A) 32P end-labelled PCR genotype analysis of floxed Rb locus. Primers flanking the LoxP sites in the Rb locus were used to amplify DNA samples from Rbf/f:MCK-Cre primary myoblasts during growth (GM) and after 5 d in differentiation conditions (D5) in three independent isolates (Rbf/f:MCK-Cre 1-3). (B) Immunoblot detection of pRb from Rbwt/wt:MCK-Cre control and Rbf/f:MCK-Cre primary myoblast protein extracts. a-Tubulin protein levels were used as loading controls. Whole cell protein extract was harvested from primary myoblasts in growth media (GM) and 5 d in DM (D5). (C) Immunofluorescent staining of Rbwt/wt:MCK-Cre control and Rbf/f:MCK-Cre primary myotubes. Myotubes were PFA fixed after 5 d in DM and stained with antibody to pRb (FITC) and MHC (rhodamine), and counterstained with DAPI.

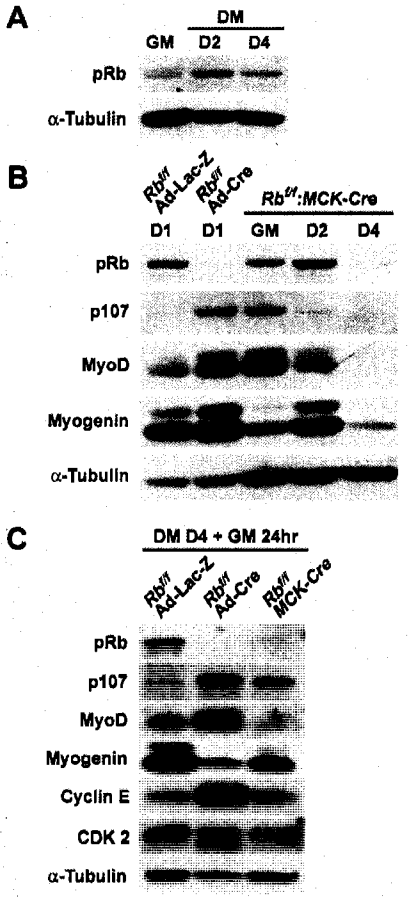

Figure 10. **Late stage removal of pRb in differentiated Rb f/f MCK-Cre myotubes does not result in the up regulation of p107, MyoD and Myogenin protein levels in low serum conditions.** (A) Immunoblot for pRb in wild-type primary myoblasts. (B) Immunoblot differentiation time course analysis of pRb, p107, MyoD, and Myogenin in Rbf/f:MCK-Cre primary myoblasts. Whole cell protein extract was harvested from Rbf/f:MCK-Cre and wild-type myoblasts at the indicated time points. (C) Immunoblot analysis of pRb, p107, MyoD, myogenin, cyclin E, and cdk2. Whole cell protein extract were harvested from Rbf/f:Ad-Lac-Z, Rbf/f:Ad-Cre, and Rbf/f:MCK-Cre after 4 d in DM followed by 24 h in GM. a-Tubulin protein levels were used as loading controls (A-C).

Serum Stimulation does not Induce DNA Synthesis in *Rb$^{f/f}$:MCK-Cre* Myotubes

The presence of pRb has been suggested to be required for inhibiting *de novo* DNA synthesis in response to mitogen restimulation in differentiated myocytes derived from *Rb$^{-/-}$* teratoma derived myocytes and MyoD-transfected fibroblasts (Novitch et al., 1996; Schneider et al., 1994). These experiments suggested that myotubes require pRb for the suppression of mitogen activated ectopic S-phases. Therefore, we investigated the effect of serum stimulation of myotubes lacking pRb that were derived from *Rb$^{f/f}$:MCK-Cre* primary myoblasts.

Primary myoblasts were cultured in DM for 4 d and either BrdU pulsed for 1 h before fixation or stimulated with growth media containing 20% FCS and supplemented with BrdU for 24 hours before fixation (Fig. 8). Our experiments revealed that stimulation of *Rb$^{f/f}$:MCK-Cre* myotubes for 24 hours with growth media did not result in any myotube nuclei entering S-phase as evidenced by an absence of BrdU incorporation (Fig. 8 F). Moreover, serum stimulation did not result in up-regulation MyoD and cyclin E proteins in *Rb$^{f/f}$:MCK-Cre* myotubes (Fig. 10 C). However, levels of p107 were reinduced in the *Rb$^{f/f}$:MCK-Cre* myotubes to approximately half the levels present in the *Rb$^{f/f}$*:Ad-Cre myocytes (Fig. 10 C). Additionally, higher levels of cyclin E protein and an activated form of Cdk2 were also present in the restimulated *Rb$^{f/f}$*:Ad-Cre myocytes but not in the *Rb$^{f/f}$*:Ad-Lac-Z and *Rb$^{f/f}$:MCK-Cre* myotubes (Fig. 10 C). These experiments therefore indicate that pRb is not required to maintain the terminally differentiated state in myotubes derived from primary myoblasts.

Discussion

We have utilized mouse genetics to demonstrate that the completion of skeletal myogenic differentiation is dependent on pRb function. The loss of pRb in myogenic precursor cells precludes their ability to properly couple cell cycle exit and the progression of differentiation following the induction of myogenin (Fig. 5-7). Importantly, pRb function was not required for maintaining the terminally differentiated state of myotubes *in vitro* (Fig. 8 and 10) or for the formation of completely differentiated skeletal muscle tissue *in vivo* (Fig. 3).

Recent studies have demonstrated that much of the developmental defects observed in the initial *Rb* knockout studies were primarily caused by a pRb-dependent extraembryonic defect in placental development (Wu et al., 2003). Functional rescue of placental defects by generation of aggregation chimeras with wild type tetraploid donor embryos results in $Rb^{-/-}$ pups that survive to birth without neuronal or erythroid phenotypes. Notably, the newborn $Rb^{-/-}$ pups exhibited ectopic S-phases and apoptosis in the lens together with extensive deficiencies in skeletal muscle differentiation (de Bruin et al., 2003). The muscle phenotype in these animals is strikingly reminiscent of the $Rb^{f/f}$*:Myf5-Cre* muscle phenotype. Importantly, our experiments provide the formal genetic proof that pRb is required in a cell autonomous manner for skeletal muscle development.

Ad-Cre infected $Rb^{f/f}$ primary myoblasts could not properly form multinucleated MHC expressing myotubes (Fig. 6). Additionally, $Rb^{f/f}$:Ad-Cre myoblasts were unable to down regulate *cyclins*, *cdks*, p107, Pax7, MyoD, and myogenin when withdrawn from serum (Fig. 7). However, upon induction of differentiation, $Rb^{f/f}$:Ad-Cre myoblasts

upregulated myogenin expression, an immediate early marker of commitment for differentiation (Bergstrom et al., 2002). Therefore we conclude that $Rb^{f/f}$:Ad-Cre myoblasts enter the differentiation program but fail to progress as evidenced by continued Pax7 expression, cell division and failure to form multinucleated myotubes.

Activation of myogenin transcription is directly mediated by MyoD binding to E-boxes located in the proximal myogenin promoter in response to differentiation inducing signals (Bergstrom et al., 2002; Gerber et al., 1997). These data are consistent with the suggestion therefore that myogenin induction occurs independently of *Rb* transcriptional induction during myogenic differentiation.

During muscle differentiation, pRb becomes hypophosphorylated and mRNA and protein levels increase about 10 fold (Corbeil et al., 1995; Martelli et al., 1994). MyoD activation during differentiation is responsible for the transcriptional activation of the *Rb* (Martelli et al., 1994). More recent studies demonstrate that MyoD activation of *Rb* transcription requires a cyclic AMP-responsive element (CRE) in the *Rb* promoter, which binds CREB protein (Magenta et al., 2003). Moreover, CREB is phosphorylated during myogenic differentiation and recruits MyoD, p300 and pCAF to the *Rb* promoter (Magenta et al., 2003). Therefore, both *Rb* and myogenin are immediate early targets of MyoD mediated transcriptional activation during the switch to myogenic differentiation. Our experiments demonstrate that pRb activity is absolutely required for MyoD-mediated cell cycle exit and completion of the differentiation program but not for activation of myogenin.

The severe myogenic differentiation defect seen in the $Rb^{f/f}$:*Myf5-Cre* mice (Figs. 1 and 2) and the $Rb^{f/f}$:Ad-Cre primary myoblasts (Figs. 5-7) was in stark contrast to the

normal phenotype observed in the *Rb$^{f/f}$:MCK-Cre* skeletal muscle in which pRb was eliminated after the completion of differentiation (Figs. 3 and 9). Furthermore, primary myoblasts isolated from *Rb$^{f/f}$:MCK-Cre* mice were also able to properly differentiate into multinucleated MHC positive myotubes. The *Rb$^{f/f}$:MCK-Cre* myotubes lacking pRb did not incorporate BrdU when restimulated with growth media for 24 hours (Fig. 8 F). However, *Rb$^{f/f}$*:Ad-Cre myocytes were fully capable of incorporating BrdU and resuming cell division upon growth media restimulation (Fig. 8 D). The persistence of activated Cdk2 (Fig. 10 C) and an abundance of its regulatory subunit cyclin E (Fig. 10 C) observed in the restimulated *Rb$^{f/f}$*:Ad-Cre myocytes, but not in the *Rb$^{f/f}$*:Ad-Lac-Z and *Rb$^{f/f}$:MCK-Cre* myotubes is indicative of the actively proliferating state of the restimulated *Rb$^{f/f}$*:Ad-Cre myocytes (Cenciarelli et al., 1999). Interestingly, serum restimulation of *Rb$^{f/f}$:MCK-Cre* myotubes results in the induction of p107 protein (Fig. 10 C). However, despite the induction of p107 in differentiated myotubes, the cell cycle continues to be checked. Up regulation of cell cycle genes has previously been reported in serum treated terminally differentiated C2C12 myotubes. Serum restimulation of C2C12 myotubes induces immediate early genes such as *c-fos*, *c-jun*, *c-myc*, and *Id-1* (Tiainen et al., 1996a). Moreover, cell cycle genes such as *cyclin D1* and *cdc2* were similarly serum induced to levels comparable to that of proliferation (Jahn et al., 1994), yet no evidence of cell cycle re-entry was ever observed. *Rb$^{f/f}$:MCK-Cre* myotubes are thereby capable of inhibiting DNA synthesis and maintaining the terminally differentiated state in the absence of pRb.

The maintenance of the terminally differentiated state is likely the effect of multiple mechanisms that may include p130-E2F-4 complexes (Corbeil et al., 1995;

Takahashi et al., 2000), cyclinD3 complexes (Cenciarelli et al., 1999), p21 activity (Jiang et al., 2000; Mal et al., 2000) and inhibition of *Cyclin D1* expression (Latella et al., 2001; Skapek et al., 1995). Notably, forced expression of E2F1 in differentiated C2C12 myotubes is insufficient to induce ectopic DNA synthesis (Tiainen et al., 1996a). However, the expression of viral oncoproteins such as E1A (Tiainen et al., 1996b) and SV40 large T antigen (Gu et al., 1993) in C2C12 myotubes can induce ectopic DNA synthesis, but they are both known to inactivate multiple checkpoint mechanisms (Helt and Galloway, 2003). Therefore, terminal differentiation is a very stable state that appears tolerant to inactivation of single pathways.

A high proportion of pRb-deficient myoblasts undergo apoptosis in response to induction of differentiation. Interestingly, attenuation of N-*ras* signaling has been suggested to rescue this apoptotic response of *Rb*-mutant myoblasts (Takahashi et al., 2003). The set of genes activated by mitogens via the Ras/MAPK pathway are very similar to the genes activated following E2F induction (Muller et al., 2001). Moreover, forced expression of E2Fs results in high rates of apoptosis (Stevaux and Dyson, 2002) and elevated rates of apoptosis in the cortex of $Rb^{-/-}$ embryos is attenuated by crossing into *E2F1* and *E2F3* mutant backgrounds (Ziebold et al., 2001). Several pro-apoptotic genes including *caspase 3* have been suggested to represent E2F target genes (Muller et al., 2001). Notably, *caspase 3* is upregulated upon myogenic differentiation and is required for normal progression of the differentiation program (Fernando et al., 2002). Therefore it is interesting to speculate that pRb may play a protective role in preventing an apoptotic response to activated caspase 3 during myogenic differentiation.

In this article we demonstrate that pRb is essential for progressing through to terminal myogenic differentiation. Several pRb dependent mechanisms have been suggested to play important roles in the regulation of myogenesis. Dominant negative N-*ras* enhances MyoD mediated expression from an MCK reporter construct in $Rb^{-/-}$ fibroblasts (Lee et al., 1999). Additionally, N-$ras^{-/-}$:$Rb^{-/-}$ compound mutant muscle appears to relatively normal suggesting N-*ras* plays a role in mediating the defect in differentiation of pRb-deficient myoblasts (Takahashi et al., 2003). Other studies have suggested that dynamic interactions between pRb, HDAC1, and MyoD play an important role (Puri et al., 2001). Alternatively, pRb inhibition of Id2 has been suggested to potentiate MyoD activity (Lasorella et al., 2000). Clearly, the weight of importance of these interactions must be reassessed under a unified context in light of our findings.

We have demonstrated that pRb is required during the early stages of differentiation in order to properly control cell cycle exit and regulate the progression of the differentiation program. However, maintenance of myogenic terminal differentiation does not require pRb. Identifying the early pRb dependent downstream regulatory network could potentially be valuable in developing highly efficient stem cell therapeutics for a broad range of myopathies. Future studies will thus address the mechanistic and the downstream targets of pRb regulation during the early stages of skeletal muscle differentiation.

Materials and Methods

Mice and Cell Culture

Mice carrying the *LoxP* targeted *Rb* allele (*Rb floxed*; provided by M. Vooijs and A. Berns, Netherlands Cancer Institute, Amsterdam, Netherlands; Marino et al., 2000) were backcrossed into the Balb/cJ and FVB strain and bred with either *Myf5-Cre* mice (provided by P. Soriano, Fred Hutchinson Cancer Research Center, Seattle, WA; Tallquist et al., 2000), or transgenic *MCK-Cre* mice (provided by R. Kahn, Joslin Diabetes Center, Boston, MA; Wang et al., 1999). Primary myoblasts were derived from lower hind limb skeletal muscle of 4-8 wk-old mice as described previously (Sabourin et al., 1999). All primary myoblast isolations were expanded and enriched to >99% purity (assessed by Desmin and MyoD staining) prior to experimental use. Primary myoblasts were differentiated in 5% horse serum in DMEM for the duration of time indicated in the figure legends. $Rb^{f/f}$*:MCK-Cre* myoblasts were differentiated for 3 days in 5% horse serum, followed by 2 days in 5% horse serum DMEM supplemented with 5mg/ml cytosine arabinoside (CA). CA was used to eliminate dividing mononuclear cells in culture. For adenoviral infections of primary myoblasts, 300,000 cells were seeded per 60 mm dish and infected with Ad-Cre or Ad-Lac-Z at an M.O.I. of 5 for 1 hour using established techniques (Parks et al., 1999). To assess the efficiency of Cre-mediated excision, genomic DNA was isolated from Ad-Cre infected myoblasts and was PCR genotyped using primers that flank the LoxP targeted *Rb* locus (Marino et al., 2000).

Single Fiber Isolation

Single fiber isolation procedure was performed on the extensor digitorum longus muscle of 8 wk-old *$Rb^{f/f}$:MCK-Cre* and *$Rb^{f/wt}$* control littermates as described previously (Rosenblatt et al., 1995). 20 fibers were lysed in DNA lysis buffer (100 mM Tris.HCl pH 8.5, 5 mM EDTA, 0.2% SDS, 200 mM NaCl, 100 μg Proteinase L/ml) and the DNA was precipitated by isopropanol and washed once in 70% ethanol. 200 fibers were lysed in protein extraction buffer (50 mM Tris.HCl, pH 7.4, 0.1% Triton X-100, 5 mM EDTA, 250 mM NaCl, 50 mM NaF) supplemented with protease inhibitors (0.1 mM Na3VO4, 1 mM PMSF, 10 μg/ml leupeptin).

^{32}P End-labelled PCR and Densitometry Analysis

Rb flox forward primer was end-labelled with ^{32}P γATP (Amersham Pharmacia) by T4 kinase (Invitrogen) in a final reaction volume of 20μl. Rb flox PCR was performed under standard conditions using 0.4μl of end-labelled primer in each 10μl PCR reaction. 20ng of DNA was used as starting template in each PCR reaction. Radiolabelled PCR products were resolved on a 7% denaturing acrylamide gel and exposed on film. Band densities were quantified by ImageJ analysis software. *Rb^{flox}:$Rb^{excised}$* allele ratios were determined by densitometry analysis and an allele ratio standard curve was constructed. Sensitivity of detection was determined by decreasing the total ratio of *Rb^{flox}* DNA to *$Rb^{excised}$* DNA in 10 fold steps.

BrdU Pulsed Cell Cycle Analysis

Exponentially growing asynchronous Ad-Cre and Ad-Lac-Z infected $Rb^{f/f}$ primary myoblasts were pulsed with BrdU for 20 minutes at a concentration of 30 μM. Myoblasts were trypsinized, pelleted and washed twice in ice cold PBS. Myoblasts were stained for BrdU incorporation and total DNA content using the BrdU Flow Kit (BD Pharmingen) as per manufacturer's instructions. Flow cytometry was performed on a Coulter FacStar.

TUNEL Assay

Ad-Cre and Ad-Lac-Z infected $Rb^{f/f}$ myoblasts were grown on collagen coated 4-well poly L-lysine chamber slides (Lab-Tek). Cells were fixed with 4% formaldehyde in PBS at the 6 hour differentiation time point. TUNEL assays were performed using ApoAlert DNA Fragmentation Kit (Clontech) according to manufacturer's instructions. TUNEL staining was analyzed and photographed on a Zeiss Axioscope equipped with a UV source and FITC, rhodamine, and hoechst detection filters.

RNase Protection and Western Analysis

Total RNA was extracted from Ad-Cre and Ad-Lac-Z $Rb^{f/f}$ primary myoblasts using the RNeasy mini-kit (Qiagen). RNase protection assay was performed using the RiboQuant kit along with the multi-probe template sets m-CYC-1 and m-CC-1 (BD Pharmingen). 2 μg of total RNA from each time point was used for the ribo-probe hybridization incubation. The RNase protection assay was completed according to manufacturer's protocols.

Primary myoblasts were harvested and lysed in RIPA extraction buffer (50 mM Tris-HCl pH 7.4, 1% nonidet P-40, 0.5% NaDeoxycholate, 0.1% Sodium-dodecyl-sulphate, 5 mM EDTA, 150 mM NaCl, 50 mM NaF) supplemented with protease inhibitors (Complete , Roche) on ice. Western blots were probed with antibodies to pRb, 1:1000 (41302, BD Pharmingen); p107, 1:500 (c-18, Santa-Cruz); p130, 1:2000 (ab6545-100, Ab-Cam); Pax7 1:10 (Developmental Studies Hybridoma Bank [DSHB]); Myogenin 1:10 (F5D, DSHB); MyoD 1:1000 (c-20, Santa-Cruz); Myosin Heavy Chain (MHC)1:10 (MF-20, DSHB); Cyclin E 1:1000 (06-459, Upstate); Cdk2 1:1000 (M2, Santa-Cruz); α-Tubulin 1:3500 (T 9026, Sigma). Secondary detection was performed with horseradish peroxidase (HRP) conjugated antibodies (BioRad). Membrane bound immune complexes were visualized by ECL Plus kit (Amersham).

Immuno-staining

Tissue samples were fixed in 4% para-formaldehyde (PFA) at 4°C overnight. Samples were washed in PBS for 30 minutes and processed for paraffin embedding. Sections were dewaxed in 2 washes of Citri-Solv for 5 minutes each and rehydrated in graded alcohol washes. Antigen retrieval was performed by immersing sections in boiling citrate buffer (0.21% w/v citric acid monohydrate in dH_2O) for 10 minutes while continuously agitating. Slides were allowed to cool down to room temperature and transferred into PBS. Sections were stained with antibodies to Desmin 1:200 (clone D33, DAKO) and MHC 1:10 (MF-20, DSHB) using the Fluorescent M.O.M. kit (Vector).

Primary myoblasts were grown on collagen coated 4-well poly L-lysine chamber slides (Lab-Tek). Cells were fixed with 2% PFA and permeabilized with 0.2% Triton-X.

Cells were stained with antibodies for MyoD 1:200 (M-318, Santa-Cruz), MHC 1:10 (MF-20, DSHB), Myogenin 1:10 (F5D, DSHB), and pRb 1:250 (41302, BD Pharmingen). Secondary detection was performed with flourescein conjugated or rhodamine conjugated antibodies (Chemicon). Cells were counterstained with DAPI and mounted in aqueous fluorescent mounting media (DAKO). Bright field, phase, and fluorescent images were viewed using an Axioplan2 (Zeiss) fluorescent microscope and digitally acquired (Axiocam, Zeiss; Axiovision 3.1, Zeiss) at room temperature. Image processing software (Photoshop 7, Adobe) was used to overlay images and to enhance colour and clarity. Images were viewed through (40x/0.75; 20x/0.5; 5x/0.12) Zeiss air objective lenses.

DNA Synthesis Assay

Primary myoblasts were grown on collagen coated 4-well poly L-lysine chamber slides (Lab-Tek). Cells were induced to differentiate in differentiation media for 4 days. Prior to fixation, cells were pulsed with 30 μM BrdU for 1 hour or restimulated in growth media supplemented with 30 μM BrdU for 24 hours. Fixed cells were processed for BrdU staining using the BrdU in situ staining kit (BD Pharmingen) according to manufacturer's protocols. The final HRP-streptavidin incubation was omitted and replaced with fluoroscein conjugated streptavidin 1:200 (Vector). Cells were washed twice in PBS and double stained using rabbit anti-myosin skeletal muscle 1:500 (M7523, Sigma). Anti-rabbit rhodamine conjugated secondary was used to detect the myosin antibody.

Acknowledgements

The authors would like to thank Drs. Marc Vooijs and Anton Berns for providing the $Rb^{f/f}$ mice, Dr. Philippe Soriano for providing *Myf5-Cre* mice, and Dr. Ronald Kahn for providing *MCK-Cre* mice, Dr. Sophie Charge for help isolating single fibers, and Karl Parato for flow cytometry. M.A.R. holds the Canada Research Chair in Molecular Genetics and is a Howard Hughes Medical Institute International Scholar. This work was supported by grants to M.A.R. from the Canadian Institutes of Health Research (36538), the National Institutes for Health (RO1AR44031), and the Canada Research Chair Program.

Cited Literature

Andrechek, E.R., W.R. Hardy, A.A. Girgis-Gabardo, R.L. Perry, R. Butler, F.L. Graham, R.C. Kahn, M.A. Rudnicki, and W.J. Muller. 2002. ErbB2 is required for muscle spindle and myoblast cell survival. *Mol Cell Biol.* 22:4714-22.

Anton, M., and F.L. Graham. 1995. Site-specific recombination mediated by an adenovirus vector expressing the Cre recombinase protein: a molecular switch for control of gene expression. *J Virol.* 69:4600-6.

Bergstrom, D.A., B.H. Penn, A. Strand, R.L. Perry, M.A. Rudnicki, and S.J. Tapscott. 2002. Promoter-specific regulation of MyoD binding and signal transduction cooperate to pattern gene expression. *Mol Cell.* 9:587-600.

Cenciarelli, C., F. De Santa, P.L. Puri, E. Mattei, L. Ricci, F. Bucci, A. Felsani, and M. Caruso. 1999. Critical role played by cyclin D3 in the MyoD-mediated arrest of cell cycle during myoblast differentiation. *Mol Cell Biol.* 19:5203-17.

Classon, M., S. Salama, C. Gorka, R. Mulloy, P. Braun, and E. Harlow. 2000. Combinatorial roles for pRB, p107, and p130 in E2F-mediated cell cycle control. *Proc Natl Acad Sci U S A.* 97:10820-5.

Corbeil, H.B., P. Whyte, and P.E. Branton. 1995. Characterization of transcription factor E2F complexes during muscle and neuronal differentiation. *Oncogene.* 11:909-20.

de Bruin, A., L. Wu, H.I. Saavedra, P. Wilson, Y. Yang, T.J. Rosol, M. Weinstein, M.L. Robinson, and G. Leone. 2003. Rb function in extraembryonic lineages suppresses apoptosis in the CNS of Rb-deficient mice. *Proc Natl Acad Sci U S A.* 100:6546-51.

Fernando, P., J.F. Kelly, K. Balazsi, R.S. Slack, and L.A. Megeney. 2002. Caspase 3 activity is required for skeletal muscle differentiation. *Proc Natl Acad Sci U S A.* 99:11025-30.

Gerber, A.N., T.R. Klesert, D.A. Bergstrom, and S.J. Tapscott. 1997. Two domains of MyoD mediate transcriptional activation of genes in repressive chromatin: a mechanism for lineage determination in myogenesis. *Genes Dev.* 11:436-50.

Gu, W., J.W. Schneider, G. Condorelli, S. Kaushal, V. Mahdavi, and B. Nadal-Ginard. 1993. Interaction of myogenic factors and the retinoblastoma protein mediates muscle cell commitment and differentiation. *Cell.* 72:309-24.

Helt, A.M., and D.A. Galloway. 2003. Mechanisms by which DNA tumor virus oncoproteins target the Rb family of pocket proteins. *Carcinogenesis.* 24:159-69.

Herrera, R.E., V.P. Sah, B.O. Williams, T.P. Makela, R.A. Weinberg, and T. Jacks. 1996. Altered cell cycle kinetics, gene expression, and G1 restriction point regulation in Rb-deficient fibroblasts. *Mol Cell Biol.* 16:2402-7.

Ho, A.T., Q.H. Li, R. Hakem, T.W. Mak, and E. Zacksenhaus. 2004. Coupling of caspase-9 to Apaf1 in response to loss of pRb or cytotoxic drugs is cell-type-specific. *Embo J.*

Jahn, L., J. Sadoshima, and S. Izumo. 1994. Cyclins and cyclin-dependent kinases are differentially regulated during terminal differentiation of C2C12 muscle cells. *Exp Cell Res.* 212:297-307.

Jiang, Z., P. Liang, R. Leng, Z. Guo, Y. Liu, X. Liu, S. Bubnic, A. Keating, D. Murray, P. Goss, and E. Zacksenhaus. 2000. E2F1 and p53 are dispensable, whereas

p21(Waf1/Cip1) cooperates with Rb to restrict endoreduplication and apoptosis during skeletal myogenesis. *Dev Biol.* 227:8-41.

Kim, J.K., A. Zisman, J.J. Fillmore, O.D. Peroni, K. Kotani, P. Perret, H. Zong, J. Dong, C.R. Kahn, B.B. Kahn, and G.I. Shulman. 2001. Glucose toxicity and the development of diabetes in mice with muscle-specific inactivation of GLUT4. *J Clin Invest.* 108:153-60.

Lasorella, A., M. Noseda, M. Beyna, Y. Yokota, and A. Iavarone. 2000. Id2 is a retinoblastoma protein target and mediates signalling by Myc oncoproteins. *Nature.* 407:592-8.

Latella, L., A. Sacco, D. Pajalunga, M. Tiainen, D. Macera, M. D'Angelo, A. Felici, A. Sacchi, and M. Crescenzi. 2001. Reconstitution of cyclin D1-associated kinase activity drives terminally differentiated cells into the cell cycle. *Mol Cell Biol.* 21:5631-43.

Lee, K.Y., M.H. Ladha, C. McMahon, and M.E. Ewen. 1999. The retinoblastoma protein is linked to the activation of Ras. *Mol Cell Biol.* 19:7724-32.

Magenta, A., C. Cenciarelli, F. De Santa, P. Fuschi, F. Martelli, M. Caruso, and A. Felsani. 2003. MyoD stimulates RB promoter activity via the CREB/p300 nuclear transduction pathway. *Mol Cell Biol.* 23:2893-906.

Mal, A., D. Chattopadhyay, M.K. Ghosh, R.Y. Poon, T. Hunter, and M.L. Harter. 2000. p21 and retinoblastoma protein control the absence of DNA replication in terminally differentiated muscle cells. *J Cell Biol.* 149:281-92.

Marino, S., M. Vooijs, H. van Der Gulden, J. Jonkers, and A. Berns. 2000. Induction of medulloblastomas in p53-null mutant mice by somatic inactivation of Rb in the external granular layer cells of the cerebellum. *Genes Dev.* 14:994-1004.

Martelli, F., C. Cenciarelli, G. Santarelli, B. Polikar, A. Felsani, and M. Caruso. 1994. MyoD induces retinoblastoma gene expression during myogenic differentiation. *Oncogene*. 9:3579-90.

Muller, H., A.P. Bracken, R. Vernell, M.C. Moroni, F. Christians, E. Grassilli, E. Prosperini, E. Vigo, J.D. Oliner, and K. Helin. 2001. E2Fs regulate the expression of genes involved in differentiation, development, proliferation, and apoptosis. *Genes Dev*. 15:267-85.

Norris, A.W., L. Chen, S.J. Fisher, I. Szanto, M. Ristow, A.C. Jozsi, M.F. Hirshman, E.D. Rosen, L.J. Goodyear, F.J. Gonzalez, B.M. Spiegelman, and C.R. Kahn. 2003. Muscle-specific PPARgamma-deficient mice develop increased adiposity and insulin resistance but respond to thiazolidinediones. *J Clin Invest*. 112:608-18.

Novitch, B.G., G.J. Mulligan, T. Jacks, and A.B. Lassar. 1996. Skeletal muscle cells lacking the retinoblastoma protein display defects in muscle gene expression and accumulate in S and G2 phases of the cell cycle. *J Cell Biol*. 135:441-56.

Novitch, B.G., D.B. Spicer, P.S. Kim, W.L. Cheung, and A.B. Lassar. 1999. pRb is required for MEF2-dependent gene expression as well as cell-cycle arrest during skeletal muscle differentiation. *Curr Biol*. 9:449-59.

Parker, M.H., P. Seale, and M.A. Rudnicki. 2003. Looking back to the embryo: defining transcriptional networks in adult myogenesis. *Nat Rev Genet*. 4:497-507.

Parks, R.J., J.L. Bramson, Y. Wan, C.L. Addison, and F.L. Graham. 1999. Effects of stuffer DNA on transgene expression from helper-dependent adenovirus vectors. *J Virol.* 73:8027-34.

Perry, R.L., and M.A. Rudnick. 2000. Molecular mechanisms regulating myogenic determination and differentiation. *Front Biosci.* 5:D750-67.

Peschiaroli, A., R. Figliola, L. Coltella, A. Strom, A. Valentini, I. D'Agnano, and R. Maione. 2002. MyoD induces apoptosis in the absence of RB function through a p21(WAF1)-dependent re-localization of cyclin/cdk complexes to the nucleus. *Oncogene.* 21:8114-27.

Puri, P.L., S. Iezzi, P. Stiegler, T.T. Chen, R.L. Schiltz, G.E. Muscat, A. Giordano, L. Kedes, J.Y. Wang, and V. Sartorelli. 2001. Class I histone deacetylases sequentially interact with MyoD and pRb during skeletal myogenesis. *Mol Cell.* 8:885-97.

Puri, P.L., and V. Sartorelli. 2000. Regulation of muscle regulatory factors by DNA-binding, interacting proteins, and post-transcriptional modifications. *J Cell Physiol.* 185:155-73.

Rosenblatt, J.D., A.I. Lunt, D.J. Parry, and T.A. Partridge. 1995. Culturing satellite cells from living single muscle fiber explants. *In Vitro Cell Dev Biol Anim.* 31:773-9.

Sabourin, L.A., A. Girgis-Gabardo, P. Seale, A. Asakura, and M.A. Rudnicki. 1999. Reduced differentiation potential of primary MyoD-/- myogenic cells derived from adult skeletal muscle. *J Cell Biol.* 144:631-43.

Schneider, J.W., W. Gu, L. Zhu, V. Mahdavi, and B. Nadal-Ginard. 1994. Reversal of terminal differentiation mediated by p107 in Rb-/- muscle cells. *Science*. 264:1467-71.

Seale, P., L.A. Sabourin, A. Girgis-Gabardo, A. Mansouri, P. Gruss, and M.A. Rudnicki. 2000. Pax7 is required for the specification of myogenic satellite cells. *Cell*. 102:777-86.

Skapek, S.X., J. Rhee, D.B. Spicer, and A.B. Lassar. 1995. Inhibition of myogenic differentiation in proliferating myoblasts by cyclin D1-dependent kinase. *Science*. 267:1022-4.

Stevaux, O., and N.J. Dyson. 2002. A revised picture of the E2F transcriptional network and RB function. *Curr Opin Cell Biol*. 14:684-91.

Takahashi, C., R.T. Bronson, M. Socolovsky, B. Contreras, K.Y. Lee, T. Jacks, M. Noda, R. Kucherlapati, and M.E. Ewen. 2003. Rb and N-ras function together to control differentiation in the mouse. *Mol Cell Biol*. 23:5256-68.

Takahashi, Y., J.B. Rayman, and B.D. Dynlacht. 2000. Analysis of promoter binding by the E2F and pRB families in vivo: distinct E2F proteins mediate activation and repression. *Genes Dev*. 14:804-16.

Tallquist, M.D., K.E. Weismann, M. Hellstrom, and P. Soriano. 2000. Early myotome specification regulates PDGFA expression and axial skeleton development. *Development*. 127:5059-70.

Tiainen, M., D. Pajalunga, F. Ferrantelli, S. Soddu, G. Salvatori, A. Sacchi, and M. Crescenzi. 1996a. Terminally differentiated skeletal myotubes are not confined to

G0 but can enter G1 upon growth factor stimulation. *Cell Growth Differ.* 7:1039-50.

Tiainen, M., D. Spitkovsky, P. Jansen-Durr, A. Sacchi, and M. Crescenzi. 1996b. Expression of E1A in terminally differentiated muscle cells reactivates the cell cycle and suppresses tissue-specific genes by separable mechanisms. *Mol Cell Biol.* 16:5302-12.

Walsh, K., and H. Perlman. 1997. Cell cycle exit upon myogenic differentiation. *Curr Opin Genet Dev.* 7:597-602.

Wang, J., H. Wilhelmsson, C. Graff, H. Li, A. Oldfors, P. Rustin, J.C. Bruning, C.R. Kahn, D.A. Clayton, G.S. Barsh, P. Thoren, and N.G. Larsson. 1999. Dilated cardiomyopathy and atrioventricular conduction blocks induced by heart-specific inactivation of mitochondrial DNA gene expression. *Nat Genet.* 21:133-7.

Wu, L., A. de Bruin, H.I. Saavedra, M. Starovic, A. Trimboli, Y. Yang, J. Opavska, P. Wilson, J.C. Thompson, M.C. Ostrowski, T.J. Rosol, L.A. Woollett, M. Weinstein, J.C. Cross, M.L. Robinson, and G. Leone. 2003. Extra-embryonic function of Rb is essential for embryonic development and viability. *Nature.* 421:942-7.

Yee, A.S., H.H. Shih, and S.G. Tevosian. 1998. New perspectives on retinoblastoma family functions in differentiation. *Front Biosci.* 3:D532-47.

Zacksenhaus, E., Z. Jiang, D. Chung, J.D. Marth, R.A. Phillips, and B.L. Gallie. 1996. pRb controls proliferation, differentiation, and death of skeletal muscle cells and other lineages during embryogenesis. *Genes Dev.* 10:3051-64.

Zhang, J.M., Q. Wei, X. Zhao, and B.M. Paterson. 1999a. Coupling of the cell cycle and myogenesis through the cyclin D1-dependent interaction of MyoD with cdk4. *Embo J.* 18:926-33.

Zhang, J.M., X. Zhao, Q. Wei, and B.M. Paterson. 1999b. Direct inhibition of G(1) cdk kinase activity by MyoD promotes myoblast cell cycle withdrawal and terminal differentiation. *Embo J.* 18:6983-93.

Ziebold, U., T. Reza, A. Caron, and J.A. Lees. 2001. E2F3 contributes both to the inappropriate proliferation and to the apoptosis arising in Rb mutant embryos. *Genes Dev.* 15:386-91.

Zisman, A., O.D. Peroni, E.D. Abel, M.D. Michael, F. Mauvais-Jarvis, B.B. Lowell, J.F. Wojtaszewski, M.F. Hirshman, A. Virkamaki, L.J. Goodyear, C.R. Kahn, and B.B. Kahn. 2000. Targeted disruption of the glucose transporter 4 selectively in muscle causes insulin resistance and glucose intolerance. *Nat Med.* 6:924-8.

Chapter 3

Rb Dependent Repression and Activation of Opposing Transcriptional Networks in Skeletal Muscle Differentiation

Purpose

To globally survey Rb dependent transcriptional networks in primary myoblasts and myotubes by expression array and chromatin immunoprecipitation location analysis.

Contribution of Co-Authors

Michael Huh did all of the experimental work and MAPPFinder analysis on the microarray data.

Jeff Ishibashi analyzed the raw microarray data with MicroArray Suite 5.0 and provided database and spreadsheet support.

Chris Porter provided scripts for the ChIP-RDA location analysis.

Rb Dependent Repression and Activation of Opposing Transcriptional Networks in Skeletal Muscle Differentiation

Michael S. Huh[1,2], Jeff Ishibashi[1,2], Chris Porter[1],
and Michael A. Rudnicki[1,2,3]

1. Ottawa Health Research Institute
   Molecular Medicine Program
   501 Smyth Road,
   Ottawa, Ontario
   Canada, K1H 8L6
   Tel: 613-739-6740
   Fax: 613-737-8803

2. University of Ottawa
   Cellular and Molecular Medicine
   Ottawa, Ontario
   Canada

3. Correspondence should be addressed to M.A.R.
   E-mail: mrudnicki@ohri.ca

Running Title: Rb directly represses transcription of *Myf5*

Key words: Rb, Myf5, MyoD, ChIP-RDA, Differentiation, Opposing Networks

Summary

Myogenic differentiation entails permanent cell cycle arrest along with the faithful regulation of differentiation specific genes by MyoD and Rb. Global expression analysis of differentiated primary myotubes revealed two opposing sets of transcriptional regulatory networks that were deregulated in the absence of Rb. Loss of Rb function resulted in the de-repression of numerous genes involved in cell cycle regulation. Quite strikingly, expression of genes encoding contractile proteins and glycolytic enzymes were coordinately down-regulated. A combination of chromatin IP and representational difference analysis (ChIP-RDA) was used to identify Rb binding sites in differentiated myotubes. We identified a number of putative Rb target genes that included *Myf5* and *E2F7*. Real-time PCR analysis of Rb ChIPs confirmed Rb complex binding within the *Myf5* 5' UTR region. Therefore, Rb's direct repression of *Myf5* is required for cell cycle withdrawal and the induction of myogenic differentiation.

Introduction

Skeletal muscle differentiation requires the induction of myogenic transcriptional regulatory pathways. The basic helix-loop-helix (bHLH) family of myogenic transcription factors are recognized as the master regulators of skeletal muscle specification and differentiation (Pownall et al. 2002; Berkes et al. 2004). The mechanisms of bHLH mediated transcriptional activity are tightly coupled to the cell cycle machinery, hence disruptions in key cell cycle regulatory components frequently result in skeletal muscle defects (Walsh 1997; De Falco and De Luca 2006).

The myogenic bHLH transcription factors MyoD and Myf5 respond to the periodic fluctuations of cell cycle factors in that the stability of both MyoD and Myf5 proteins are directly modulated by cell cycle dependent phosphorylation events (Kitzmann et al. 1998; Lindon et al. 1998; Kitzmann et al. 1999; Lindon et al. 2000; Tintignac et al. 2000; Doucet et al. 2005). MyoD activation potently activates transcriptional targets required for differentiation and cell cycle arrest, such as the myogenic transcription factor *myogenin*, the cdk inhibitor *p21*, cyclin *D3* and *Rb* (Halevy et al. 1995; Kiess et al. 1995; Bergstrom et al. 2002; de la Serna et al. 2005). Furthermore, activated MyoD in association with CREB/p300 directly targets the promoter of *Rb* to induce transcription (Magenta et al. 2003).

Retinoblastoma (Rb) and its family members p107 and p130 regulate the G1/S cell cycle transition (Dannenberg et al. 2000; Sage et al. 2000), and are modulated by the cyclical associations with cyclin dependent kinase (cdk) complexes. Studies in mouse models have given us some general insight into the functional importance of Rb in skeletal muscle development (Zacksenhaus et al. 1996; Jiang et al. 2000; Lasorella et al.

2000; Mal et al. 2000; de Bruin et al. 2003; Takahashi et al. 2003; Huh et al. 2004). We have previously described Rb as critical for the progression of the myogenic differentiation program in primary myoblasts. This progression is defined initially from the point of cell cycle withdrawal, to the induction of the differentiation program and concludes with terminal differentiation. Elimination of Rb in myogenic precursor cells prior to differentiation causes a severe deficiency in muscle differentiation (Huh et al. 2004), indeed histological examination of Rb deficient residual muscle fibers reveals large amounts apoptotic nuclei and ectopic DNA synthesis (Zacksenhaus et al. 1996). Interestingly, concurrent ablation of *Rb* and *N-ras* rescues the defect in skeletal muscle differentiation (Takahashi et al. 2003). Identifying the direct targets of Rb would therefore provide valuable insight into its role in cellular differentiation, and provide a molecular basis for understanding the functional consequences of Rb loss.

Based on the current state of knowledge, Rb is hypothesized to be an important regulator of cell cycle and muscle specific transcriptional networks. This notion however, has yet to be physically and comprehensively validated. Location analysis studies have been an effective means to identify direct targets of a protein complex, indeed such a method has been used to identify Rb binding targets in synchronized human Raji cells (Wells et al. 2003). The study by Wells et al. identified target sites that were bound by Rb at G0/G1 and S phase of the cell cycle. However, due to the fact that Raji cells are a human lymphoma cell line, these results must be interpreted within reasonable context. There are also technical limitations to some location analysis techniques. Specifically, use of CpG arrays or promoter arrays for the identification of enriched binding targets is highly biased based on limited assumptions on promoter

regions. In order to circumvent these problems, we have devised a dual pronged approach combining the use of expression microarrays and ChIP location analysis. Through the use of our novel ChIP representational difference analysis (ChIP-RDA) technique, we identified genomic binding targets of Rb in an unbiased manner.

This report exploits the availability of current technologies to understand Rb directed transcriptional regulation in myogenic differentiation. Comparison of global expression profiles between Rb deficient myoblast and myotubes revealed a dramatic contrast in expression deregulation. Gene expression in proliferating Rb deficient myoblasts were minimally perturbed. In stark contrast, *MCK-Cre* driven *Rb* deleted differentiated myotubes had increased levels of transcripts involved in cell cycle and DNA metabolism. Moreover, expression levels of genes encoding contractile proteins and glycolytic enzymes were coordinately downregulated. The expression data was subsequently re-examined in conjunction with the physical binding data from our ChIP-RDA experiment. Most significantly, the identification of *Myf5* and *E2F7* as Rb targets physically validates Rb's function in a myogenic context. We therefore have demonstrated an effective means to comprehend and deconstruct specifics of a complex transcriptional network.

Results

Loss of Functional Rb Deregulates Global Gene Expression in Terminally Differentiated Myotubes

We set out to test the notion that Rb would regulate a distinct subset of target genes in proliferating and differentiated primary myotubes. To this end, we utilized homozygous *Rb-LoxP* primary myoblasts infected with Cre recombinase expressing adenovirus (Mb^{Rb-}) and differentiated *Rb-LoxP* myoblast lines harboring the *MCK-Cre* transgene (Mt^{Rb-}) (Huh et al. 2004). Total RNA was harvested in biological triplicates of Mb^{Rb-}, Mt^{Rb-}, wildtype myoblasts (Mb^{wt}), and wildtype myotubes (Mt^{wt}). All together, 12 independent RNA samples were processed and hybridized onto the Mouse Expression Set 430 (MOE430) Affymetrix microarray.

Changes in gene expression due to the functional loss of Rb were determined by comparing the normalized intensity ratio of Mb^{Rb-}/Mb^{wt} and Mt^{Rb-}/Mt^{wt} of each probeset (entire dataset available in stembase). A list of deregulated genes was generated for Mb^{Rb-} and Mt^{Rb-} by selecting for probes that changed at least 2-fold with significant signal values. Under this selection criterion, the number of probesets identified in Mb^{Rb-} amounted to only 37 (13 increased and 24 decreased). In comparison, 1146 probesets were deregulated in Mt^{Rb-} (638 increased and 508 decreased) (Figure 1). Among the deregulated probesets in Mb^{Rb-} and Mt^{Rb-}, only 5 probesets (4 genes) were common between both (*Cd24a*, *Actn3*, *Mypn*, and *Slc8a3*). *Actn3*, *Mypn*, and *Slc8a3* were down regulated in both Mb^{Rb-} and Mt^{Rb-} while *Cd24a* was down regulated in Mb^{Rb-} but highly up regulated in Mt^{Rb-}. Our initial intention was to determine the extent of overlap in

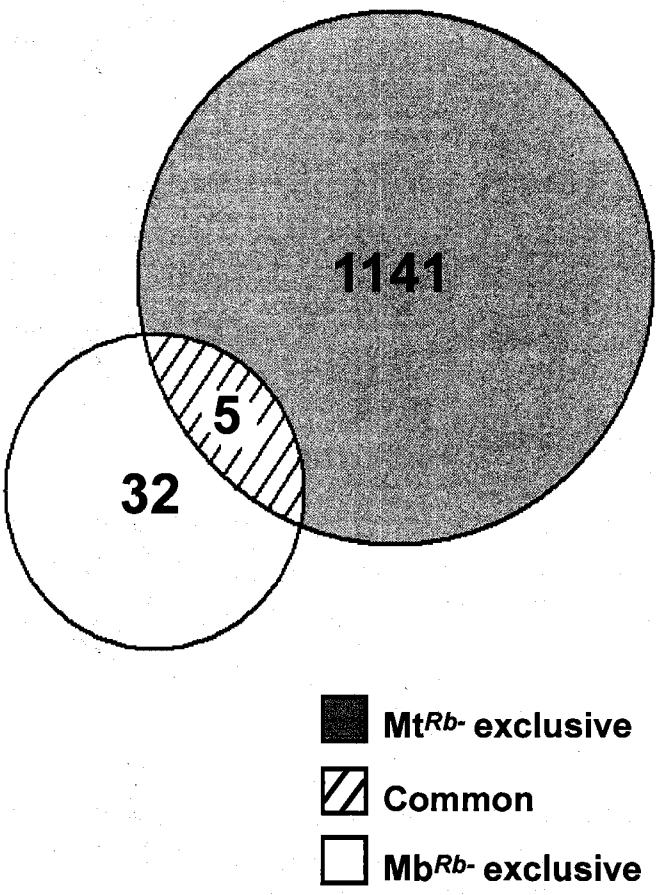

Figure 1. **Gene expression changes in Rbf/f:Ad-Cre myoblasts (MbRb-) are distinct and fewer than the changes observed in Rbf/f:MCK-Cre myotubes (MtRb-) by Affymetrix microarray analysis.** Venn diagram of genes that are 2 fold up and down regulated in MbRb- (white and hatched areas) and MtRb- (grey and hatched areas). The hatched area represents 2 fold deregulated genes identified in both MbRb- and MtRb-.

deregulated genes between Mb^{Rb-} and Mt^{Rb-}. However, the extremely small number of changed genes in Mb^{Rb-} confounded such a comparison. In summary, the loss of Rb function minimally affects gene expression patterns in proliferating myoblasts, but has a profoundly greater impact in terminally differentiated myotubes.

Rb is Required for the Repression and Activation of Distinct Classes of Genes in Terminally Differentiated Myotubes

The expression data generated by our experimental approach produced an inherently complex output due to the cascading effects of functional Rb loss. As a result, it was an infeasible pursuit to determine direct targets of Rb solely from the microarray data. With this is mind; we chose to further analyze our list of deregulated genes in Mb^{Rb-} and Mt^{Rb-} in a collective manner. We performed a statistical based Gene Ontology (GO) grouping of the deregulated list of genes identified from our microarray experiments by MAPPFinder (Doniger et al. 2003). MAPPFinder analysis of the Mb^{Rb-} dataset produced a ranked list of GO categories based on permuted *p*-values. The 3 highest ranked GO categories generated by MAPPFinder for genes that were at least 2-fold deregulated were: insulin-like growth factor binding (2 genes out of 21 genes measured in category), development (10 genes out of 1539 genes measured in category), and extra-cellular region (12 genes out of 2288 genes measured in category) (Table1). The GO categories of development and extra-cellular region each encompass many nested GO categories, thus explaining the large numbers of genes in both. GO family classification of the Mb^{Rb-} dataset is limited due to the low number of genes meeting the

Table 1. MAPPFinder Ranked GO Categories for MbRb-

Gene Ontology Category	Changed/Total	Z Score	*p*-value
insulin-like growth factor binding	2 of 21	9.764	0
development	10 of 1539	4.359	0
extracellular region	12 of 2288	3.992	0
sarcomere	2 of 36	7.352	0.002
transcription factor activity	5 of 564	3.845	0.005
regulation of smoothened signaling pathway	1 of 3	13.098	0.007
FAD binding	1 of 8	7.945	0.024

List of genes in GO category shown in **Table S1.**

significant expression cutoff. Therefore, we chose to focus our resources to the analysis of the Mt^{Rb-} system.

MAPPFinder analysis of the Mt^{Rb-} dataset generated a complete list of statistically ranked GO categories. From this list, a selection of the most significant nonsynonymous GO categories was chosen for further examination (Table 2). The top 3 ranked GO category associations for genes with at least a 2-fold change in Mt^{Rb-} were: cyclin-dependent protein kinase activity (5 genes out of 5 genes measured in category), sarcomere (14 genes out of 36 measured in category), and muscle development (27 out of 120 genes measured in category). The deregulated genes that fell within the top 3 GO categories for Mt^{Rb-} were remarkably coherent based on the Westfall-Young adjustment for multiple testing (adjusted $p = 0$ for cyclin-dependent kinase activity, sarcomere, and muscle development). Furthermore, we observed a striking consistency with respects to the activation or repression of the genes within individual GO categories. Most notably the GO categories of: cyclin-dependent protein kinase activity (4 of 5; 80% of genes upregulated), sarcomere (13 of 14; 93% of genes downregulated), muscle development (22 of 27; 81% of genes downregulated), DNA metabolism (28 of 34; 82% of genes upregulated), glycolysis (6 of 7; 86% of genes downregulated), and cell cycle (24 of 31; 77% of genes upregulated) (Table S2). Taken together, we have demonstrated that Rb is required for the proper regulation of both skeletal muscle and cell cycle specific transcriptional networks in terminally differentiated myotubes. Moreover, MAPPFinder analysis revealed a significant bias for either co-activation or co-repression of the deregulated genes in individual GO categories.

Table 2. MAPPFinder Ranked GO Categories for MtRb-

Gene Ontology Category	Changed/Total	Z Score	*p*-value
cyclin-dependent protein kinase activity*	5 of 5	12.029	0
sarcomere*	14 of 36	11.884	0
muscle development*	27 of 120	11.732	0
actin binding	22 of 172	6.942	0
phosphotransferases	4 of 10	6.453	0
DNA metabolism	34 of 404	5.766	0
glycolysis	7 of 45	5.28	0
cell cycle	31 of 445	4.33	0
positive regulation of apoptosis	11 of 106	4.047	0.001

* Adjusted permute $p = 0$

List of genes in GO category shown in **Table S2.**

Identifying Physical Binding Targets of the Rb Complex in Differentiated Myotubes

In order to identify direct transcriptional targets of Rb we combined the techniques of chromatin immunoprecipitation (ChIP) and representational difference analysis (RDA) (Figure S1), whereby the RDA allows for the subtraction of non-specific or background chromatin from the ChIP. This results in a higher relative enrichment of ChIPed targets. Furthermore, identification of ChIP targets are not restricted to specific regions of the genome, as is the case with promoter arrays. Through the use of the ChIP-RDA approach, we identified potential Rb target genes in differentiated myotubes. Amplified Mt^{wt} ChIP and Mt^{Rb-} ChIP were used as the Tester and Driver respectively for the RDA protocol, and the difference products were cloned, sequenced, and BLATed to identify their positions on the genome. In total, more than 100 independent mouse genomic fragments were identified with at least 60% identity (hits), from which 226 candidate genes fell within 50kb of a ChIP-RDA hit sequence.

Rb Complexes Preferentially Bind Within Genes

ChIP-RDA candidate genes included transcription factors, receptors, metabolic proteins, cell cycle proteins, DNA synthesis and damage response proteins. For each of the 226 candidate genes, we associated the corresponding expression data from the Mt^{Rb-} microarray (Table S3). Using this compiled dataset, we analyzed specific relationships in the data. In particular, we enumerated the frequency of ChIP-RDA target gene pairings within 50 kb. We considered 11 separate distance classes (0kb; 0 to ±10kb; ±10 to ±20kb; ±20 to ±30kb; ±30 to ±40kb; ±40 to ±50kb) (Figure 2A). In total, 582 ChIP-RDA target gene pairings were placed in their respective distance categories and their

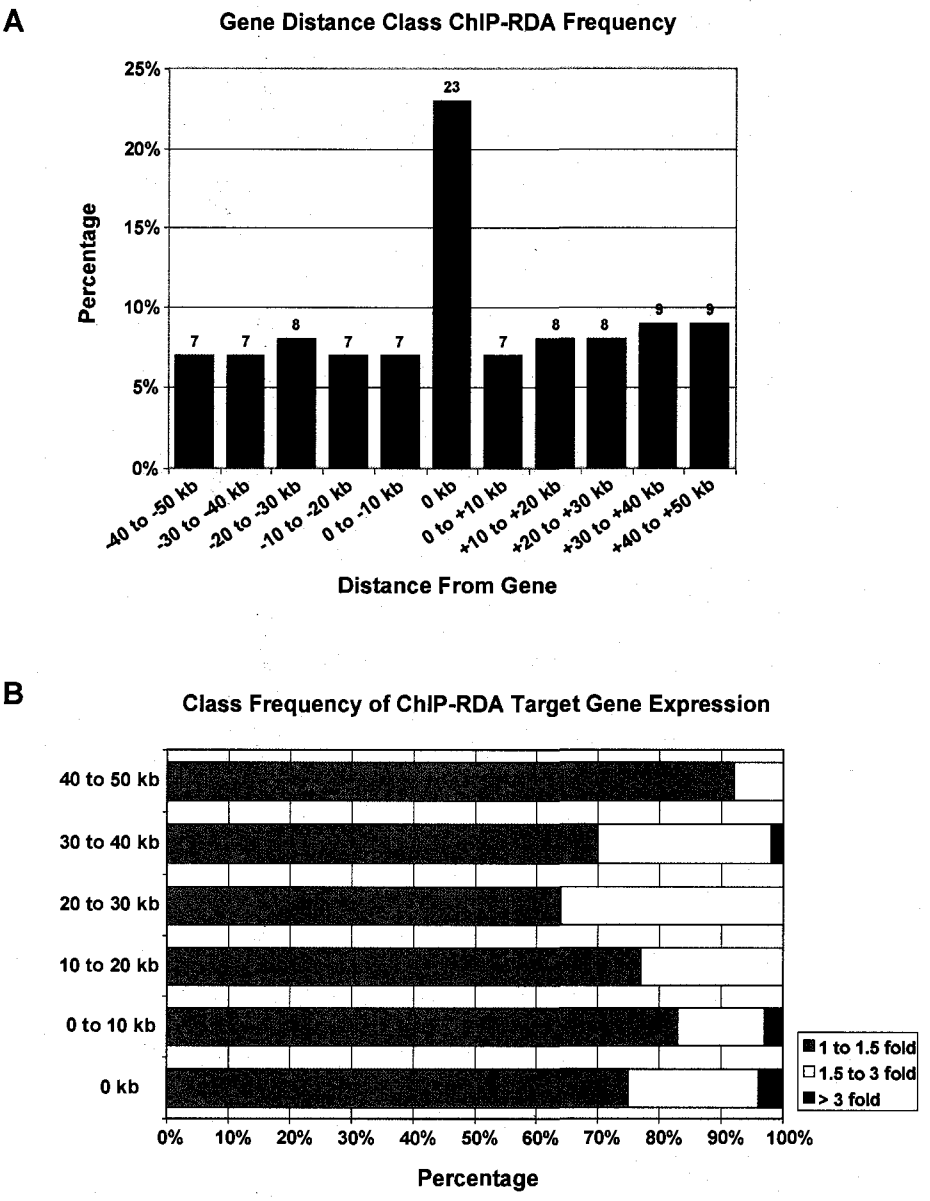

Figure 2. **Rb binds preferentially within genes.** (A) Frequency of target gene pairings within 50 kb of putative Rb binding sites. Each bar represents the percentage of total hits found within the designated region. 0kb bar represents percentage of hits within genes. (B) Fold change profile of target genes within 50 kb of putative Rb binding sites. Fold change profiles are illustrated as the percentage of genes within 3 classes [1 to 1.5 fold (grey); 1.5 to 3 fold (white); >3 fold (black)] in each distance category.

frequencies per class was calculated as a percentage. We discovered that approximately a quarter of all the ChIP-RDA sequences identified resided within a transcribed gene locus. However, with the exception of the 0kb class, it appears that Rb complexes on average bind to the other distance classes with a relative constant frequency (~8% per distance class).

We expanded our analysis by combining the physical binding data generated from the ChIP-RDA procedure with the microarray expression data. Our intention was to determine if gene expression change was related to the proximity of Rb complex binding to its target gene. For every distance class, we calculated the proportion of genes that changed expression levels (low, 1 to 1.5 fold; medium, 1.5 to 3 fold; high, > 3 fold) (Figure 2B). Our analysis revealed that the majority of the candidate genes had minimal gene expression changes (~70% < 1.5 fold change). With the exception of the 40 to 50 kb distance class, the proportion of gene expression changes ranging in the medium to high class (> 1.5 fold change) was between ~20 to ~30%. It was only in the furthest distance class of 40 to 50kb where we observed a reduced effect on gene expression change (8% > 1.5 fold change). Taken together, Rb complexes have a higher affinity for binding within genes. Furthermore, Rb complexes appear to be able to exert effects on target gene transcription from as far away as 40kb.

Rb Complexes Directly Regulate the Transcription of *Myf5* and *E2F7*

In order to prioritize the complete list of candidate Rb target genes, we utilized the following criteria (candidates with ≥ 2 hits and > 1.3 fold expression change). This filtering process reduced the candidate list to 12 genes (9 genes upregulated and 3 genes

downregulated) (Table 3). Among these candidates were genes encoding metabolic enzymes (*Nat2* and *Tkt*), signal transducers (*Ptpns1* and *Gngt1*), transcription factors (*Myf5*, *MRF4*, and *E2F7*) and nuclear membrane protein (*Tor1aip1*).

To ensure the validity of the Affymetrix expression data, we reverse transcribed the original RNA samples used in the microarray experiments for quantitative SYBR Green real-time PCR analysis. Specific primers were designed for our transcripts of interest (*Myf5*, *MRF4*, *E2F7*, *Rab4a*, *Rai2*, *Slc2a*, *Mip*, and *Timeless*) (Figure 3A). These primers were designed to span introns whenever possible and specificity of the PCR products were confirmed by denaturing curve analysis and direct product sequencing. Additionally, primers for *Eif4g1* and *Eif4e* transcripts were designed similarly and used for mRNA normalization. Real-time PCR analysis reiterated the fold change estimated by microarray analysis with the exception of *E2F7* and *Mip* (Figure 3B). *E2F7* was expressed at a much higher level in Mt^{Rb-} as determined by real-time PCR (compare 234 fold increase by real-time to 4.74 fold by microarray). While *Mip* expression was actually upregulated, opposite to that of the microarray data (compare 2.7 fold increase by real-time to –1.3 fold decrease by microarray). This illustrates the limitation of microarrays when there are either large or modest changes between two samples. We were also intrigued by the location of the hits in relation to the gene locus. More specifically, more than half of the ChIP-RDA targets found within genes occurred within 10 kb of the 5' or 3' end. Indeed, our findings support the notion that Rb complexes do not exclusively bind the proximal 5' region of genes.

Hypophosphorylated Rb predominantly binds to members of the E2F family of transcription factors, thus providing the means to specifically target and regulate the

Table 3. ChIP-RDA Identified Rb Target Candidate Genes

GeneSymbol	GeneID	GeneTitle	Hits	Min Dist	Max Dist	Fold Change
Myf5*	17877	myogenic factor 5	6	0	0	8.38
MRF4*	17878	myogenic regulatory factor 4	6	6827	6827	-8.77
Nat2	17961	N-acetyltransferase 2 (arylamine N-acetyltransferase)	3	0	0	2.06
E2f7*	52679	E2F transcription factor 7	2	0	0	4.74
Dpysl2	12934	dihydropyrimidinase-like 2	2	0	43040	2.70
Ptpns1	19261	protein tyrosine phosphatase, non-receptor type substrate 1	2	36485	36485	2.03
MGI:1929890	64164	interferon alpha responsive gene	2	0	0	1.60
Tkt	21881	transketolase	2	35799	35907	1.59
Tor1aip1	208263	torsin A interacting protein 1	2	30481	30484	1.40
Plekhb2	226971	pleckstrin homology domain containing, family B (evectins) member 2	2	0	19324	1.37
Gngt1	14699	guanine nucleotide binding protein (G protein)	2	24396	24396	-1.32
Ndufa10	67273	NADH dehydrogenase (ubiquinone) 1 alpha subcomplex 10	2	27230	27240	-1.58

Hits represent frequency of independent ChIP-RDA clones sequenced.
Min Dist and **Max Dist** calculated from the most proximal terminus of transcribed gene locus.
* Candidate genes identified with less than 60% total sequence match, but greater than 100bp consecutive sequence identity
Complete list of ChIP-RDA candidate genes provided in **Table S3.**

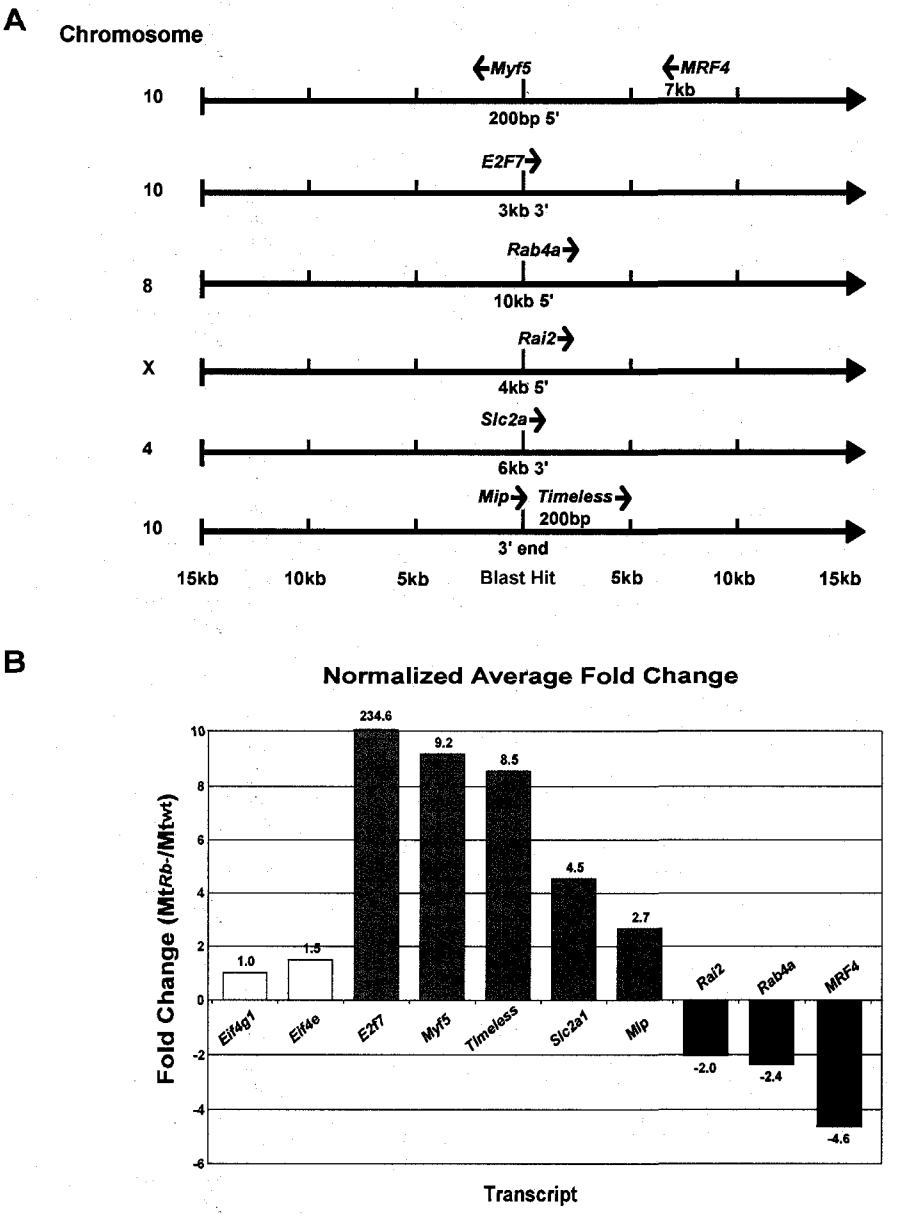

Figure 3. **E2F7 and Myf5 expression is derepressed with the loss of functional Rb in differentiated myotubes.** (A) Illustration of candidate Rb target genes and the physical location of the corresponding ChIP-RDA hit. (B) SYBR Green real-time PCR quantification of candidate Rb target gene transcripts. Fold change of target transcripts in MtRb- were calculated from the ?Ct values in relation to the respective wildtype myotube transcript levels. Ct values were normalized to the transcript levels of Eif4G1.

transcription of genes. Therefore we posited that Rb-E2F complexes were directly responsible for the repression of *Myf5* and *E2F7* in terminally differentiated myotubes. To test this hypothesis, ChIPs were performed using antibodies for Rb, p107, and E2F4 on proliferating and differentiated C2C12 myoblasts. We specifically examined E2F4 due to its prominence over its family members in terminally differentiated myotubes (Corbeil et al. 1995). E2F4 was therefore a prime candidate as the DNA binding partner of Rb at our putative target loci. Primers specific for the *E2F7* and *Myf5* ChIP-RDA target loci were designed for interrogating these regions for relative enrichment by ChIP. Additionally, *cdc2* proximal promoter was used as a known high affinity binding region for anti-p107 and anti-E2F4 ChIPs (Takahashi et al. 2000). Relative fold enrichment of our genomic targets of interest was measured using SYBR Green real-time PCR. Chromatin IPs using anti-p107 and anti-E2F4 produced an enrichment of the proximal *cdc2* promoter in proliferating myoblasts as expected (9 fold and 12 fold enrichment respectively relative to anti-Rb ChIP) (Figure 4). Furthermore, the *cdc2* promoter was highly enriched by anti-E2F4 ChIP in relation to anti-p107 ChIP (26 fold relative enrichment) (Figure 5). Comparatively, anti-Rb ChIP at the E2F7 locus resulted in a lower relative enrichment in both proliferation and differentiation (~2 fold enrichment and ~1.5 fold enrichment respectively) (Figures 4 & 5).

Interestingly, a differential pattern of enrichment spanning the Myf5 target region was observed between proliferation and differentiation. In proliferating myoblasts, anti-Rb ChIP on average was enriched compared to anti-E2F4 ChIP, but similar to anti-p107 ChIP (Figure 4). In contrast, a much different binding profile was observed in terminally differentiated myotubes. Anti-Rb ChIP at the *Myf5* hit locus produced a 3-fold

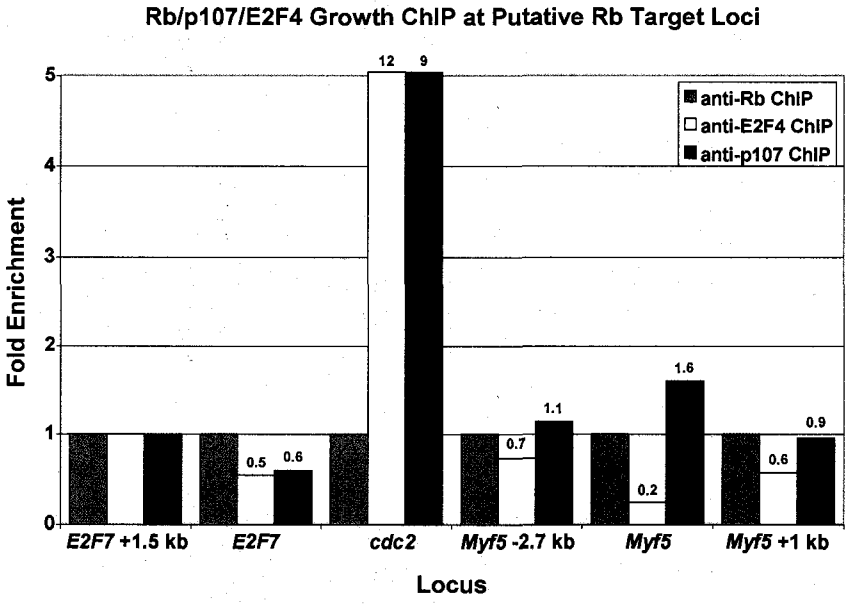

Figure 4. **E2F7 target locus is bound by Rb complex in proliferating myoblasts.** SYBR Green real-time quantification measuring fold enrichment of anti-E2F4 and anti-p107 ChIPs relative to anti-Rb ChIP. Ct values for the detection of specific loci were normalized to Ct values obtained at E2F7 +1.5 kb locus primers. The E2F7 +1.5 kb locus is not preferentially enriched by anti-Rb, anti-E2F4, and anti-p107 ChIPs. Normalized Ct values for ChIPs were subsequently calculated for relative fold enrichment.

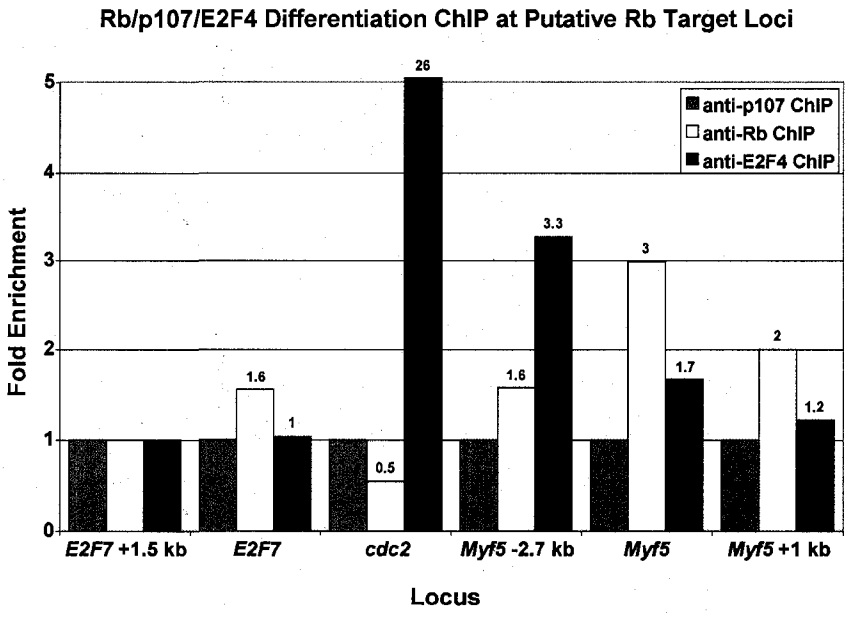

Figure 5. **Myf5 target region is bound by Rb and E2F4 complexes in differentiated myotubes.** SYBR Green real-time quantification measuring fold enrichment of anti-Rb and anti-pE2F4 ChIPs relative to anti-p107 ChIP. Ct values for the detection of specific loci were normalized to Ct values obtained at E2F7 +1.5 kb locus primers. The E2F7 +1.5 kb locus is not preferentially enriched by anti-Rb, anti-E2F4, and anti-p107 ChIPs. Normalized Ct values for ChIPs were subsequently calculated for relative fold enrichment.

enrichment in relation to anti-p107 ChIP. ChIP enrichment by anti-Rb diminished further upstream and downstream of the ChIP-RDA target locus (*Myf5* –2.7 kb, 1.5 fold enrichment and *Myf5* +1 kb, 2 fold enrichment). Intriguingly, anti-E2F4 ChIP also enriched for the region spanning the *Myf5* target locus. However, the highest relative enrichment by anti-E2F4 ChIP was observed in the upstream *Myf5* –2.7 kb locus (~3 fold enrichment). With the *Myf5* hit locus found at a lower level (~1.5 fold enrichment relative to anti-p107 ChIP).

In summary, functional Rb is required for faithful regulation of differentiation, metabolic, and cell cycle specific genes in terminally differentiated myotubes. We have demonstrated that this is possible through an Rb dependent direct regulation of myogenic and cell cycle transcription factors.

Discussion

Through the combination of global expression and genomic location analysis, we have identified a list of putative Rb complex targets in a terminally differentiated myogenic system (Table S3). Most importantly, our data for the first time elucidates an Rb dependent transcriptional repression of *Myf5* and *E2F7* in this context. Knowledge of these targets evolves our current understanding of Rb dependent regulation of myogenesis.

Collectively, the retinoblastoma family of Rb, p107, and p130 are critical regulators of the G1/S transition of the cell cycle. Mounting evidence now supports the notion that Rb plays a critical role in the process of permanent cell cycle withdrawal. Specifically, Rb is essential in establishing cellular senescence and terminal differentiation (Narita et al. 2003). Based on these observations, the relatively sparse number of deregulated genes found by microarray analysis in Mb^{Rb-} cells supports this model (Figure 1). Even with a lower expression cutoff (1.5 fold change), the numbers of deregulated probesets were still relatively low (27 probesets upregulated and 77 probesets downregulated). The subtle gene deregulation observed in Mb^{Rb-} may be a direct correlate to the lack of Rb complex targets in proliferating myoblasts. Given this scenario, Rb does not directly regulate the progression of the cell cycle. However, it must be noted that Wells et al. have successfully identified Rb target sites in synchronized Raji cells (Wells et al. 2003). Therefore, it is plausible that different cell types can account for the discrepancies reported in the literature.

Microarray analysis of Mt^{Rb-} in contrast produced a much higher number of deregulated probesets (Figure 1). The scope and magnitude of gene deregulation in Mt^{Rb-}

provides overwhelming evidence for the importance of Rb mediated transcriptional regulation in terminally differentiated myotubes. We further characterized the nature of the deregulated genes by grouping them, based on a stringent statistical protocol, into functional GO categories by MAPPFinder (Table 2). From this analysis, a striking functional separation emerged from the deregulated collective of genes identified in Mt^{Rb-}. The majority of the genes identified by MAPPFinder analysis were defined either as a component of the cell cycle and DNA synthesis machinery or structural and metabolic components of differentiated muscle. Hence, these GO categories represent two distinct and opposing cellular states. Rb's profound effects on two seemingly opposing set of gene regulatory networks may be a function of its ability to repress and activate transcription (Figure 6). The classical model of Rb dependent transcriptional regulation involves the interaction with E2F family of transcription factors. In this model, Rb's interaction with E2Fs is believed to repress transcription via two separate mechanisms. The binding of Rb can both directly inhibit E2F transcriptional activity and recruit repressive histone modifiers and ATPase dependent chromatin remodeling enzymes to E2F target promoters. Assuming this model, we would predict that loss of Rb function would result in the activation of E2F target genes. Indeed, this appears to be the case as we observe a coordinated activation of genes associated with the progression of the cell cycle (Table S2). Therefore the cell cycle phenotype suggests an E2F mediated repressive model of Rb. In addition to the activation of cell cycle associated genes, we also observed a significant repression of muscle structural proteins and glycolytic enzymes. This was an unanticipated effect in Mt^{Rb-} primarily due to their overtly stable phenotype (Huh et al. 2004). The depression of such genes may be an indirect effect of

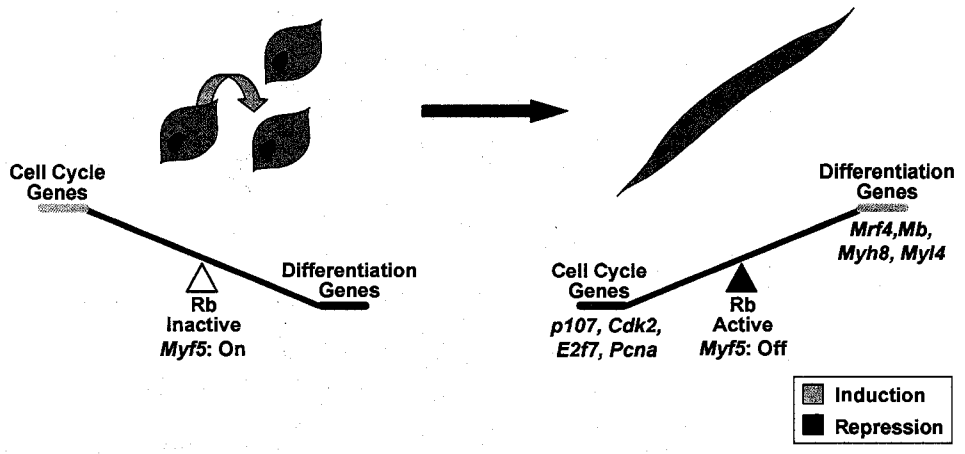

Figure 6. **Rb dependent transcriptional regulatory model in proliferating myoblasts and differentiated myotubes.**

the activation of cell cycle genes, however there is evidence in the literature that describe the transcriptional activation potential of Rb (Novitch et al. 1999; Thomas et al. 2001). Indeed, MEF2C dependent muscle gene induction and CBFA1 osteogenic gene induction both require functional Rb. Taken together, our data would suggest that Rb does have a positive role in regulating the physiology of skeletal muscle fibers. Perhaps in upkeeping skeletal muscle homeostasis by regulating the turnover of contractile proteins and glycolytic enzymes.

ChIP based location analysis techniques have been particularly effective in identifying new and functional targets of numerous DNA binding complexes. In this report, we have introduced a novel variation into the ChIP based location analysis by combining representation difference analysis (ChIP-RDA). Our ChIP-RDA based approach was applied to specifically identify functional Rb complex targets in a terminally differentiated myogenic system. This method resulted in the identification of ChIPed targets in an unbiased manner (Table S3). Similar to the studies that have utilized high density tiled arrays (Cawley et al. 2004; Carroll et al. 2005), modified SAGE (Impey et al. 2004), and paired-end ditag methods (Wei et al. 2006). Whilst this particular study was not able to attain a saturation point in target identification due to technical limitations, our ChIP-RDA dataset provided sufficient information for some general observations. In particular, studies such as ours are challenging the simplistic classical paradigm of transcription factor binding. This is the notion that transcriptional regulatory complexes bind predominantly in the proximal 5' region of genes. Our data seems to suggest that outside of the transcribed region of a gene, there is an equal frequency of Rb binding its' targets up to 50 kb on either terminus of a gene locus

(Figure 2A). A similar distribution of p53 binding sites has also been described (Cawley et al. 2004; Wei et al. 2006). If there is no distance based bias for transcription factor binding, one would predict that target proximity would not be relevant in altering gene expression. Indeed, this is largely what we observe in our data (Figure 2B). The percentage of genes that are deregulated (> 1.5 fold change) in the absence of Rb function is approximately 30% on average, up to 40kb away. In light of these findings, the concept of a typical promoter must include a broader physical distance upstream and even possibly downstream of a transcribed locus.

The diversity of putative target genes is congruous with the notion that Rb is an effector of a diverse palette of cell biological processes (Table S3). Additionally, it is conceivable that Rb's global effects are mediated by a minimal set of direct targets. Targets such as transcription factors can adequately facilitate this hypothesis. An individual transcription factor in essence represents a functional gene regulatory network (Blais et al. 2005). Among the most intriguing of our putative Rb targets were the genes *Myf5* and *E2F7*. The increased transcriptional activity of *E2F7* and *Myf5* in Mt^{Rb-} suggested that Rb complexes were normally repressive at these genes (Figure 3B). Due to the predominance of E2F4 in differentiated myotubes (Corbeil et al. 1995), we chose E2F4 as a potential Rb binding candidate at our target loci. Anti-E2F4 ChIPs did not appear to be co-enriched with anti-Rb ChIP at the *E2F7* target locus in growth and differentiation (Figure 4 & 5). However, the relatively low level of enrichment by the anti-Rb ChIP at the *E2F7* locus precludes a confident assessment on the nature of interactions. Binding of Rb complex to the *Myf5* target locus achieved a 3-fold enrichment relative to the anti-p107 ChIP (Figure 5). Due to the diminishing of the ChIP

enrichment on either side of the ChIP-RDA target locus, we inferred that the optimal binding region is within the 5' UTR of *Myf5*. Interestingly, the highest level of enrichment produced by the anti-E2F4 ChIP was the 2.7 kb region upstream of the *Myf5* target locus. Assuming that Rb and E2F4 are either in complex together or are in mutually independent complexes, we offer the following explanations. If Rb-E2F4 complexes are present, then their optimal target would most likely be downstream of the 2.7 kb region. However, Rb and E2F4 complexes may be mutually exclusive thus explaining our current results. Resolution of these two possibilities would require finer enrichment mapping of this region. Despite the ambiguity of Rb's DNA binding cofactor, our central observation stands as a significant advancement in knowledge of myogenic differentiation.

MyoD and Myf5 activity is closely coupled to components of the cell cycle machinery. Although MyoD protein is present in significant amounts in proliferating myoblasts, it is inactive until the initiation of differentiation (Skapek et al. 1995). MyoD's arrest of the cell cycle is potentiated through the direct induction of p21, cyclin D3, and Rb (Martelli et al. 1994; Halevy et al. 1995; Cenciarelli et al. 1999). MyoD's direct induction of Rb marks a significant event in causing cell cycle arrest (Magenta et al. 2003), and our findings implicate Rb as the key mediator in MyoD induced repression of *Myf5* transcription during differentiation. Rb's primary role may thus be one of promoting cell cycle arrest and induction of differentiation through repression of targets such as *Myf5*. Ultimately, the repression of *Myf5* may provide a more permissive state in which to progress the differentiation program.

Herein our studies present novel mechanistic insight into an Rb dependent repression of *Myf5* during skeletal muscle differentiation. Importantly, our findings delineate a sequential and functional cascade of myogenic transcriptional regulation.

Materials and Methods

Cell Culture

Primary myoblasts were derived from mice carrying the *LoxP*-targeted *Rb* allele and *MCK-Cre* transgenic mice (Huh et al. 2004). Myoblasts were isolated from the lower hind limb skeletal muscle of 4-8 weeks old mice. Primary myoblasts were maintained in culture and differentiated as previously described (Sabourin et al. 1999). Adenoviral infections of primary myoblasts were carried out as described previously (Huh et al. 2004). Efficiency of Cre-mediated excision were verified by PCR primers flanking the *LoxP* targeted Rb locus (Marino et al. 2000).

C2C12 myoblast cell line was obtained from the ATCC. C2C12s were maintained in 10% FBS DME under sub-confluent conditions and differentiated in 2% HS DME.

RNA Isolation

$6x10^6$ cells were harvested from proliferating primary myoblasts and day 6 differentiated primary myotubes using RNeasy Mini-Kit (QIAGEN) as per manufacturer's instructions. Total RNA samples were ethanol precipitated and resuspended to a concentration of 2 μg/ul for subsequent microarray analysis.

Affymetrix Analysis

Biological triplicate RNA samples were sent to the Ottawa Genome Centre for hybridization to the MOE430 GeneChips (Affymetrix, Inc.). The MOE430 contains over

45,000 probesets representing more than 34,000 known mouse genes. Manufacturer's quality controls were verified by the Centre. Raw data files were processed using MicroArray Suite 5.0 (Affymetrix, Inc.), according to the parameters previously described (Ishibashi et al. 2005). The processed data was then imported into GenMAPP 2.1 (Gladstone Institutes, UCSF). MAPPFinder analysis was performed on the microarray data to identify deregulated biological processes in Mb^{Rb-} and Mt^{Rb-} primary cultures. Expression deregulation was defined by the following criteria: Mb^{Rb-}/Mb^{wt} and Mt^{Rb-}/Mt^{wt} ratios of probeset signal intensities achieved an absolute value of greater than 2 fold change, > 7 pair-wise concordance, and presence of significant signal intensities. Genes within supplementary tables were subsequently inspected and appended manually.

ChIP-RDA

Chromatin Immunoprecipitations (ChIP) were performed using the ChIP Assay Kit according to the manufacturer's directions (Upstate Biotechnology). Formaldehyde crosslinked protein-chromatin suspension were immunoprecipitated with a specific antibody to Rb (C-15X; Santa Cruz Biotechnology, Inc.). Each ChIP preparation utilized $7x10^7$ primary cells and 36 μg of antibody. The immunoprecipitated chromatin samples were representationally amplified using the GenomePlex Whole Genome Amplification (WGA) Kit according to the manufacturer's instructions (WGA1; Sigma). The WGA amplified samples were subsequently subjected to representational difference analysis (RDA) as previously described (Seale et al. 2004). The Tester:Driver subtractive hybridization ratio used to produce sequentially enriched difference products (DP1-3) were: (DP1, 1:50; DP2, 1:100; DP3, 1:200). DP3 was cloned into pBluescript and

transformed into One Shot OmniMAX 2 T1 Phage-Resistant Cells (C8540-03, Invitrogen). Positive clones were picked and sequenced at the Ottawa Genome Centre.

SYBR Green Real-Time PCR Quantification of Transcripts

1 μg of each RNA sample was reverse transcribed using the RNA PCR Core Kit (Perkin Elmer) as per manufacturer's instructions. Reverse transcribed reactions were diluted 3 fold in water and used as the working template solution. Each real-time PCR reaction contained the following components: 2 μl of reverse transcribed template, 10 μl of 2X iQ SYBR Green Supermix (BioRad Laboratories), 30 nM ROX reference dye (Stratagene), and 200 nM of forward and reverse primers. Real-time PCR C_t values were calculated with the MX4000 software by using moving window averaging and adaptive baseline.

SYBR Green Real-Time PCR Quantification of ChIPs

In total, $9x10^6$ C2C12 cells were crosslinked in 1% formaldehyde and harvested during growth and 6 days into differentiation. Sonicated growth and differentiation protein-chromatin suspensions were equally divided into 3 samples. 3 independent ChIPs were performed for both growth and differentiation samples using 8 μg of the following antibodies: Rb (C-15X; Santa Cruz Biotechnology, Inc.), p107 (C-18X; Santa Cruz Biotechnology, Inc.), and E2F4 (A-20; Santa Cruz Biotechnology, Inc.). Reverse crosslinked ChIPs were purified by phenol/chloroform extractions and ethanol precipitated. Relative enrichment of target loci by ChIPs were determined by SYBR Green real-time PCR analysis.

Acknowledgements

The authors would like to thank Drs. Marc Vooijs and Anton Berns for providing the *Rb flox* mice, Dr. Ronald Kahn for providing *MCK-Cre* mice, and Dr. Iain McKinnell for helpful suggestions and critical reading of the manuscript. M.A.R. holds the Canada Research Chair in Molecular Genetics and is a Howard Hughes Medical Institute International Scholar. This work was supported by grants to M.A.R. from the Canadian Institutes of Health Research, the National Institutes for Health, and the Canada Research Chair Program.

Literature Cited

Bergstrom, D.A., Penn, B.H., Strand, A., Perry, R.L., Rudnicki, M.A., and Tapscott, S.J. 2002. Promoter-specific regulation of MyoD binding and signal transduction cooperate to pattern gene expression. *Mol Cell* **9**(3): 587-600.

Berkes, C.A., Bergstrom, D.A., Penn, B.H., Seaver, K.J., Knoepfler, P.S., and Tapscott, S.J. 2004. Pbx marks genes for activation by MyoD indicating a role for a homeodomain protein in establishing myogenic potential. *Mol Cell* **14**(4): 465-477.

Blais, A., Tsikitis, M., Acosta-Alvear, D., Sharan, R., Kluger, Y., and Dynlacht, B.D. 2005. An initial blueprint for myogenic differentiation. *Genes Dev* **19**(5): 553-569.

Carroll, J.S., Liu, X.S., Brodsky, A.S., Li, W., Meyer, C.A., Szary, A.J., Eeckhoute, J., Shao, W., Hestermann, E.V., Geistlinger, T.R., Fox, E.A., Silver, P.A., and Brown, M. 2005. Chromosome-wide mapping of estrogen receptor binding reveals long-range regulation requiring the forkhead protein FoxA1. *Cell* **122**(1): 33-43.

Cawley, S., Bekiranov, S., Ng, H.H., Kapranov, P., Sekinger, E.A., Kampa, D., Piccolboni, A., Sementchenko, V., Cheng, J., Williams, A.J., Wheeler, R., Wong, B., Drenkow, J., Yamanaka, M., Patel, S., Brubaker, S., Tammana, H., Helt, G., Struhl, K., and Gingeras, T.R. 2004. Unbiased mapping of transcription factor binding sites along human chromosomes 21 and 22 points to widespread regulation of noncoding RNAs. *Cell* **116**(4): 499-509.

Cenciarelli, C., De Santa, F., Puri, P.L., Mattei, E., Ricci, L., Bucci, F., Felsani, A., and Caruso, M. 1999. Critical role played by cyclin D3 in the MyoD-mediated arrest of cell cycle during myoblast differentiation. *Mol Cell Biol* **19**(7): 5203-5217.

Corbeil, H.B., Whyte, P., and Branton, P.E. 1995. Characterization of transcription factor E2F complexes during muscle and neuronal differentiation. *Oncogene* **11**(5): 909-920.

Dannenberg, J.H., van Rossum, A., Schuijff, L., and te Riele, H. 2000. Ablation of the retinoblastoma gene family deregulates G(1) control causing immortalization and increased cell turnover under growth-restricting conditions. *Genes Dev* **14**(23): 3051-3064.

de Bruin, A., Wu, L., Saavedra, H.I., Wilson, P., Yang, Y., Rosol, T.J., Weinstein, M., Robinson, M.L., and Leone, G. 2003. Rb function in extraembryonic lineages suppresses apoptosis in the CNS of Rb-deficient mice. *Proc Natl Acad Sci U S A* **100**(11): 6546-6551.

De Falco, M. and De Luca, A. 2006. Involvement of cdks and cyclins in muscle differentiation. *Eur J Histochem* **50**(1): 19-23.

de la Serna, I.L., Ohkawa, Y., Berkes, C.A., Bergstrom, D.A., Dacwag, C.S., Tapscott, S.J., and Imbalzano, A.N. 2005. MyoD targets chromatin remodeling complexes to the myogenin locus prior to forming a stable DNA-bound complex. *Mol Cell Biol* **25**(10): 3997-4009.

Doniger, S.W., Salomonis, N., Dahlquist, K.D., Vranizan, K., Lawlor, S.C., and Conklin, B.R. 2003. MAPPFinder: using Gene Ontology and GenMAPP to create a global gene-expression profile from microarray data. *Genome Biol* **4**(1): R7.

Doucet, C., Gutierrez, G.J., Lindon, C., Lorca, T., Lledo, G., Pinset, C., and Coux, O. 2005. Multiple phosphorylation events control mitotic degradation of the muscle transcription factor Myf5. *BMC Biochem* **6**: 27.

Halevy, O., Novitch, B.G., Spicer, D.B., Skapek, S.X., Rhee, J., Hannon, G.J., Beach, D., and Lassar, A.B. 1995. Correlation of terminal cell cycle arrest of skeletal muscle with induction of p21 by MyoD. *Science* **267**(5200): 1018-1021.

Huh, M.S., Parker, M.H., Scime, A., Parks, R., and Rudnicki, M.A. 2004. Rb is required for progression through myogenic differentiation but not maintenance of terminal differentiation. *J Cell Biol* **166**(6): 865-876.

Impey, S., McCorkle, S.R., Cha-Molstad, H., Dwyer, J.M., Yochum, G.S., Boss, J.M., McWeeney, S., Dunn, J.J., Mandel, G., and Goodman, R.H. 2004. Defining the CREB regulon: a genome-wide analysis of transcription factor regulatory regions. *Cell* **119**(7): 1041-1054.

Ishibashi, J., Perry, R.L., Asakura, A., and Rudnicki, M.A. 2005. MyoD induces myogenic differentiation through cooperation of its NH2- and COOH-terminal regions. *J Cell Biol* **171**(3): 471-482.

Jiang, Z., Liang, P., Leng, R., Guo, Z., Liu, Y., Liu, X., Bubnic, S., Keating, A., Murray, D., Goss, P., and Zacksenhaus, E. 2000. E2F1 and p53 are dispensable, whereas p21(Waf1/Cip1) cooperates with Rb to restrict endoreduplication and apoptosis during skeletal myogenesis. *Dev Biol* **227**(1): 8-41.

Kiess, M., Gill, R.M., and Hamel, P.A. 1995. Expression of the positive regulator of cell cycle progression, cyclin D3, is induced during differentiation of myoblasts into quiescent myotubes. *Oncogene* **10**(1): 159-166.

Kitzmann, M., Carnac, G., Vandromme, M., Primig, M., Lamb, N.J., and Fernandez, A. 1998. The muscle regulatory factors MyoD and myf-5 undergo distinct cell cycle-specific expression in muscle cells. *J Cell Biol* **142**(6): 1447-1459.

Kitzmann, M., Vandromme, M., Schaeffer, V., Carnac, G., Labbe, J.C., Lamb, N., and Fernandez, A. 1999. cdk1- and cdk2-mediated phosphorylation of MyoD Ser200 in growing C2 myoblasts: role in modulating MyoD half-life and myogenic activity. *Mol Cell Biol* **19**(4): 3167-3176.

Lasorella, A., Noseda, M., Beyna, M., Yokota, Y., and Iavarone, A. 2000. Id2 is a retinoblastoma protein target and mediates signalling by Myc oncoproteins. *Nature* **407**(6804): 592-598.

Lindon, C., Albagli, O., Domeyne, P., Montarras, D., and Pinset, C. 2000. Constitutive instability of muscle regulatory factor Myf5 is distinct from its mitosis-specific disappearance, which requires a D-box-like motif overlapping the basic domain. *Mol Cell Biol* **20**(23): 8923-8932.

Lindon, C., Montarras, D., and Pinset, C. 1998. Cell cycle-regulated expression of the muscle determination factor Myf5 in proliferating myoblasts. *J Cell Biol* **140**(1): 111-118.

Magenta, A., Cenciarelli, C., De Santa, F., Fuschi, P., Martelli, F., Caruso, M., and Felsani, A. 2003. MyoD stimulates RB promoter activity via the CREB/p300 nuclear transduction pathway. *Mol Cell Biol* **23**(8): 2893-2906.

Mal, A., Chattopadhyay, D., Ghosh, M.K., Poon, R.Y., Hunter, T., and Harter, M.L. 2000. p21 and retinoblastoma protein control the absence of DNA replication in terminally differentiated muscle cells. *J Cell Biol* **149**(2): 281-292.

Marino, S., Vooijs, M., van Der Gulden, H., Jonkers, J., and Berns, A. 2000. Induction of medulloblastomas in p53-null mutant mice by somatic inactivation of Rb in the external granular layer cells of the cerebellum. *Genes Dev* **14**(8): 994-1004.

Martelli, F., Cenciarelli, C., Santarelli, G., Polikar, B., Felsani, A., and Caruso, M. 1994. MyoD induces retinoblastoma gene expression during myogenic differentiation. *Oncogene* **9**(12): 3579-3590.

Narita, M., Nunez, S., Heard, E., Lin, A.W., Hearn, S.A., Spector, D.L., Hannon, G.J., and Lowe, S.W. 2003. Rb-mediated heterochromatin formation and silencing of E2F target genes during cellular senescence. *Cell* **113**(6): 703-716.

Novitch, B.G., Spicer, D.B., Kim, P.S., Cheung, W.L., and Lassar, A.B. 1999. pRb is required for MEF2-dependent gene expression as well as cell-cycle arrest during skeletal muscle differentiation. *Curr Biol* **9**(9): 449-459.

Pownall, M.E., Gustafsson, M.K., and Emerson, C.P., Jr. 2002. Myogenic regulatory factors and the specification of muscle progenitors in vertebrate embryos. *Annu Rev Cell Dev Biol* **18**: 747-783.

Sabourin, L.A., Girgis-Gabardo, A., Seale, P., Asakura, A., and Rudnicki, M.A. 1999. Reduced differentiation potential of primary MyoD-/- myogenic cells derived from adult skeletal muscle. *J Cell Biol* **144**(4): 631-643.

Sage, J., Mulligan, G.J., Attardi, L.D., Miller, A., Chen, S., Williams, B., Theodorou, E., and Jacks, T. 2000. Targeted disruption of the three Rb-related genes leads to loss of G(1) control and immortalization. *Genes Dev* **14**(23): 3037-3050.

Seale, P., Ishibashi, J., Holterman, C., and Rudnicki, M.A. 2004. Muscle satellite cell-specific genes identified by genetic profiling of MyoD-deficient myogenic cell. *Dev Biol* **275**(2): 287-300.

Skapek, S.X., Rhee, J., Spicer, D.B., and Lassar, A.B. 1995. Inhibition of myogenic differentiation in proliferating myoblasts by cyclin D1-dependent kinase. *Science* **267**(5200): 1022-1024.

Takahashi, C., Bronson, R.T., Socolovsky, M., Contreras, B., Lee, K.Y., Jacks, T., Noda, M., Kucherlapati, R., and Ewen, M.E. 2003. Rb and N-ras function together to control differentiation in the mouse. *Mol Cell Biol* **23**(15): 5256-5268.

Takahashi, Y., Rayman, J.B., and Dynlacht, B.D. 2000. Analysis of promoter binding by the E2F and pRB families in vivo: distinct E2F proteins mediate activation and repression. *Genes Dev* **14**(7): 804-816.

Thomas, D.M., Carty, S.A., Piscopo, D.M., Lee, J.S., Wang, W.F., Forrester, W.C., and Hinds, P.W. 2001. The retinoblastoma protein acts as a transcriptional coactivator required for osteogenic differentiation. *Mol Cell* **8**(2): 303-316.

Tintignac, L.A., Leibovitch, M.P., Kitzmann, M., Fernandez, A., Ducommun, B., Meijer, L., and Leibovitch, S.A. 2000. Cyclin E-cdk2 phosphorylation promotes late G1-phase degradation of MyoD in muscle cells. *Exp Cell Res* **259**(1): 300-307.

Walsh, K. 1997. Coordinate regulation of cell cycle and apoptosis during myogenesis. *Prog Cell Cycle Res* **3**: 53-58.

Wei, C.L., Wu, Q., Vega, V.B., Chiu, K.P., Ng, P., Zhang, T., Shahab, A., Yong, H.C., Fu, Y., Weng, Z., Liu, J., Zhao, X.D., Chew, J.L., Lee, Y.L., Kuznetsov, V.A., Sung, W.K., Miller, L.D., Lim, B., Liu, E.T., Yu, Q., Ng, H.H., and Ruan, Y.

2006. A global map of p53 transcription-factor binding sites in the human genome. *Cell* **124**(1): 207-219.

Wells, J., Yan, P.S., Cechvala, M., Huang, T., and Farnham, P.J. 2003. Identification of novel pRb binding sites using CpG microarrays suggests that E2F recruits pRb to specific genomic sites during S phase. *Oncogene* **22**(10): 1445-1460.

Zacksenhaus, E., Jiang, Z., Chung, D., Marth, J.D., Phillips, R.A., and Gallie, B.L. 1996. pRb controls proliferation, differentiation, and death of skeletal muscle cells and other lineages during embryogenesis. *Genes Dev* **10**(23): 3051-3064.

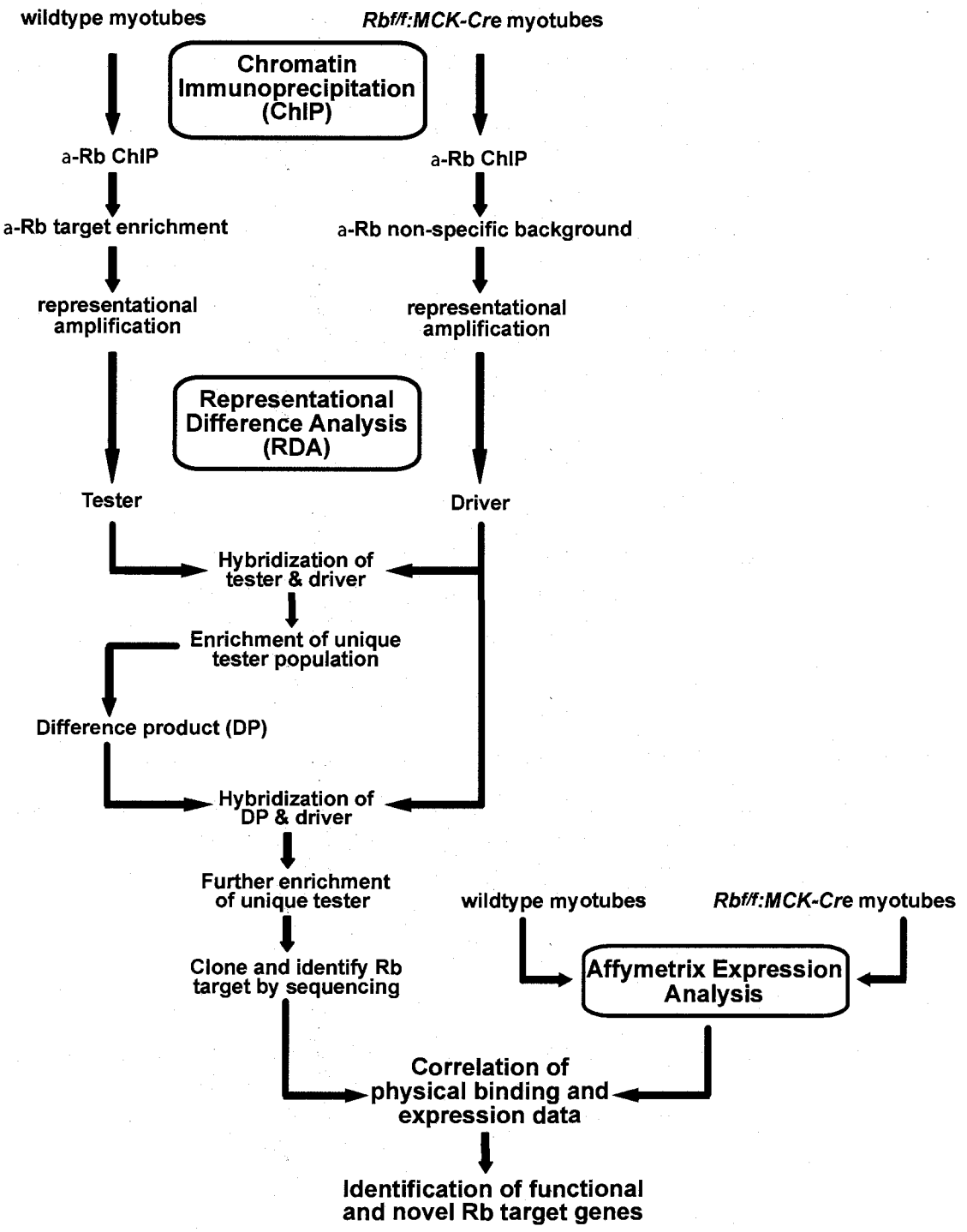

Figure S1. **Flow chart representation of experimental approach utilized for the identification of functional Rb target genes.**

Table S1. Deregulated genes in MbRb- by GO Classifications

Gene Symbol	Gene ID	Description	Fold Change
growth factor binding			
Igfbp2	16008	insulin-like growth factor binding protein 2	-3.85
Igfbp5	16011	insulin-like growth factor binding protein 5	-4.76
development			
Zic1	22771	zinc finger protein of the cerebellum 1	4.00
Rnase4	58809	angiogenin, ribonuclease A family, member 1	2.98
Nr4a2	18227	nuclear receptor subfamily 4, group A, member 2	2.06
Dmp1	13406	dentin matrix protein 1	2.04
Gal	14419	galanin	-2.04
Myom2	17930	myomesin 2	-2.94
Igfbp2	16008	insulin-like growth factor binding protein 2	-3.85
Igfbp5	16011	insulin-like growth factor binding protein 5	-4.76
cellular component			
Coq6	217707	coenzyme Q6 homolog (yeast)	6.10
Smoc2	64074	SPARC related modular calcium binding 2	4.73
Rnase4	58809	angiogenin, ribonuclease A family, member 1	2.98
Mfap1	67532	microfibrillar-associated protein 1	2.85
Dmp1	13406	dentin matrix protein 1	2.04
Cd80	12519	CD80 antigen	1.86
Gal	14419	galanin	-2.04
Nid1	18073	nidogen 1	-3.70
Igfbp2	16008	insulin-like growth factor binding protein 2	-3.85
Serinc3	26943	serine incorporator 3	-4.09
Igfbp5	16011	insulin-like growth factor binding protein 5	-4.76
contractile fiber			
Actn3	11474	actinin alpha 3	-2.17
Myom2	17930	myomesin 2	-2.94
DNA binding			
Zic1	22771	zinc finger protein of the cerebellum 1	4.00
Nr4a2	18227	nuclear receptor subfamily 4, group A, member 2	2.06
signal transduction			
Zic1	22771	zinc finger protein of the cerebellum 1	4.00
nucleotide binding			
Coq6	217707	coenzyme Q6 homolog (yeast)	6.10

Table S2. Deregulated genes in MtRb- by GO Classifications

Gene Symbol	Gene ID	Description	Fold Change
serine/threonine kinases			
Cks1b	54124	CDC28 protein kinase 1b	5.65
Cks2	66197	CDC28 protein kinase regulatory subunit 2	5.57
Plk2	20620	polo-like kinase 2	4.22
Atm	11920	ataxia telangiectasia mutated homolog	2.65
Cdk4	12567	cyclin-dependent kinase 4	2.31
Cdk2	12566	cyclin-dependent kinase 2	2.06
Raf1	110157	v-raf-1 leukemia viral oncogene 1	-1.89
Akt1	11651	thymoma viral proto-oncogene 1	-2.00
Mapkapk2	17164	MAP kinase-activated protein kinase 2	-2.13
Tesk1	21751	testis specific protein kinase 1	-2.17
Prkaca	18747	protein kinase, cAMP dependent, catalytic, alpha	-2.38
Nrk	27206	Nik related kinase	-2.44
Als2cr2	227154	amyotrophic lateral sclerosis 2	-2.63
Alpk3	116904	alpha-kinase 3	-2.78
Camk2a	12322	calcium/calmodulin-dependent protein kinase II alpha	-2.86
Sbk1	104175	SH3-binding kinase 1	-2.94
Dcamkl1	13175	double cortin and calcium/calmodulin-dependent protein kinase-like 1	-3.85
contractile fiber			
Pdlim3	53318	PDZ and LIM domain	2.33
Tpm1	22003	tropomyosin 1, alpha	-2.13
Sync	68828	syncoilin	-2.33
Pdlim5	56376	PDZ and LIM domain 5	-2.38
Tpm2	22004	tropomyosin 2, beta	-2.44
Actn3	11474	actinin alpha 3	-2.50
Tnnt2	21956	troponin T2, cardiac	-2.70
Myom1	17929	myomesin 1	-2.94
Actn2	11472	actinin alpha 2	-4.17
Itgb1bp2	26549	integrin beta 1 binding protein 2	-4.76
8030451F13Rik	109272	myosin binding protein C, slow type	-5.00
Mybph	53311	myosin binding protein H	-7.69
Myh8	17885	myosin, heavy polypeptide 8, skeletal muscle, perinatal	-7.69
muscle development			
Myf5	17877	myogenic factor 5	8.37
Tpm4	326618	tropomyosin 4	2.91
Tpm3	59069	tropomyosin 3, gamma	2.82
Ifrd1	15982	interferon-related developmental regulator 1	2.76
Ezh2	14056	enhancer of zeste homolog 2	2.56
Pdlim3	53318	PDZ and LIM domain	2.33
Hdac5	15184	histone deacetylase	-1.56
Myl9	98932	myosin, light polypeptide 9, regulatory	-2.04
Tpm1	22003	tropomyosin 1, alpha	-2.13
Vamp5	53620	vesicle-associated membrane protein 5	-2.13
Tnnt3	21957	troponin T3, skeletal, fast	-2.22

Hspb2	69253	heatshock protein 2	-2.42
Tpm2	22004	tropomyosin 2, beta	-2.44
Tnnc2	21925	troponin C2, fast	-2.56
Tnnt2	21956	troponin T2, cardiac	-2.70
Tnni1	21952	troponin I, skeletal, slow 1	-2.86
Myl4	17896	myosin, light polypeptide 4	-2.94
Myom1	17929	myomesin 1	-2.94
Tnni2	21953	troponin I, skeletal, fast 2	-3.23
Capn3	12335	calpain 3	-4.76
Myh6	140781	myosin, heavy polypeptide 6, cardiac muscle, alpha	-5.56
Mb	17189	myoglobin	-5.70
Mybph	53311	myosin binding protein H	-7.69
Myh8	17885	myosin, heavy polypeptide 8, skeletal muscle, perinatal	-7.69
Myf6	17878	myogenic factor 6	-9.09
cytoskeletal protein binding			
Fscn1	14086	fascin homolog 1, actin bundling protein	3.81
Tpm4	326618	tropomyosin 4	2.91
Tpm3	59069	tropomyosin 3, gamma	2.82
Myh9	17886	myosin, heavy polypeptide 9, non-muscle	2.44
Tpm1	22003	tropomyosin 1, alpha	-2.13
Cfl2	12632	cofilin 2, muscle	-2.27
Daam2	76441	dishevelled associated activator of morphogenesis 2	-2.38
Shrm	27428	shroom	-2.38
Synpo2l	68760	synaptopodin 2-like	-2.38
Tpm2	22004	tropomyosin 2, beta	-2.44
Actn3	11474	actinin alpha 3	-2.50
Tmod1	21916	tropomodulin 1	-2.78
Tnni1	21952	troponin I, skeletal, slow 1	-2.86
Fhod3	225288	formin homology 2 domain containing 3	-3.03
Tnni2	21953	troponin I, skeletal, fast 2	-3.23
Actn2	11472	actinin alpha 2	-4.17
Myh8	17885	myosin, heavy polypeptide 8, skeletal muscle, perinatal	-7.69
Ablim3	319713	actin binding LIM protein family, member 3	-33.33
intramolecular transferase			
Pmm1	29858	phosphomannomutase 1	3.37
Pgam1	18648	phosphoglycerate mutase 1	2.26
Pgam2	56012	phosphoglycerate mutase 2	-2.94
Pgm5	226041	phosphoglucomutase 5	-2.94
DNA metabolism			
Rrm2	20135	ribonucleotide reductase M2	14.14
Mcm2	17216	minichromosome maintenance deficient 2 mitotin	13.50
Pcna	18538	proliferating cell nuclear antigen	10.55
Ris2	67177	retroviral integration site 2	7.29
Rpa1	68275	replication protein A1	6.39
Msh6	17688	mutS homolog 6	5.57
Mcm7	17220	minichromosome maintenance deficient 7	5.48
Rpa3	68240	replication protein A3	4.28

Mcm4	17217	minichromosome maintenance deficient 4 homolog	4.03
Rpa2	19891	replication protein A2	3.00
Chaf1b	110749	chromatin assembly factor 1, subunit B	2.96
Rev1l	56210	REV1-like	2.96
Polk	27015	polymerase (DNA directed), kappa	2.78
Rrm1	20133	ribonucleotide reductase M1	2.74
Ercc1	13870	Excision repair cross-complementing rodent repair deficiency	-2.02
Pold4	69745	polymerase (DNA-directed), delta 4	-2.26
Pold4	69745	polymerase (DNA-directed), delta 4	-2.27
H3h2a	319162	histone 3, H2a	-2.35
Hist1h1c	50708	histone 1, H1c	-2.50
Smyd1	12180	SET and MYND domain containing 1	-3.25
Hist1h2bc	68024	histone 1, H2bc	-5.12
glucose catabolism			
Pgam1	18648	phosphoglycerate mutase 1	2.26
Tpi1	21991	triosephosphate isomerase 1	-1.92
Mdh1	17449	malate dehydrogenase 1, NAD	-2.08
Pfkm	18642	phosphofructokinase, muscle	-2.08
Aldoa	11674	aldolase 1, A isoform	-2.17
Pgam2	56012	phosphoglycerate mutase 2	-2.94
Eno3	13808	enolase 3, beta muscle	-3.03
cell cycle			
Mcm2	17216	minichromosome maintenance deficient 2 mitotin	13.50
Ris2	67177	retroviral integration site 2	7.29
Cks1b	54124	CDC28 protein kinase 1b	5.65
Cks2	66197	CDC28 protein kinase regulatory subunit 2	5.57
Mcm7	17220	minichromosome maintenance deficient 7	5.48
E2f7	52679	E2F transcription factor 7	4.73
Pmp22	18858	peripheral myelin protein	3.79
Rbl1	19650	retinoblastoma-like 1 (p107)	3.73
Tfdp1	21781	transcription factor Dp 1	3.50
Anxa1	16952	annexin A1	2.96
Chaf1b	110749	chromatin assembly factor 1, subunit B	2.96
Gadd45g	23882	growth arrest and DNA-damage-inducible 45 gamma	2.85
Smc1l1	24061	SMC (structural maintenance of chromosomes 1)-like 1	2.74
Atm	11920	ataxia telangiectasia mutated homolog	2.65
Ccng1	12450	cyclin G1	2.38
Cdk4	12567	cyclin-dependent kinase 4	2.31
Cspg6	13006	chondroitin sulfate proteoglycan 6	2.29
Anapc5	59008	anaphase-promoting complex subunit 5	2.21
Cdkn2a	12578	cyclin-dependent kinase inhibitor 2A	2.11
Cdk2	12566	cyclin-dependent kinase 2	2.06
Rad50	19360	RAD50 homolog	2.06
Rbbp4	19646	retinoblastoma binding protein 4	1.93
Pkd2	18764	polycystic kidney disease 2	1.90
Apbb1	11785	amyloid beta (A4) precursor protein-binding, family B, member 1	-2.04

Fgf7	14178	fibroblast growth factor 7	-2.38
S100a6	20200	S100 calcium binding protein A6 (calcyclin)	-2.44
Camk2a	12322	calcium/calmodulin-dependent protein kinase II alpha	-2.44
Ccnd3	12445	cyclin D3	-2.53
Ccnd3	12445	cyclin D3	-2.56
Ccng2	12452	cyclin G2	-2.72
apoptosis			
Msh6	17688	mutS homolog 6	5.57
Pmaip1	58801	phorbol-12-myristate-13-acetate-induced protein 1	3.00
Scotin	66940	scotin gene	2.40
Casp8ap2	26885	caspase 8 associated protein 2	2.12
Ercc5	22592	excision repair cross-complementing rodent repair deficiency, complementation group 5	2.06
Bax	12028	Bcl2-associated X protein	2.00
Akt1	11651	thymoma viral proto-oncogene 1	-1.79
Rnf7	19823	ring finger protein 7	-2.04
Ndufa13	67184	NADH dehydrogenase 1 alpha subcomplex, 13	-2.17

Table S3. ChIP-RDA Candidate Genes

GeneSymbol	GeneID	GeneTitle	Hits	Min Dist	Max Dist	Fold Change
Tnip2	231130	TNFAIP3 interacting protein 2	4	30324	30333	-1.01
Nat2	17961	N-acetyltransferase 2 (arylamine N-acetyltransferase)	3	0	0	2.06
Nat1	17960	N-acetyltransferase 1 (arylamine N-acetyltransferase)	3	9303	9303	1.11
Nat3	17962	N-acetyltransferase 3	3	22188	22188	1.02
St6gal1	20440	beta galactoside alpha 2,6 sialyltransferase 1	3	3994	4017	-1.24
Dpysl2	12934	dihydropyrimidinase-like 2	2	0	43040	2.7
Ptpns1	19261	protein tyrosine phosphatase, non-receptor type substrate 1	2	36485	36485	2.03
MGI:1929890	64164	interferon alpha responsive gene	2	0	0	1.6
Tkt	21881	transketolase	2	35799	35907	1.59
Tor1aip1	208263	torsin A interacting protein 1	2	30481	30484	1.4
1300018I05Rik	74157	RIKEN cDNA 1300018I05 gene (1300018I05Rik), mRNA	2	0	0	1.38
Plekhb2	226971	pleckstrin homology domain containing, family B (evectins) member 2	2	0	19324	1.37
Foxi1	14233	forkhead box I1	2	39603	39603	1.21
Llglh	16897	lethal giant larvae homolog	2	15428	28467	1.16
Dcp1a	75901	decapping enzym	2	0	0	1.04
Hba-a1	15122	hemoglobin alpha, adult chain 1	2	33743	46560	1.01
Tor1aip2	240832	torsin A interacting protein 2	2	0	0	-1.02
Lama4	16775	laminin, alpha 4	2	0	19147	-1.08
Gngt1	14699	G protein, gamma transducing activity polypeptide 1	2	24396	24396	-1.32
Ndufa10	67273	NADH dehydrogenase (ubiquinone) 1 alpha subcomplex 10	2	27230	27240	-1.58
Fliih	14248	flightless I homolog (Drosophila)	2	29854	42893	-1.64
Rai2	24004	retinoic acid induced 2	2	0	0	-3.68
Pml	18854	promyelocytic leukemia	1	9566	9566	7.02
Nup210	54563	nucleoporin 210	1	0	0	4.96
Rsbn1	229675	rosbin, round spermatid basic protein 1	1	28809	28809	2.92
Hspa14	50497	heat shock 70kDa protein 14	1	23017	23017	2.66
Timeless	21853	timeless homolog (Drosophila)	1	206	206	2.6
Pnp	18950	purine-nucleoside phosphorylase	1	22116	22116	2.56
Parp2	11546	poly (ADP-ribose) polymerase family, member 2	1	11910	11910	2.44
Vldlr	22359	very low density lipoprotein receptor	1	831	831	2.35
BC005662	210992	cDNA sequence BC005662	1	34797	34797	2.26
Prg1	19073	proteoglycan 1, secretory granule	1	31050	31050	2.16
Xrcc6	14375	X-ray repair complementing defective repair in Chinese hamster cells 6	1	0	0	2.16

Lhcgr	16867	luteinizing hormone/choriogonadotropin receptor	1	23510	23510	1.98
Stat2	20847	signal transducer and activator of transcription 2	1	38690	38690	1.97
Krt1-17	16667	keratin complex 1, acidic, gene 17	1	0	0	1.88
Tram1	72265	translocating chain-associating membrane protein 1	1	361	361	1.78
St7	64213	Suppression of tumorigenicity 7	1	12991	12991	1.71
Rcc2	108911	regulator of chromosome condensation 2	1	48774	48774	1.7
Gpc3	14734	Glypican 3	1	0	0	1.65
Ang1	11727	angiogenin, ribonuclease A family, member 1	1	42854	42854	1.65
Morc4	75746	microrchidia 4	1	0	0	1.62
Tubgcp3	259279	tubulin, gamma complex associated protein 3	1	13106	13106	1.58
Tbx5	21388	T-box 5	1	35766	35766	1.54
Ptbp2	56195	polypyrimidine tract binding protein 2	1	22169	22169	1.54
Ptk2	14083	PTK2 protein tyrosine kinase 2	1	0	0	1.52
2700062C07Rik	68046	RIKEN cDNA 2700062C07 gene	1	58	58	1.52
Creld1	171508	cysteine-rich with EGF-like domains 1	1	0	0	1.52
Sorcs3	66673	sortilin-related VPS10 domain containing receptor 3	1	0	0	1.5
3300001G02Rik	78372	RIKEN cDNA 3300001G02 gene	1	40654	40654	1.49
Mapre1	13589	microtubule-associated protein, RP/EB family, member 1	1	0	0	1.48
Phtf1	18685	putative homeodomain transcription factor 1	1	0	0	1.47
Alg1	208211	asparagine-linked glycosylation 1 homolog	1	47537	47537	1.43
Kcna4	16492	potassium voltage-gated channel, shaker-related subfamily, member 4	1	42536	42536	1.43
Mpg	268395	N-methylpurine-DNA glycosylase	1	16939	16939	1.41
D15Wsu75e	28075	DNA segment, Chr 15, Wayne State University 75, expressed	1	18364	18364	1.4
Brd2	14312	bromodomain containing 2	1	32844	32844	1.39
Slc39a7	14977	solute carrier family 39 (zinc transporter), member 7	1	48835	48835	1.39
Agtrap	11610	angiotensin II, type I receptor-associated protein	1	47487	47487	1.38
Cald1	109624	caldesmon 1	1	0	0	1.38
Rusc2	100213	RUN and SH3 domain containing 2	1	43022	43022	1.36
Nppb	18158	natriuretic peptide precursor type B	1	41992	41992	1.33
Tnrc5	72029	trinucleotide repeat containing 5	1	19791	19791	1.31
Ptk9	19230	protein tyrosine kinase 9	1	11208	11208	1.3
Amacr	17117	alpha-methylacyl-CoA racemase	1	45243	45243	1.3
BC027231	212547	cDNA sequence BC027231	1	0	0	1.29
Nhp2l1	20826	NHP2 non-histone chromosome protein 2-like 1	1	6529	6529	1.27
Rbm10	236732	RNA binding motif protein 10	1	0	0	1.25
Trim33	94093	tripartite motif protein 33	1	0	0	1.25

Mbtps1	56453	membrane-bound transcription factor peptidase, site 1	1	0	0	1.24
Dnaja3	83945	DnaJ (Hsp40) homolog, subfamily A, member 3	1	686	686	1.22
Supv3l1	338359	suppressor of var1, 3-like 1 (S. cerevisiae)	1	13492	13492	1.2
Dbh	13166	dopamine beta hydroxylase	1	0	0	1.2
Abcg1	11307	ATP-binding cassette, sub-family G (WHITE), member 1	1	44752	44752	1.19
0610039A15Rik	66087	RIKEN cDNA 0610039A15 gene	1	27044	27044	1.19
Man1a	17155	Mannosidase 1, alpha, mRNA (cDNA clone MGC:18448 IMAGE:4223319)	1	2736	2736	1.19
Clcn6	26372	chloride channel 6	1	0	0	1.19
0610010K06Rik	71678	RIKEN cDNA 0610010K06 gene	1	40937	40937	1.18
Cldn2	12738	claudin 2	1	45941	45941	1.18
Stx3	20908	syntaxin 3	1	36558	36558	1.17
Akr1d1	208665	aldo-keto reductase family 1, member D1	1	36463	36463	1.17
Ppp4r2	232314	protein phosphatase 4, regulatory subunit 2	1	33329	33329	1.17
Abcf2	27407	ATP-binding cassette, sub-family F (GCN20), member 2	1	30235	30235	1.17
H2afy3	404634	H2A histone family, member Y3 (H2afy3), mRNA	1	0	0	1.15
Ushbp1	234395	Usher syndrome 1C binding protein 1	1	8114	8114	1.14
Nell2	54003	nel-like 2 homolog (chicken)	1	0	0	1.13
Sardh	192166	sarcosine dehydrogenase	1	13804	13804	1.13
Cryzl1	66609	crystallin, zeta (quinone reductase)-like 1	1	43598	43598	1.11
Ptprc	19264	protein tyrosine phosphatase, receptor type, C	1	0	0	1.11
Magi3	99470	membrane associated guanylate kinase, WW and PDZ domain containing 3	1	19261	19261	1.11
Suclg2	20917	succinate-Coenzyme A ligase, GDP-forming, beta subunit	1	0	0	1.11
AW050020	268420	expressed sequence AW050020	1	19511	19511	1.1
1200009B18Rik	67456	RIKEN cDNA 1200009B18 gene	1	20540	20540	1.08
Dbnl	13169	drebrin-like	1	48124	48124	1.07
Bms1l	213895	BMS1-like, ribosome assembly protein (yeast)	1	45949	45949	1.07
Cntnap2	66797	Contactin associated protein-like 2	1	0	0	1.07
Mare	17168	alpha globin regulatory element containing gene	1	0	0	1.07
Il17re	57890	interleukin 17 receptor E	1	16798	16798	1.06
Syk	20963	spleen tyrosine kinase	1	39278	39278	1.06
Als2cr13	72750	amyotrophic lateral sclerosis 2 (juvenile) chromosome region	1	0	0	1.06
Abt1	30946	activator of basal transcription	1	32707	32707	1.05
Smad6	17130	MAD homolog 6 (Drosophila)	1	9502	9502	1.05
2600005C20Rik	72462	RIKEN cDNA 2600005C20 gene	1	5001	5001	1.05
Cmah	12763	cytidine monophospho-N-acetylneuraminic acid hydroxylase	1	0	0	1.05

Tiam2	24001	T-cell lymphoma invasion and metastasis 2	1	0	0	1.05
Mrps24	64660	mitochondrial ribosomal protein S24	1	32409	32409	1.04
Irak4	266632	interleukin-1 receptor-associated kinase 4	1	19473	19473	1.04
C1galt1	94192	core 1 UDP-galactose:N-acetylgalactosamine-alpha-R beta	1	0	0	1.04
Ublcp1	79560	ubiquitin-like domain containing CTD phosphatase 1	1	2932	2932	1.03
Cklfsf8	70031	chemokine-like factor super family 8	1	0	0	1.02
Zfp238	30928	zinc finger protein 238	1	34147	34147	1
Ube1x	22201	ubiquitin-activating enzyme E1, Chr X	1	28016	28016	1
Accn1	11418	amiloride-sensitive cation channel 1, neuronal (degenerin)	1	0	0	-1.01
Npepl1	228961	aminopeptidase-like 1	1	0	0	-1.01
Bzw2	66912	basic leucine zipper and W2 domains 2	1	30080	30080	-1.02
Apon	28194	apolipoprotein N	1	22245	22245	-1.02
Tff2	21785	trefoil factor 2 (spasmolytic protein 1)	1	16240	16240	-1.02
Ang2	11731	angiogenin, ribonuclease A family, member 2	1	46113	46113	-1.02
Grin2a	14811	glutamate receptor, ionotropic, NMDA2A (epsilon 1)	1	46658	46658	-1.02
Slitl2	246154	Slit-like 2 (Drosophila)	1	32444	32444	-1.02
MGI:1930773	56695	brain protein 17	1	0	0	-1.02
Il17rc	171095	interleukin 17 receptor C	1	4435	4435	-1.03
Slc11a1	18173	solute carrier family 11, member 1	1	39669	39669	-1.04
Adra1a	11549	adrenergic receptor, alpha 1a	1	27643	27643	-1.04
Padi3	18601	peptidyl arginine deiminase, type III	1	13214	13214	-1.04
5430437P03Rik	68251	RIKEN cDNA 5430437P03 gene	1	0	0	-1.04
Btn1a1	12231	butyrophilin, subfamily 1, member A1	1	1906	1906	-1.05
Asb10	117590	ankyrin repeat and SOCS box-containing protein 10	1	0	0	-1.05
Myo15	17910	myosin XV	1	47039	47039	-1.06
Gnmt	14711	glycine N-methyltransferase	1	42764	42764	-1.06
Tep1	21745	telomerase associated protein 1	1	0	0	-1.06
Nppa	230899	natriuretic peptide precursor type A	1	27123	27123	-1.06
Nr5a2	26424	nuclear receptor subfamily 5, group A, member 2	1	0	0	-1.06
Rnf13	24017	ring finger protein 13	1	38061	38061	-1.06
Mthfr	17769	5,10-methylenetetrahydrofolate reductase	1	11647	11647	-1.06
Nsdhl	18194	NAD(P) dependent steroid dehydrogenase-like	1	0	0	-1.06
Tcrb-V13	269846	T-cell receptor beta, variable 13	1	0	0	-1.06
Lrrc50	68270	leucine rich repeat containing 50	1	30420	30420	-1.07
Rgs6	50779	regulator of G-protein signaling 6	1	0	0	-1.07
Slc38a4	69354	solute carrier family 38, member 4	1	0	0	-1.07

Lactb2	212442	lactamase, beta 2	1	44003	44003	-1.08
Apln	30878	apelin	1	21646	21646	-1.08
Rnase4	58809	ribonuclease, RNase A family 4	1	42854	42854	-1.09
Hba-x	15126	hemoglobin X, alpha-like embryonic chain in Hba complex	1	26673	26673	-1.09
9430098E02Rik	77090	RIKEN cDNA 9430098E02 gene	1	30596	30596	-1.1
Hmox2	15369	heme oxygenase (decycling) 2	1	43005	43005	-1.11
Bcl9	77578	B-cell CLL/lymphoma 9	1	0	0	-1.11
Cd200r1	57781	CD200 receptor 1	1	37354	37354	-1.11
1700054N08Rik	73420	RIKEN cDNA 1700054N08 gene	1	24873	24873	-1.11
Ndufb11	104130	NADH dehydrogenase (ubiquinone) 1 beta subcomplex, 11	1	12676	12676	-1.11
Oosp1	170834	oocyte secreted protein 1	1	47210	47210	-1.12
Ppl	19041	periplakin	1	44104	44104	-1.12
Rxrb	20182	retinoid X receptor beta	1	41588	41588	-1.12
Hkdc1	216019	hexokinase domain containing 1	1	40720	40720	-1.12
2310039H08Rik	67101	RIKEN cDNA 2310039H08 gene	1	263	263	-1.12
Dok5	76829	docking protein 5	1	31542	31542	-1.13
Kif21b	16565	kinesin family member 21B	1	29852	29852	-1.13
Hexa	15211	hexosaminidase A	1	11061	11061	-1.13
Tlx1	21908	T-cell leukemia, homeobox 1	1	21142	21142	-1.13
Scgn	214189	secretagogin, EF-hand calcium binding protein	1	18317	18317	-1.13
Rae1	66679	RAE1 RNA export 1 homolog (S. pombe)	1	44833	44833	-1.14
Irf2bp1	272359	interferon regulatory factor 2 binding protein 1	1	34225	34225	-1.14
Centg3	213990	centaurin, gamma 3	1	32596	32596	-1.14
Pank1	75735	pantothenate kinase 1	1	0	0	-1.14
Tcl1	21432	T-cell lymphoma breakpoint 1	1	39337	39337	-1.15
Krt1-16	16666	keratin complex 1, acidic, gene 16	1	9505	9505	-1.15
Kcnk13	217826	Potassium channel, subfamily K, member 13 (Kcnk13), mRNA	1	2706	2706	-1.15
Rnase1	19752	ribonuclease, RNase A family, 1 (pancreatic)	1	2451	2451	-1.15
Padi4	18602	peptidyl arginine deiminase, type IV	1	0	0	-1.15
Ga17	98221	dendritic cell protein GA17	1	45437	45437	-1.18
Cetn2	26370	centrin 2	1	38298	38298	-1.18
Itsn1	16443	intersectin 1 (SH3 domain protein 1A)	1	9674	9674	-1.18
Mrpl16	94063	mitochondrial ribosomal protein L16	1	31830	31830	-1.18
Asb7	117589	ankyrin repeat and SOCS box-containing protein 7	1	22827	22827	-1.18
MGI:2446472	232934	Myb protein P42POP	1	21491	21491	-1.18
Epas1	13819	endothelial PAS domain protein 1	1	0	0	-1.18

Nr2f6	13864	nuclear receptor subfamily 2, group F, member 6	1	22087	22087	-1.19
Cadps2	320405	Ca2+-dependent activator protein for secretion 2	1	0	0	-1.19
H2afy	26914	H2A histone family, member Y	1	3453	3453	-1.19
Kcnma1	16531	Large conductance calcium activated potassium BK channel STREX-1 (Slo)	1	0	0	-1.21
Foxa3	15377	forkhead box A3	1	43455	43455	-1.22
Capza2	12343	capping protein (actin filament) muscle Z-line, alpha 2	1	14105	14105	-1.22
Npas2	18143	neuronal PAS domain protein 2	1	0	0	-1.22
Tff1	21784	trefoil factor 1	1	0	0	-1.22
Tbcd	108903	tubulin-specific chaperone d	1	0	0	-1.23
Ppm1a	19042	protein phosphatase 1A, magnesium dependent, alpha isoform	1	0	0	-1.24
Gif	14603	gastric intrinsic factor	1	8998	8998	-1.24
Vps26	30930	vacuolar protein sorting 26 (yeast)	1	0	0	-1.24
Il12b	16160	interleukin 12b	1	38557	38557	-1.27
Psmc1	19179	protease (prosome, macropain) 26S subunit, ATPase 1	1	48465	48465	-1.28
Padi1	18599	peptidyl arginine deiminase, type I	1	40826	40826	-1.29
4633402N23Rik	66701	RIKEN cDNA 4633402N23 gene	1	19951	19951	-1.29
C1qtnf3	81799	C1q and tumor necrosis factor related protein 3	1	15819	15819	-1.3
Mip	17339	major intrinsic protein of eye lens fiber	1	0	0	-1.3
Parp6	67287	Poly (ADP-ribose) polymerase family, member 6	1	40792	40792	-1.33
1100001I22Rik	68436	RIKEN cDNA 1100001I22 gene	1	9925	9925	-1.33
Tcf7l2	21416	HMG box transcription factor TCF7L2 (Tcf7l2) mRNA	1	0	0	-1.35
Slc17a1	20504	solute carrier family 17 (sodium phosphate), member 1	1	39090	39090	-1.35
Tfb1m	224481	transcription factor B1, mitochondrial	1	39705	39705	-1.37
Prss16	54373	protease, serine, 16 (thymus)	1	17660	17660	-1.37
Zic3	22773	zinc finger protein of the cerebellum 3	1	15572	15572	-1.37
Astn2	56079	astrotactin 2	1	0	0	-1.38
Acp6	66659	acid phosphatase 6, lysophosphatidic	1	43053	43053	-1.39
Loxl1	16949	lysyl oxidase-like 1	1	27945	27945	-1.43
Pex6	224824	peroxisomal biogenesis factor 6	1	46391	46391	-1.44
Ptprc	19264	Alternatively spliced Ly-5 glycoprotein mRNA, 5' end	1	0	0	-1.44
Cldn14	56173	claudin 14	1	26161	26161	-1.45
BC021395	225283	cDNA sequence BC021395	1	6798	6798	-1.5
Nf1	18015	NF1GRP, neurofibromatosis type-1-GTPase activating-protein type IV	1	22101	22101	-1.56
Cybrd1	73649	cytochrome b reductase 1	1	15021	15021	-1.56
Ear5	54159	eosinophil-associated, ribonuclease A family, member 5	1	13091	13091	-1.6

Oact2	67216	O-acyltransferase (membrane bound) domain containing 2	1	0	0	-1.62
Pacrg	69310	Park2 co-regulated	1	0	0	-1.62
Tmbim1	69660	transmembrane BAX inhibitor motif containing 1	1	31200	31200	-1.64
Rhbdf1	13650	rhomboid family 1 (Drosophila)	1	27400	27400	-1.65
Acadm	11364	acetyl-Coenzyme A dehydrogenase, medium chain	1	39050	39050	-1.66
2010315L10Rik	67023	RIKEN cDNA 2010315L10 gene	1	34025	34025	-1.66
V2r13	22304	vomeronasal 2, receptor, 13	1	36047	36047	-1.68
Zfp185	22673	zinc finger protein 185	1	30436	30436	-1.68
BC051244	232078	cDNA sequence BC051244	1	13713	13713	-1.84
Ttc5	219022	Tetratricopeptide repeat domain 5 (Ttc5), mRNA	1	47700	47700	-1.92
Rab4a	19341	RAB4A, member RAS oncogene family	1	0	0	-1.94
Apof	103161	apolipoprotein F	1	36111	36111	-2.14
Rnpc1	56190	RNA-binding region (RNP1, RRM) containing 1	1	25831	25831	-2.26
H2-Oa	15001	histocompatibility 2, O region alpha locus	1	13162	13162	-2.54
Tff3	21786	trefoil factor 3, intestinal	1	30911	30911	-3.76

Chapter 4

General Discussion

Overview of Findings

The retinoblastoma pathway is almost always inactivated during the course of neoplastic transformation. Rb functions not only to inhibit cell proliferation, but also enables specific cells type to properly differentiate. Hence, it is presumed that Rb is an important molecular coupler of cell cycle arrest and differentiation. Mouse knockout models have demonstrated that Rb is physiologically required for the proper maturation of numerous cell types. Despite the necessity for Rb in these cell types, germline transmission of a mutant *Rb* allele predisposes an individual to a limited subset of tumour types. Rb has been demonstrated to be required for skeletal myogenesis, but has not been directly implicated in tumour formation in this context. Thus understanding Rb's molecular function in skeletal muscle, may potentially provide insight into the determinants of disease and non-disease states.

This thesis has addressed the following questions. The elimination of Rb function prior to myogenic lineage commitment compromises skeletal muscle terminal differentiation. However, Rb's function subsequent to myogenic lineage commitment was yet unclear. Through genetic means, these data unequivocally demonstrates that progression towards terminal differentiation cannot be completed in *Rb* null primary myoblasts. Specifically, Rb is critically required for permanent cell cycle arrest, inhibition of apoptosis, and the activation of late markers of muscle differentiation. Rb integrates its functions through the transcriptional repression of genes associated with proliferation. In terminally differentiated myotubes, Rb complexes directly inhibit the transcription of *E2F7* and *Myf5*. These findings for the first time demonstrate *Myf5* and *E2F7* as functional targets of Rb in myogenic differentiation. Moreover, identifying

Myf5 as a direct target of Rb is of major significance in delineating a unified model of myogenic transcriptional regulation. Taken together, these data redefine a transcriptional regulatory model of myogenic differentiation that involves MyoD induced repression of *Myf5* through Rb.

Context Driven Function of Rb

Mouse knockout studies have validated the functional importance of Rb in specific cell types. Processes such neurogenesis, osteogenesis, and myogenesis all require functional Rb to faithfully execute their developmental program (Lipinski and Jacks 1999; Wikenheiser-Brokamp 2006). This is especially relevant in the case of inherited Rb mutations that predisposes an individual to early onset retinoblastomas and osteosarcomas. Interestingly, the abnormalities associated with Rb loss in these cell types results in different sets of deficiencies in mice. Understanding the molecular basis for this difference will undoubtedly be useful in devising strategies to treat cancers.

Functional compensation of Rb loss can be assumed by its family members p107 and p130. This is most likely the case in tissues and cell types that are not affected by the elimination of Rb. Rb and its family members together serve to regulate the G1/S cell cycle transition through their interaction with the E2F transcription factors (Dannenberg et al. 2000; Sage et al. 2000). However, a clear and important distinction has been made recently in relation to Rb and p107/p130 function. It is proposed that Rb complexes function to target promoters during scenarios that entail permanent cell cycle withdrawal (senescence and terminal differentiation) (Narita et al. 2003). Conversely, p107/p130 complexes primarily serve to regulate promoters under reversible arrest conditions

(progression through cell cycle, contact inhibition, serum withdrawal and p16 induced). This proposal is consistent with the findings that p107/p130 complexes are the predominant Rb family-E2F complexes in cycling and reversibly arrested cells (Cam et al. 2004; Balciunaite et al. 2005). Rb's hypothetical role in permanent cell cycle withdrawal is then consistent with its function as an important regulator of differentiation and why it is so frequently targeted in tumour cells.

Myogenic and Osteogenic Models for Rb Function

The fusion of myoblasts into fully differentiated myotubes results in a permanent cell cycle arrest and the activation of differentiation specific muscle genes. The induction of differentiation immediately marks the increase in levels of cdk inhibitors p21, p27, and p57. The lack of cdk activity in turn activates Rb to promote permanent cell cycle arrest and the progression of the differentiation program. In line with this idea, *Rb* deleted myoblasts displayed a severe deficiency in muscle differentiation (Chapter 2). The deficiency in differentiation is not unlike what is observed in the osteogenic system. However, there are some key differences between the two. Indeed, *Rb* deficient mouse embryonic fibroblasts (MEFs) are incapable of terminal osteogenic differentiation (Thomas et al. 2001). Furthermore, the master osteogenic transcription factor CBFA1 can induce terminal cell cycle exit by inducing the cdk inhibitor p27 (Thomas et al. 2004), analogous to MyoD induction of p21 (Guo et al. 1995). Interestingly, Rb activity in terms of osteogenesis is linked to its physical binding with CBFA1. This type of direct interaction has yet to be confidently reproduced in the myogenic system. Finally, forced induction of osteogenesis by BMP-2 in *Rb* null MEFs did not induce apoptosis. This lack

of apoptosis is contrary to what is observed in *Rb* null myoblasts. This difference may be a critical factor in why osteosarcomas arise when a mutant *Rb* allele is inherited humans. Therefore, mechanistic knowledge of Rb dependent apoptotic response in osteoblasts can potentially be of therapeutic value for osteosarcomas.

Rb Dependent Mechanistic Model of Myogenic Differentiation

It was shown in Chapter 2 that functional loss of Rb in skeletal myoblasts precludes proper cell cycle withdrawal and terminal differentiation. In Chapter 3, the identification of transcriptional targets of Rb provided a novel mechanistic perspective on the Rb phenotype. This new model reinforces the notion of functional incompatibility of MyoD and Myf5. Myf5 and MyoD are members of the bHLH family of skeletal muscle transcription factors. Despite the high degree of homology in the bHLH domain, they are not equivalent in function (Ishibashi et al. 2005). Myf5 expression is associated with the capacity to proliferate, while MyoD expression is associated with the capacity to differentiate. This phenomenon is supported by the phenotypes exhibited by Myf5 and MyoD deficient primary myoblasts (Sabourin et al. 1999; Montarras et al. 2000). Under this assumption, MyoD activity would promote the exclusion of Myf5 expression. Indeed this is likely to be the case, as Rb directly represses *Myf5* transcription during differentiation (Chapter 3). Therefore, Rb repression of *Myf5* may doubly serve to promote cell cycle arrest and the progression of differentiation. Basic helix-loop-helix transcription factors are also important in neurogenic determination and differentiation. Therefore, an analogous relationship may exist between Rb and the neurogenic bHLH

factors. A comprehensive description of Rb targets in this system is also required to assess these functional relationships.

Biomedical Implications

Dissecting Rb's function under different cellular contexts is of primary interest in understanding pertinent cell intrinsic oncogenic mechanisms. Detailed understanding of these cell specific idiosyncrasies can eventually be exploited for more effective molecular based therapies for cancer. Cancer cells are highly resistant to single modes of treatment, largely due to the phenotypic heterogeneity associated with an inherently unstable genome. Therefore, drug based molecular disruption of multiple therapeutic targets is a much more effective means to eliminate cancerous cells. Due to the importance of Rb in suppressing tumour formation, understanding the tissue specific molecular mechanisms that are pertinent to triggering apoptosis will provide valuable targets for this purpose. Furthermore, basic mechanistic knowledge of Rb gene targets can also help in the design of more effective targeting strategies for cancer cells. This can be achieved by allowing clinicians to predict sets of deregulated genes according to the initiating genetic lesion (*Rb*) and tissue of origin of tumour cells.

Conclusion

Rb is a molecular conductor of transcriptional networks that lead to cell cycle inhibition and myogenic induction. Rb's function potentiates the activity of MyoD through the repression of Myf5 in the formation of skeletal muscle. This relationship represents an essential dynamic for skeletal muscle differentiation.

References

References

Ach, R.A., Durfee, T., Miller, A.B., Taranto, P., Hanley-Bowdoin, L., Zambryski, P.C., and Gruissem, W. 1997a. RRB1 and RRB2 encode maize retinoblastoma-related proteins that interact with a plant D-type cyclin and geminivirus replication protein. *Mol Cell Biol* **17**(9): 5077-5086.

Ach, R.A., Taranto, P., and Gruissem, W. 1997b. A conserved family of WD-40 proteins binds to the retinoblastoma protein in both plants and animals. *Plant Cell* **9**(9): 1595-1606.

Andrechek, E.R., Hardy, W.R., Girgis-Gabardo, A.A., Perry, R.L., Butler, R., Graham, F.L., Kahn, R.C., Rudnicki, M.A., and Muller, W.J. 2002. ErbB2 is required for muscle spindle and myoblast cell survival. *Mol Cell Biol* **22**(13): 4714-4722.

Anton, M. and Graham, F.L. 1995. Site-specific recombination mediated by an adenovirus vector expressing the Cre recombinase protein: a molecular switch for control of gene expression. *J Virol* **69**(8): 4600-4606.

Balciunaite, E., Spektor, A., Lents, N.H., Cam, H., Te Riele, H., Scime, A., Rudnicki, M.A., Young, R., and Dynlacht, B.D. 2005. Pocket protein complexes are recruited to distinct targets in quiescent and proliferating cells. *Mol Cell Biol* **25**(18): 8166-8178.

Bergstrom, D.A., Penn, B.H., Strand, A., Perry, R.L., Rudnicki, M.A., and Tapscott, S.J. 2002. Promoter-specific regulation of MyoD binding and signal transduction cooperate to pattern gene expression. *Mol Cell* **9**(3): 587-600.

Berkes, C.A., Bergstrom, D.A., Penn, B.H., Seaver, K.J., Knoepfler, P.S., and Tapscott, S.J. 2004. Pbx marks genes for activation by MyoD indicating a role for a

homeodomain protein in establishing myogenic potential. *Mol Cell* **14**(4): 465-477.

Bladt, F., Riethmacher, D., Isenmann, S., Aguzzi, A., and Birchmeier, C. 1995. Essential role for the c-met receptor in the migration of myogenic precursor cells into the limb bud. *Nature* **376**(6543): 768-771.

Blais, A., Tsikitis, M., Acosta-Alvear, D., Sharan, R., Kluger, Y., and Dynlacht, B.D. 2005. An initial blueprint for myogenic differentiation. *Genes Dev* **19**(5): 553-569.

Bober, E., Franz, T., Arnold, H.H., Gruss, P., and Tremblay, P. 1994. Pax-3 is required for the development of limb muscles: a possible role for the migration of dermomyotomal muscle progenitor cells. *Development* **120**(3): 603-612.

Boehmelt, G., Ulrich, E., Kurzbauer, R., Mellitzer, G., Bird, A., and Zenke, M. 1994. Structure and expression of the chicken retinoblastoma gene. *Cell Growth Differ* **5**(2): 221-230.

Borycki, A.G., Brunk, B., Tajbakhsh, S., Buckingham, M., Chiang, C., and Emerson, C.P., Jr. 1999a. Sonic hedgehog controls epaxial muscle determination through Myf5 activation. *Development* **126**(18): 4053-4063.

Borycki, A.G., Li, J., Jin, F., Emerson, C.P., and Epstein, J.A. 1999b. Pax3 functions in cell survival and in pax7 regulation. *Development* **126**(8): 1665-1674.

Braun, T. and Arnold, H.H. 1995. Inactivation of Myf-6 and Myf-5 genes in mice leads to alterations in skeletal muscle development. *Embo J* **14**(6): 1176-1186.

Braun, T., Rudnicki, M.A., Arnold, H.H., and Jaenisch, R. 1992. Targeted inactivation of the muscle regulatory gene Myf-5 results in abnormal rib development and perinatal death. *Cell* **71**(3): 369-382.

Brehm, A., Miska, E.A., McCance, D.J., Reid, J.L., Bannister, A.J., and Kouzarides, T. 1998. Retinoblastoma protein recruits histone deacetylase to repress transcription. *Nature* **391**(6667): 597-601.

Brunelli, J.P. and Thorgaard, G.H. 1999. Sequence, expression and genetic mapping of a rainbow trout retinoblastoma cDNA. *Gene* **226**(2): 175-180.

Buchkovich, K., Duffy, L.A., and Harlow, E. 1989. The retinoblastoma protein is phosphorylated during specific phases of the cell cycle. *Cell* **58**(6): 1097-1105.

Cam, H., Balciunaite, E., Blais, A., Spektor, A., Scarpulla, R.C., Young, R., Kluger, Y., and Dynlacht, B.D. 2004. A common set of gene regulatory networks links metabolism and growth inhibition. *Mol Cell* **16**(3): 399-411.

Cam, H. and Dynlacht, B.D. 2003. Emerging roles for E2F: beyond the G1/S transition and DNA replication. *Cancer Cell* **3**(4): 311-316.

Carroll, J.S., Liu, X.S., Brodsky, A.S., Li, W., Meyer, C.A., Szary, A.J., Eeckhoute, J., Shao, W., Hestermann, E.V., Geistlinger, T.R., Fox, E.A., Silver, P.A., and Brown, M. 2005. Chromosome-wide mapping of estrogen receptor binding reveals long-range regulation requiring the forkhead protein FoxA1. *Cell* **122**(1): 33-43.

Castano, E., Kleyner, Y., and Dynlacht, B.D. 1998. Dual cyclin-binding domains are required for p107 to function as a kinase inhibitor. *Mol Cell Biol* **18**(9): 5380-5391.

Cawley, S., Bekiranov, S., Ng, H.H., Kapranov, P., Sekinger, E.A., Kampa, D., Piccolboni, A., Sementchenko, V., Cheng, J., Williams, A.J., Wheeler, R., Wong, B., Drenkow, J., Yamanaka, M., Patel, S., Brubaker, S., Tammana, H., Helt, G., Struhl, K., and Gingeras, T.R. 2004. Unbiased mapping of transcription factor binding sites along human chromosomes 21 and 22 points to widespread regulation of noncoding RNAs. *Cell* **116**(4): 499-509.

Cenciarelli, C., De Santa, F., Puri, P.L., Mattei, E., Ricci, L., Bucci, F., Felsani, A., and Caruso, M. 1999. Critical role played by cyclin D3 in the MyoD-mediated arrest of cell cycle during myoblast differentiation. *Mol Cell Biol* **19**(7): 5203-5217.

Chen, P.L., Scully, P., Shew, J.Y., Wang, J.Y., and Lee, W.H. 1989. Phosphorylation of the retinoblastoma gene product is modulated during the cell cycle and cellular differentiation. *Cell* **58**(6): 1193-1198.

Chow, K.N. and Dean, D.C. 1996. Domains A and B in the Rb pocket interact to form a transcriptional repressor motif. *Mol Cell Biol* **16**(9): 4862-4868.

Chow, K.N., Starostik, P., and Dean, D.C. 1996. The Rb family contains a conserved cyclin-dependent-kinase-regulated transcriptional repressor motif. *Mol Cell Biol* **16**(12): 7173-7181.

Clarke, A.R., Maandag, E.R., van Roon, M., van der Lugt, N.M., van der Valk, M., Hooper, M.L., Berns, A., and te Riele, H. 1992. Requirement for a functional Rb-1 gene in murine development. *Nature* **359**(6393): 328-330.

Classon, M., Salama, S., Gorka, C., Mulloy, R., Braun, P., and Harlow, E. 2000. Combinatorial roles for pRB, p107, and p130 in E2F-mediated cell cycle control. *Proc Natl Acad Sci U S A* **97**(20): 10820-10825.

Claudio, P.P., Tonini, T., and Giordano, A. 2002. The retinoblastoma family: twins or distant cousins? *Genome Biol* **3**(9): reviews3012.

Cobrinik, D. 2005. Pocket proteins and cell cycle control. *Oncogene* **24**(17): 2796-2809.

Cobrinik, D., Lee, M.H., Hannon, G., Mulligan, G., Bronson, R.T., Dyson, N., Harlow, E., Beach, D., Weinberg, R.A., and Jacks, T. 1996. Shared role of the pRB-related p130 and p107 proteins in limb development. *Genes Dev* **10**(13): 1633-1644.

Cobrinik, D., Whyte, P., Peeper, D.S., Jacks, T., and Weinberg, R.A. 1993. Cell cycle-specific association of E2F with the p130 E1A-binding protein. *Genes Dev* 7(12A): 2392-2404.

Corbeil, H.B., Whyte, P., and Branton, P.E. 1995. Characterization of transcription factor E2F complexes during muscle and neuronal differentiation. *Oncogene* **11**(5): 909-920.

Costanzo, M., Nishikawa, J.L., Tang, X., Millman, J.S., Schub, O., Breitkreuz, K., Dewar, D., Rupes, I., Andrews, B., and Tyers, M. 2004. CDK activity antagonizes Whi5, an inhibitor of G1/S transcription in yeast. *Cell* **117**(7): 899-913.

Dannenberg, J.H. and te Riele, H.P. 2006. The retinoblastoma gene family in cell cycle regulation and suppression of tumorigenesis. *Results Probl Cell Differ* **42**: 183-225.

Dannenberg, J.H., van Rossum, A., Schuijff, L., and te Riele, H. 2000. Ablation of the retinoblastoma gene family deregulates G(1) control causing immortalization and increased cell turnover under growth-restricting conditions. *Genes Dev* **14**(23): 3051-3064.

Daston, G., Lamar, E., Olivier, M., and Goulding, M. 1996. Pax-3 is necessary for migration but not differentiation of limb muscle precursors in the mouse. *Development* **122**(3): 1017-1027.

de Bruin, A., Wu, L., Saavedra, H.I., Wilson, P., Yang, Y., Rosol, T.J., Weinstein, M., Robinson, M.L., and Leone, G. 2003. Rb function in extraembryonic lineages suppresses apoptosis in the CNS of Rb-deficient mice. *Proc Natl Acad Sci U S A* **100**(11): 6546-6551.

De Falco, M. and De Luca, A. 2006. Involvement of cdks and cyclins in muscle differentiation. *Eur J Histochem* **50**(1): 19-23.

de la Serna, I.L., Ohkawa, Y., Berkes, C.A., Bergstrom, D.A., Dacwag, C.S., Tapscott, S.J., and Imbalzano, A.N. 2005. MyoD targets chromatin remodeling complexes to the myogenin locus prior to forming a stable DNA-bound complex. *Mol Cell Biol* **25**(10): 3997-4009.

DeCaprio, J.A., Ludlow, J.W., Figge, J., Shew, J.Y., Huang, C.M., Lee, W.H., Marsilio, E., Paucha, E., and Livingston, D.M. 1988. SV40 large tumor antigen forms a specific complex with the product of the retinoblastoma susceptibility gene. *Cell* **54**(2): 275-283.

DeCaprio, J.A., Ludlow, J.W., Lynch, D., Furukawa, Y., Griffin, J., Piwnica-Worms, H., Huang, C.M., and Livingston, D.M. 1989. The product of the retinoblastoma susceptibility gene has properties of a cell cycle regulatory element. *Cell* **58**(6): 1085-1095.

Destree, O.H., Lam, K.T., Peterson-Maduro, L.J., Eizema, K., Diller, L., Gryka, M.A., Frebourg, T., Shibuya, E., and Friend, S.H. 1992. Structure and expression of the Xenopus retinoblastoma gene. *Dev Biol* **153**(1): 141-149.

Dimova, D.K., Stevaux, O., Frolov, M.V., and Dyson, N.J. 2003. Cell cycle-dependent and cell cycle-independent control of transcription by the Drosophila E2F/RB pathway. *Genes Dev* **17**(18): 2308-2320.

Doniger, S.W., Salomonis, N., Dahlquist, K.D., Vranizan, K., Lawlor, S.C., and Conklin, B.R. 2003. MAPPFinder: using Gene Ontology and GenMAPP to create a global gene-expression profile from microarray data. *Genome Biol* **4**(1): R7.

Doucet, C., Gutierrez, G.J., Lindon, C., Lorca, T., Lledo, G., Pinset, C., and Coux, O. 2005. Multiple phosphorylation events control mitotic degradation of the muscle transcription factor Myf5. *BMC Biochem* **6**: 27.

Du, W. and Pogoriler, J. 2006. Retinoblastoma family genes. *Oncogene* **25**(38): 5190-5200.

Dunaief, J.L., Strober, B.E., Guha, S., Khavari, P.A., Alin, K., Luban, J., Begemann, M., Crabtree, G.R., and Goff, S.P. 1994. The retinoblastoma protein and BRG1 form a complex and cooperate to induce cell cycle arrest. *Cell* **79**(1): 119-130.

Epstein, J.A., Shapiro, D.N., Cheng, J., Lam, P.Y., and Maas, R.L. 1996. Pax3 modulates expression of the c-Met receptor during limb muscle development. *Proc Natl Acad Sci U S A* **93**(9): 4213-4218.

Ewen, M.E., Faha, B., Harlow, E., and Livingston, D.M. 1992. Interaction of p107 with cyclin A independent of complex formation with viral oncoproteins. *Science* **255**(5040): 85-87.

Faha, B., Ewen, M.E., Tsai, L.H., Livingston, D.M., and Harlow, E. 1992. Interaction between human cyclin A and adenovirus E1A-associated p107 protein. *Science* **255**(5040): 87-90.

Ferguson, K.L., McClellan, K.A., Vanderluit, J.L., McIntosh, W.C., Schuurmans, C., Polleux, F., and Slack, R.S. 2005. A cell-autonomous requirement for the cell cycle regulatory protein, Rb, in neuronal migration. *Embo J* **24**(24): 4381-4391.

Ferguson, K.L., Vanderluit, J.L., Hebert, J.M., McIntosh, W.C., Tibbo, E., MacLaurin, J.G., Park, D.S., Wallace, V.A., Vooijs, M., McConnell, S.K., and Slack, R.S. 2002. Telencephalon-specific Rb knockouts reveal enhanced neurogenesis, survival and abnormal cortical development. *Embo J* **21**(13): 3337-3346.

Fernando, P., Kelly, J.F., Balazsi, K., Slack, R.S., and Megeney, L.A. 2002. Caspase 3 activity is required for skeletal muscle differentiation. *Proc Natl Acad Sci U S A* **99**(17): 11025-11030.

Ferreira, R., Magnaghi-Jaulin, L., Robin, P., Harel-Bellan, A., and Trouche, D. 1998. The three members of the pocket proteins family share the ability to repress E2F activity through recruitment of a histone deacetylase. *Proc Natl Acad Sci U S A* **95**(18): 10493-10498.

Flemington, E.K., Speck, S.H., and Kaelin, W.G., Jr. 1993. E2F-1-mediated transactivation is inhibited by complex formation with the retinoblastoma susceptibility gene product. *Proc Natl Acad Sci U S A* **90**(15): 6914-6918.

Friend, S.H., Bernards, R., Rogelj, S., Weinberg, R.A., Rapaport, J.M., Albert, D.M., and Dryja, T.P. 1986. A human DNA segment with properties of the gene that predisposes to retinoblastoma and osteosarcoma. *Nature* **323**(6089): 643-646.

Frolov, M.V. and Dyson, N.J. 2004. Molecular mechanisms of E2F-dependent activation and pRB-mediated repression. *J Cell Sci* **117**(Pt 11): 2173-2181.

Gerber, A.N., Klesert, T.R., Bergstrom, D.A., and Tapscott, S.J. 1997. Two domains of MyoD mediate transcriptional activation of genes in repressive chromatin: a mechanism for lineage determination in myogenesis. *Genes Dev* **11**(4): 436-450.

Goodrich, D.W. 2003. How the other half lives, the amino-terminal domain of the retinoblastoma tumor suppressor protein. *J Cell Physiol* **197**(2): 169-180.

Goodrich, D.W. and Lee, W.H. 1993. Molecular characterization of the retinoblastoma susceptibility gene. *Biochim Biophys Acta* **1155**(1): 43-61.

Goulding, M., Lumsden, A., and Paquette, A.J. 1994. Regulation of Pax-3 expression in the dermomyotome and its role in muscle development. *Development* **120**(4): 957-971.

Grafi, G., Burnett, R.J., Helentjaris, T., Larkins, B.A., DeCaprio, J.A., Sellers, W.R., and Kaelin, W.G., Jr. 1996. A maize cDNA encoding a member of the retinoblastoma protein family: involvement in endoreduplication. *Proc Natl Acad Sci U S A* **93**(17): 8962-8967.

Gu, W., Schneider, J.W., Condorelli, G., Kaushal, S., Mahdavi, V., and Nadal-Ginard, B. 1993. Interaction of myogenic factors and the retinoblastoma protein mediates muscle cell commitment and differentiation. *Cell* **72**(3): 309-324.

Guo, K., Wang, J., Andres, V., Smith, R.C., and Walsh, K. 1995. MyoD-induced expression of p21 inhibits cyclin-dependent kinase activity upon myocyte terminal differentiation. *Mol Cell Biol* **15**(7): 3823-3829.

Halevy, O., Novitch, B.G., Spicer, D.B., Skapek, S.X., Rhee, J., Hannon, G.J., Beach, D., and Lassar, A.B. 1995. Correlation of terminal cell cycle arrest of skeletal muscle with induction of p21 by MyoD. *Science* **267**(5200): 1018-1021.

Hannon, G.J., Demetrick, D., and Beach, D. 1993. Isolation of the Rb-related p130 through its interaction with CDK2 and cyclins. *Genes Dev* 7(12A): 2378-2391.

Hasty, P., Bradley, A., Morris, J.H., Edmondson, D.G., Venuti, J.M., Olson, E.N., and Klein, W.H. 1993. Muscle deficiency and neonatal death in mice with a targeted mutation in the myogenin gene. *Nature* **364**(6437): 501-506.

Heanue, T.A., Reshef, R., Davis, R.J., Mardon, G., Oliver, G., Tomarev, S., Lassar, A.B., and Tabin, C.J. 1999. Synergistic regulation of vertebrate muscle development by Dach2, Eya2, and Six1, homologs of genes required for Drosophila eye formation. *Genes Dev* **13**(24): 3231-3243.

Helin, K., Harlow, E., and Fattaey, A. 1993. Inhibition of E2F-1 transactivation by direct binding of the retinoblastoma protein. *Mol Cell Biol* **13**(10): 6501-6508.

Helin, K., Lees, J.A., Vidal, M., Dyson, N., Harlow, E., and Fattaey, A. 1992. A cDNA encoding a pRB-binding protein with properties of the transcription factor E2F. *Cell* **70**(2): 337-350.

Helt, A.M. and Galloway, D.A. 2003. Mechanisms by which DNA tumor virus oncoproteins target the Rb family of pocket proteins. *Carcinogenesis* **24**(2): 159-169.

Herrera, R.E., Chen, F., and Weinberg, R.A. 1996. Increased histone H1 phosphorylation and relaxed chromatin structure in Rb-deficient fibroblasts. *Proc Natl Acad Sci U S A* **93**(21): 11510-11515.

Ho, A.T., Li, Q.H., Hakem, R., Mak, T.W., and Zacksenhaus, E. 2004. Coupling of caspase-9 to Apaf1 in response to loss of pRb or cytotoxic drugs is cell-type-specific. *Embo J.*

Holland, L.Z., Schubert, M., Kozmik, Z., and Holland, N.D. 1999. AmphiPax3/7, an amphioxus paired box gene: insights into chordate myogenesis, neurogenesis, and the possible evolutionary precursor of definitive vertebrate neural crest. *Evol Dev* **1**(3): 153-165.

Holterman, C.E. and Rudnicki, M.A. 2005. Molecular regulation of satellite cell function. *Semin Cell Dev Biol* **16**(4-5): 575-584.

Hu, N., Gutsmann, A., Herbert, D.C., Bradley, A., Lee, W.H., and Lee, E.Y. 1994. Heterozygous Rb-1 delta 20/+mice are predisposed to tumors of the pituitary gland with a nearly complete penetrance. *Oncogene* **9**(4): 1021-1027.

Hu, Q.J., Lees, J.A., Buchkovich, K.J., and Harlow, E. 1992. The retinoblastoma protein physically associates with the human cdc2 kinase. *Mol Cell Biol* **12**(3): 971-980.

Huang, H.J., Yee, J.K., Shew, J.Y., Chen, P.L., Bookstein, R., Friedmann, T., Lee, E.Y., and Lee, W.H. 1988. Suppression of the neoplastic phenotype by replacement of the RB gene in human cancer cells. *Science* **242**(4885): 1563-1566.

Huh, M.S., Parker, M.H., Scime, A., Parks, R., and Rudnicki, M.A. 2004. Rb is required for progression through myogenic differentiation but not maintenance of terminal differentiation. *J Cell Biol* **166**(6): 865-876.

Hurford, R.K., Jr., Cobrinik, D., Lee, M.H., and Dyson, N. 1997. pRB and p107/p130 are required for the regulated expression of different sets of E2F responsive genes. *Genes Dev* **11**(11): 1447-1463.

Impey, S., McCorkle, S.R., Cha-Molstad, H., Dwyer, J.M., Yochum, G.S., Boss, J.M., McWeeney, S., Dunn, J.J., Mandel, G., and Goodman, R.H. 2004. Defining the CREB regulon: a genome-wide analysis of transcription factor regulatory regions. *Cell* **119**(7): 1041-1054.

Ishibashi, J., Perry, R.L., Asakura, A., and Rudnicki, M.A. 2005. MyoD induces myogenic differentiation through cooperation of its NH2- and COOH-terminal regions. *J Cell Biol* **171**(3): 471-482.

Jacks, T., Fazeli, A., Schmitt, E.M., Bronson, R.T., Goodell, M.A., and Weinberg, R.A. 1992. Effects of an Rb mutation in the mouse. *Nature* **359**(6393): 295-300.

Jenuwein, T. and Allis, C.D. 2001. Translating the histone code. *Science* **293**(5532): 1074-1080.

Jiang, Z., Liang, P., Leng, R., Guo, Z., Liu, Y., Liu, X., Bubnic, S., Keating, A., Murray, D., Goss, P., and Zacksenhaus, E. 2000. E2F1 and p53 are dispensable, whereas p21(Waf1/Cip1) cooperates with Rb to restrict endoreduplication and apoptosis during skeletal myogenesis. *Dev Biol* **227**(1): 8-41.

Johnson, D.G., Schwarz, J.K., Cress, W.D., and Nevins, J.R. 1993. Expression of transcription factor E2F1 induces quiescent cells to enter S phase. *Nature* **365**(6444): 349-352.

Jones, P.L., Veenstra, G.J., Wade, P.A., Vermaak, D., Kass, S.U., Landsberger, N., Strouboulis, J., and Wolffe, A.P. 1998. Methylated DNA and MeCP2 recruit histone deacetylase to repress transcription. *Nat Genet* **19**(2): 187-191.

Jostes, B., Walther, C., and Gruss, P. 1990. The murine paired box gene, Pax7, is expressed specifically during the development of the nervous and muscular system. *Mech Dev* **33**(1): 27-37.

Kablar, B., Krastel, K., Ying, C., Asakura, A., Tapscott, S.J., and Rudnicki, M.A. 1997. MyoD and Myf-5 differentially regulate the development of limb versus trunk skeletal muscle. *Development* **124**(23): 4729-4738.

Kablar, B., Krastel, K., Ying, C., Tapscott, S.J., Goldhamer, D.J., and Rudnicki, M.A. 1999. Myogenic determination occurs independently in somites and limb buds. *Dev Biol* **206**(2): 219-231.

Kaelin, W.G., Jr., Krek, W., Sellers, W.R., DeCaprio, J.A., Ajchenbaum, F., Fuchs, C.S., Chittenden, T., Li, Y., Farnham, P.J., Blanar, M.A., and et al. 1992. Expression cloning of a cDNA encoding a retinoblastoma-binding protein with E2F-like properties. *Cell* **70**(2): 351-364.

Kang, H., Cui, K., and Zhao, K. 2004. BRG1 controls the activity of the retinoblastoma protein via regulation of p21CIP1/WAF1/SDI. *Mol Cell Biol* **24**(3): 1188-1199.

Kassar-Duchossoy, L., Gayraud-Morel, B., Gomes, D., Rocancourt, D., Buckingham, M., Shinin, V., and Tajbakhsh, S. 2004. Mrf4 determines skeletal muscle identity in Myf5:Myod double-mutant mice. *Nature* **431**(7007): 466-471.

Kaul, A., Koster, M., Neuhaus, H., and Braun, T. 2000. Myf-5 revisited: loss of early myotome formation does not lead to a rib phenotype in homozygous Myf-5 mutant mice. *Cell* **102**(1): 17-19.

Kiess, M., Gill, R.M., and Hamel, P.A. 1995. Expression of the positive regulator of cell cycle progression, cyclin D3, is induced during differentiation of myoblasts into quiescent myotubes. *Oncogene* **10**(1): 159-166.

Kim, J.K., Zisman, A., Fillmore, J.J., Peroni, O.D., Kotani, K., Perret, P., Zong, H., Dong, J., Kahn, C.R., Kahn, B.B., and Shulman, G.I. 2001. Glucose toxicity and the development of diabetes in mice with muscle-specific inactivation of GLUT4. *J Clin Invest* **108**(1): 153-160.

Kitzmann, M., Carnac, G., Vandromme, M., Primig, M., Lamb, N.J., and Fernandez, A. 1998. The muscle regulatory factors MyoD and myf-5 undergo distinct cell cycle-specific expression in muscle cells. *J Cell Biol* **142**(6): 1447-1459.

Kitzmann, M., Vandromme, M., Schaeffer, V., Carnac, G., Labbe, J.C., Lamb, N., and Fernandez, A. 1999. cdk1- and cdk2-mediated phosphorylation of MyoD Ser200 in growing C2 myoblasts: role in modulating MyoD half-life and myogenic activity. *Mol Cell Biol* **19**(4): 3167-3176.

Knudson, A.G., Jr. 1971. Mutation and cancer: statistical study of retinoblastoma. *Proc Natl Acad Sci U S A* **68**(4): 820-823.

Lasorella, A., Noseda, M., Beyna, M., Yokota, Y., and Iavarone, A. 2000. Id2 is a retinoblastoma protein target and mediates signalling by Myc oncoproteins. *Nature* **407**(6804): 592-598.

Latella, L., Sacco, A., Pajalunga, D., Tiainen, M., Macera, D., D'Angelo, M., Felici, A., Sacchi, A., and Crescenzi, M. 2001. Reconstitution of cyclin D1-associated kinase activity drives terminally differentiated cells into the cell cycle. *Mol Cell Biol* **21**(16): 5631-5643.

LeCouter, J.E., Kablar, B., Hardy, W.R., Ying, C., Megeney, L.A., May, L.L., and Rudnicki, M.A. 1998a. Strain-dependent myeloid hyperplasia, growth deficiency, and accelerated cell cycle in mice lacking the Rb-related p107 gene. *Mol Cell Biol* **18**(12): 7455-7465.

LeCouter, J.E., Kablar, B., Whyte, P.F., Ying, C., and Rudnicki, M.A. 1998b. Strain-dependent embryonic lethality in mice lacking the retinoblastoma-related p130 gene. *Development* **125**(23): 4669-4679.

Lee, E.Y., Chang, C.Y., Hu, N., Wang, Y.C., Lai, C.C., Herrup, K., Lee, W.H., and Bradley, A. 1992. Mice deficient for Rb are nonviable and show defects in neurogenesis and haematopoiesis. *Nature* **359**(6393): 288-294.

Lee, K.Y., Ladha, M.H., McMahon, C., and Ewen, M.E. 1999. The retinoblastoma protein is linked to the activation of Ras. *Mol Cell Biol* **19**(11): 7724-7732.

Lees, E., Faha, B., Dulic, V., Reed, S.I., and Harlow, E. 1992. Cyclin E/cdk2 and cyclin A/cdk2 kinases associate with p107 and E2F in a temporally distinct manner. *Genes Dev* **6**(10): 1874-1885.

Lees, J.A., Buchkovich, K.J., Marshak, D.R., Anderson, C.W., and Harlow, E. 1991. The retinoblastoma protein is phosphorylated on multiple sites by human cdc2. *Embo J* **10**(13): 4279-4290.

Lewis, J.D., Meehan, R.R., Henzel, W.J., Maurer-Fogy, I., Jeppesen, P., Klein, F., and Bird, A. 1992. Purification, sequence, and cellular localization of a novel chromosomal protein that binds to methylated DNA. *Cell* **69**(6): 905-914.

Li, Y., Graham, C., Lacy, S., Duncan, A.M., and Whyte, P. 1993. The adenovirus E1A-associated 130-kD protein is encoded by a member of the retinoblastoma gene

family and physically interacts with cyclins A and E. *Genes Dev* **7**(12A): 2366-2377.

Lindon, C., Albagli, O., Domeyne, P., Montarras, D., and Pinset, C. 2000. Constitutive instability of muscle regulatory factor Myf5 is distinct from its mitosis-specific disappearance, which requires a D-box-like motif overlapping the basic domain. *Mol Cell Biol* **20**(23): 8923-8932.

Lindon, C., Montarras, D., and Pinset, C. 1998. Cell cycle-regulated expression of the muscle determination factor Myf5 in proliferating myoblasts. *J Cell Biol* **140**(1): 111-118.

Lipinski, M.M. and Jacks, T. 1999. The retinoblastoma gene family in differentiation and development. *Oncogene* **18**(55): 7873-7882.

Lu, X. and Horvitz, H.R. 1998. lin-35 and lin-53, two genes that antagonize a C. elegans Ras pathway, encode proteins similar to Rb and its binding protein RbAp48. *Cell* **95**(7): 981-991.

Luo, R.X., Postigo, A.A., and Dean, D.C. 1998. Rb interacts with histone deacetylase to repress transcription. *Cell* **92**(4): 463-473.

Magenta, A., Cenciarelli, C., De Santa, F., Fuschi, P., Martelli, F., Caruso, M., and Felsani, A. 2003. MyoD stimulates RB promoter activity via the CREB/p300 nuclear transduction pathway. *Mol Cell Biol* **23**(8): 2893-2906.

Magnaghi-Jaulin, L., Groisman, R., Naguibneva, I., Robin, P., Lorain, S., Le Villain, J.P., Troalen, F., Trouche, D., and Harel-Bellan, A. 1998. Retinoblastoma protein represses transcription by recruiting a histone deacetylase. *Nature* **391**(6667): 601-605.

Mal, A., Chattopadhyay, D., Ghosh, M.K., Poon, R.Y., Hunter, T., and Harter, M.L. 2000. p21 and retinoblastoma protein control the absence of DNA replication in terminally differentiated muscle cells. *J Cell Biol* **149**(2): 281-292.

Marino, S., Vooijs, M., van Der Gulden, H., Jonkers, J., and Berns, A. 2000. Induction of medulloblastomas in p53-null mutant mice by somatic inactivation of Rb in the external granular layer cells of the cerebellum. *Genes Dev* **14**(8): 994-1004.

Martelli, F., Cenciarelli, C., Santarelli, G., Polikar, B., Felsani, A., and Caruso, M. 1994. MyoD induces retinoblastoma gene expression during myogenic differentiation. *Oncogene* **9**(12): 3579-3590.

Martinez-Balbas, M.A., Bauer, U.M., Nielsen, S.J., Brehm, A., and Kouzarides, T. 2000. Regulation of E2F1 activity by acetylation. *Embo J* **19**(4): 662-671.

Marzio, G., Wagener, C., Gutierrez, M.I., Cartwright, P., Helin, K., and Giacca, M. 2000. E2F family members are differentially regulated by reversible acetylation. *J Biol Chem* **275**(15): 10887-10892.

Mayol, X., Grana, X., Baldi, A., Sang, N., Hu, Q., and Giordano, A. 1993. Cloning of a new member of the retinoblastoma gene family (pRb2) which binds to the E1A transforming domain. *Oncogene* **8**(9): 2561-2566.

Meehan, R.R., Lewis, J.D., McKay, S., Kleiner, E.L., and Bird, A.P. 1989. Identification of a mammalian protein that binds specifically to DNA containing methylated CpGs. *Cell* **58**(3): 499-507.

Mennerich, D., Schafer, K., and Braun, T. 1998. Pax-3 is necessary but not sufficient for lbx1 expression in myogenic precursor cells of the limb. *Mech Dev* **73**(2): 147-158.

Mihara, K., Cao, X.R., Yen, A., Chandler, S., Driscoll, B., Murphree, A.L., T'Ang, A., and Fung, Y.K. 1989. Cell cycle-dependent regulation of phosphorylation of the human retinoblastoma gene product. *Science* **246**(4935): 1300-1303.

Montarras, D., Lindon, C., Pinset, C., and Domeyne, P. 2000. Cultured myf5 null and myoD null muscle precursor cells display distinct growth defects. *Biol Cell* **92**(8-9): 565-572.

Morris, E.J. and Dyson, N.J. 2001. Retinoblastoma protein partners. *Adv Cancer Res* **82**: 1-54.

Morris, L., Allen, K.E., and La Thangue, N.B. 2000. Regulation of E2F transcription by cyclin E-Cdk2 kinase mediated through p300/CBP co-activators. *Nat Cell Biol* **2**(4): 232-239.

Muller, H., Bracken, A.P., Vernell, R., Moroni, M.C., Christians, F., Grassilli, E., Prosperini, E., Vigo, E., Oliner, J.D., and Helin, K. 2001. E2Fs regulate the expression of genes involved in differentiation, development, proliferation, and apoptosis. *Genes Dev* **15**(3): 267-285.

Munger, K., Werness, B.A., Dyson, N., Phelps, W.C., Harlow, E., and Howley, P.M. 1989. Complex formation of human papillomavirus E7 proteins with the retinoblastoma tumor suppressor gene product. *Embo J* **8**(13): 4099-4105.

Nabeshima, Y., Hanaoka, K., Hayasaka, M., Esumi, E., Li, S., and Nonaka, I. 1993. Myogenin gene disruption results in perinatal lethality because of severe muscle defect. *Nature* **364**(6437): 532-535.

Nakagami, H., Sekine, M., Murakami, H., and Shinmyo, A. 1999. Tobacco retinoblastoma-related protein phosphorylated by a distinct cyclin-dependent kinase complex with Cdc2/cyclin D in vitro. *Plant J* **18**(3): 243-252.

Narita, M., Nunez, S., Heard, E., Lin, A.W., Hearn, S.A., Spector, D.L., Hannon, G.J., and Lowe, S.W. 2003. Rb-mediated heterochromatin formation and silencing of E2F target genes during cellular senescence. *Cell* **113**(6): 703-716.

Nevins, J.R. 1992. E2F: a link between the Rb tumor suppressor protein and viral oncoproteins. *Science* **258**(5081): 424-429.

Ng, H.H., Zhang, Y., Hendrich, B., Johnson, C.A., Turner, B.M., Erdjument-Bromage, H., Tempst, P., Reinberg, D., and Bird, A. 1999. MBD2 is a transcriptional repressor belonging to the MeCP1 histone deacetylase complex. *Nat Genet* **23**(1): 58-61.

Nguyen, D.X. and McCance, D.J. 2005. Role of the retinoblastoma tumor suppressor protein in cellular differentiation. *J Cell Biochem* **94**(5): 870-879.

Nielsen, S.J., Schneider, R., Bauer, U.M., Bannister, A.J., Morrison, A., O'Carroll, D., Firestein, R., Cleary, M., Jenuwein, T., Herrera, R.E., and Kouzarides, T. 2001. Rb targets histone H3 methylation and HP1 to promoters. *Nature* **412**(6846): 561-565.

Norris, A.W., Chen, L., Fisher, S.J., Szanto, I., Ristow, M., Jozsi, A.C., Hirshman, M.F., Rosen, E.D., Goodyear, L.J., Gonzalez, F.J., Spiegelman, B.M., and Kahn, C.R. 2003. Muscle-specific PPARgamma-deficient mice develop increased adiposity and insulin resistance but respond to thiazolidinediones. *J Clin Invest* **112**(4): 608-618.

Novitch, B.G., Mulligan, G.J., Jacks, T., and Lassar, A.B. 1996. Skeletal muscle cells lacking the retinoblastoma protein display defects in muscle gene expression and accumulate in S and G2 phases of the cell cycle. *J Cell Biol* **135**(2): 441-456.

Novitch, B.G., Spicer, D.B., Kim, P.S., Cheung, W.L., and Lassar, A.B. 1999. pRb is required for MEF2-dependent gene expression as well as cell-cycle arrest during skeletal muscle differentiation. *Curr Biol* **9**(9): 449-459.

Olson, E.N., Arnold, H.H., Rigby, P.W., and Wold, B.J. 1996. Know your neighbors: three phenotypes in null mutants of the myogenic bHLH gene MRF4. *Cell* **85**(1): 1-4.

Parker, M.H., Seale, P., and Rudnicki, M.A. 2003. Looking back to the embryo: defining transcriptional networks in adult myogenesis. *Nat Rev Genet* **4**(7): 497-507.

Patapoutian, A., Yoon, J.K., Miner, J.H., Wang, S., Stark, K., and Wold, B. 1995. Disruption of the mouse MRF4 gene identifies multiple waves of myogenesis in the myotome. *Development* **121**(10): 3347-3358.

Perry, R.L. and Rudnick, M.A. 2000. Molecular mechanisms regulating myogenic determination and differentiation. *Front Biosci* **5**: D750-767.

Peschiaroli, A., Figliola, R., Coltella, L., Strom, A., Valentini, A., D'Agnano, I., and Maione, R. 2002. MyoD induces apoptosis in the absence of RB function through a p21(WAF1)-dependent re-localization of cyclin/cdk complexes to the nucleus. *Oncogene* **21**(53): 8114-8127.

Pownall, M.E., Gustafsson, M.K., and Emerson, C.P., Jr. 2002. Myogenic regulatory factors and the specification of muscle progenitors in vertebrate embryos. *Annu Rev Cell Dev Biol* **18**: 747-783.

Puri, P.L., Iezzi, S., Stiegler, P., Chen, T.T., Schiltz, R.L., Muscat, G.E., Giordano, A., Kedes, L., Wang, J.Y., and Sartorelli, V. 2001. Class I histone deacetylases sequentially interact with MyoD and pRb during skeletal myogenesis. *Mol Cell* **8**(4): 885-897.

Puri, P.L. and Sartorelli, V. 2000. Regulation of muscle regulatory factors by DNA-binding, interacting proteins, and post-transcriptional modifications. *J Cell Physiol* **185**(2): 155-173.

Rawls, A., Morris, J.H., Rudnicki, M., Braun, T., Arnold, H.H., Klein, W.H., and Olson, E.N. 1995. Myogenin's functions do not overlap with those of MyoD or Myf-5 during mouse embryogenesis. *Dev Biol* **172**(1): 37-50.

Rayman, J.B., Takahashi, Y., Indjeian, V.B., Dannenberg, J.H., Catchpole, S., Watson, R.J., te Riele, H., and Dynlacht, B.D. 2002. E2F mediates cell cycle-dependent transcriptional repression in vivo by recruitment of an HDAC1/mSin3B corepressor complex. *Genes Dev* **16**(8): 933-947.

Rea, S., Eisenhaber, F., O'Carroll, D., Strahl, B.D., Sun, Z.W., Schmid, M., Opravil, S., Mechtler, K., Ponting, C.P., Allis, C.D., and Jenuwein, T. 2000. Regulation of chromatin structure by site-specific histone H3 methyltransferases. *Nature* **406**(6796): 593-599.

Relaix, F., Rocancourt, D., Mansouri, A., and Buckingham, M. 2004. Divergent functions of murine Pax3 and Pax7 in limb muscle development. *Genes Dev* **18**(9): 1088-1105.

-. 2005. A Pax3/Pax7-dependent population of skeletal muscle progenitor cells. *Nature* **435**(7044): 948-953.

Ren, B., Cam, H., Takahashi, Y., Volkert, T., Terragni, J., Young, R.A., and Dynlacht, B.D. 2002. E2F integrates cell cycle progression with DNA repair, replication, and G(2)/M checkpoints. *Genes Dev* **16**(2): 245-256.

Ridgeway, A.G. and Skerjanc, I.S. 2001. Pax3 is essential for skeletal myogenesis and the expression of Six1 and Eya2. *J Biol Chem* **276**(22): 19033-19039.

Robertson, K.D., Ait-Si-Ali, S., Yokochi, T., Wade, P.A., Jones, P.L., and Wolffe, A.P. 2000. DNMT1 forms a complex with Rb, E2F1 and HDAC1 and represses transcription from E2F-responsive promoters. *Nat Genet* **25**(3): 338-342.

Ross, J.F., Liu, X., and Dynlacht, B.D. 1999. Mechanism of transcriptional repression of E2F by the retinoblastoma tumor suppressor protein. *Mol Cell* **3**(2): 195-205.

Ross, J.F., Naar, A., Cam, H., Gregory, R., and Dynlacht, B.D. 2001. Active repression and E2F inhibition by pRB are biochemically distinguishable. *Genes Dev* **15**(4): 392-397.

Rotchell, J.M., Blair, J.B., Shim, J.K., Hawkins, W.E., and Ostrander, G.K. 2001. Cloning of the Retinoblastoma cDNA from the Japanese medaka (Oryzias latipes) and preliminary evidence of mutational alterations in chemically-induced retinoblastomas. *Gene* **263**(1-2): 231-237.

Roy, N.K., Ballesteros, A., and Garte, S.J. 1993. Cloning and sequence of the rat retinoblastoma (Rb) gene cDNA. *Nucleic Acids Res* **21**(1): 170.

Rudnicki, M.A., Braun, T., Hinuma, S., and Jaenisch, R. 1992. Inactivation of MyoD in mice leads to up-regulation of the myogenic HLH gene Myf-5 and results in apparently normal muscle development. *Cell* **71**(3): 383-390.

Rudnicki, M.A., Schnegelsberg, P.N., Stead, R.H., Braun, T., Arnold, H.H., and Jaenisch, R. 1993. MyoD or Myf-5 is required for the formation of skeletal muscle. *Cell* **75**(7): 1351-1359.

Ruzinova, M.B. and Benezra, R. 2003. Id proteins in development, cell cycle and cancer. *Trends Cell Biol* **13**(8): 410-418.

Saavedra, H.I., Wu, L., de Bruin, A., Timmers, C., Rosol, T.J., Weinstein, M., Robinson, M.L., and Leone, G. 2002. Specificity of E2F1, E2F2, and E2F3 in mediating phenotypes induced by loss of Rb. *Cell Growth Differ* **13**(5): 215-225.

Sabourin, L.A., Girgis-Gabardo, A., Seale, P., Asakura, A., and Rudnicki, M.A. 1999. Reduced differentiation potential of primary MyoD-/- myogenic cells derived from adult skeletal muscle. *J Cell Biol* **144**(4): 631-643.

Sage, J., Mulligan, G.J., Attardi, L.D., Miller, A., Chen, S., Williams, B., Theodorou, E., and Jacks, T. 2000. Targeted disruption of the three Rb-related genes leads to loss of G(1) control and immortalization. *Genes Dev* **14**(23): 3037-3050.

Schneider, J.W., Gu, W., Zhu, L., Mahdavi, V., and Nadal-Ginard, B. 1994. Reversal of terminal differentiation mediated by p107 in Rb-/- muscle cells. *Science* **264**(5164): 1467-1471.

Seale, P., Ishibashi, J., Holterman, C., and Rudnicki, M.A. 2004a. Muscle satellite cell-specific genes identified by genetic profiling of MyoD-deficient myogenic cell. *Dev Biol* **275**(2): 287-300.

Seale, P., Ishibashi, J., Scime, A., and Rudnicki, M.A. 2004b. Pax7 is necessary and sufficient for the myogenic specification of CD45+:Sca1+ stem cells from injured muscle. *PLoS Biol* **2**(5): E130.

Seale, P., Sabourin, L.A., Girgis-Gabardo, A., Mansouri, A., Gruss, P., and Rudnicki, M.A. 2000. Pax7 is required for the specification of myogenic satellite cells. *Cell* **102**(6): 777-786.

Skapek, S.X., Rhee, J., Kim, P.S., Novitch, B.G., and Lassar, A.B. 1996. Cyclin-mediated inhibition of muscle gene expression via a mechanism that is independent of pRB hyperphosphorylation. *Mol Cell Biol* **16**(12): 7043-7053.

Skapek, S.X., Rhee, J., Spicer, D.B., and Lassar, A.B. 1995. Inhibition of myogenic differentiation in proliferating myoblasts by cyclin D1-dependent kinase. *Science* **267**(5200): 1022-1024.

Song, A., Wang, Q., Goebl, M.G., and Harrington, M.A. 1998. Phosphorylation of nuclear MyoD is required for its rapid degradation. *Mol Cell Biol* **18**(9): 4994-4999.

Stevaux, O., Dimova, D., Frolov, M.V., Taylor-Harding, B., Morris, E., and Dyson, N. 2002. Distinct mechanisms of E2F regulation by Drosophila RBF1 and RBF2. *Embo J* **21**(18): 4927-4937.

Stevaux, O. and Dyson, N.J. 2002. A revised picture of the E2F transcriptional network and RB function. *Curr Opin Cell Biol* **14**(6): 684-691.

Tajbakhsh, S., Rocancourt, D., and Buckingham, M. 1996. Muscle progenitor cells failing to respond to positional cues adopt non-myogenic fates in myf-5 null mice. *Nature* **384**(6606): 266-270.

Tajbakhsh, S., Rocancourt, D., Cossu, G., and Buckingham, M. 1997. Redefining the genetic hierarchies controlling skeletal myogenesis: Pax-3 and Myf-5 act upstream of MyoD. *Cell* **89**(1): 127-138.

Takahashi, C., Bronson, R.T., Socolovsky, M., Contreras, B., Lee, K.Y., Jacks, T., Noda, M., Kucherlapati, R., and Ewen, M.E. 2003. Rb and N-ras function together to control differentiation in the mouse. *Mol Cell Biol* **23**(15): 5256-5268.

Takahashi, Y., Rayman, J.B., and Dynlacht, B.D. 2000. Analysis of promoter binding by the E2F and pRB families in vivo: distinct E2F proteins mediate activation and repression. *Genes Dev* **14**(7): 804-816.

Tallquist, M.D., Weismann, K.E., Hellstrom, M., and Soriano, P. 2000. Early myotome specification regulates PDGFA expression and axial skeleton development. *Development* **127**(23): 5059-5070.

Thomas, D.M., Carty, S.A., Piscopo, D.M., Lee, J.S., Wang, W.F., Forrester, W.C., and Hinds, P.W. 2001. The retinoblastoma protein acts as a transcriptional coactivator required for osteogenic differentiation. *Mol Cell* **8**(2): 303-316.

Thomas, D.M., Johnson, S.A., Sims, N.A., Trivett, M.K., Slavin, J.L., Rubin, B.P., Waring, P., McArthur, G.A., Walkley, C.R., Holloway, A.J., Diyagama, D., Grim, J.E., Clurman, B.E., Bowtell, D.D., Lee, J.S., Gutierrez, G.M., Piscopo, D.M., Carty, S.A., and Hinds, P.W. 2004. Terminal osteoblast differentiation, mediated by runx2 and p27KIP1, is disrupted in osteosarcoma. *J Cell Biol* **167**(5): 925-934.

Tiainen, M., Pajalunga, D., Ferrantelli, F., Soddu, S., Salvatori, G., Sacchi, A., and Crescenzi, M. 1996a. Terminally differentiated skeletal myotubes are not confined to G0 but can enter G1 upon growth factor stimulation. *Cell Growth Differ* **7**(8): 1039-1050.

Tiainen, M., Spitkovsky, D., Jansen-Durr, P., Sacchi, A., and Crescenzi, M. 1996b. Expression of E1A in terminally differentiated muscle cells reactivates the cell

cycle and suppresses tissue-specific genes by separable mechanisms. *Mol Cell Biol* **16**(10): 5302-5312.

Tintignac, L.A., Leibovitch, M.P., Kitzmann, M., Fernandez, A., Ducommun, B., Meijer, L., and Leibovitch, S.A. 2000. Cyclin E-cdk2 phosphorylation promotes late G1-phase degradation of MyoD in muscle cells. *Exp Cell Res* **259**(1): 300-307.

Tremblay, P., Dietrich, S., Mericskay, M., Schubert, F.R., Li, Z., and Paulin, D. 1998. A crucial role for Pax3 in the development of the hypaxial musculature and the long-range migration of muscle precursors. *Dev Biol* **203**(1): 49-61.

Trouche, D. and Kouzarides, T. 1996. E2F1 and E1A(12S) have a homologous activation domain regulated by RB and CBP. *Proc Natl Acad Sci U S A* **93**(4): 1439-1442.

Tsai, K.Y., Hu, Y., Macleod, K.F., Crowley, D., Yamasaki, L., and Jacks, T. 1998. Mutation of E2f-1 suppresses apoptosis and inappropriate S phase entry and extends survival of Rb-deficient mouse embryos. *Mol Cell* **2**(3): 293-304.

Umen, J.G. and Goodenough, U.W. 2001. Control of cell division by a retinoblastoma protein homolog in Chlamydomonas. *Genes Dev* **15**(13): 1652-1661.

Venuti, J.M., Morris, J.H., Vivian, J.L., Olson, E.N., and Klein, W.H. 1995. Myogenin is required for late but not early aspects of myogenesis during mouse development. *J Cell Biol* **128**(4): 563-576.

Vogan, K.J., Underhill, D.A., and Gros, P. 1996. An alternative splicing event in the Pax-3 paired domain identifies the linker region as a key determinant of paired domain DNA-binding activity. *Mol Cell Biol* **16**(12): 6677-6686.

Wade, P.A., Gegonne, A., Jones, P.L., Ballestar, E., Aubry, F., and Wolffe, A.P. 1999. Mi-2 complex couples DNA methylation to chromatin remodelling and histone deacetylation. *Nat Genet* **23**(1): 62-66.

Walsh, K. 1997. Coordinate regulation of cell cycle and apoptosis during myogenesis. *Prog Cell Cycle Res* **3**: 53-58.

Walsh, K. and Perlman, H. 1997. Cell cycle exit upon myogenic differentiation. *Curr Opin Genet Dev* **7**(5): 597-602.

Wang, J., Wilhelmsson, H., Graff, C., Li, H., Oldfors, A., Rustin, P., Bruning, J.C., Kahn, C.R., Clayton, D.A., Barsh, G.S., Thoren, P., and Larsson, N.G. 1999. Dilated cardiomyopathy and atrioventricular conduction blocks induced by heart-specific inactivation of mitochondrial DNA gene expression. *Nat Genet* **21**(1): 133-137.

Wei, C.L., Wu, Q., Vega, V.B., Chiu, K.P., Ng, P., Zhang, T., Shahab, A., Yong, H.C., Fu, Y., Weng, Z., Liu, J., Zhao, X.D., Chew, J.L., Lee, Y.L., Kuznetsov, V.A., Sung, W.K., Miller, L.D., Lim, B., Liu, E.T., Yu, Q., Ng, H.H., and Ruan, Y. 2006. A global map of p53 transcription-factor binding sites in the human genome. *Cell* **124**(1): 207-219.

Wells, J., Graveel, C.R., Bartley, S.M., Madore, S.J., and Farnham, P.J. 2002. The identification of E2F1-specific target genes. *Proc Natl Acad Sci U S A* **99**(6): 3890-3895.

Wells, J., Yan, P.S., Cechvala, M., Huang, T., and Farnham, P.J. 2003. Identification of novel pRb binding sites using CpG microarrays suggests that E2F recruits pRb to specific genomic sites during S phase. *Oncogene* **22**(10): 1445-1460.

Whyte, P., Buchkovich, K.J., Horowitz, J.M., Friend, S.H., Raybuck, M., Weinberg, R.A., and Harlow, E. 1988. Association between an oncogene and an anti-oncogene: the adenovirus E1A proteins bind to the retinoblastoma gene product. *Nature* **334**(6178): 124-129.

Wikenheiser-Brokamp, K.A. 2006. Retinoblastoma family proteins: insights gained through genetic manipulation of mice. *Cell Mol Life Sci* **63**(7-8): 767-780.

Williams, B.A. and Ordahl, C.P. 1994. Pax-3 expression in segmental mesoderm marks early stages in myogenic cell specification. *Development* **120**(4): 785-796.

Woo, M.S., Sanchez, I., and Dynlacht, B.D. 1997. p130 and p107 use a conserved domain to inhibit cellular cyclin-dependent kinase activity. *Mol Cell Biol* **17**(7): 3566-3579.

Wu, L., de Bruin, A., Saavedra, H.I., Starovic, M., Trimboli, A., Yang, Y., Opavska, J., Wilson, P., Thompson, J.C., Ostrowski, M.C., Rosol, T.J., Woollett, L.A., Weinstein, M., Cross, J.C., Robinson, M.L., and Leone, G. 2003. Extra-embryonic function of Rb is essential for embryonic development and viability. *Nature* **421**(6926): 942-947.

Wu, L., Timmers, C., Maiti, B., Saavedra, H.I., Sang, L., Chong, G.T., Nuckolls, F., Giangrande, P., Wright, F.A., Field, S.J., Greenberg, M.E., Orkin, S., Nevins, J.R., Robinson, M.L., and Leone, G. 2001. The E2F1-3 transcription factors are essential for cellular proliferation. *Nature* **414**(6862): 457-462.

Yee, A.S., Shih, H.H., and Tevosian, S.G. 1998. New perspectives on retinoblastoma family functions in differentiation. *Front Biosci* **3**: D532-547.

Zacksenhaus, E., Jiang, Z., Chung, D., Marth, J.D., Phillips, R.A., and Gallie, B.L. 1996. pRb controls proliferation, differentiation, and death of skeletal muscle cells and other lineages during embryogenesis. *Genes Dev* **10**(23): 3051-3064.

Zhang, J.M., Wei, Q., Zhao, X., and Paterson, B.M. 1999a. Coupling of the cell cycle and myogenesis through the cyclin D1-dependent interaction of MyoD with cdk4. *Embo J* **18**(4): 926-933.

Zhang, J.M., Zhao, X., Wei, Q., and Paterson, B.M. 1999b. Direct inhibition of G(1) cdk kinase activity by MyoD promotes myoblast cell cycle withdrawal and terminal differentiation. *Embo J* **18**(24): 6983-6993.

Zhang, W., Behringer, R.R., and Olson, E.N. 1995. Inactivation of the myogenic bHLH gene MRF4 results in up-regulation of myogenin and rib anomalies. *Genes Dev* **9**(11): 1388-1399.

Zhu, L. 2005. Tumour suppressor retinoblastoma protein Rb: a transcriptional regulator. *Eur J Cancer* **41**(16): 2415-2427.

Ziebold, U., Reza, T., Caron, A., and Lees, J.A. 2001. E2F3 contributes both to the inappropriate proliferation and to the apoptosis arising in Rb mutant embryos. *Genes Dev* **15**(4): 386-391.

Zisman, A., Peroni, O.D., Abel, E.D., Michael, M.D., Mauvais-Jarvis, F., Lowell, B.B., Wojtaszewski, J.F., Hirshman, M.F., Virkamaki, A., Goodyear, L.J., Kahn, C.R., and Kahn, B.B. 2000. Targeted disruption of the glucose transporter 4 selectively in muscle causes insulin resistance and glucose intolerance. *Nat Med* **6**(8): 924-928.

Appendix A

Rb and p107 Regulate Preadipocyte Differentiation into White Versus Brown Fat Through Repression of PGC1-α

Purpose

To understand the function of p107 and Rb in determining preadipocyte differentiation into white or brown adipocytes, by means of mouse knockout and cell culture models.

Submission Information

Submitted: 27 February 2005
Accepted: 11 October 2005
Published: 08 November 2005

Reprinted from Cell Metabolism, Vol. 2, Scimè A, Grenier G, Huh M, Gillespie M, Bevilacqua L, Harper M, and Rudnicki M., Rb and p107 Regulate Preadipocyte Differentiation into White Versus Brown Fat Through Repression of PGC1-α, pp. 283-295, copyright (2005), with permission from Elsevier.

Contribution of Co-Authors

Michael Huh conducted the chromatin immunoprecipitation experiments as shown in Figure 7A of the article.

Preface and Discussion of Figure 7 A

White adipose tissue (WAT) is dramatically reduced in *p107*$^{-/-}$ mice. The residual WAT in *p107*$^{-/-}$ displayed elevated levels of UCP-1 and PGC-1α, that are known to be markers of brown adipocytes. Additionally, *p107*$^{-/-}$ WAT tissue had a marked reduction in Rb expression and a much higher proportion of resident preadipocytes. These results suggested to a p107 and Rb dependent inhibition of white adipocyte differentiation. Expression of PGC-1α causes brown adipocyte differentiation, therefore it was posited that Rb may directly inhibit *PGC-1α* expression in differentiating adipocytes. To test this hypothesis, we performed chromatin IPs (ChIPs) using an antibody directed towards Rb on the *PGC-1α* promoter. Binding of Rb on the promoter would indicate a direct relationship between Rb binding and levels of PGC-1α.

Anti-Rb ChIPs on differentiated 3T3-L1 adipocytes revealed binding of Rb complexes on the –1 kb and –4 kb regions of *PGC-1α* promoter (Figure 7A). This provides physical evidence as to Rb's role in directed inhibiting the expression of *PGC-1α* during white adipose differentiation. This mechanism thus explains the in vivo white to brown adipocyte conversion phenotype in the *p107*$^{-/-}$ mice.

Rb and p107 regulate preadipocyte differentiation into white versus brown fat through repression of PGC-1α

Anthony Scimè,[1] Guillaume Grenier,[1,4] Michael S. Huh,[1,2] Mark A. Gillespie,[1,2] Lisa Bevilacqua,[3] Mary-Ellen Harper,[3] and Michael A. Rudnicki[1,2,*]

[1]Molecular Medicine Program, Ottawa Health Research Institute, 501 Smyth Road, Ottawa, Ontario K1H 8L6, Canada
[2]Department of Cellular and Molecular Medicine, Faculty of Medicine, University of Ottawa, 451 Smyth Rd., Ottawa, Ontario K1H 8M5, Canada
[3]Department of Biochemistry, Microbiology and Immunology, Faculty of Medicine, University of Ottawa, 451 Smyth Rd., Ottawa, Ontario K1H 8M5, Canada
[4]Present address: Research Centre on Aging, Faculty of Medicine, University of Sherbrooke, Sherbrooke, Quebec, J1H 4C4, Canada
*Correspondence: mrudnicki@ohri.ca

Summary

The Rb family, Rb, p107, and p130, play important roles in cell cycle control and cellular differentiation, and Rb has been suggested to regulate adipocyte differentiation. We report here that mice lacking *p107* displayed a uniform replacement of white adipose tissue (WAT) with brown adipose tissue (BAT). Mutant WAT depots contained mutilocular adipocytes that expressed elevated levels of PGC-1α and UCP-1 typical of BAT. WAT from *p107*$^{-/-}$ mice contained markedly elevated numbers of adipogenic precursors that displayed downregulated expression of pRb. Consistent with the hypothesis that pRb is required for adult adipocyte differentiation, Cre-mediated deletion of *Rb* in adult primary preadipocytes blocked their differentiation into white adipocytes. Importantly, pRb was observed to bind the *PGC-1α* promoter and repress transcription. Therefore, p107 and pRb regulate PGC-1α expression to control the switch between white and brown adipocyte differentiation from a common pool of presumptive adult progenitors in fat tissue.

Introduction

Adipose tissue is composed of white adipose tissue (WAT) and brown adipose tissue (BAT), two functionally distinct cell types characterized by their opposing metabolic properties (Ailhaud et al., 1992; Cinti, 2000, 2001; Rosen, 2002). Morphologically, white adipocytes are unilocular containing a single lipid-filled vacuole, while brown adipocytes have a multilocular appearance with cytoplasmic lipids arranged as numerous small droplets surrounding the nucleus. The principal role of WAT is the storage and release of triglycerides in response to energy levels. By contrast, BAT dissipates energy in the form of heat through the process of adaptive thermogenesis in response to cold exposure or diet (Cannon and Nedergaard, 2004).

The difference between white and brown adipocytes is apparent at the level of gene expression and by the number and properties of their mitochondria. Brown adipocytes contain many more mitochondria and express increased levels of proteins involved in oxidation. In addition, brown adipocytes specifically express uncoupling protein-1 (UCP-1) which uncouples the electron gradient of the mitochondrial respiratory chain such that O_2 consumption is no longer linked to ATP synthesis (Argyropoulos and Harper, 2002; Cannon and Nedergaard, 2004). Hence, the resulting energy is given off as heat required for newborn mammals, rodents, and hibernators. Adipogenesis of both brown and white adipocytes requires the peroxisome proliferator activated receptor γ (pparγ) and the CCAAT/enhancer binding protein (c/ebp) family of transcription factors. These factors interact to orchestrate a cascade of gene regulatory events culminating in the development of a highly specialized cell type (Rosen and Spiegelman, 2000). In vitro studies with cell lines reveal that differentiation is divided into three phases. An initial growth arrest phase is followed by a period of two or more cell divisions known as mitotic clonal expansion (MCE) (Tang et al., 2003). In the last phase of differentiation, the factors required for adipocyte differentiation and triglyceride storage are expressed.

The anatomical localization of WAT and BAT is normally mutually exclusive with BAT located predominately between the scapulae as a distinct bilobic structure. However, brown adipocytes can be found in WAT and vice versa (Cinti, 2000, 2001). It has not been clear if brown adipocytes within WAT depots are derived from brown specific preadipocytes or the same preadipocytes that give rise to WAT. pparγ coactivator-1 α (PGC-1α) has been implicated as a potential switch for brown adipocyte differentiation (Puigserver and Spiegelman, 2003; Puigserver et al., 1998). PGC-1α is expressed at higher levels in BAT, where it is involved in mitochondrial biogenesis and activation of the *UCP-1* promoter (Puigserver et al., 1998; Wu et al., 1999). Furthermore, the exogenous addition of PGC-1α promoted brown cell features in human white adipocytes as noted by the elevated expression of UCP-1 and increased mitochondrial biogenesis (Tiraby et al., 2003).

There is a large body of evidence that implicates the retinoblastoma susceptibility protein (Rb) family (pocket proteins), including pRb, p107, p130, and their associated proteins, in adipogenesis. Pocket proteins have unique and overlapping functions. The classic role for the Rb family is in the regulation of the cell cycle as repressors of the E2F family of transcription factors (Classon and Dyson, 2001). An additional role for the Rb family is in development and differentiation of many tissues. Mice lacking pRb die in utero displaying defects in erythroid,

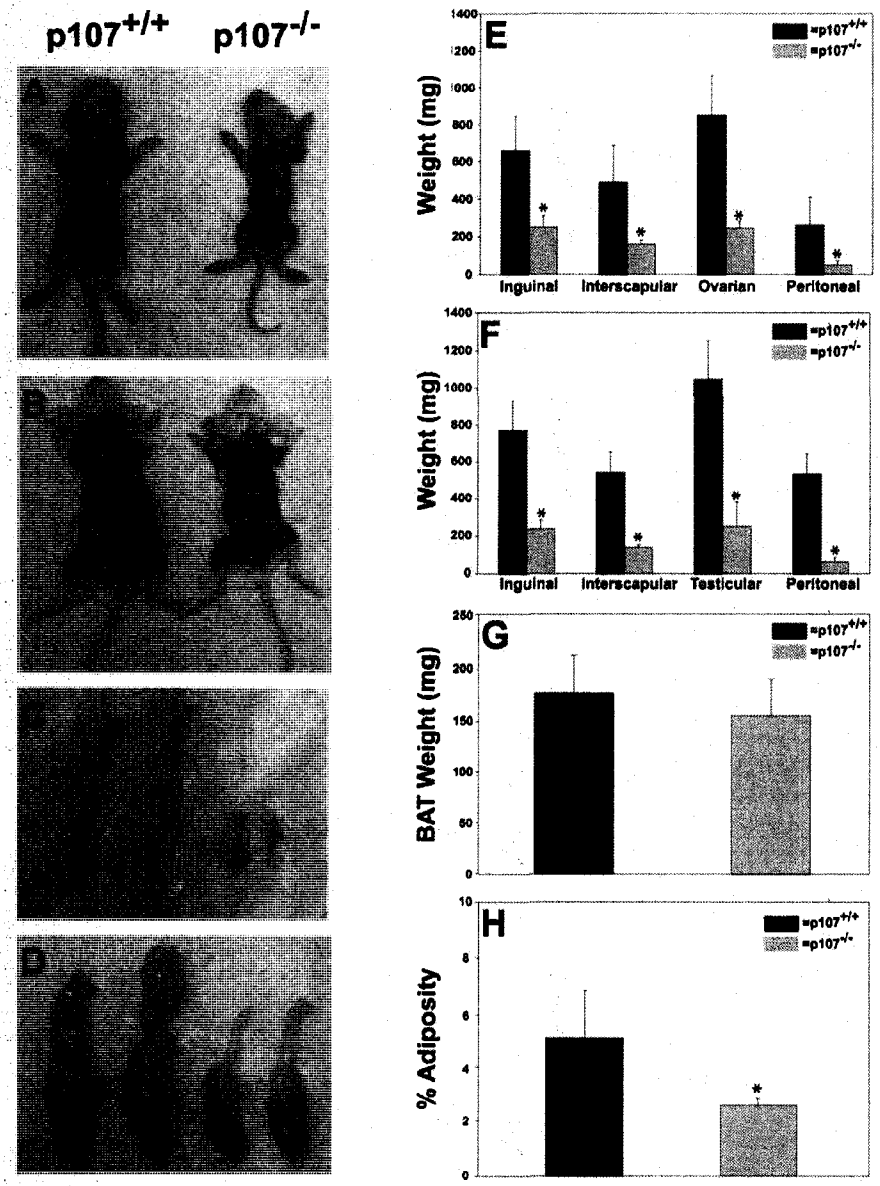

Figure 1. *p107*$^{-/-}$ mice display under developed WAT depots

A) Dorsal view of one-week-old *p107*$^{-/-}$ mouse with *p107*$^{+/+}$, its littermate control. Note the decrease deposition of fat in the inguinal and interscapular regions for the mutant animal.

B) Dorsal view of *p107*$^{-/-}$ and control adult mice. The decrease in fat deposition is apparent in the interscapular and inguinal fat pads.

C) Gross comparison of ovarian fat depots between adult *p107*$^{-/-}$ and wild-type mice.

D) Gross comparison of testicular fat depots between adult *p107*$^{-/-}$ and wild-type mice.

E) Graphical representation for the weight of various fat depots between *p107*$^{-/-}$ and wild-type female mice. Asterisks denote significance for inguinal ($p < 0.002$), interscapular ($p < 0.0002$), ovarian ($p < 0.0005$), and peritoneal ($p < 0.001$).

F) Graphical representation for the weight of various fat depots between *p107*$^{-/-}$ and wild-type male mice. Asterisks denote significance for inguinal ($p < 0.0005$), interscapular ($p < 0.01$), testicular ($p < 0.0002$) and peritoneal ($p < 0.005$).

G) Graphical representation for the weight of interscapular BAT between *p107*$^{-/-}$ and wild-type mice.

H) Graphical representation for the percent adiposity between *p107*$^{-/-}$ and wild-type mice, n = 5. Asterisk denotes significance ($p < 0.007$).

neuronal, and muscle differentiation (Clarke et al., 1992; Jacks et al., 1992; Lee et al., 1992), whereas mice lacking p107 come to term but display myeloid differentiation and cell cycle kinetic abnormalities (LeCouter et al., 1998). The Rb family has been shown to be differentially regulated during adipogenic differentiation of preadipocyte cell lines (Hansen et al., 2004b; Reichert and Eick, 1999; Richon et al., 1997).

Sequestration of Rb family members by SV40 large T antigen inhibits adipocyte differentiation (Cherington et al., 1988; Higgins et al., 1996). Antisense suppression of p107 inhibits adipocyte differentiation of a preadipocyte cell line (May et al., 2001). However, *p107*$^{-/-}$ mouse embryonic fibroblasts (MEFs) exhibit an increase in their adipogenic potential over wild-type controls (Classon et al., 2000; Landsberg et al., 2003). In addition, *Rb*$^{-/-}$ MEFs are unable to differentiate without exogenous pparγ activators (Chen et al., 1996; Hansen et al., 2004a, 1999). Paradoxically, pRb can inhibit adipogenesis by attenuating pparγ's capacity to drive gene expression. This is accomplished by the simultaneous binding of underphosphorylated pRb to pparγ and histone deacetylase 3 (HDAC3) (Fajas et al., 2002a). Lastly, MEFs lacking *Rb* preferentially differentiated into brown adipocytes rather than white adipocytes when differentiation was forced by treatment with a pparγ activator, Rosiglitazone, and triiodothryonine (Hansen et al., 2004a).

In the current study, we demonstrate that the targeted loss of *p107* leads to a severe deficiency in WAT development. WAT depots in *p107*$^{-/-}$ mice were poorly differentiated with elevated numbers of preadipocytes and brown-like adipocytes. More-

over, $p107^{-/-}$ WAT depots exhibited markedly reduced expression of pRb. Using Cre-mediated deletion, we show that pRb directs brown versus white adipocyte fate from a common adult progenitor via regulation of PGC-1α expression. Our experiments reveal for the first time an in vivo role for the Rb family members p107 and pRb in regulating the bipotential capacity of adult preadipocytes to differentiate into white versus brown adipocytes.

Results

Defective WAT development in the absence of p107

The targeted disruption of *p107* in a pure *Balb/c* background caused a runted phenotype, a myeloid proliferative disorder, and altered cell cycle kinetics (LeCouter et al., 1998). Unexpectedly, we also found that $p107^{-/-}$ mice have a severe differentiation deficiency in WAT development. At birth, $p107^{-/-}$ mice appear identical to their heterozygous and wild-type littermates. However, by 5 days, $p107^{-/-}$ neonates were noticeably runted despite the ability to suckle, and about 70% did not survive beyond three weeks of age. Dissection revealed that neonatal mutant mice exhibited extensive deficiencies in WAT depots at all sites examined (Figure 1A).

Decreased WAT mass in $p107^{-/-}$ animals persisted into adulthood. The striking lack of WAT in the interscapular and inguinal depots, as well as the smaller sized testicular and ovarian depots of $p107^{-/-}$ mice were readily apparent (Figures 1B–1D). The size of various WAT depots between mutant and wild-type animals was enumerated by carefully weighing dissected tissue samples (Figures 1E and 1F). In all WAT depots analyzed, including the interscapular, inguinal, testicular, ovarian, and intraperitoneal compartment, both $p107^{-/-}$ male and female mice exhibited severe reductions in the mass of fat pads (Figures 1E and 1F). By contrast, interscapular BAT depots were not significantly different in weight between wild-type and $p107^{-/-}$ mice (Figure 1G). In addition, $p107^{-/-}$ mice had a significantly lower percentage of adipose tissue relative to body weight as compared to their littermate controls (Figure 1H).

The size of WAT in $p107^{-/-}$ animals is not due to hypophagia as food intake for both mutant and control animals was essentially the same at 3.9 ± 0.5g/mouse/day for wild-type as compared to $p107^{-/-}$ mice at 3.5 ± 0.4g/mouse/day. Furthermore, as stool mass and composition for $p107^{-/-}$ mice were found to be normal, the malabsorption of nutrients was ruled out as a factor leading to their small WAT depots.

The reduction of adipose tissue size is reflected by a significantly higher metabolic rate. Indeed the 24 hr mass adjusted total energy expenditure for $p107^{-/-}$ mice is about 12% higher at 0.066 ± 0.001 ml O_2/min/g as compared to 0.058 ± 0.002 ml O_2/min/g for wild-type controls ($n = 6$; $p < 0.05$). Taken together, these results suggest that $p107^{-/-}$ mice have drastically reduced WAT depots perhaps based on a partial replacement of white fat with brown-type fat, providing the basis for an increased metabolic rate.

Histological examination of sections of $p107^{-/-}$ fat pads revealed abnormal WAT adipocyte development at the cellular level in all depots (Figures 2A–2D). $p107^{-/-}$ WAT exhibited very small sized unilocular adipocytes with many multilocular appearing cells. The brown-type characteristic of WAT in the $p107^{-/-}$ mice was corroborated by the presence of UCP-1 in white and brown adipocytes of inguinal fat depots by immunohistochemistry (compare Figure 2E with Figure 2F). In addition, transmission electron microscopy (TEM) revealed that the $p107^{-/-}$ adipocytes within the inguinal pads contained a large number of multilocular cells with small lipid droplets and mitochondria containing many cristae that are consistent with a brown-type phenotype (Cinti, 2001) (compare Figure 2G with Figure 2H). The histological appearance suggested that the reduced fat pad mass was the result of a severe reduction in the differentiation potential of white adipocytes and/or a brown-type differentiation potential.

Increased levels of PGC-1α and UCP-1 in $p107^{-/-}$ WAT

The nature of WAT in $p107^{-/-}$ mice suggested the possibility of a pro-brown adipocyte differentiation program or lack of white adipocyte differentiation (Tsukiyama-Kohara et al., 2001). Substantial evidence exists that UCP-1 and PGC-1α are factors contributing to leanness in various mouse models (Tiraby et al., 2003). UCP-1 is typically not expressed in adult WAT depots and correspondingly, we did not detect UCP-1 in the interscapular WAT depot (IWAT) of adult wild-type mice (Figure 3A). By contrast, $p107^{-/-}$ interscapular fat pads expressed high levels of UCP-1 supporting the assertion of greatly enhanced brown adipogenesis in the absence of WAT development (Figure 3A, lanes 3–6).

The transcription factor PGC-1α regulates the expression levels of *UCP-1* mRNA within white adipocytes and is also involved in the expression of genes required for oxidative phosphorylation (Puigserver and Spiegelman, 2003). Hence, the transcriptional expression pattern of *PGC-1α* and *UCP-1* was evaluated in the inguinal WAT (IgWAT) and IWAT of mutant and wild-type mice by qRT-PCR. We detected markedly upregulated levels of *PGC-1α* and *UCP-1* mRNA in $p107^{-/-}$ WAT of the interscapular and inguinal fat pads (Figures 3B and 3C). These results confirm an uncharacteristically high number of brown-type adipocytes within WAT of $p107^{-/-}$ mice. Taken together, these experiments indicate that in the absence of p107, preadipocytes that would normally differentiate into white adipocytes have undergone default differentiation into brown-type adipocytes.

WAT differentiation deficit of $p107^{-/-}$ adult preadipocytes in vivo but not in vitro

An indication that the WAT defect was due to inefficient differentiation of adult adipocyte precursors was the appearance of the postnatal liver. Macroscopic observation of $p107^{-/-}$ livers at five days of age revealed an unhealthy yellow appearance, indicative of excess lipid deposition (Figure 4A). Lipid deposition was confirmed by histological examination of H&E-stained liver sections that revealed microvesicular vacuolization. Sudan Black lipid staining further demonstrated a profound lipid accumulation and steatosis in the liver (Figure 4B). The liver pathology was strongly consistent with the notion that insufficient functional WAT was present at this stage of the mutant animal's life, which is normally required to store the dietary fat load contained in the mother's milk. Fatty livers for $p107^{-/-}$ mice were manifested only during this stage in their life. After weaning

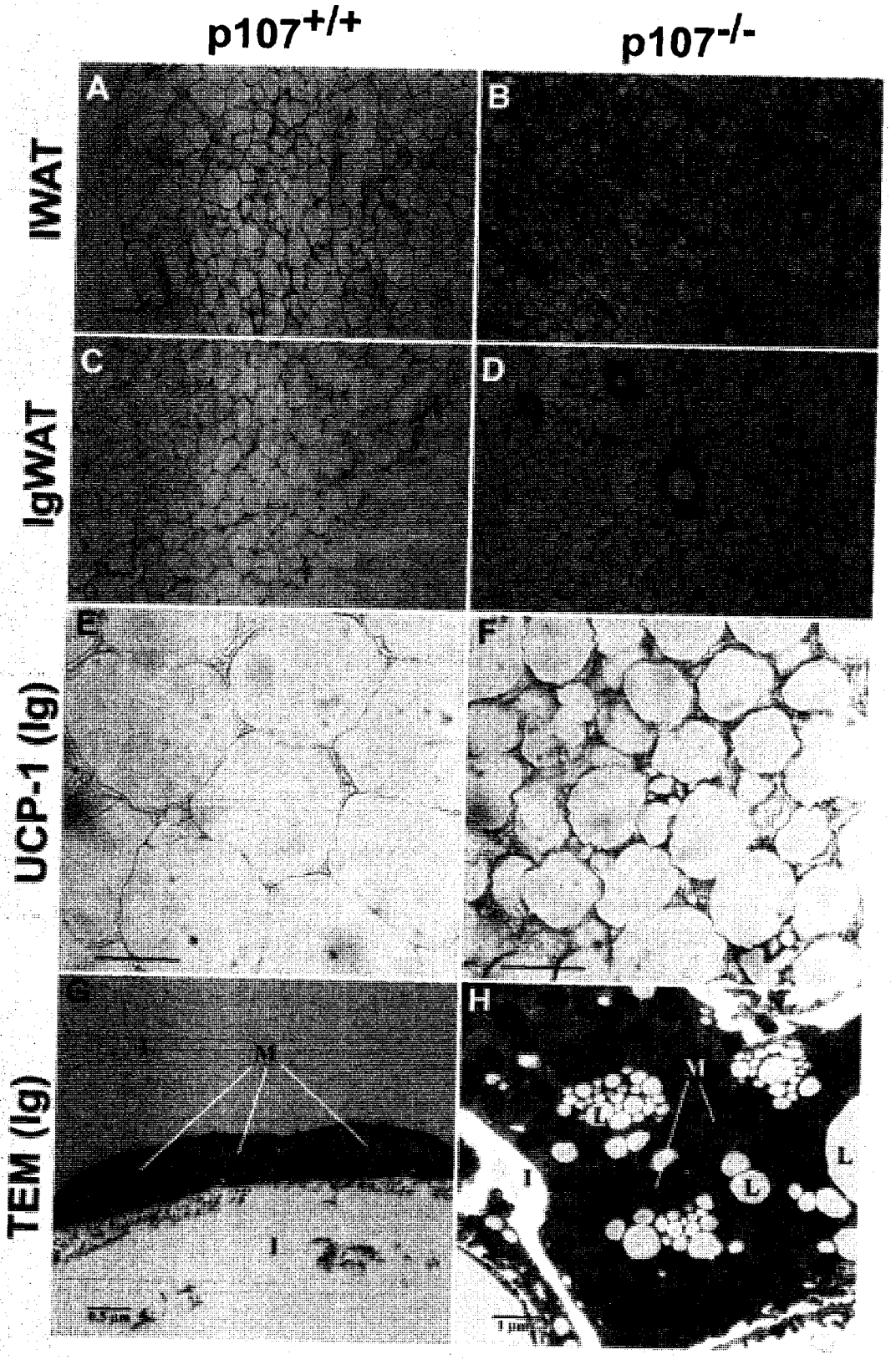
p107+/+
p107-/-
IWAT
IgWAT
UCP-1 (Ig)
TEM (Ig)
A
B
C
D
E
F
G
H
M
I
L
0.5 μm
1 μm

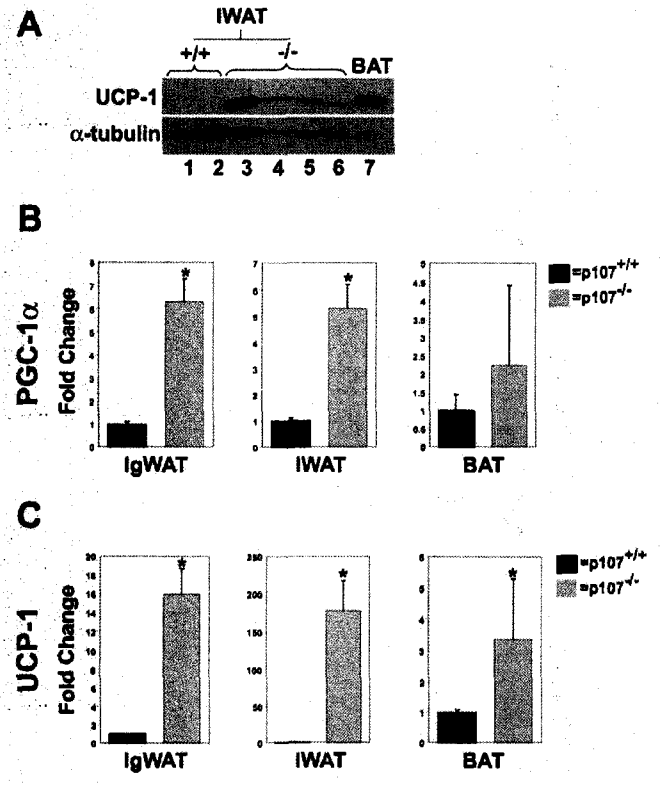

Figure 3. WAT from *p107*$^{-/-}$ mice has elevated levels of UCP-1 and PGC-1α

A) Western blot for UCP-1 on tissue lysates from the interscapular regions excluding the BAT bilobe portion. Two different adult wild-type mice (lanes 1 and 2) and four different adult *p107*$^{-/-}$ mice (lanes 3–6) were used for analysis. UCP-1 expression persists in the *p107*$^{-/-}$ animals through adulthood.

B) Graphical representation of the relative fold change expression between *p107*$^{-/-}$ and wild-type mice for *PGC-1α* in IgWAT, IWAT, and BAT using qRT-PCR. Asterisks denotes significance ($p < 0.002$) and ($p < 0.0008$) for IgWAT and IWAT, respectively.

C) Graphical representation of the relative fold change expression between *p107*$^{-/-}$ and wild-type mice for *UCP-1* in IgWAT, IWAT, and BAT, using qRT-PCR. Asterisks denotes significance ($p < 0.005$), ($p < 0.003$), and ($p < 0.03$) for IgWAT, IWAT, and BAT, respectively. For all experiments, BAT was derived solely from the interscapular bilobe section, whereas WAT was derived from inguinal depots only.

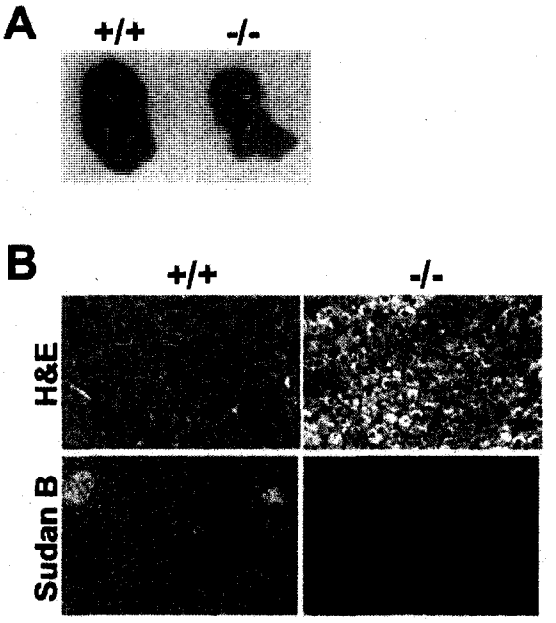

Figure 4. Newborn *p107*$^{-/-}$ mice have profound lipid deposition in their livers

A) Gross physical observation of the livers from *p107*$^{-/-}$ and wild-type littermate at 7 days postnatal. Note the yellow hue of the mutant liver.

B) H&E and Sudan Black staining of liver tissue sections. For H&E staining, clear areas represent lipid droplets within *p107*$^{-/-}$ hepatocytes (400×). For Sudan Black staining, darker areas represent lipid droplets (200×).

onto a standard mouse chow diet, their liver returned to a normal appearance, aided by an increase in daily energy expenditure. Together, these results revealed a hitherto unknown requirement for the Rb family member p107 in the development and maturation of WAT.

Transplantation experiments were performed to test if the deficit in *p107*$^{-/-}$ WAT was due to a cell-autonomous defect of precursor cells to differentiate into adipocytes. IgWAT was excised from a 2-month-old wild-type donor animal and transplanted on the flank of a *p107*$^{-/-}$ recipient from the same litter (Chao et al., 2000; Gavrilova et al., 2000) (Figure 5A). The donor wild-type tissue before transplantation was essentially composed of uniform white unilocular adipocytes (Figure 5B). One month posttransplant, the adipocytes within the transplanted tissue had dramatically increased in size (compare Figure 5B with Figure 5C). By contrast, the endogenous inguinal white adipocytes of the recipient mutant mouse remained small (Figure 5D). Moreover, transplantation of *p107*$^{-/-}$ fat pad did not result in formation of a normal WAT depot (data not shown). Therefore, these experiments demonstrate that the lipid storage deficit in mutant WAT was caused by a cell-autonomous insufficiency, consistent with an inability of *p107*$^{-/-}$ adipose precursors to differentiate into white adipocytes. However, at this time we cannot rule out the possibility that white adipocytes from *p107*$^{-/-}$ mice have a fatty acid storage defect.

To investigate whether p107 deficiency results in a preadipocyte differentiation shortfall, cells were isolated from *p107*$^{-/-}$

Figure 2. WAT lacking *p107* exhibit brown type adipocytes and poorly differentiated white adipocytes

Hematoxylin and Eosin (H&E) staining of interscapular WAT (IWAT) for *p107*$^{+/+}$ and *p107*$^{-/-}$, respectively (**A and B**), and inguinal WAT (IgWAT) for *p107*$^{+/+}$ and *p107*$^{-/-}$, respectively (**C and D**). *p107*$^{-/-}$ mice have smaller adipocytes and many undifferentiated cells in all their fat depots. Arrows denote areas of multilocular appearance for *p107*$^{-/-}$ inguinal depots. The scale bar represents 50 μm for (**A**)–(**D**). Immunostaining of UCP-1 *p107*$^{+/+}$ (**E**) and *p107*$^{-/-}$ (**F**) IgWAT; the scale bar represents 25 μm. TEM for *p107*$^{+/+}$ (**G**) and *p107*$^{-/-}$ (**H**) IgWAT. Abbreviations are as follows: M, mitochondria; L, lipid; I, intracellular space; and N, nucleus.

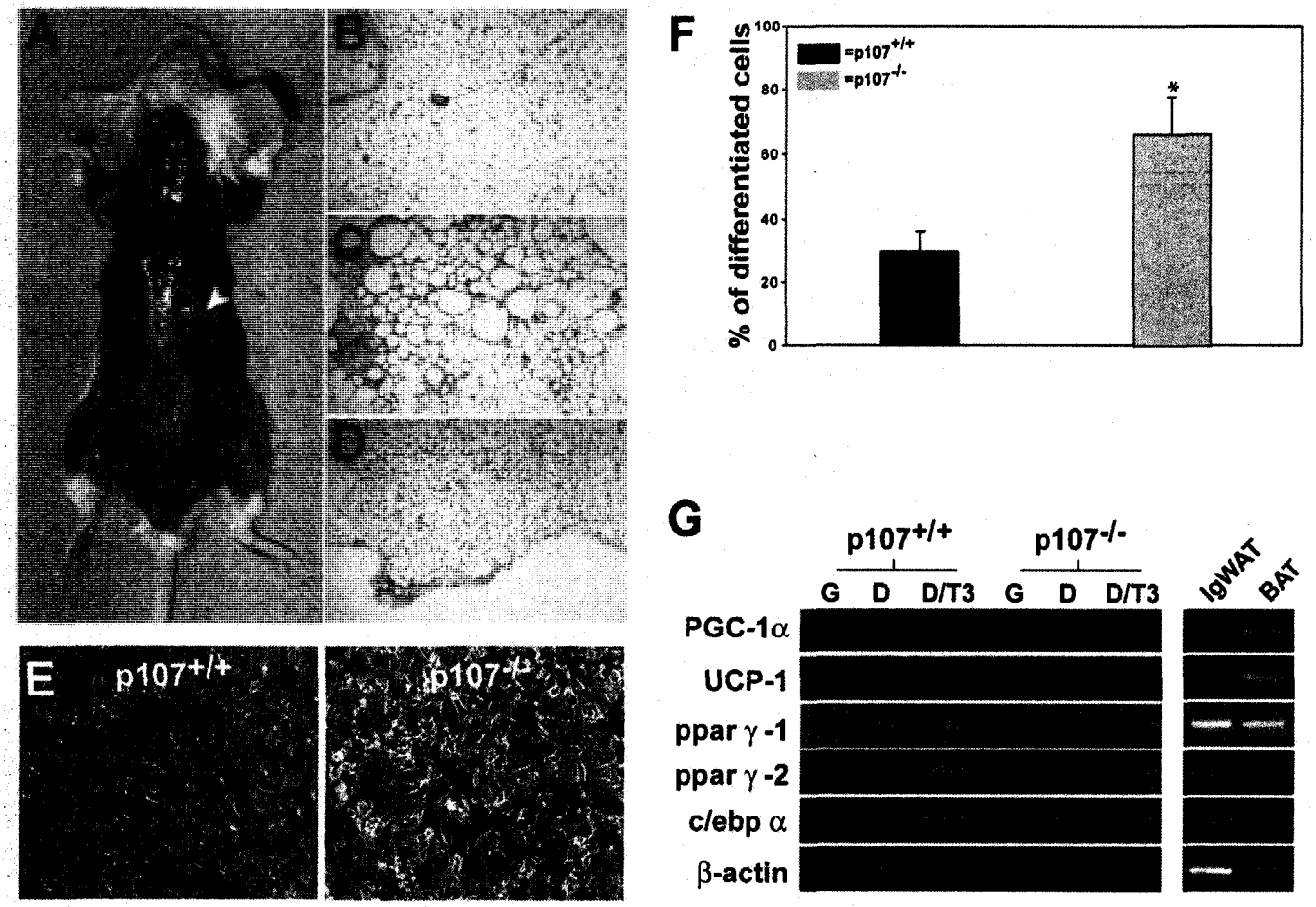

Figure 5. Adult preadipocytes lacking p107 display an in vivo differentiation deficit

A) Wild-type white adipocytes transplanted into mutant recipients dramatically increase in size. Dorsal view of *p107*$^{-/-}$ recipient mouse with wild-type transplanted tissue denoted by arrowhead.

B) H&E staining of wild-type tissue before transplant.

C) H&E section of tissue one month after transplant, showing a large amount of lipid deposition.

D) H&E staining of recipient's endogenous inguinal tissue. Note the small sized adipocytes suggesting *p107*$^{-/-}$ WAT differentiation deficiency. Magnification was at 100× for all tissue sections.

E) Oil Red O staining of representative views for differentiated Sca-1^{+}CD31^{-}Lin^{-}-sorted cells from wild-type and *p107*$^{-/-}$ mice.

F) Graphical representation of the differentiation potential of sorted cells between *p107*$^{-/-}$ and wild-type mice. Asterisk denotes significance ($p < 0.004$). The Sca-1^{+} CD31^{-}Lin^{-} fraction from *p107*$^{-/-}$ mice contains many more undifferentiated adipocyte precursors.

G) RT-PCR evaluation of adipogenic factors of growing (G), 7 days postdifferentiation (D), and 7 days postdifferentiation in the presence of Ros and T_3 (D/T3) for WAT preadipocytes from *p107*$^{+/+}$ and *p107*$^{-/-}$ mice. Note the expression of *PGC-1α* and *UCP-1* only in the *p107*$^{-/-}$ treated samples.

and wild-type adult interscapular BAT and IgWAT, enumerated, and their differentiation potential assessed.

BAT from both *p107* mutant and wild-type animals contained about the same number of cells per gram of isolated tissue (Figure 1G and data not shown). However, *p107*$^{-/-}$ IgWAT contained 61% ± 15% more cells (excluding adipocytes), as compared to wild-type IgWAT. These results suggested that WAT-derived p107-deficient preadipocytes exhibit a cell-autonomous differentiation deficit that results in a high portion of the cells to either remain undifferentiated or undergo default differentiation into brown adipose.

This idea was addressed by analyzing the differentiation capacity of *p107*$^{-/-}$ adult white primary adipocyte precursors in vitro. To facilitate isolation of adult preadipocytes, we developed a novel method for purification of an enriched population from adult tissues. The cell surface antigen Sca-1, used routinely in purification protocols for various progenitor cells (Asakura and Rudnicki, 2002), is expressed on primary preadipocytes as assayed by in vitro differentiation studies (unpublished data). Therefore, fluorescent-activated cell sorting was used to isolate a population enriched in preadipocytes by positively selecting for Sca-1 and by removing endothelial cells that express CD31 and mature blood cell lineages (Lin). Interestingly, mutant fat pads contained 30% more Sca-1^{+}CD31^{-}Lin^{-} cells relative to wild-type adipose tissue, supporting the notion that *p107* deficiency impairs preadipocyte differentiation. To investi-

gate their in vitro differentiation capacity, equal numbers of Sca-1$^+$CD31$^-$Lin$^-$ cells isolated from IgWAT from wild-type and mutant animals were plated, grown to confluence, and allowed to differentiate in normal differentiation media for 10 days. Surprisingly, isolated adult *p107*$^{-/-}$ precursor cells displayed robust adipocyte differentiation potential, as assessed by Oil Red O staining (Figures 5E and 5F). Taken together, this data suggested that undifferentiated WAT precursors account for some of the increased cell number observed in isolated mutant tissue and that the in vivo differentiation deficiency was rescued in part by cell culture conditions in vitro.

We also analyzed the in vitro brown adipocyte differentiation potential of *p107*$^{-/-}$ preadipocytes using gene expression analysis for *PGC-1α* and *UCP-1* (Figure 5G). With a pro-brown adipocyte differentiation regimen, containing the pparγ ligand, Rosiglitazone (Ros), and the hormone, triiodothyronine (T_3), *p107*$^{-/-}$ preadipocytes expressed *PGC-1α* and *UCP-1* after 7 days postdifferentiation. Wild-type preadipocytes failed to express these thermogenic markers suggesting that under the appropriate environment *p107*$^{-/-}$ preadipocytes from WAT are prone to differentiate into brown-type adipocytes.

Rb levels are dramatically reduced in *p107*$^{-/-}$ adult preadipocytes

Rb is essential for adipogenesis to occur yet paradoxically it inhibits adipogenesis by binding to pparγ with HDAC3. To investigate the potential involvement of Rb in the differentiation deficiency, we examined its expression in fat tissues in vivo and cultured adult primary preadipocytes during differentiation in vitro.

Western blot analysis of wild-type primary adult adipocyte precursors from IgWAT revealed that modulation of p107 and pRb levels occurred during the growth and differentiation program. p107 along with pRb were upregulated within 72 hr of differentiation in serum containing media (Figure 6A). However, when differentiating in the presence of serum free media, without a growth phase, the expression of p107 immediately disappeared within 24 hr, yet pRb expression was maintained albeit at drastically reduced levels.

We also assessed the expression and relevance of pRb in wild-type and *p107*$^{-/-}$ WAT differentiation. Importantly, as precursors for white adipocytes are thought to express pRb (Hansen et al., 2004a), the level of pRb in isolated primary adult preadipocytes from IgWAT was assessed. Interestingly, pRb was barely detectable in freshly isolated mutant preadipocytes by Western blot analysis (Figure 6B). In addition, lowly expressed pRb in *p107*$^{-/-}$ preadipocytes was present in an under phosphorylated state. Hence, these results correlated with the in vivo reduction in white adipocyte differentiation in the absence of p107.

We hypothesized that the apparent difference between in vivo and in vitro differentiation of preadipocytes from *p107*$^{-/-}$ mice was a consequence of differential expression of pRb. Whereas freshly isolated adult preadipocytes from *p107*-deficient mice displayed markedly reduced under phosphorylated pRb expression, cultured *p107*$^{-/-}$ preadipocytes displayed a normal expression of pRb during growth and differentiation in vitro (Figure 6C). This suggests that the large proportion of undifferentiated adipocyte precursors observed in vivo (Figures 5E and 5F), differentiated after isolation and culture in vitro due to the upregulation of pRb. Furthermore, our experiments reveal an unexpected difference in the regulation of pRb by p107 that is active in tissue but is obscured under tissue culture conditions.

pRb is required for adult preadipocyte differentiation

Our experiments suggested that p107-deficient adult preadipocytes were incapable of upregulating *Rb* in vivo. Therefore, the role for pRb in adult primary preadipocyte differentiation was directly assessed in vitro. Previous studies have not evaluated the differentiation capacity of pRb-deficient adult primary preadipocytes due to embryonic lethality (Clarke et al., 1992; Jacks et al., 1992; Lee et al., 1992). To investigate the requirement for pRb in adult adipogenesis, we FACS-purified Sca-1$^+$CD31$^-$Lin$^-$preadipocytes from the inguinal depots of adult mice carrying homozygously floxed *Rb* allele (*Rb*$^{loxP/loxP}$) (Marino et al., 2000). Uninfected *Rb*$^{loxP/loxP}$ cells express pRb normally, whereas cells infected with an adenovirus expressing Cre recombinase (Ad-Cre) (Anton and Graham, 1995) have the *Rb*$^{loxP/loxP}$ allele deleted resulting in a null mutation.

Preadipocytes isolated from IgWAT of *Rb*$^{loxP/loxP}$ adult mice were infected with Ad-Cre or control adenovirus expressing LacZ (Ad-LacZ). After 14 days of differentiation, the Ad-LacZ-infected cells exhibited normal kinetics of differentiation (Figure 6D). By contrast, cells infected with Ad-Cre exhibited an almost complete block in adipogenic differentiation. These data confirm that pRb is required for the differentiation of preadipocytes into white adipose in adult animals.

Rb-deficient preadipocytes exhibited reduced expression of a key regulator of adipogenic differentiation *pparγ-2* (Figure 6E). Importantly, addition of Ros and T_3, to the differentiation medium, resulted in a dramatic increase in the levels of *pparγ-2* and rescued adipogenic differentiation (Figures 6D and 6E). However, the consequence of forced differentiation in the absence of pRb resulted in the formation of brown adipocytes as evidenced by the expression of *PGC-1α* and *UCP-1* (Figure 6E). Therefore, as has been observed for *Rb*$^{-/-}$ MEFs (Hansen et al., 2004a), Ros can bypass the need for pRb for differentiation of adult primary preadipocytes and, under the correct stimuli, produce brown-type adipocytes as is the case for p107$^{-/-}$ preadipocytes.

pRb regulates the expression of *PGC-1α*

We further tested the relationship between Rb and PGC-1α by chromatin immunoprecipitation (ChIP) assay on the preadipocyte cell line 3T3-L1 (Figure 7A). pRb binding was assessed on regions representing 4 Kb upstream of the transcriptional start site of the *PGC-1α* gene. pRb was demonstrated to bind at locations –1 Kb and –4 Kb of the *PGC-1α* promoter, but not the –2 Kb (and –3 Kb data not shown) region during differentiation, with or without the addition of Ros (Figure 7A). The interaction was specific to the *PGC-1α* promoter as pRb did not bind to the *histone H4* promoter and the ability of the pRb antibody to recognize itself bound to other promoters was verified with ChIP on a known target, the *p107* locus.

We next tested the ability of pRb to regulate the *PGC-1α* promoter. Reporter assays revealed full-length pRb significantly inhibited *PGC-1α* expression from the 3.1 Kb proximal promoter of mouse *PGC-1α* in a dose dependent manner, but it had no effect on the control promoter consisting of four repeats of the right E-box of the muscle creatine kinase enhancer (Figure 7B). In addition, pRb might direct the activation of PGC-

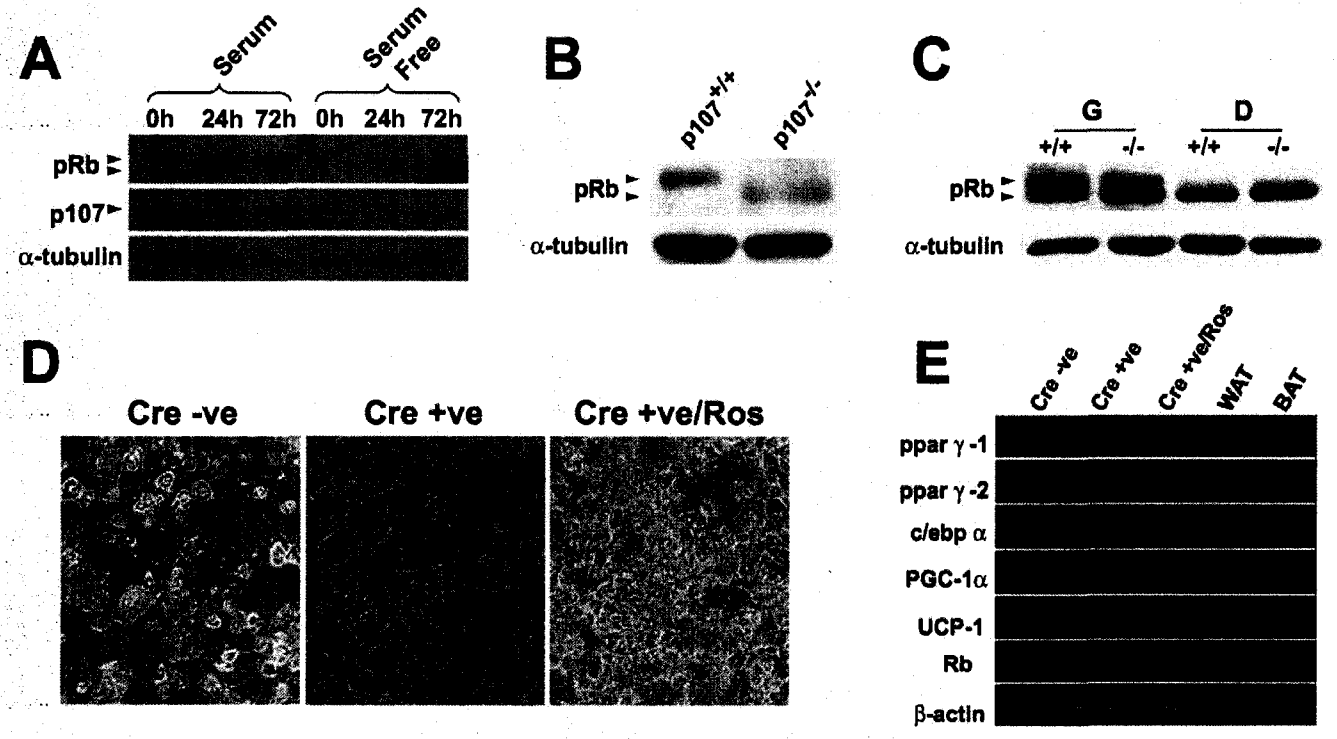

Figure 6. Differentiation of adult primary white preadipocytes requires pRb

A) pRb and p107 differentiation expression pattern in primary adipocytes from IgWAT over a 72 hr time period under serum and serum-free conditions. pRb is expressed under both conditions, but p107 is not.

B) Western blot for pRb in freshly isolated adult primary preadipocyte lysates. Note the barely detectable levels of and under phosphorylated state of pRb for $p107^{-/-}$ adipocyte precursors.

C) Western blot for pRb in growing (G) and 5 days differentiated (D) for both wild-type (+/+) and $p107^{-/-}$ (–/–) adult primary preadipocytes. pRb levels are upregulated once plated as compared to freshly isolated adult preadipocytes.

D) Representative microscopic view of $Rb^{loxP/loxP}$ Sca-1$^+$CD31$^-$Lin$^-$ sorted cells with Cre recombinase untreated (Cre –ve), Cre recombinase treated (Cre +ve), and Cre recombinase treated and supplemented with rosiglitazone and T_3 (Cre +ve/Ros) under serum-differentiation conditions for 7 days. Note the lack of differentiation with Cre-treated cells and the robust differentiation of these cells with Ros and T_3.

E) RT-PCR evaluation of adipogenic factors and pRb in Cre recombinase untreated, Cre recombinase treated, and Cre recombinase treated with Ros and T_3 of $Rb^{loxP/loxP}$ Sca-1$^+$CD31$^-$Lin$^-$ sorted cells under differentiation conditions for 7 days. Note that pRb independent differentiation results in activation of *PGC1-α* and *UCP-1*.

1α through interactions with E2F. Indeed, the repression by pRb was significantly augmented in the presence of E2F4, whereas an pRb deletion mutant deficient in E2F binding (Δ663) had no influence on the promoter (Sellers et al., 1998).

Hence, these experiments unequivocally demonstrate that pRb functions as a switch to regulate the developmental fate between white over brown adipocyte differentiation of bona fide adult preadipocytes by negatively regulating the expression of *PGC-1α* that is involved in promoting UCP-1 expression. We thus conclude that the preferential differentiation of preadipocytes into brown fat in $p107^{-/-}$ mice is likely due to a dysregulation of pRb that is manifested only in vivo.

Discussion

The Rb family of proteins play an important role in regulating adipocyte differentiation (Altiok et al., 1997; Chen et al., 1996; Cherington et al., 1988; Fajas et al., 2002b; Hansen et al., 2004a, 1999, 2004b; Higgins et al., 1996; May et al., 2001; Porse et al., 2001; Reichert and Eick, 1999; Richon et al., 1997; Slomiany et al., 2000). Our experiments demonstrate that p107 is required for white adipocyte differentiation in vivo and suggest that this lack of differentiation is a result of an inability to appropriately regulate pRb.

We show, by multiple lines of evidence, that $p107^{-/-}$ mice have a WAT differentiation disorder, exemplified by poorly differentiated white adipocytes and undifferentiated adipocyte precursors. $p107^{-/-}$ WAT depots appear smaller than their wild-type counterparts, their size substantially reduced in every depot that was assessed (Figure 1). Moreover, the histological appearance of WAT in $p107^{-/-}$ mice also reveals atypical differentiation with small unilocular and multilocular cells expressing UCP-1 (Figure 2). $p107^{-/-}$ mice never fully develop WAT in their interscapular depot, as evidenced by the expression of UCP-1 protein, a marker for brown adipocytes (Figure 3A). The impaired development of WAT is underscored by the significant increase of the transcriptional expression of *UCP-1* and its activator *PGC-1α* in the $p107^{-/-}$ inguinal depots (Figures 3B and

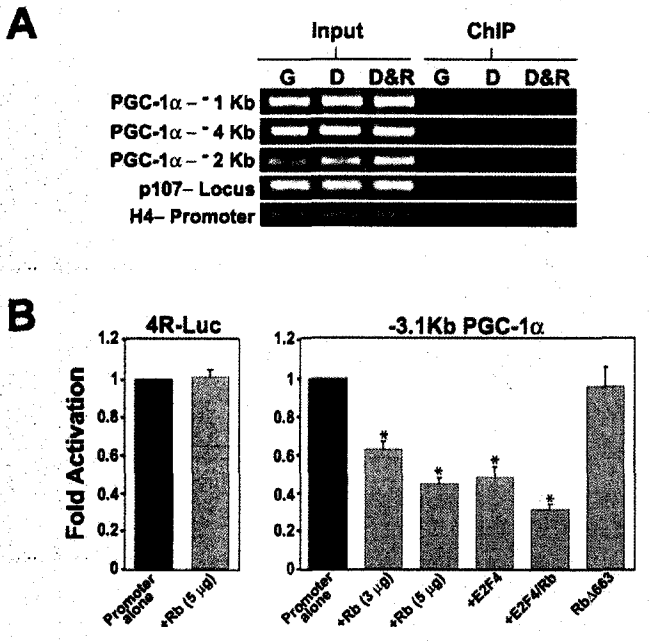

Figure 7. pRb regulates the expression of PGC-1α

A) Chromatin immunoprecipitation revealed pRb binding to the *PGC-1α* promoter. Distances upstream of the *PGC-1α* transcription start denoted by –1 Kb, –2 Kb, and –4 Kb, the *histone H4* promoter and the p107 locus. G, D, and D&R denote growth, differentiation, and differentiation with Ros, respectively.

B) pRb represses *PGC1α*-promoter activity following calcium stimulation. 3T3-L1 cells were transfected with a luciferase reporter driven by four repeats of the right E-box of the MCK enhancer (4R-Luc) or the 3.1kb region upstream of the ATG start site of the *PGC-1α* gene alone and with indicated amounts of pcmvRb pcmvHAE2F-4, pcmvRB and pcmvHAE2F-4, or RbΔ663. Transfection efficiency was normalized to *Renilla*-luciferase expression. Error bars represent the standard error of the mean (n = 9). Asterisks correspond to significant difference ($p < 0.0001$).

3C). The presence of brown adipocytes within WAT depots represents a lean phenotype in many different genetic settings (Cederberg et al., 2001; Tiraby and Langin, 2003; Tsukiyama-Kohara et al., 2001).

The histological and cell sorting data discloses a large number of undifferentiated preadipocytes within the different $p107^{-/-}$ WAT sections. p107 might simply regulate adipocyte progenitor self-renewal, its absence increasing their availability. This idea is analogous to a recent finding that demonstrates p107-deficient adult brains contain expanded neural stem cell pools in vivo that are capable of differentiating in vitro (Vanderluit et al., 2004).

There is a large body of evidence describing the necessity of pRb for proper adipogenesis to occur. This has previously been documented with isolated preadipocyte cell lines or immortalized MEFs. For example, the ability of SV40 large T to block adipocyte differentiation is at the level of sequestering pRb (Cherington et al., 1988; Higgins et al., 1996). To date, there has been no in vivo evidence for the requirement of pRb for adipose development and adult primary cell adipogenesis, unlike the evidence available for muscle development (de Bruin et al., 2003; Wu et al., 2003; Zacksenhaus et al., 1996) and adult primary myoblast differentiation (Huh et al., 2004). Our studies reveal the in vivo prerequisite of pRb for proper white adipocyte development and adult primary preadipocyte differentiation.

For the $p107^{-/-}$ mice we observed extremely low levels of pRb in preadipocytes isolated from WAT that is correlated with a lack of white adipocyte differentiation (Figure 6B). Previously, it has been impossible to study a direct role for pRb in primary adipogenesis. $pRb^{-/-}$ mice die in utero and those that come to term, by bypassing pRb's embryonic function, die shortly after with many skeletal muscle abnormalities (Cobrinik et al., 1996; Wu et al., 2003). In this study, the Cre/lox-P system provides a powerful tool to dissect a role for pRb in adult primary preadipocytes. With the Cre inactivation of *Rb*, we demonstrate that primary adipocyte precursors isolated from pure white fat depots of adult animals require pRb for differentiation. In vitro, the requirement for p107 is potentially bypassed by the serum conditions that contain supra-physiological levels of growth factors. This results in higher expression and subsequent inactivation of pRb, allowing $p107^{-/-}$ adult preadipocytes to differentiate (Figure 6B and 6C). Taken together, this data underscores the central importance of pRb in white adipocyte differentiation.

Our results suggest that $p107^{-/-}$ preadipocytes that are unable to differentiate in vivo are able to differentiate in vitro and that this difference is due to variable expression of pRb. One possibility is that in vivo p107 is required for pRb to function efficiently during differentiation. This might occur at the level of MCE promoting the expression, and subsequent posttranslational modification of pRb by phosphorylation that is required to dissociate the pparγ-histone deacytalase 3-pRb complex (Fajas et al., 2002a). Indeed, the expression level of p107 has been demonstrated to be elevated during MCE in adipocyte cell lines (Hansen et al., 2004b; May et al., 2001; Reichert and Eick, 1999; Richon et al., 1997). Our observations indicate that p107 and pRb protein expression is elevated during adult primary adipocyte differentiation in serum conditions at a time when MCE is taking place. However, in serum free conditions where MCE is absent, p107 is no longer expressed and pRb is expressed marginally (Figure 6A). Hence, adult preadipocytes (Figures 2 and 5) and $Rb^{-/-}$ MEFs (Fajas et al., 2002a) might differentiate inefficiently into white adipocytes, differentiate into brown-type adipocytes (Figures 2, 3, 5, 6D, and 6E) or accumulate in G2/M, endoreduplicate and undergo apoptosis (Fajas et al., 2003). In vitro, the requirement for p107 is potentially bypassed by the serum conditions inducing the expression and subsequent posttranslational modification of pRb (Figure 6C). Future experimentation to examine the capacity of $p107^{-/-}$ preadipocytes to enter MCE in vivo is required to settle this issue.

Our experiments demonstrate that Rb family members, p107 and pRb, act as a molecular switch to regulate the differentiation of brown versus white adipose from a common progenitor. Our data suggests that pRb acts as a negative regulator of PGC-1α expression. Induction of PGC-1 α is capable of transforming WAT cells into brown adipocytes by forcing the expression of UCP-1 and other prooxidative molecules (Tiraby et al., 2003). Here we show that $Rb^{-/-}$ primary adult preadipocytes of WAT origin can differentiate into brown type cells that express UCP-1 and PGC-1α. Our data also suggests that the fat type differentiation occurs via the control of *PGC-1α* expression by pRb. ChIP revealed that pRb is bound to at least two regions of the *PGC-1α* promoter in differentiated preadipocytes (Figure

7A). In addition, reporter assays with the 3.1 Kb proximal promoter of *PGC-1α* confirm that pRb binding represses promoter activity (Figure 7B). pRb might act with HDACs to silence the activity of the *PGC-1α* promoter (Czubryt et al., 2003). The loss of pRb before differentiation would drive the activity of PGC-1α, thus promoting a brown-type cell phenotype. On the other hand, posttranslational modification of pRb by phosphorylation, would also derepress the promoter. This would be required for cellular remodeling during adaptive thermogenesis, for example, pRb is inactivated by phosphorylation during sustained cold exposure (Hansen et al., 2004a). The concept for pRb interacting with a metabolic gene promoter is not out of the ordinary. Indeed, a recent report describes the association of E2F4 on gene promoters involved with mitochondrial biogenesis, coregulated by nuclear respiratory factor-1 (NRF1) (Cam et al., 2004). Interestingly, p107 has also been shown to be located on adipogenic gene promoters in a complex with E2F (Fajas et al., 2002b; Timchenko et al., 1999). Moreover, recent in vivo findings, where the mice have an upregulation of E2F transactivation potential because of truncated expression of c/ebp α, also demonstrate a similar WAT phenotype to our *p107*$^{-/-}$ mice (Porse et al., 2001). Future experiments should reveal the precise nature of the molecular mechanisms by which p107 and pRb act to regulate preadipocyte differentiation.

Our findings indicate that adipocyte precursors are bipotent, capable of differentiating into brown or white adipocytes, and that this developmental choice is regulated by an Rb-dependent mechanism. We demonstrate that Rb-null preadipocytes isolated from strictly WAT depots differentiated into brown adipocytes when differentiation was forced by addition of Ros, a ppary ligand, and T_3 (Figures 6D and 6E). In addition, *p107*$^{-/-}$ inguinal depots exhibit BAT differentiation and *p107*$^{-/-}$ preadipocytes express markedly reduced levels of pRb (Figures 2 and 6B). The bipotentiality of adipocyte precursors would account for the low numbers of brown adipocytes found residing in WAT (Guerra et al., 1998; Koza et al., 2000; Oberkofler et al., 1997; Tsukiyama-Kohara et al., 2001). Bipotentiality of precursors would also provide the animal with a ready source of brown adipocytes within WAT following cold stress or diet induced thermogenesis (Cannon and Nedergaard, 2004; Himms-Hagen et al., 2000). Similarly, although BAT contains preadipocytes committed to the brown adipocyte lineage (Boeuf et al., 2001; Moulin et al., 2001), a bipotential precursor can explain for the low numbers of white unilocular cells that do not express UCP-1 that are also resident in BAT (Cancello et al., 1998; Cinti et al., 1997). Therefore, our data in combination with the above observations suggest that both adult brown and white adipocytes are derived from a common adult progenitor in postnatal animals regardless of tissue location. Presumably, the type of fat produced would be contingent on the stimuli received (Cannon and Nedergaard, 2004; Rosen and Spiegelman, 2000).

Intriguingly, p107 acts in the PI3K pathway by modulating the activity of phosphoinositide-dependent kinase-1 (PDK1) (Makris et al., 2002). p107 is shown to inhibit mRNA translation by interfering with the recruitment of PDK1 to the plasma membrane. Interestingly, the targeted disruption of genes that can block mRNA translation such as 4E-BP1 (Komazawa et al., 2004; Tsukiyama-Kohara et al., 2001), result in a similar phenotype as the targeted disruption of *p107* suggesting a common pathway in WAT development.

Our results contrast with other studies that show loss of p107 promotes adipocyte differentiation (Classon et al., 2000; Landsberg et al., 2003). These discrepancies can be attributed to the difference in the mouse strains and cell types that were used to analyze p107 deficiency in adipogenesis. Classon and coworkers derived embryonic cells from a *129/SVxC57BL/6* mixed mouse genetic background that has no observable developmental anomalies apparent including WAT differentiation (Cobrinik et al., 1996). Our analysis used an independently generated p107 mutant allele backcrossed into the *Balb/c* mouse strain. Secondly, we employed bona fide adult primary preadipocytes cultured to confluence and differentiated using standard adipocyte differentiation protocols. Moreover, our experiments revealed a hitherto unappreciated difference between the requirement for p107 during the in vivo versus the in vitro differentiation of preadipocytes.

Understanding the underlying mechanisms of adipocyte differentiation and development can lead to effective prevention and treatment strategies for the escalating obesity crisis in society. Indeed, the identification of the role for p107 and pRb in specifying brown versus white adipose cell differentiation raises the possibility that this pathway may be amenable for therapeutic manipulation for the treatment of obesity.

Experimental procedures

Mice, dissections, and tissue culture

Experimental procedures were performed on the *Balb*/c genetic background, including those with a targeted deletion of *p107* (LeCouter et al., 1998) and the loxP-targeted *Rb* locus (*Rb*$^{loxP/loxP}$) kindly provided by M. Vooijs and A. Berns (Marino et al., 2000). Procedures on mice were performed according to the guidelines of the University of Ottawa. Fat pads were dissected from 6–10 week old mice. Percent adiposity was determined by dividing the total adipose tissue weight by the weight of the animal. All primary cells were grown in DMEM supplemented with 10% fetal bovine serum (FBS) and penicillin/streptamicin.

Isolation of Sca-1$^+$CD31$^-$Lin$^-$ primary adult preadipocytes

Primary preadipocytes from adipose stromal cells were fractionated to increase their homogeneity. IgWAT from five wild-type, *p107*$^{-/-}$ or *Rb*$^{loxP/loxP}$ aged 4–8 weeks were excised, weighed, minced, and digested with 1 mg/ml collagenase I (Sigma) in DMEM with 10% FBS and antibiotics at 37°C for 45 min. After digestion, the slurry was passed through a cell strainer (100 μm) and cells pelleted by centrifugation at 250 g for 5 min. Cells were resuspended and incubated on ice for 20 min with conjugated antibodies (BD Pharmingen) recognizing the following cell surface markers: Stem Cell Antigen-1 conjugated to APC (Caltag), CD31 conjugated to FITC (BD Pharmingen) and Lineage antibodies (BD Pharmingen Lineage kit) including the blood markers Mac-1, Gr-1, Ter119, CD45R/B220, and CD3e conjugated to biotin (Lin-biotin). Detection of Lin-biotin was accomplished by avidin conjugated to PE (BD Pharmingen). Immuno-labeled cells were sorted on a MoFlo facs sorter on the basis of Sca-1$^+$CD31$^-$Lin$^-$. The Sca-1$^-$CD31$^-$Lin$^-$ cells do not adhere to tissue culture plastic and were discarded. The Sca-1$^+$ CD31$^-$Lin$^-$ cell sorted fraction was plated at a density of 15,000 cells/cm^2.

Primary adult preadipocyte differentiation

Unsorted or sorted cells were differentiated after reaching confluency or 24 hr after adenoviral infection according to the standard protocols employing the serum-based or serum-free regimens. For the serum-based differentiation method, DMEM 10% FBS supplemented with 5 μg/ml insulin, 1 μM dexamethazone and 0.5 μM of 3-isobutyl-1-methylxanthine was added to cultures. After 48 hr, the media was replaced for 8 days by DMEM containing 10% FBS supplemented with 5 μg/ml of insulin. 200 pM of triiodothyronine (T_3) and 1μM of rosiglitazone (Ros) (Cayman Chemical) was added

throughout the differentiation protocol where indicated. For the serum-free technique, cells were differentiated for 10 days using serum-free DMEM:F12 basal media containing 200 pM T_3, 5 μg/ml of insulin, and 10 μg/ml transferin.

Excision of pRb from $Rb^{loxP/loxP}$ adult primary preadipocytes

Sca-1$^-$CD31$^-$Lin$^-$ fraction from *$Rb^{loxP/loxP}$* lgWAT cells were infected with adenovirus expressing Cre recombinase to excise *Rb* or LacZ as a control (both kindly provided by Dr. Robin Parks) according to the method described by Huh et al. (2004).

Cell staining and counting

Sca-1$^+$CD31$^-$Lin$^-$-sorted cells from wild-type and *$p107^{-/-}$* mice were allowed to differentiate for 10 days. After, cells were fixed and stained with Oil Red O for lipid and counterstained with DAPI. The differentiated cell percentage was obtained by scoring the number of red cells containing lipid droplets per number of nuclei within a field. At least five different fields were enumerated for each of three independent experiments. For tissue sections, hematoxylin and eosin (H&E) staining was performed on paraffin sections, and Sudan Black staining, for detection of lipids, was performed on frozen sections.

PCR analyses

RNA was extracted from BAT and WAT from the inguinal depot (lgWAT) of *$p107^{-/-}$* and wild-type mice ranging in age from 6 to 10 weeks, using the RNeasy Lipid Tissue Kit (QIAGEN) according to the manufacturer's instructions. 500 ng of RNA was reverse transcribed employing the GeneAmp Kit (Applied Biosystems). 25 ng of reverse-transcribed RNA was employed for PCR analysis. Primer sets and conditions used were described elsewhere (Hansen et al., 2004a). For Quantitative Real Time PCR (qRT-PCR), assays were performed on the Stratagene MX 4000 using SYBR green PCR Master mix (Sigma). All reactions were run at least in triplicate and the results graphed by normalizing to β-actin.

Western blot analysis

Proteins were extracted from fat tissue by first homogenizing in Ripa buffer (0.5% NP-40, 0.1% sodium deoxycholate, 150 mM NaCl, 50 mM Tris-HCl [pH 7.5]) containing protease inhibitors, pepstatin, aprotinin, and leupeptin. The homogenate was centrifuged at 4°C for 30 min at 15,000 g and the supernatant portion containing the protein fraction recovered. For the differentiation time-course, primary preadipocytes from lgWAT were grown and differentiated for the stated times. Cells were lysed with Ripa and the lysate loaded onto a 7.5% polyacrylamide gel, and Western blotted according to standard protocol. Antibodies recognizing UCP-1 (Calbiochem), pRb (BD Biosciences), p107 c-20 (Santa Cruz), and α–tubulin (Sigma) were used.

Transplant experiments

Transplant experiments were performed essentially as those already published (Chao et al., 2000; Gavrilova et al., 2000). Two month of age wild-type donor and mutant recipient littermates were used. In brief, the inguinal fat pad was excised from a wild-type donor mouse, washed in saline, and cut into pieces representing the graft; a portion was kept for tissue sectioning. Grafts were implanted subcutaneously on the flank of the recipient mouse through a small incision. Grafts were implanted for a month after which their success was assessed by noting revascularization from the recipient animal's blood vessels. Tissue from the implant and recipient inguinal tissue was dissected, paraffin embedded, and sectioned for H&E staining.

Indirect calorimetry

Whole-body oxygen consumption was measured using an open circuit four-chamber indirect calorimetry system with automatic temperature and light controls (Columbus Instruments). Mice had access ad libitum to chow and water in respiration chambers, and data were recorded for a 24 hr period with temperature at 24°C and light between 0700–1900 hr.

Transmission electron microscopy

Fat pads were fixed with 0.1 M sodium cacodylate buffer containing 2% glutaraldehyde, [pH 7.5], at 4°C overnight and postfixed with 1% osmium tetroxide. After dehydration, the samples were embedded in Spurr and observed on a Joel 1230 EM.

Immunohistochemistry analysis

Paraffin sections of wild-type and mutant inguinal fat pads were dewaxed, endogenous peroxidase activity quenched with 3% hydrogen peroxide in methanol, and incubated with the M.O.M. blocking kit (Vector Labs). Antibody directed against UCP-1 (1:500; Calbiochem) was visualized by using a streptavidin-biotin method (Vector Labs) with diaminobenzidine (Sigma).

Chromatin immunoprecipitation

Chromatin immunoprecipitation (ChIP) was performed on growing, and 7 day-differentiated (with and without Ros) 3T3-L1 preadipocytes with an assay kit (Upstate) according to the manufacturers instructions. ChIP primer sequences are available upon request.

Reporter assays

3T3-L1 cells were transfected using the calcium phosphate protocol (Perry et al., 2001). 40 hr posttransfection, cells were treated with 5mM caffeine for 4.5 hr prior to harvest. The 3.1 Kb proximal PGC1α-promoter-luciferase construct and RbΔ663 were kindly provided by Drs. Michael Czubryt and William Kaelin Jr., respectively (Czubryt et al., 2003) (Sellers et al., 1998). Luciferase assays were performed using the Dual-Luciferase Reporter Assay System (Promega).

Acknowledgments

We thank Dr. Patrick Seale for critical reading of the manuscript; Dr. Anne-Marie Gagnon and Dr. Jacob Hansen for guidance and comments; Dr. Robin Parks for the LacZ and Cre adenovirus; and Peter Rippstein for TEM support. G.G. is a recipient of a postdoctoral fellowship from the Fonds de la Recherche en Santé du Québec. M.A.R. holds the Canada Research Chair in Molecular Genetics and is a Howard Hughes Medical Institute International Scholar. This work was supported by grants to M.A.R. from the Canadian Institutes of Health Research, and the Canada Research Chair Program.

Received: February 27, 2005
Revised: June 28, 2005
Accepted: October 11, 2005
Published: November 8, 2005

References

Ailhaud, G., Grimaldi, P., and Negrel, R. (1992). Cellular and molecular aspects of adipose tissue development. Annu. Rev. Nutr. *12*, 207–233.

Altiok, S., Xu, M., and Spiegelman, B.M. (1997). PPARgamma induces cell cycle withdrawal: inhibition of E2F/DP DNA-binding activity via down-regulation of PP2A. Genes Dev. *11*, 1987–1998.

Anton, M., and Graham, F.L. (1995). Site-specific recombination mediated by an adenovirus vector expressing the Cre recombinase protein: a molecular switch for control of gene expression. J. Virol. *69*, 4600–4606.

Argyropoulos, G., and Harper, M.E. (2002). Uncoupling proteins and thermoregulation. J. Appl. Physiol. *92*, 2187–2198.

Asakura, A., and Rudnicki, M.A. (2002). Side population cells from diverse adult tissues are capable of in vitro hematopoietic differentiation. Exp. Hematol. *30*, 1339–1345.

Boeuf, S., Klingenspor, M., Van Hal, N.L., Schneider, T., Keijer, J., and Klaus, S. (2001). Differential gene expression in white and brown preadipocytes. Physiol. Genomics *7*, 15–25.

Cam, H., Balciunaite, E., Blais, A., Spektor, A., Scarpulla, R.C., Young, R., Kluger, Y., and Dynlacht, B.D. (2004). A common set of gene regulatory networks links metabolism and growth inhibition. Mol. Cell *16*, 399–411.

Cancello, R., Zingaretti, M.C., Sarzani, R., Ricquier, D., and Cinti, S. (1998).

Leptin and UCP1 genes are reciprocally regulated in brown adipose tissue. Endocrinology *139*, 4747–4750.

Cannon, B., and Nedergaard, J. (2004). Brown adipose tissue: function and physiological significance. Physiol. Rev. *84*, 277–359.

Cederberg, A., Gronning, L.M., Ahren, B., Tasken, K., Carlsson, P., and Enerback, S. (2001). FOXC2 is a winged helix gene that counteracts obesity, hypertriglyceridemia, and diet-induced insulin resistance. Cell *106*, 563–573.

Chao, L., Marcus-Samuels, B., Mason, M.M., Moitra, J., Vinson, C., Arioglu, E., Gavrilova, O., and Reitman, M.L. (2000). Adipose tissue is required for the antidiabetic, but not for the hypolipidemic, effect of thiazolidinediones. J. Clin. Invest. *106*, 1221–1228.

Chen, P.L., Riley, D.J., Chen, Y., and Lee, W.H. (1996). Retinoblastoma protein positively regulates terminal adipocyte differentiation through direct interaction with C/EBPs. Genes Dev. *10*, 2794–2804.

Cherington, V., Brown, M., Paucha, E., St Louis, J., Spiegelman, B.M., and Roberts, T.M. (1988). Separation of simian virus 40 large-T-antigen-transforming and origin-binding functions from the ability to block differentiation. Mol. Cell. Biol. *8*, 1380–1384.

Cinti, S. (2000). Anatomy of the adipose organ. Eat. Weight Disord. *5*, 132–142.

Cinti, S. (2001). The adipose organ: morphological perspectives of adipose tissues. Proc. Nutr. Soc. *60*, 319–328.

Cinti, S., Frederich, R.C., Zingaretti, M.C., De Matteis, R., Flier, J.S., and Lowell, B.B. (1997). Immunohistochemical localization of leptin and uncoupling protein in white and brown adipose tissue. Endocrinology *138*, 797–804.

Clarke, A.R., Maandag, E.R., van Roon, M., van der Lugt, N.M., van der Valk, M., Hooper, M.L., Berns, A., and te Riele, H. (1992). Requirement for a functional Rb-1 gene in murine development. Nature *359*, 328–330.

Classon, M., and Dyson, N. (2001). p107 and p130: versatile proteins with interesting pockets. Exp. Cell Res. *264*, 135–147.

Classon, M., Kennedy, B.K., Mulloy, R., and Harlow, E. (2000). Opposing roles of pRB and p107 in adipocyte differentiation. Proc. Natl. Acad. Sci. USA *97*, 10826–10831.

Cobrinik, D., Lee, M.H., Hannon, G., Mulligan, G., Bronson, R.T., Dyson, N., Harlow, E., Beach, D., Weinberg, R.A., and Jacks, T. (1996). Shared role of the pRB-related p130 and p107 proteins in limb development. Genes Dev. *10*, 1633–1644.

Czubryt, M.P., McAnally, J., Fishman, G.I., and Olson, E.N. (2003). Regulation of peroxisome proliferator-activated receptor gamma coactivator 1 alpha (PGC-1 alpha) and mitochondrial function by MEF2 and HDAC5. Proc. Natl. Acad. Sci. USA *100*, 1711–1716.

de Bruin, A., Wu, L., Saavedra, H.I., Wilson, P., Yang, Y., Rosol, T.J., Weinstein, M., Robinson, M.L., and Leone, G. (2003). Rb function in extraembryonic lineages suppresses apoptosis in the CNS of Rb-deficient mice. Proc. Natl. Acad. Sci. USA *100*, 6546–6551.

Fajas, L., Egler, V., Reiter, R., Hansen, J., Kristiansen, K., Debril, M.B., Miard, S., and Auwerx, J. (2002a). The retinoblastoma-histone deacetylase 3 complex inhibits PPARgamma and adipocyte differentiation. Dev. Cell *3*, 903–910.

Fajas, L., Egler, V., Reiter, R., Miard, S., Lefebvre, A.M., and Auwerx, J. (2003). PPARgamma controls cell proliferation and apoptosis in an RB-dependent manner. Oncogene *22*, 4186–4193.

Fajas, L., Landsberg, R.L., Huss-Garcia, Y., Sardet, C., Lees, J.A., and Auwerx, J. (2002b). E2Fs regulate adipocyte differentiation. Dev. Cell *3*, 39–49.

Gavrilova, O., Marcus-Samuels, B., Graham, D., Kim, J.K., Shulman, G.I., Castle, A.L., Vinson, C., Eckhaus, M., and Reitman, M.L. (2000). Surgical implantation of adipose tissue reverses diabetes in lipoatrophic mice. J. Clin. Invest. *105*, 271–278.

Guerra, C., Koza, R.A., Yamashita, H., Walsh, K., and Kozak, L.P. (1998). Emergence of brown adipocytes in white fat in mice is under genetic control. Effects on body weight and adiposity. J. Clin. Invest. *102*, 412–420.

Hansen, J.B., Jorgensen, C., Petersen, R.K., Hallenborg, P., De Matteis, R., Boye, H.A., Petrovic, N., Enerback, S., Nedergaard, J., Cinti, S., et al. (2004a). Retinoblastoma protein functions as a molecular switch determining white versus brown adipocyte differentiation. Proc. Natl. Acad. Sci. USA *101*, 4112–4117.

Hansen, J.B., Petersen, R.K., Larsen, B.M., Bartkova, J., Alsner, J., and Kristiansen, K. (1999). Activation of peroxisome proliferator-activated receptor gamma bypasses the function of the retinoblastoma protein in adipocyte differentiation. J. Biol. Chem. *274*, 2386–2393.

Hansen, J.B., te Riele, H., and Kristiansen, K. (2004b). Novel function of the retinoblastoma protein in fat: regulation of white versus brown adipocyte differentiation. Cell Cycle *3*, 774–778.

Higgins, C., Chatterjee, S., and Cherington, V. (1996). The block of adipocyte differentiation by a C-terminally truncated, but not by full-length, simian virus 40 large tumor antigen is dependent on an intact retinoblastoma susceptibility protein family binding domain. J. Virol. *70*, 745–752.

Himms-Hagen, J., Melnyk, A., Zingaretti, M.C., Ceresi, E., Barbatelli, G., and Cinti, S. (2000). Multilocular fat cells in WAT of CL-316243-treated rats derive directly from white adipocytes. Am. J. Physiol. Cell Physiol. *279*, C670–C681.

Huh, M.S., Parker, M.H., Scime, A., Parks, R., and Rudnicki, M.A. (2004). Rb is required for progression through myogenic differentiation but not maintenance of terminal differentiation. J. Cell Biol. *166*, 865–876.

Jacks, T., Fazeli, A., Schmitt, E.M., Bronson, R.T., Goodell, M.A., and Weinberg, R.A. (1992). Effects of an Rb mutation in the mouse. Nature *359*, 295–300.

Komazawa, N., Matsuda, M., Kondoh, G., Mizunoya, W., Iwaki, M., Takagi, T., Sumikawa, Y., Inoue, K., Suzuki, A., Mak, T.W., et al. (2004). Enhanced insulin sensitivity, energy expenditure and thermogenesis in adipose-specific Pten suppression in mice. Nat. Med. *10*, 1208–1215.

Koza, R.A., Hohmann, S.M., Guerra, C., Rossmeisl, M., and Kozak, L.P. (2000). Synergistic gene interactions control the induction of the mitochondrial uncoupling protein (Ucp1) gene in white fat tissue. J. Biol. Chem. *275*, 34486–34492.

Landsberg, R.L., Sero, J.E., Danielian, P.S., Yuan, T.L., Lee, E.Y., and Lees, J.A. (2003). The role of E2F4 in adipogenesis is independent of its cell cycle regulatory activity. Proc. Natl. Acad. Sci. USA *100*, 2456–2461.

LeCouter, J.E., Kablar, B., Hardy, W.R., Ying, C., Megeney, L.A., May, L.L., and Rudnicki, M.A. (1998). Strain-dependent myeloid hyperplasia, growth deficiency, and accelerated cell cycle in mice lacking the Rb-related p107 gene. Mol. Cell. Biol. *18*, 7455–7465.

Lee, E.Y., Chang, C.Y., Hu, N., Wang, Y.C., Lai, C.C., Herrup, K., Lee, W.H., and Bradley, A. (1992). Mice deficient for Rb are nonviable and show defects in neurogenesis and haematopoiesis. Nature *359*, 288–294.

Makris, C., Voisin, L., Giasson, E., Tudan, C., Kaplan, D.R., and Meloche, S. (2002). The Rb-family protein p107 inhibits translation by a PDK1-dependent mechanism. Oncogene *21*, 7891–7896.

Marino, S., Vooijs, M., van Der Gulden, H., Jonkers, J., and Berns, A. (2000). Induction of medulloblastomas in p53-null mutant mice by somatic inactivation of Rb in the external granular layer cells of the cerebellum. Genes Dev. *14*, 994–1004.

May, J.S., Prince, A.M., Lyle, R.E., and McGehee, R.E., Jr. (2001). Antisense suppression of p107 inhibits 3T3-L1 adipocyte differentiation. Biochem. Biophys. Res. Commun. *283*, 837–842.

Moulin, K., Arnaud, E., Nibbelink, M., Viguerie-Bascands, N., Penicaud, L., and Casteilla, L. (2001). Cloning of BUG demonstrates the existence of a brown preadipocyte distinct from a white one. Int. J. Obes. Relat. Metab. Disord. *25*, 1431–1441.

Oberkofler, H., Dallinger, G., Liu, Y.M., Hell, E., Krempler, F., and Patsch, W. (1997). Uncoupling protein gene: quantification of expression levels in adipose tissues of obese and non-obese humans. J. Lipid Res. *38*, 2125–2133.

Perry, R.L., Parker, M.H., and Rudnicki, M.A. (2001). Activated MEK1 binds the nuclear MyoD transcriptional complex to repress transactivation. Mol. Cell 8, 291–301.

Porse, B.T., Pedersen, T.A., Xu, X., Lindberg, B., Wewer, U.M., Friis-Hansen, L., and Nerlov, C. (2001). E2F repression by C/EBPalpha is required for adipogenesis and granulopoiesis in vivo. Cell *107*, 247–258.

Puigserver, P., and Spiegelman, B.M. (2003). Peroxisome proliferator-activated receptor-gamma coactivator 1 alpha (PGC-1 alpha): transcriptional coactivator and metabolic regulator. Endocr. Rev. *24*, 78–90.

Puigserver, P., Wu, Z., Park, C.W., Graves, R., Wright, M., and Spiegelman, B.M. (1998). A cold-inducible coactivator of nuclear receptors linked to adaptive thermogenesis. Cell *92*, 829–839.

Reichert, M., and Eick, D. (1999). Analysis of cell cycle arrest in adipocyte differentiation. Oncogene *18*, 459–466.

Richon, V.M., Lyle, R.E., and McGehee, R.E., Jr. (1997). Regulation and expression of retinoblastoma proteins p107 and p130 during 3T3–L1 adipocyte differentiation. J. Biol. Chem. *272*, 10117–10124.

Rosen, E.D. (2002). Molecular mechanisms of adipocyte differentiation. Ann. Endocrinol. (Paris) *63*, 79–82.

Rosen, E.D., and Spiegelman, B.M. (2000). Molecular regulation of adipogenesis. Annu. Rev. Cell Dev. Biol. *16*, 145–171.

Sellers, W.R., Novitch, B.G., Miyake, S., Heith, A., Otterson, G.A., Kaye, F.J., Lassar, A.B., and Kaelin, W.G., Jr. (1998). Stable binding to E2F is not required for the retinoblastoma protein to activate transcription, promote differentiation, and suppress tumor cell growth. Genes Dev. *12*, 95–106.

Slomiany, B.A., D'Arigo, K.L., Kelly, M.M., and Kurtz, D.T. (2000). C/EBPalpha inhibits cell growth via direct repression of E2F-DP-mediated transcription. Mol. Cell. Biol. *20*, 5986–5997.

Tang, Q.Q., Otto, T.C., and Lane, M.D. (2003). Mitotic clonal expansion: a synchronous process required for adipogenesis. Proc. Natl. Acad. Sci. USA *100*, 44–49.

Timchenko, N.A., Wilde, M., Iakova, P., Albrecht, J.H., and Darlington, G.J. (1999). E2F/p107 and E2F/p130 complexes are regulated by C/EBPalpha in 3T3–L1 adipocytes. Nucleic Acids Res. *27*, 3621–3630.

Tiraby, C., and Langin, D. (2003). Conversion from white to brown adipocytes: a strategy for the control of fat mass? Trends Endocrinol. Metab. *14*, 439–441.

Tiraby, C., Tavernier, G., Lefort, C., Larrouy, D., Bouillaud, F., Ricquier, D., and Langin, D. (2003). Acquirement of brown fat cell features by human white adipocytes. J. Biol. Chem. *278*, 33370–33376.

Tsukiyama-Kohara, K., Poulin, F., Kohara, M., DeMaria, C.T., Cheng, A., Wu, Z., Gingras, A.C., Katsume, A., Elchebly, M., Spiegelman, B.M., et al. (2001). Adipose tissue reduction in mice lacking the translational inhibitor 4E–BP1. Nat. Med. *7*, 1128–1132.

Vanderluit, J.L., Ferguson, K.L., Nikoletopoulou, V., Parker, M., Ruzhynsky, V., Alexson, T., McNamara, S.M., Park, D.S., Rudnicki, M., and Slack, R.S. (2004). p107 regulates neural precursor cells in the mammalian brain. J. Cell Biol. *166*, 853–863.

Wu, L., de Bruin, A., Saavedra, H.I., Starovic, M., Trimboli, A., Yang, Y., Opavska, J., Wilson, P., Thompson, J.C., Ostrowski, M.C., et al. (2003). Extra-embryonic function of Rb is essential for embryonic development and viability. Nature *421*, 942–947.

Wu, Z., Puigserver, P., Andersson, U., Zhang, C., Adelmant, G., Mootha, V., Troy, A., Cinti, S., Lowell, B., Scarpulla, R.C., and Spiegelman, B.M. (1999). Mechanisms controlling mitochondrial biogenesis and respiration through the thermogenic coactivator PGC-1. Cell *98*, 115–124.

Zacksenhaus, E., Jiang, Z., Chung, D., Marth, J.D., Phillips, R.A., and Gallie, B.L. (1996). pRb controls proliferation, differentiation, and death of skeletal muscle cells and other lineages during embryogenesis. Genes Dev. *10*, 3051–3064.

Appendix B

Distinct Roles for Pax7 and Pax3 in Adult Regenerative Myogenesis

Purpose

To understand the role and contribution of Pax3 and Pax7 dependent myogenic cell populations in adult regenerative myogenesis.

Submission Information

Submitted: 01 August 2005
Accepted: 06 Decenber 2005
Published: 02 January 2006

Reproduced from **"The Journal of Cell Biology, 2006, Volume 172, pp. 103-113"** by copyright permission of The Rockefeller University Press.

Contribution of Co-Authors

Michael Huh contributed the pan-tissue/cell-type *Pax* RNase protection assay included as a supplementary figure in Appendix B (Figure S1).

Preface and Discussion of Figure S1

Satellite cells provide the majority of the regenrative capacity in adult muscle. *Pax7*$^{-/-}$ mice are completely devoid of satellite cells in the limb musculature. Cardiotoxin damage to *Pax7*$^{-/-}$ muscle results in a very poor regeneration of the muscle. However, some residual regeneration is observed in *Pax7*$^{-/-}$ mice. During fetal myogenesis, Pax3/Pax7 expressing myoblasts contribute to the initial starting pool of post-natal satellite cells. It is believed, that some Pax3 dependent myogenic cells contribute to the residual regenerative response in *Pax7*$^{-/-}$ muscle. Evidence of this population of Pax3 myogenic cells is needed to support this hypothesis. Therefore, the expression of *Pax3* was assessed in primary myoblasts cultures by RNase protection assay (Figure S1).

The results of the RNase protection assay reveal the low expression of *Pax3* mRNA in a proliferating primary myoblast culture (Figure S1). This is indicative of the possibility that a minority population of Pax3 dependent myogenic cells reside in adult skeletal muscle. Further investigation into this possibility indeed validated this notion. Pax3 dependent myogenic cells were positioned outside of the classical satellite cell niche and resided in the interstitial region of muscle fiber.

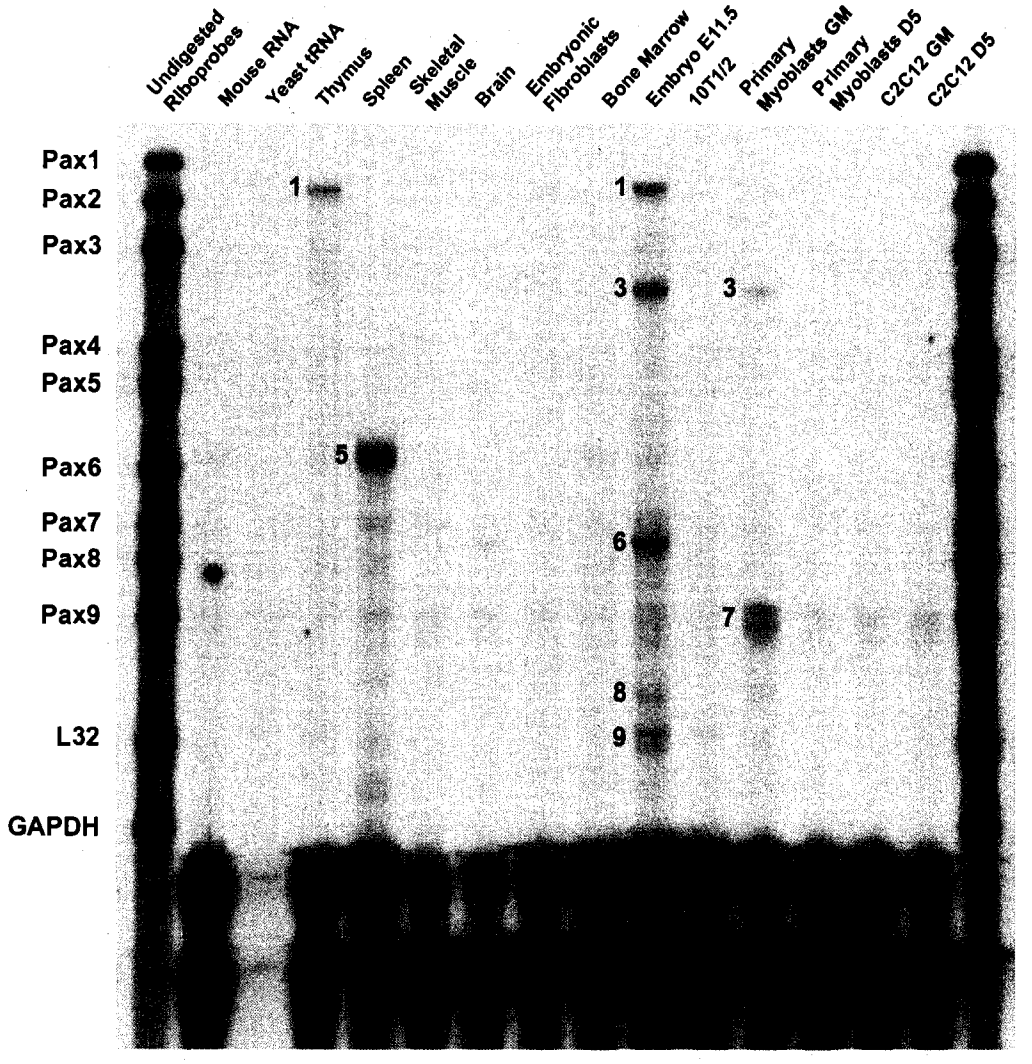

Figure S1. **Pax3 is expressed in primary myoblasts.** RNase protection assay of different tissues and cell types for Pax 1-9 mRNAs. L32 and GAPDH levels are used as loading controls.

Distinct roles for Pax7 and Pax3 in adult regenerative myogenesis

Shihuan Kuang,[1] Sophie B. Chargé,[1] Patrick Seale,[2] Michael Huh,[1,3] and Michael A. Rudnicki[1,2,3]

[1]Molecular Medicine Program, Ottawa Health Research Institute, Ottawa, Ontario, Canada K1H 8L6
[2]Department of Biology, McMaster University, Hamilton, Ontario, Canado L8S 4K1
[3]Department of Cellulor and Molecular Medicine, University of Ottawa, Ottawa, Ontario, Canada K1H 8M5

We assessed viable *Pax7*$^{-/-}$ mice in 129Sv/J background and observed reduced growth and marked muscle wasting together with a complete absence of functional satellite cells. Acute injury resulted in an extreme deficit in muscle regeneration. However, a small number of regenerated myofibers were detected, suggesting the presence of residual myogenic cells in *Pax7*-deficient muscle. Rare Pax3^{+}/MyoD^{+} myoblasts were recovered from *Pax7*$^{-/-}$ muscle homogenates and cultures of myofiber bundles but not from single myofibers free of interstitial tissues. Finally, we identified Pax3^{+} cells in the muscle interstitial environment and demonstrated that they coexpressed MyoD during regeneration. Sublaminar satellite cells in hind limb muscle did not express detectable levels of Pax3 protein or messenger RNA. Therefore, we conclude that interstitial Pax3^{+} cells represent a novel myogenic population that is distinct from the sublaminar satellite cell lineage and that Pax7 is essential for the formation of functional myogenic progenitors from sublaminar satellite cells.

Introduction

Muscle satellite cells are thought to represent the only population of committed myogenic progenitors in adult skeletal muscle. The activation of muscle satellite cells generates proliferative myogenic precursor cells that differentiate to repair and replace damaged fibers (Charge and Rudnicki, 2004). The transcription factors regulating the specification and differentiation of satellite cell–derived myogenic progenitors is analogous to the molecular mechanisms regulating embryonic myogenesis (Parker et al., 2003). Pax7, a paired-box transcription factor, is specifically expressed in quiescent and newly activated satellite cells. Importantly, the absence of myogenic cells in young *Pax7*$^{-/-}$ skeletal muscle demonstrates a requirement for Pax7 in the function of the satellite cell lineage (Seale et al., 2000). *Pax7*$^{-/-}$ mice appear normal at birth but fail to thrive and subsequently die at 2–3 wk from unknown causes (Mansouri et al., 1996; Seale et al., 2000). The decreased caliber of *Pax7*$^{-/-}$ myofibers is attributable to the lack of satellite cell fusion during the postnatal growth of muscle (Seale et al., 2000). However, the normal appearance of newborn *Pax7*$^{-/-}$ muscle suggests that embryonic and fetal myogenesis is unaffected and identifies a unique requirement for Pax7 in the satellite cell lineage.

Recent work has identified stem cell populations capable of giving rise to satellite cells during regeneration. Muscle-derived side-population cells separated on the basis of Hoechst dye exclusion give rise to satellite cells after intramuscular or intravenous injection (Gussoni et al., 1999; Asakura et al., 2002). In addition, bone marrow–derived cells similarly have the capacity to engraft skeletal muscle and form myogenic satellite cells after whole-body irradiation and transplantation (Ferrari et al., 1998; Bittner et al., 1999; Gussoni et al., 1999; LaBarge and Blau, 2002). More recently, we demonstrated that endogenous CD45^{+} muscle-derived cells give rise to Pax7^{+} myogenic cells in response to Wnt proteins during regeneration (Polesskaya et al., 2003). Furthermore, ectopic expression of Pax7 in CD45^{+}/Sca1^{+} cells is sufficient for their myogenic specification (Seale et al., 2004). Together, these data support the notion that a developmental relationship exists between adult stem cells and Pax7-dependent satellite cell myogenic lineages.

Pax3, a paralogue of Pax7, is critical for the delamination and migration of the somitic muscle progenitor cells to the limb buds, as *Pax3* mutant mice lack limb muscles (Bober et al., 1994; Goulding et al., 1994; Tajbakhsh et al., 1997). Despite these distinct functions of Pax3 and -7 in muscle development (Relaix et al., 2004), recent studies have begun to elucidate a

S. Kuang and S.B. Chargé contributed equally to this paper.

Correspondence to Michael A. Rudnicki: mrudnicki@ohri.co

P. Seale's present address is Dana-Farber Cancer Institute, Boston, MA 02115.

Abbreviations used in this paper: β-gal, β-galactosidase; CTX, cardiotoxin; EDL, extensor digitorum longus; MyHC, myosin heavy chain; P, postnatal doy; TA, tibialis anterior.

The online version of this article contains supplemental material.

The Journal of Cell Biology, Vol. 172, No. 1, January 2, 2006 103–113
http://www.jcb.org/cgi/doi/10.1083/jcb.200508001

Supplemental Material can be found at:
http://www.jcb.org/cgi/content/full/jcb.200508001/DC1

common playground for these paralogues. Specifically, a novel population of Pax3/Pax7 double-positive ($Pax3^+/Pax7^+$) stem cells were identified in the dermomyotome of the embryonic somites (Ben-Yair and Kalcheim, 2005; Gros et al., 2005; Kassar-Duchossoy et al., 2005; Relaix et al., 2005). Proliferating $Pax3^+/Pax7^+$ cells were observed to persist throughout embryonic and fetal development and later to give rise to a subset of muscle satellite cells. In the absence of muscle environment or Pax3/Pax7 expression, these somitic stem cells apoptose or adopt alternative nonmuscle lineages. Interestingly, Pax3 expression in satellite cells is mostly down-regulated before birth, although a subset of satellite cells appears to express Pax3 (Kassar-Duchossoy et al., 2005; Montarras et al., 2005; Relaix et al., 2005).

In this study, we set out to determine the relative role of Pax7 and -3 in postnatal muscle growth and regeneration. The original $Pax7^{-/-}$ mice in C57/B6 background appear normal at birth but fail to thrive and subsequently die at 2–3 wk of age (Mansouri et al., 1996; Seale et al., 2000), preventing them from further postnatal analysis. Therefore, *Pax7* carrying a knockin of a β-galactosidase (β-gal) cassette ($Pax7^{lacZ/lacZ}$) were backcrossed nine generations into the 129Sv/J genetic background, where some mutant mice were viable. These $Pax7^{lacZ/lacZ}$ 129Sv/J mice allow us to examine not only muscle growth and regeneration in the absence of Pax7 expression but also the function of Pax3 independent of Pax7 in postnatal muscles. We found that the growth and regeneration of $Pax7^{lacZ/lacZ}$ muscle was greatly compromised, suggesting an essential role for Pax7 in these processes. Furthermore, we identified a novel population of Pax3-expressing myogenic progenitors in the interstitial space of adult skeletal muscles. Together, these results demonstrate an essential role for Pax7 in the productive formation of myogenic progenitors during postnatal growth and regeneration of skeletal muscle.

Results

Decreased fiber size but not fiber number characterizes the decreased muscle growth in $Pax7^{lacZ/lacZ}$ mice

To investigate the role of Pax7 in postnatal muscle development, we examined the growth of $Pax7^{lacZ/lacZ}$ muscles during the postnatal period in the 129Sv/J genetic background. Growth of $Pax7^{lacZ/lacZ}$ mice appeared normal during embryonic development until birth, as demonstrated by the normal body weight as compared with control littermates at postnatal day (P) 0 (Table I). However, after birth, $Pax7^{lacZ/lacZ}$ mice failed to maintain normal postnatal growth. At P3, $Pax7^{lacZ/lacZ}$ mice were only two thirds of the weight of wild-type littermates, and at P10, they were less than half the weight of wild-type littermates. No significant weight difference was detected between $Pax7^{+/lacZ}$ and wild-type littermates (Table I). The decreased body mass of $Pax7^{lacZ/lacZ}$ mice was at least partially attributable to decreased skeletal muscle growth as revealed by the significant size/weight decreases in tibialis anterior (TA) and other skeletal muscles (Table I; unpublished data). To further determine whether the decreased muscle mass in $Pax7^{lacZ/lacZ}$ mice resulted from reduced myofiber size or number or both, we enumerated the total number of myofibers at muscle mid-belly and determined the myofiber cross-sectional area. The total fiber number in both extensor digitorum longus (EDL) and soleus muscles was not different between $Pax7^{lacZ/lacZ}$ and wild-type littermates at P10 (Table I). In contrast, myofiber size, regardless of their myosin heavy chain (MyHC) phenotypes, was found to be significantly decreased in $Pax7^{lacZ/lacZ}$ mice. More precisely, the cross-sectional areas of Types II and I myofibers (253 ± 16 and 289 ± 15 μm^2, $n = 4$, respectively) in the mutant soleus were ~1.5- and 1.8-fold smaller than those of wild-type fibers (374 ± 25 and 512 ± 29 μm^2, $n = 4$, respectively) at P10, whereas no significant difference in the cross-sectional area of Type I myofiber was detected at P0 ($Pax7^{lacZ/lacZ}$: 205 ± 37 μm^2, $n = 2$; $Pax7^{+/+}$: 192 ± 29 μm^2, $n = 2$). Together, these results suggest that the smaller fiber size found in $Pax7^{lacZ/lacZ}$ mice directly resulted from defects in postnatal growth. Furthermore, the myonuclei number per myofiber was significantly reduced to ~50% of the normal amount in adult $Pax7^{lacZ/lacZ}$ mice in both soleus and EDL muscles (Table I), suggesting a deficiency in (or lack of) satellite cell function to supply myonuclei to the growing myofibers. Altogether, these data demonstrate that postnatal growth of $Pax7^{lacZ/lacZ}$ skeletal muscles is severely retarded because of inadequate myonuclei increase and myofiber growth.

Muscle atrophy and fiber loss in aged $Pax7^{lacZ/lacZ}$ mice

To investigate the maintenance of $Pax7^{lacZ/lacZ}$ muscle during aging, we analyzed the muscle phenotype of aging mice. By 6 mo of age, $Pax7^{lacZ/lacZ}$ mice displayed prominent kyphosis (curvature of the spinal column), which is typical of extensive muscle wasting and a hallmark of aging (Fig. 1, A and B; Megeney et

Table I. **Decreases in muscle mass but normal fiber number in $Pax7^{lacZ/lacZ}$ muscle**

	Body mass (g)			TA mass (mg)	EDL fiber number	Soleus fiber number	EDL nuclei/fiber	Soleus nuclei/fiber
	P0	P3	P10	P10	P10	P10	P100	P100
$Pax7^{+/+}$	1.3 ± 0.05 (n = 9)	3.1 ± 0.1 (n = 11)	7.1 ± 0.3 (n = 11)	5.6 ± 0.6 (n = 8)	947 ± 40 (n = 5)	897 ± 107 (n = 3)	ND	ND
$Pax7^{+/lacZ}$	1.2 ± 0.04 (n = 10)	3.0 ± 0.1 (n = 15)	6.8 ± 0.3 (n = 13)	5.4 ± 0.3 (n = 10)	ND	ND	227 ± 5 (n = 20)	402 ± 8 (n = 20)
$Pax7^{lacZ/lacZ}$	1.3 ± 0.05 (n = 5)	1.9 ± 0.1* (n = 9)	3.0 ± 0.3* (n = 8)	1.6 ± 0.3* (n = 6)	1,028 ± 61 (n = 5)	865 ± 250 (n = 3)	142 ± 6* (n = 20)	170 ± 8* (n = 10)

*Significant at $P < 0.01$.

al., 1996). Evidence for muscle wasting was strikingly depicted by a progressive decline in the number of TA myofibers from 2–3 mo of age (Fig. 1 C). At 6–7 mo, the number of TA fibers in $Pax7^{lacZ/lacZ}$ mice was decreased to one third of that in $Pax7^{+/+}$ muscle (Fig. 1 C). The decreased myofiber number was attributable to a specific loss of fast IIb fibers as demonstrated by TA fiber–type analysis (not depicted) and by the normal fiber number found in the slow soleus muscle of adult $Pax7^{lacZ/lacZ}$ mice (Fig. 1 D). Despite the massive fiber loss in adult $Pax7^{lacZ/lacZ}$ TA, the number of newly regenerated myofibers, as indicated by the centrally located nuclei (5 ± 1 per cross section, $n = 8$), remained comparable to that of wild-type littermates (4 ± 1, $n = 7$). Therefore, these observations suggest that an impaired regeneration process is failing to replace the rapid loss of fast myofibers associated with aging in $Pax7^{lacZ/lacZ}$ mice. The presence of calcium deposits in adult $Pax7^{lacZ/lacZ}$ TA muscles further demonstrated the defective regenerative response during aging (Fig. 1, E and F). Finally, $Pax7^{lacZ/lacZ}$ muscle fibers did not display signs of extensive damage, suggesting that the loss of muscle did not result in a reduction in fiber integrity. Specifically, $Pax7^{lacZ/lacZ}$ fibers were resistant to Evans blue dye incorporation (unpublished data), and serum creatine kinase levels were normal at all ages studied (216 ± 92 U/liter [$n = 2$] and 579 ± 179 U/liter [$n = 6$] in $Pax7^{lacZ/lacZ}$; 328 ± 206 U/liter [$n = 2$] and 1148 ± 500 U/liter [$n = 6$] in $Pax7^{+/+}$ at P3 and in adults, respectively). Together, these results demonstrate that muscle wasting accompanied by a specific loss of fast fibers in $Pax7^{lacZ/lacZ}$ mice is accelerated as a function of age, and the accelerated fiber loss is not adequately compensated because of an impairment in muscle regenerative ability.

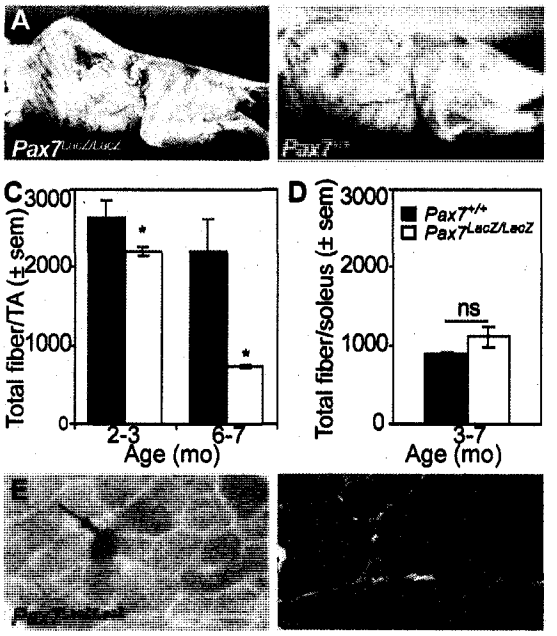

Figure 1. **Accelerated muscle wasting in adult $Pax7^{lacZ/lacZ}$ mice.** (A and B) By 6 mo of age, $Pax7^{lacZ/lacZ}$ (A) mice develop a curvature of the spine characteristic of extensive muscle wasting compared with wild-type littermates (B). (C) Total fiber number per TA is significantly reduced in $Pax7^{lacZ/lacZ}$ mice compared with wild-type littermates ($n = 4$ and 5 for 2–4 mo and $n = 2$ and 2 for 6–7 mo for $Pax7^{+/+}$ and $Pax7^{lacZ/lacZ}$, respectively). *, $P < 0.05$. (D) Total fiber number per soleus is not affected in $Pax7^{lacZ/lacZ}$ mice compared with wild-type littermates ($n = 2$ for each genotype). (E and F) Small calcium deposits (arrows) stained with Alizarin red (E) are present in between $Pax7^{lacZ/lacZ}$ myofibers, which otherwise appear normal, albeit smaller, on a spaced serial cross section stained with hematoxylin–eosin (F).

Severely deficient regeneration of $Pax7^{lacZ/lacZ}$ muscle after acute injury

To assess the regenerative capacity of $Pax7^{lacZ/lacZ}$ muscle, we injected cardiotoxin (CTX) into TA muscles to chemically induce injury. At 10 d and 1 mo after CTX injection, $Pax7^{+/+}$ TA regained the overall normal appearance of regenerated muscle characterized by numerous centrally nucleated regenerating myofibers (Fig. 2, A and B). There were >700 regenerating fibers per TA cross section at both 10 d ($n = 2$) and 1 mo ($n = 3$) after injury, without appreciable deposition of calcium, adipose, or fibrotic tissues (Fig. 2, A–D). In sharp contrast, $Pax7^{lacZ/lacZ}$ TA displayed a severe regeneration deficit, with only rare centrally nucleated myofibers observed at 10 d (9 ± 6 fibers/TA cross section, $n = 3$) and 1 mo (61 ± 50 fibers/TA cross section, $n = 4$) after injection (Fig. 2, E and F). The centrally nucleated myofibers in $Pax7^{lacZ/lacZ}$ TA failed to mature and remained significantly smaller than those in $Pax7^{+/+}$ controls even 1 mo after injury (compare Fig. 2 B with Fig. 2 F [arrows]). Furthermore, by 1 mo after injury, $Pax7^{lacZ/lacZ}$ TA had been replaced by extensive adipose tissue (Fig. 2 F, arrowheads), fibrotic tissue (Fig. 2 G, arrowhead), and deposition of calcium (Fig. 2 H). Similar results were obtained after CTX injection in gastrocnemius muscles (unpublished data). This almost complete absence of muscle repair in adult $Pax7^{lacZ/lacZ}$ mice appears to be the most striking regeneration deficit reported in any mouse model.

Muscle regeneration was also analyzed in $Pax7^{lacZ/lacZ}$ mice after physically (crush) induced injuries. Similar to CTX-induced muscle regeneration, $Pax7^{lacZ/lacZ}$ TA and gastrocnemius muscles (Fig. 2 K, arrows, and not depicted) contained only rare centrally nucleated myofibers with extensive calcium deposition (Fig. 2 L) and fibrosis (not depicted) 10 d after crush. In contrast, muscles from $Pax7^{+/+}$ littermates were fully regenerated with large centrally nucleated fibers (Fig. 2 I and not depicted) and without calcium deposits (Fig. 2 J). Together, these experiments indicate that Pax7 is necessary for efficient muscle regeneration.

The presence of small numbers of centrally nucleated myofibers in $Pax7^{lacZ/lacZ}$ muscle at 10 d and 1 mo after injury did, however, suggest a limited capacity for muscle differentiation. As in wild-type mice, the centrally nucleated fibers in $Pax7^{lacZ/lacZ}$ mutant expressed embryonic MyHC and high levels of Desmin (Fig. 2, O and P), confirming their newly regenerated state. In addition, regenerated fibers in both $Pax7^{+/+}$ and $Pax7^{lacZ/lacZ}$ muscles contained BrdU-labeled nuclei at 10 d after injury, indicating that proliferating cells had differentiated and fused into these myofibers (Fig. 2, M and N). Consistent with the regenerative deficit of $Pax7^{lacZ/lacZ}$ muscle, only 3.5% of BrdU-labeled nuclei were found within muscle fibers, compared with 45% of BrdU-positive nuclei within myofibers in

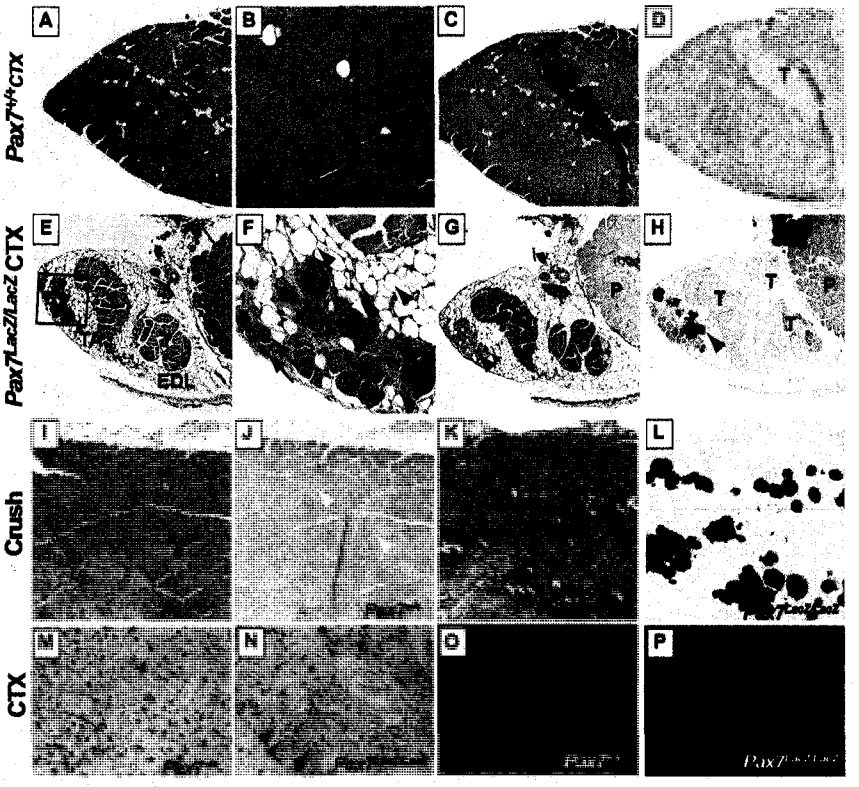

Figure 2. **Profound regeneration deficit in $Pax7^{lacZ/lacZ}$ muscle after acute injury.** Lower hind limb sections from $Pax7^{+/+}$ (A–D) or $Pax7^{lacZ/lacZ}$ (E–H) mice 1 mo after CTX stained with hematoxylin–eosin (A, B, E, and F), Van Gieson's (C and G; pink stain), and Alizarin red (D and H; red stain). (B and F) Higher magnifications of A and E, respectively. Note the efficient muscle regeneration in $Pax7^{+/+}$ TA characterized by numerous large centrally nucleated regenerating myofibers (B, arrows), with no extensive calcium deposition, adipogenesis, or fibrogenesis (A–D). In contrast, injured $Pax7^{lacZ/lacZ}$ TA (E–H) displays only rare and small centrally nucleated myofibers (F, arrows); instead, the muscle was replaced by calcium deposits (H, arrowhead), adipocytes (F, arrowheads), or fibrosis (G, arrowhead). Sections from $Pax7^{+/+}$ (I and J) and $Pax7^{lacZ/lacZ}$ littermates (K and L) 10 d after crush injury reveal an efficient muscle regeneration process in $Pax7^{+/+}$ TA (I), whereas only rare centrally nucleated myofibers are observed in $Pax7^{lacZ/lacZ}$ TA (K, arrows). Instead, muscle is infiltrated by inflammatory cells and replaced by fibrosis and large calcium deposits (L). The arrowheads in J indicate normal regenerative fibers in wild type. Central myonuclei in regenerated TA myofibers from $Pax7^{+/+}$ (M) and $Pax7^{lacZ/lacZ}$ (N) muscle 10 d after CTX injection are BrdU$^+$ (DAB, brown; N, arrowheads) after multiple BrdU injections during the period of regeneration. Low efficiency of muscle regeneration in the $Pax7^{lacZ/lacZ}$ (P) is contrasted with the robust regeneration in $Pax7^{+/+}$ (O), as demonstrated by the expression of Desmin (FITC, green). P, plantarus; T, tendon.

regenerated $Pax7^{+/+}$ muscles. Finally, analysis of spaced serial cross sections demonstrated that regenerated $Pax7^{lacZ/lacZ}$ myofibers were multinucleated and extended over several hundred micrometers (unpublished data). Thus, by these criteria, the centrally nucleated $Pax7^{lacZ/lacZ}$ myofibers observed after muscle injury were regenerated rather than surviving myofibers.

Absence of functional satellite cells in $Pax7^{lacZ/lacZ}$ adult muscle

It has been reported that satellite cells are formed in the absence of Pax7 and that these cells have some capacity for myogenic function (Oustanina et al., 2004). Therefore, we examined whether we could similarly detect $Pax7^{lacZ/lacZ}$ satellite cells and whether these cells were capable of following the myogenic developmental program. First, we asked whether cells derived from Pax7 lineage, as marked by the expression of β-gal (see Materials and methods), were present on single muscle fibers in $Pax7^{lacZ/lacZ}$ mice. In $Pax7^{+/lacZ}$ mice, all β-gal$^+$ cells also coexpressed Pax7 (Fig. 3 A) and vice versa, validating the absolute specificity of β-gal labeling. Rare β-gal$^+$ cells were detected on EDL fibers isolated from younger (P25) $Pax7^{lacZ/lacZ}$ mice (Fig. 3 B). Although the Pax7$^+$/β-gal$^+$ cells on $Pax7^{+/lacZ}$ myofibers typically displayed a small round shape indicative of activation by the single fiber isolation procedure, most $Pax7^{lacZ/lacZ}$ β-gal$^+$ cells displayed a morphology characterized by a large cell body with long filopodium-like processes (Fig. 3, A and B). Furthermore, the frequency of β-gal$^+$ cells on $Pax7^{lacZ/lacZ}$ mutant fibers (1.1 ± 0.2/fiber, n = 28) was ~7% of that of the $Pax7^{+/lacZ}$ control (15.9 ± 2.2/fiber, n = 25) at P25. Even at birth (P0), the frequency of β-gal$^+$ cells in the $Pax7^{lacZ/lacZ}$ mutant muscle (6.9 ± 1.3/microscopic field under 20×, n = 7) was less than half that of the $Pax7^{+/lacZ}$ control (16.0 ± 3.8/field, n = 5; Fig. S1, available at http://www.jcb.org/cgi/content/full/jcb.200508001/DC1). To examine whether the $Pax7^{lacZ/lacZ}$ β-gal$^+$ cells were capable of proliferation upon activation, single fibers were isolated and cultured in horse serum–coated Petri dishes to prevent attachment of fibers. After 6 d of suspension culture, floating $Pax7^{+/lacZ}$ myofibers displayed characteristic large aggregates of proliferative satellite cell–derived myoblasts that expressed MyoD and/or Pax7 (Fig. 3, C and E). Under similar culture conditions, no aggregates of cells were found on $Pax7^{lacZ/lacZ}$ fibers (n = 29). Occasionally, pairs of nuclei that expressed low levels of MyoD were found within arrested single-blobbing cell bodies (Fig. 3, D and F). We did not detect Caspase3 expression in these cells (unpublished data), suggesting that Pax7 mutant satellite cells underwent an abortive mitosis and failed to complete cell division.

We next examined whether the Pax7-remnant cells on isolated single myofibers still retained typical satellite cell features. All satellite cells associated with freshly isolated $Pax7^{+/+}$ or $Pax7^{+/lacZ}$ fibers coexpressed Pax7 and Syndecan4 (Fig. 4, A and B) or CD34 (Fig. 4 H), suggesting that Syndecan4 (Cornelison et al., 2001) and CD34 (Beauchamp et al., 2000) are reliable markers of satellite cells. Specifically, 8.7 ± 1.9 Syndecan4$^+$ cells/fiber and 3.9 ± 1.8 CD34$^+$ cells/fiber were

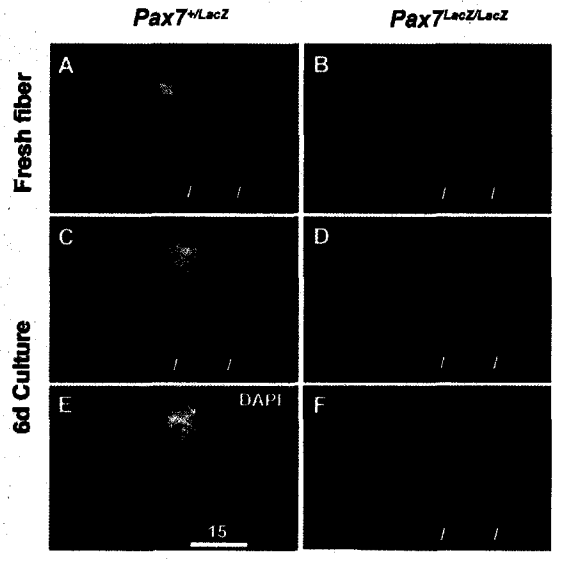

Figure 3. **Remnant nonfunctional β-gal$^+$ cells associated with muscle fibers in Pax7 mutant mice.** Expression of β-gal, knocked into the first coding exon of *Pax7* gene to generate the *Pax7* knockouts, in $Pax7^{+/lacZ}$ (A) and $Pax7^{lacZ/lacZ}$ (B) muscle fibers isolated from 1-mo-old mice. In $Pax7^{+/lacZ}$ muscle fibers, expression of β-gal is always colocalized with Pax7 expression. In $Pax7^{lacZ/lacZ}$ fibers, the β-gal$^+$ cells display large cell bodies and extensive filopodia-like processes (B), which are in contrast to the smaller, round morphologies of the β-gal$^+$ cells in the $Pax7^{+/lacZ}$ fibers (A). (C–F) After 6 d of suspended culture of single muscle fibers from $Pax7^{+/lacZ}$ mice, the Pax7$^+$ cells proliferate and differentiate to form aggregates of cells that express Pax7, MyoD, or both (C and E). Under identical culture conditions, the β-gal$^+$ cells associated with muscle fibers of $Pax7^{lacZ/lacZ}$ mice are unable to proliferate or differentiate (D and F). Bar, 15 μm.

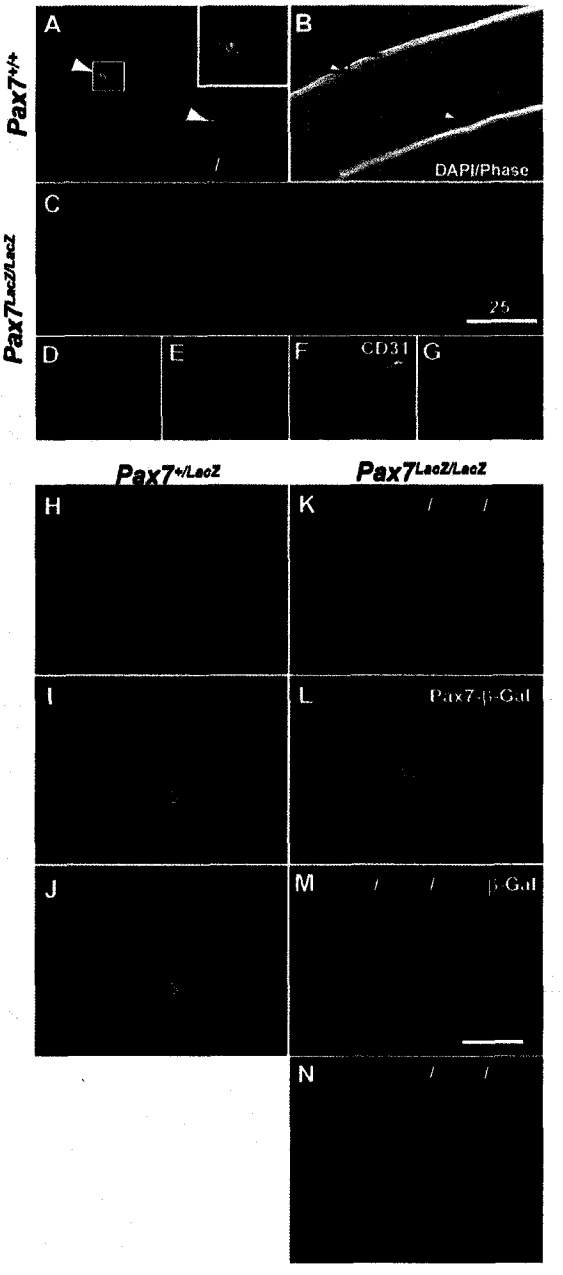

Figure 4. **Absence of satellite cell marker expression associated with adult $Pax7^{lacZ/lacZ}$ muscle fibers.** (A and B) Pax7 and Syndecan4 are coexpressed in satellite cells on freshly isolated $Pax7^{+/+}$ EDL fibers. Arrowheads show satellite cells and corresponding nuclei stained with DAPI. (C) In the $Pax7^{lacZ/lacZ}$ myofibers, few β-gal$^+$ cells (red) were identified, but they did not express the satellite cell marker Syndecan4 (green). (C–G) Conversely, the low frequencies of Syndecan4$^+$ cells associated with $Pax7^{lacZ/lacZ}$ myofibers were negative for β-gal but positive for the endothelial cells marker CD31. (H–J) Similarly, Pax7$^+$ and β-gal$^+$ cells on the $Pax7^{+/lacZ}$ myofibers are also positive for another satellite cell marker, CD34. (K–N) In the $Pax7^{lacZ/lacZ}$ myofibers, however, rare β-gal$^+$ and CD34$^+$ cells were never colocalized: the β-gal$^+$ cells were negative for CD34, and the CD34$^+$ cells were negative for β-gal. Bars, 25 μm.

detected in 6–8-wk-old adult $Pax7^{+/+}$ fibers (n = 16 fibers/3 mice for Syndecan4; n = 35 fibers/2 mice for CD34). In contrast, syndecan4 or CD34-expressing cells were never found on clean capillary-free $Pax7^{lacZ/lacZ}$ fibers (n = 56 fibers/3 mice for Syndecan4; n = 65 fibers/2 mice for CD34). Importantly, all β-gal–expressing cells on $Pax7^{lacZ/lacZ}$ fibers were negative for syndecan4 (Fig. 4 C) and CD34 (Fig. 4, K–M). However, occasionally syndecan4$^+$ or CD34$^+$ cells were found on $Pax7^{lacZ/lacZ}$ fibers when care was deliberately not taken during single fiber preparation. These cells were uniformly negative for β-gal immunostaining (Fig. 4, C–E and N). Notably, these syndecan4$^+$, β-gal$^-$ cells were also positive for the endothelial marker CD31 (Fig. 4, D–G). Together, these data demonstrate that although rare β-gal$^+$ cells are localized to the satellite cell niche in young $Pax7^{lacZ/lacZ}$ musculature, these cells have lost the characteristics and function of wild-type satellite cells.

In support of these findings, only 9% of $Pax7^{lacZ/lacZ}$ fiber (n = 76 fibers/3 mice) yielded any mononuclear cells (mean of 1.85 ± 0.34 cells/fiber) after several days of attached culture in growth medium. Importantly, the mononuclear cells associated with $Pax7^{lacZ/lacZ}$ fibers were uniformly negative for the myoblast-specific markers MyoD, Myf5, and Desmin (unpublished data). In contrast, all $Pax7^{+/+}$ fibers (n = 60 fibers/3 mice) gave rise to an average of 11.8 ± 0.97 cells/fiber. Furthermore, numerous proliferative bursts of $MyoD^+$ myoblasts were generated by all $Pax7^{+/+}$ fibers (unpublished data). Together, these data indicate that the defects in postnatal muscle growth and regeneration are attributable to an absence of functional satellite cells in $Pax7^{lacZ/lacZ}$ mutant mice.

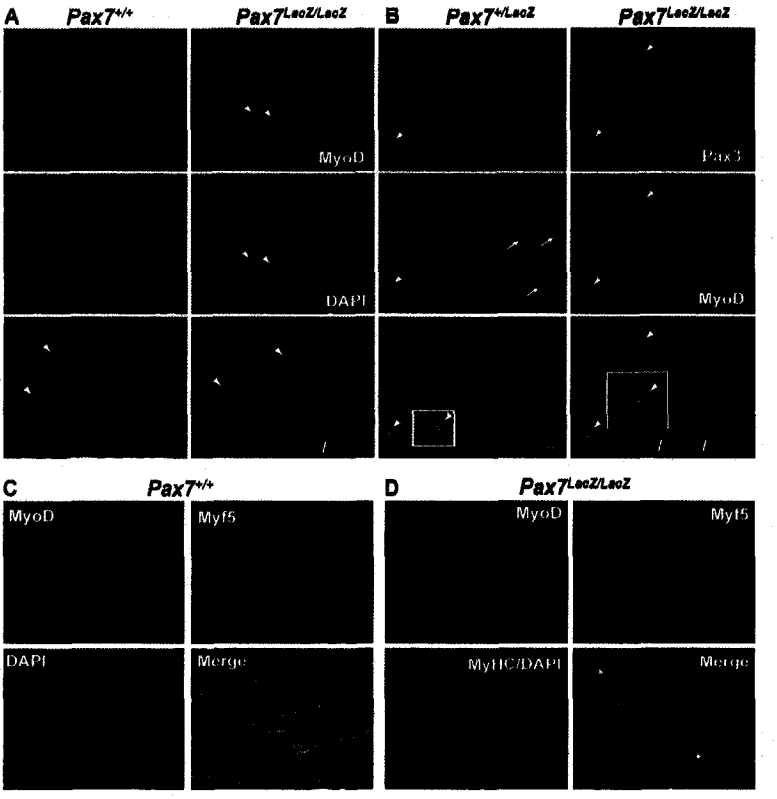

Figure 5. **Identification of Pax7-independent myogenic cells expressing Pax3.** (A, top and middle) Cell suspensions from $Pax7^{+/+}$ hind limb muscles grown in growth media for 15 h yielded large numbers of MyoD$^+$ cells (FITC) compared with rare MyoD$^+$ cells (arrowheads) observed in $Pax7^{lacZ/lacZ}$ preparations. (bottom) Myogenic cells obtained from both $Pax7^{+/+}$ and $Pax7^{lacZ/lacZ}$ hind limb muscles were capable of terminal differentiation as shown by MyHC expression (green; arrowheads) and fusion following 3 d in differentiation media. (B) Double immunostaining for Pax3 (red) and MyoD (green) of cell suspensions from $Pax7^{+/lacZ}$ or $Pax7^{lacZ/lacZ}$ limb muscle revealed that Pax3 and MyoD were coexpressed in certain myogenic cells (arrowheads). Cells expressing MyoD but not Pax3 were also detected in $Pax7^{+/+}$ and $Pax7^{lacZ/lacZ}$ cultures (arrows; not depicted). Insets show enlargements of the cells to the left. (C and D) Myogenic cells derived from cultures myofiber bundles of $Pax7^{+/+}$ (C) and $Pax7^{lacZ/lacZ}$ (D) mice. Myofiber bundle (20–30 fibers) were plated in a Matrigel-coated dish and culture in growth medium for 3 d followed by 1 d in differentiation medium. The green signals in the merged panels are intensified to help visualize myotubes. Bars, 12.5 μm.

Isolation of myogenic cells from $Pax7^{lacZ/lacZ}$ musculature

To identify the myogenic cells responsible for the small regenerative capacity in $Pax7^{lacZ/lacZ}$ hind limb muscle, single-cell suspensions were prepared from hind limb muscles and analyzed after 15 h in growth conditions or after an additional 3 d in differentiation medium. Interestingly, freshly isolated cell preparations from hind limb and diaphragm $Pax7^{lacZ/lacZ}$ muscles yielded some myogenic cells expressing MyoD (Fig. 5, A and B) or Myf5 (Fig. 5 D). Although present, $Pax7^{lacZ/lacZ}$ myogenic cells were recovered at an extremely low frequency (~1/150; Fig. 5) compared with wild-type muscle (363,012 ± 34,247 [n = 2] and 2,961 ± 1,096 [n = 4] MyoD$^+$ cells and 242,132 ± 5,843 [n = 2] and 1,277 ± 578 [n = 3] Myf5$^+$ cells/g of hind limb muscle for $Pax7^{+/+}$ and $Pax7^{lacZ/lacZ}$, respectively). The frequency of MyoD$^+$ cells was not increased in cultures prepared from regenerating $Pax7^{lacZ/lacZ}$ TA 3–4 d after CTX injection (unpublished data).

At clonal density, $Pax7^{lacZ/lacZ}$ cells isolated from limb muscle formed small colonies of 6–20 MyoD$^+$ and Desmin$^+$ myoblasts after 10–20 d compared with proliferative bursts of >500 myoblasts in $Pax7^{+/+}$ cultures (unpublished data). The inability for $Pax7^{lacZ/lacZ}$ cells to expand in culture suggested a profound proliferative deficit under standard myoblast growth conditions as compared with myoblasts isolated from wild-type littermates. Even when cultured in the presence of high concentrations of growth factors (5% chick embryo extract; 50 ng/ml of stem cell growth factor; 1 μg/ml of insulin; Methocult M3434 [StemCell Technologies, Inc.] or in Matrigel-coated dishes), $Pax7^{lacZ/lacZ}$ myogenic cells did not proliferate. Nevertheless, $Pax7^{lacZ/lacZ}$ myogenic cells underwent myogenic differentiation and expressed MyHC after culture in low-mitogen medium after 3–5 d (Fig. 5 A). In myoblast preparations from $Pax7^{+/+}$ or $Pax7^{+/lacZ}$ muscles, an average of 311.3 ± 49.3 (n = 6) nuclei/20× field were found within MyHC$^+$ cell bodies. In myoblast preparations from $Pax7^{lacZ/lacZ}$ muscle, an average of 3.0 ± 1.5 (n = 11) nuclei were found within MyHC$^+$ cell bodies. In myoblast preparations from $Pax7^{lacZ/lacZ}$ muscle, all MyoD$^+$ cells expressed MyHC after 6 d of culture in differentiation conditions. In contrast, in the $Pax7^{+/lacZ}$ control, ~10% of MyoD$^+$ cells did not express MyHC.

Lastly, EDL fiber bundles containing interstitial connective and other tissues from P30 $Pax7^{+/lacZ}$ and $Pax7^{lacZ/lacZ}$ mice were plated on Matrigel and cultured for 3 d in growth media followed by 1 d in differentiation media. $Pax7^{+/lacZ}$ EDL muscle yielded large numbers of MyoD-, Myf5-, and MyHC-expressing cells together with formation of large myotubes (Fig. 5 C). Notably, $Pax7^{lacZ/lacZ}$ EDL myofiber bundles gave rise to low numbers of MyoD- and Myf5-expressing cells that were capable of forming myotubes (Fig. 5 D). However, under identical conditions, $Pax7^{lacZ/lacZ}$ single fibers free of interstitial tissues did not yield any Myf5-, MyoD-, or MyHC-expressing cells (see Absence of functional satellite cells...). Together, these results indicate that a low number of $Pax7^{lacZ/lacZ}$ myogenic cells resides in an alternate anatomical location and support the contention that $Pax7^{lacZ/lacZ}$ myogenic cells represent an interstitial myogenic-progenitor population distinct from the satellite cell compartment.

Coexpression of Pax3 and myogenic markers in *Pax7*$^{lacZ/lacZ}$ cells

To investigate the possibility that the Pax7-independent myogenic cells in adult muscle represent a Pax3-dependent lineage, cell cultures from limb and diaphragm were analyzed for Pax3 expression by immunohistochemistry. Cultures from both wild-type and *Pax7*$^{lacZ/lacZ}$ diaphragm (unpublished data) and limb (Fig. 5 B) muscles yielded similar numbers of MyoD$^+$/Pax3$^+$ cells (Fig. 5 B). The majority of wild-type MyoD$^+$ cells did not express Pax3 (Fig. 5 B, arrows) but expressed Pax7 (not depicted). However, in cultures derived from *Pax7*$^{lacZ/lacZ}$ muscle, virtually all MyoD$^+$ cells coexpressed Pax3 (Fig. 5 B, arrowheads), with very few MyoD$^+$/Pax3$^-$ cells detected. Altogether, these results suggest that Pax3 is expressed in a population of myogenic progenitors in adult *Pax7*$^{lacZ/lacZ}$ muscle.

Pax3$^+$ myogenic cells in adult skeletal muscle

To demonstrate the presence of the Pax3$^+$ myogenic cell population in wild-type animals, we performed RNase protection assay, in situ hybridization, and immunostaining on wild-type muscles. By RNase protection assay, primary myoblasts isolated from adult limb muscles and expanded over several weeks expressed extremely low levels of *Pax3* mRNA, and we were unable to detect Pax3 protein by Western blot analysis (unpublished data). In addition, *Pax3* mRNA was below the limit of detection in C2C12 myoblasts and myotubes. Furthermore, immunolabeling for Pax3 confirmed the presence of Pax3-expressing cells in wild type and *Pax7*$^{lacZ/lacZ}$ limb musculature outside the basal lamina (Fig. 6, A–E and G–K). In contrast, Pax7$^+$ cells in *Pax7*$^{+/lacZ}$ muscle were uniformly observed in a sublaminar position (Fig. 6, B and E). Limb muscle of wild-type mice at P1 was also examined and we found a similar interstitial localization of Pax3$^+$ cells and sublaminar positioning of Pax7$^+$ cells (Fig. S2, available at http://www.jcb.org/cgi/content/full/jcb.200508001/DC1). In situ hybridization also detected the presence of Pax3-expressing cells within the musculature of both wild type and *Pax7*$^{lacZ/lacZ}$ diaphragm (Fig. 6, F and L). Immunolabeling of the basal lamina confirmed the location of the Pax3$^+$ cells outside the satellite cell location in the diaphragm (unpublished data). In agreement with the in vitro data, Pax3$^+$ cells were found at a similar abundance in both *Pax7*$^{lacZ/lacZ}$ and *Pax7*$^{+/+}$ muscle (1.6 ± 0.5 and 1.1 ± 0.5 Pax3$^+$ cells/section in *Pax7*$^{+/+}$ and *Pax7*$^{lacZ/lacZ}$ by in situ hybridization, respectively). These analyses reveal the presence of myogenic Pax3$^+$ cells in the interstitial environment in a niche distinct from the satellite cell compartment in both mutant and wild-type musculature.

Coexpression of Pax3 and MyoD during muscle regeneration in vivo

Finally, we tested for whether the rare Pax3$^+$ myogenic cells have any biological function in vivo. TA and gastrocnemius muscles were examined for expression of Pax3 and MyoD 2 d after CTX-induced regeneration. In resting muscles, none of the Pax3$^+$ cells expressed MyoD in either *Pax7*$^{+/lacZ}$ or *Pax7*$^{lacZ/lacZ}$ mice (Fig. 7 and not depicted). Within 2 d after CTX injection in *Pax7*$^{+/lacZ}$ mice, ~84% Pax3$^+$ cells expressed

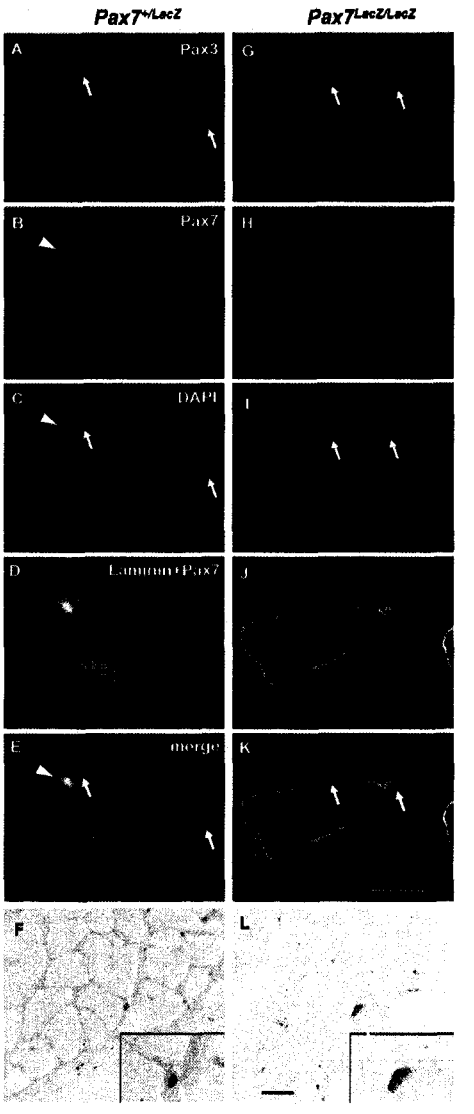

Figure 6. **Pax3 expression in *Pax7*$^{lacZ/lacZ}$ and *Pax7*$^{+/lacZ}$ musculature.** (A–E and G–K) Triple staining of adult EDL muscle sections with laminin, Pax7, and Pax3 antibodies plus DAPI labeling of nuclei. Pax3$^+$ cells (arrows), located in the interstitial space outside the basal lamina of myofibers, exist in similar frequency in both *Pax7*$^{+/lacZ}$ (C) and *Pax7*$^{lacZ/lacZ}$ (D) muscles. Note that the Pax7$^+$ cell (arrowheads) in the *Pax7*$^{+/lacZ}$ is located in a sublaminar position. Bar, 10 μm. (F and L) Pax3 in situ hybridization on *Pax7*$^{+/lacZ}$ (F) and *Pax7*$^{lacZ/lacZ}$ (L) diaphragm also revealed the presence of Pax3$^+$ cells in both genotypes. Bar, 25 μm.

MyoD (n = 74 cells from four 20× microscopic images taken from regenerative regions); ~11% of the MyoD$^+$ cells were also Pax3$^+$ (n = 569 cells from four regenerative regions; Fig. 7). In the regenerating muscles of *Pax7*$^{lacZ/lacZ}$ mice, ~29% Pax3$^+$ cells coexpressed MyoD (Fig. 7; n = 80 cells from five regenerating regions). Whereas the number of Pax3$^+$ cells was comparable in *Pax7*$^{+/lacZ}$ and *Pax7*$^{lacZ/lacZ}$ muscles, the total number of MyoD$^+$ cells in regenerating *Pax7*$^{lacZ/lacZ}$ muscle was only 5% of that in *Pax7*$^{+/lacZ}$ muscles, a result consistent with the impaired muscle regeneration in mutant mice. Among the

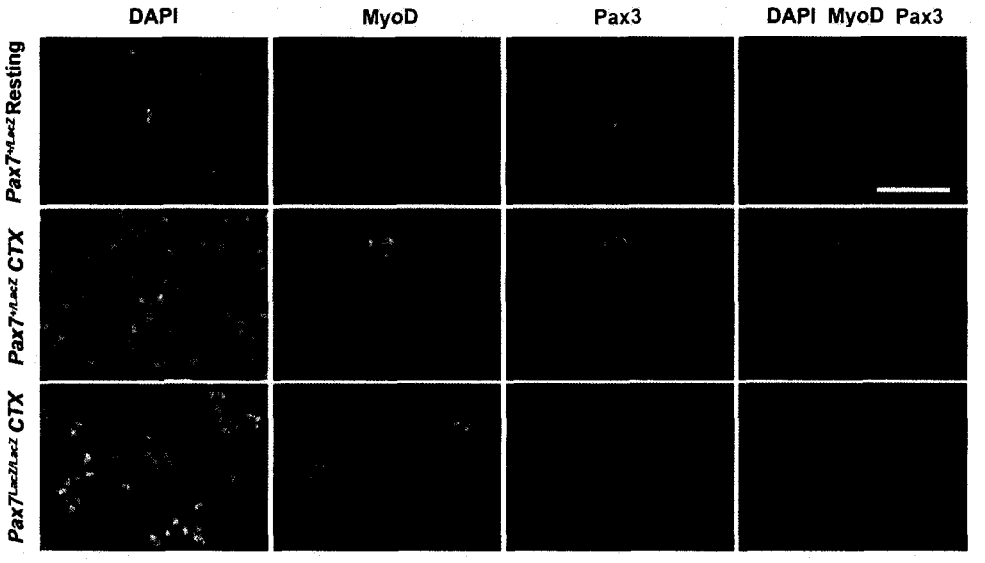

Figure 7. **Myogenic specification of Pax3$^+$ cells during muscle regeneration.** In resting muscle, Pax3$^+$ cells did not coexpress MyoD. In regenerating *Pax7$^{lacZ/lacZ}$* and *Pax7$^{+/lacZ}$* muscles 48 h after CTX injection, many Pax3$^+$ cells coexpressed MyoD, indicating that these cells had acquired a myogenic fate. Note that in *Pax7$^{+/lacZ}$*, the majority of MyoD$^+$ cells did not express Pax3 and are likely expressing Pax7. Bar, 20 μm.

MyoD$^+$ cells in *Pax7$^{lacZ/lacZ}$* regenerating muscles (n = 38 cells from five regenerative regions), ~61% coexpressed Pax3, suggesting that the majority of MyoD$^+$ cells were derived from the Pax3 myogenic cells. In addition, the frequency of Pax3$^+$ cells in the regenerating region (>10 cells/field) was higher than in the resting tissue (1–2 cells/section; see the previous paragraph), suggesting that Pax3$^+$ myogenic cells are preferentially recruited to the regenerating region and/or Pax3 expression is upregulated during regeneration. Together, these results indicate that these interstitial Pax3$^+$ cells found in limb musculature likely represent a novel lineage of myogenic progenitors that is distinct from the Pax7$^+$ satellite cell lineage of myogenic cells.

Discussion

Our analysis of *Pax7$^{lacZ/lacZ}$* mice clearly establishes an essential requirement for Pax7 during postnatal muscle growth and regeneration. Importantly, these experiments demonstrate that Pax7 is required for presatellite cells to express genes normally associated with functional satellite cells located in the sublaminar niche. Moreover, Pax7 is also required for the productive formation of committed myogenic precursor cells from sublaminar satellite cells. Furthermore, our experiments have identified a novel population of interstitial Pax3-expressing myogenic progenitors in adult limb musculature.

Using three different models of muscle injury in three different muscle groups, our results demonstrate a severe regeneration deficit in adult *Pax7$^{lacZ/lacZ}$* mice. Profound deficits in *Pax7$^{lacZ/lacZ}$* muscle regeneration have also been reported in a mixed C57/BL/Sv129 genetic background (Oustanina et al., 2004). Surprisingly, Oustanina et al. (2004) observed that postnatal muscle growth appeared "essentially normal" despite the extremely low number of satellite cells, the obviously smaller body size, and the increased number of smaller sized myofibers in *Pax7$^{lacZ/lacZ}$* mice in the mixed background. Our experiments do not support these findings. We observed significant deficits in muscle growth and regeneration capacity in *Pax7$^{lacZ/lacZ}$* mice with loss of fast myofibers, calcium deposition, and chronic degeneration associated with aging. The specific loss of fast muscle fibers can be attributed to the deficient fiber growth, as manifested by the reduced fiber size and myonuclei number per fiber, susceptibility of fast fibers to damages, and inefficient regeneration mechanisms to replace damaged fibers. In response to acute damage, such as CTX- or crush-induced injury, *Pax7$^{lacZ/lacZ}$* muscle was rapidly replaced by an inflammatory infiltration, together with large calcium deposits and extensive adipose infiltration. Only rare regenerated myofibers were formed. Lastly, our results demonstrate that Pax7 is required for the normal function of satellite cells and the productive formation of myogenic precursor cells. Therefore, our study unequivocally demonstrates that *Pax7*-dependent myogenic cells, which comprise the satellite cell compartment, are required for the efficient regeneration of skeletal muscle.

The identification of rare regenerated *Pax7$^{lacZ/lacZ}$* myofibers suggested the presence of Pax7-independent myogenic progenitors within the muscle. In our experiments, myogenic (MyoD$^+$) cells were cultured from *Pax7$^{lacZ/lacZ}$* muscle at a frequency of ~1/150 as compared with wild-type muscle. However, our in vivo data suggests that Pax3$^+$ myogenic progenitors may give rise to as much as 5% of MyoD$^+$ cells during regeneration. Importantly, sufficient numbers of *Pax7$^{lacZ/lacZ}$* myofibers were analyzed to conclusively demonstrate that these *Pax7$^{lacZ/lacZ}$* myogenic cells were not associated with myofibers and therefore were not satellite cells. Specifically, control EDL myofibers contained ~9–10 Syndecan4$^+$ satellite cells per fiber. Therefore, if satellite cells were present on

Pax7$^{lacZ/lacZ}$ fibers at a frequency of 1/150, one satellite cell would be observed for every 16 fibers. From our experiments, no Syndecan4$^+$ cells were detected on a total of 197 fibers examined either by direct immunohistochemistry or following in vitro culture. Although few β-gal$^+$ cells (7% of control) were found on *Pax7*$^{lacZ/lacZ}$ fibers, these cells did not express the satellite cell markers CD34 and Syndecan4 and were incapable of on-fiber proliferation in culture, suggesting that they were incapable of productively forming myogenic precursor cells. In addition, single fiber versus myofiber bundle culture experiments strongly support the notion that the myogenic progenitors found in *Pax7*$^{lacZ/lacZ}$ mice were not associated with myofibers, arguing against a possible contribution from any residual Pax7-deficient satellite cells.

Recent findings have demonstrated the presence of resident or circulating stem cells in the muscle (Ferrari et al., 1998; Bittner et al., 1999; Gussoni et al., 1999; Blau et al., 2001; Torrente et al., 2001; Asakura et al., 2002; LaBarge and Blau, 2002; Qu-Petersen et al., 2002; Polesskaya et al., 2003; Dreyfus et al., 2004). Our results suggest that these stem cells are insufficient to compensate for the loss of satellite cell function in the absence of Pax7 or suggest that Pax7 is a key player in the myogenic specification of most, if not all, adult stem cells. This idea is further supported by our finding that the myogenic differentiation of Pax3$^+$ cells is reduced in the *Pax7*$^{lacZ/lacZ}$ mice, by our previous studies showing that Pax7 expression is necessary for the myogenic differentiation of CD45$^+$ muscle-derived stem cells (Seale et al., 2004), and by recent studies showing that embryonic stem cells giving rise to satellite cells apoptose or undergo nonmyogenic differentiation in the absence of Pax7 and -3 (Relaix et al., 2005).

The molecular function of Pax3 and -7 in myogenic specification remains to be fully defined. Genetically, *Pax3* and *-7* function upstream of *Myf5* and *MyoD*, and Pax3-FKHD is capable of activating MyoD transcription in fibroblasts (Khan et al., 1999). In addition, several recent studies have reported that newly activated satellite cells and proliferating myoblasts coexpress Pax7 and MyoD in vitro (Halevy et al., 2004; Olguin and Olwin, 2004; Zammit et al., 2004). Together, these findings support the notion that Pax3/Pax7 directly or indirectly activates the transcription of the myogenic regulatory factors. Moreover, ectopic expression of Pax7 leads to enhanced proliferative and survival potential of myoblasts (Seale et al., 2004). Likewise, transient activation of Pax3 expression in response to Notch signaling has been reported in cultures of primary myoblast (Conboy and Rando, 2002), resulting in enhanced proliferation of these cells. Interestingly, overexpression of Pax7 also seems to down-regulate MyoD and promote cell-cycle withdrawal from the proliferating state, therefore playing a critical role in the maintenances of the satellite cell pool (Olguin and Olwin, 2004; Zammit et al., 2004). Our present data demonstrate that satellite cells lacking Pax7 undergo arrest when forming myogenic cells. Pax7 appears to function at multiple levels, including activation of the myogenic program, stimulating the proliferation and survival of myogenic progenitors, and the self-renewal of satellite cells. Our experiments unequivocally demonstrate that Pax7-deficient satellite cells that survive are incapable of giving rise to functional myogenic progenitors. Therefore, we conclude that Pax7 is required for sublaminar satellite cells to either form functional myogenic daughter cells or maintain a renewable satellite cell pool. Importantly, these data imply that myogenic commitment or specification occurs when satellite cells undergo an asymmetric cell division to form a myogenic factor–expressing daughter cell.

The rare MyoD$^+$ cells recovered from whole muscle homogenates from *Pax7*$^{lacZ/lacZ}$ mice uniformly expressed Pax3. Immunolabeling and in situ hybridization revealed the presence of Pax3$^+$ cells in interstitial locations outside the basal lamina of muscle fibers and not in the sublaminar satellite cell niche. The interstitial Pax3$^+$ cells did not express MyoD in undamaged muscle. However, after injury, the Pax3$^+$ cells rapidly increased in number and were found to express MyoD. Expression of *Pax3-GFP* or *Pax3-nLacZ* knockins has recently been reported in postnatal diaphragm in a subset of Pax7-expressing satellite cells, but expression was not detected in satellite cells in most hind limb musculature (Buckingham et al., 2003; Montarras et al., 2005; Relaix et al., 2005), as opposed to our observation that they are located outside muscle fibers. In our experiments, we only detected Pax3 protein in rare cells located outside of the basal lamina and not in satellite cells. This discrepancy may be the result of the different labeling techniques used and the different thresholds of detection between immunostaining of endogenous Pax3 versus bacterial enzymes or GFP with long half-lives. It is also possible that the extralaminar Pax3-expressing cells represent presatellite cells that require Pax7 to become functional sublaminar satellite cells. However, the presence of these cells in both wild type and mutant muscle, and the absence of detectable Pax3 protein in Pax7-deficient LacZ$^+$ cells, supports the notion that the Pax3$^+$ cells represent a novel myogenic lineage. Future studies applying immunolabeling to the knockin mice may help clarify the discrepancy.

Together, our experiments suggest that the interstitial Pax3$^+$ cells represent a novel myogenic lineage that is distinct from the sublaminar Pax7$^+$ satellite cell compartment. The normal role of these Pax3-expressing myogenic progenitors in adult muscle remains to be established. It is interesting to speculate that Pax3-expressing myogenic cells have a specialized role in adult muscle. For example, it is possible that these cells have a role in the formation of muscle spindles, neuromuscular junctions, myotendinous attachments, or other muscle specializations. Future studies characterizing the expression, differential activity, and developmental role of Pax3 and -7 in postnatal myogenesis are thus required.

Materials and methods

Mice and injury protocols

Mice carrying a targeted reporter allele of *Pax7* provided by P. Gruss (Max Plank Institute for Biophysical Chemistry, Gättingen, Germany; Mansouri et al., 1996) were backcrossed into the 129Sv/J genetic background for nine generations to generate 129Sv/J-inbred mice carrying the *Pax7-LacZ* allele. In these mice, the *Pax7* gene was knocked out by insertion of a β-gal gene and a neomycin cassette into the first exon of *Pax7*. The muscle phenotype was indistinguishable between C57BL/6- or 129Sv/J-inbred backgrounds and a C57BL/6 × 129Sv/J-outbred background. Mouse serum was prepared by coagulation and centrifugation of

blood samples and assayed by the Department of Biochemistry at the Children Hospital of Eastern Ontario. To investigate whether regeneration is age dependent, 1–7-mo-old *Pax7*$^{lacZ/lacZ}$ and *Pax7*$^{+/+}$ littermates were used for all regeneration experiments. However, no difference was found in the regeneration efficiency of age groups tested. We therefore pooled all data together in the results. For CTX-induced muscle regeneration, mice were killed at 10 d or 1 mo after injection of 25 μl CTX (10 μM; Latoxan) into the TA or the gastrocnemius muscles. For cell proliferation assays, 30 mg/kg BrdU (Sigma-Aldrich) was injected i.p. on days 4, 6, 7, and 8 after CTX injection. For crush injury, TA or gastrocnemius muscles were crushed using large forceps. Experiments were performed under University of Ottawa regulations for animal care and handlings.

Cell and tissue culture

Single myofibers were isolated by collagenase digestion as previously described (Charge et al., 2002) and subsequently plated in Matrigel-coated chamber slides for attached culture or suspended in 60-mm Petri dishes coated with horse serum to prevent fiber attachment. Myofiber bundles, which contained ~10–50 myofibers and surrounding tissue, were prepared and plated in chamber slides as per single myofiber culture but without extensive triturating. Primary myoblasts were isolated from hind limb or diaphragm muscles and cultured as previously described (Megeney et al., 1996).

Histology

For all injury and regeneration experiments, TA muscle was isolated, cut at mid-belly, embedded in optimal cutting temperature compound (Tissue-Tek)/20% sucrose, and frozen in liquid nitrogen for cryosections or fixed in 4% PFA and processed for paraffin sections. Cryosections were used for immunohistochemistry staining, and paraffin sections were used for hematoxylin–eosin, Alizarin red S (calcification), or Van Gieson's (fibrosis) staining. For postnatal fiber size analysis, lower hind legs were cryosectioned and total fiber number and fiber size were analyzed on transverse sections (10 μm) of the mid-belly soleus and EDL muscles, using NIH Image software. Fiber types were identified immunohistochemically with antibodies specific for MyHC subtypes (see next section) as described previously (Hughes et al., 1993).

Immunochemistry

In brief, cryosections, single myofibers, or cultured cells were fixed in 2–4% PFA, quenched with glycine (100 mM glycine, 0.2% Triton X-100, and 0.1% sodium azide in PBS), and blocked in PBS containing 2% BSA, 5% goat serum, and 0.2% Triton X-100. Tissues or cells were then incubated with the primary antibodies diluted in the same blocking solution and finally with biotinylated secondary antibodies or fluorophore-conjugated secondary antibodies. The primary antibodies used were as follows: mouse monoclonal anti-Pax3 (IgG2a; a gift from C. Ordhal, University of California, San Francisco, San Francisco, CA; available from the Developmental Studies Hybridoma Bank), rabbit anti-Pax3 (Active Motif and Zymed Laboratories), Pax7 (Developmental Studies Hybridoma Bank), rat anti-laminin (Qbiogene), laminin (DakoCytomation), Desmin (DakoCytomation), CD34 (BD Biosciences), MyoD (5.8A; BD Biosciences), rabbit anti-MyoD (C-20; Santa Cruz Biotechnology, Inc.), Myf5 (Santa-Cruz Biotechnology, Inc.), MyHC (MF-20; Developmental Studies Hybridoma Bank), embryonic fast MyHC (F1.652; Developmental Studies Hybridoma Bank); MyHC IIb (BF-F3; Deutsche Sammlung von Mikroorganismen und Zellkulturen), MyHC I (A4.840) and IIa (A4.74; Developmental Studies Hybridoma Bank), anti-β-gal (Invitrogen), and chicken anti-Syndecan4 (gift of B. Olwin, University of Colorado, Boulder, CO; Cornelison et al., 2001). BrdU detection was performed using the BrdU in situ detection kit (BD Biosciences) following the manufacturer's protocol. The secondary antibodies used were Alexa488 anti-mouse IgG2a; Alexa568 anti-mouse IgG1 (Invitrogen); and Fluorescein-, Rhodamine-, or Cy5-conjugated antibodies (Chemicon). Nuclei were counter-stained with DAPI.

In situ hybridization

Pax7$^{+/+}$ and *Pax7*$^{lacZ/lacZ}$ adult diaphragms were processed for in situ hybridization as previously described (Wallace and Raff, 1999). A *Pax3* cDNA template was used for synthesis of sense and antisense digoxigenin-labeled riboprobes (Goulding et al., 1993). After in situ hybridization, sections were reacted with an antibody to laminin (DakoCytomation) and a Rhodamine-conjugated secondary layer (Chemicon).

Statistical analysis and microscopy

Errors quoted are SEM throughout. Data were analyzed using unpaired *t* tests. Asterisks indicate significance at $P < 0.05$ and $P < 0.01$ throughout. Samples were visualized with a microscope (Axioplan2; Carl Zeiss MicroImaging, Inc.), and images were acquired using a camera (AxioCam; Carl Zeiss MicroImaging, Inc.) and the Axioview 3.1 software (Carl Zeiss MicroImaging, Inc.). Digital fluorescent images were captured at room temperature with a 20× (plan-apochromat, air, NA 0.75) or 63× (plan-apochromat, oil, NA 1.40) objective using the least possible exposure to minimize bleaching. The final displaying levels were subsequently adjusted similarly for all figures using Axioview or Photoshop (Adobe) software.

Online supplemental material

Fig. S1 shows the expression of β-gal in *Pax7*$^{+/lacZ}$ and *Pax7*$^{lacZ/lacZ}$ muscles at P0. Fig. S2 shows Pax7$^+$ and Pax3$^+$ cells in the limb muscle of a wild-type mouse at P1. Online supplemental material is available at http://www.jcb.org/cgi/content/full/jcb.200508001/DC1.

We thank Dr. B. Olwin for the gift of Syndecan4 antibody and Vanessa Seale for technical assistance.

S. Kuang was supported by a postdoctoral fellowship from the National Sciences and Engineering Research Council. P. Seale was supported by a doctoral research award from the Canada Institutes of Health Research. M.A. Rudnicki holds the Canada Research Chair in Molecular Genetics and is a Howard Hughes Medical Institute International Scholar. This work was supported by grants to M.A. Rudnicki from the Muscular Dystrophy Association, the National Institutes of Health, the Canada Institutes of Health Research, and the Canada Research Chair Program.

Submitted: 1 August 2005
Accepted: 6 December 2005

References

Asakura, A., P. Seale, A. Girgis-Gabardo, and M.A. Rudnicki. 2002. Myogenic specification of side population cells in skeletal muscle. *J. Cell Biol.* 159:123–134.

Beauchamp, J.R., L. Heslop, D.S. Yu, S. Tajbakhsh, R.G. Kelly, A. Wernig, M.E. Buckingham, T.A. Partridge, and P.S. Zammit. 2000. Expression of CD34 and Myf5 defines the majority of quiescent adult skeletal muscle satellite cells. *J. Cell Biol.* 151:1221–1234.

Ben-Yair, R., and C. Kalcheim. 2005. Lineage analysis of the avian dermomyotome sheet reveals the existence of single cells with both dermal and muscle progenitor fates. *Development.* 132:689–701.

Bittner, R.E., C. Schofer, K. Weipoltshammer, S. Ivanova, B. Streubel, E. Hauser, M. Freilinger, H. Hoger, A. Elbe-Burger, and F. Wachtler. 1999. Recruitment of bone-marrow-derived cells by skeletal and cardiac muscle in adult dystrophic mdx mice. *Anat. Embryol. (Berl.).* 199:391–396.

Blau, H.M., T.R. Brazelton, and J.M. Weimann. 2001. The evolving concept review of a stem cell: entity or function? *Cell.* 105:829–841.

Bober, E., T. Franz, H.H. Arnold, P. Gruss, and P. Tremblay. 1994. Pax-3 is required for the development of limb muscles: a possible role for the migration of dermomyotomal muscle progenitor cells. *Development.* 120:603–612.

Buckingham, M., L. Bajard, T. Chang, P. Daubas, J. Hadchouel, S. Meilhac, D. Montarras, D. Rocancourt, and F. Relaix. 2003. The formation of skeletal muscle: from somite to limb. *J. Anat.* 202:59–68.

Charge, S.B., and M.A. Rudnicki. 2004. Cellular and molecular regulation of muscle regeneration. *Physiol. Rev.* 84:209–238.

Charge, S.B., A.S. Brack, and S.M. Hughes. 2002. Aging-related satellite cell differentiation defect occurs prematurely after Ski-induced muscle hypertrophy. *Am. J. Physiol. Cell Physiol.* 283:C1228–C1241.

Conboy, I.M., and T.A. Rando. 2002. The regulation of Notch signaling controls satellite cell activation and cell fate determination in postnatal myogenesis. *Dev. Cell.* 3:397–409.

Cornelison, D.D., M.S. Filla, H.M. Stanley, A.C. Rapraeger, and B.B. Olwin. 2001. Syndecan-3 and syndecan-4 specifically mark skeletal muscle satellite cells and are implicated in satellite cell maintenance and muscle regeneration. *Dev. Biol.* 239:79–94.

Dreyfus, P.A., F. Chretien, B. Chazaud, Y. Kirova, P. Caramelle, L. Garcia, G. Butler-Browne, and R.K. Gherardi. 2004. Adult bone marrow-derived stem cells in muscle connective tissue and satellite cell niches. *Am. J. Pathol.* 164:773–779.

Ferrari, G., G. Cussela-De Angelis, M. Coletta, E. Paolucci, A. Stornaiuolo, G. Cossu, and F. Mavilio. 1998. Muscle regeneration by bone marrow-derived myogenic progenitors. *Science.* 279:1528–1530.

Goulding, M., S. Sterrer, J. Fleming, R. Balling, J. Nadeau, K.J. Moore, S.D. Brown, K.P. Steel, and P. Gruss. 1993. Analysis of the Pax-3 gene in the mouse mutant splotch. *Genomics.* 17:355–363.

Goulding, M., A. Lumsden, and A.J. Paquette. 1994. Regulation of Pax-3 expression in the dermomyotome and its role in muscle development. *Development.* 120:957–971.

Gros, J., M. Manceau, V. Thome, and C. Marcelle. 2005. A common somitic origin for embryonic muscle progenitors and satellite cells. *Nature.* 435:954–958.

Gussoni, E., Y. Soneoka, C.D. Strickland, E.A. Buzney, M.K. Khan, A.F. Flint, L.M. Kunkel, and R.C. Mulligan. 1999. Dystrophin expression in the mdx mouse restored by stem cell transplantation. *Nature.* 401:390–394.

Halevy, O., Y. Piestun, M.Z. Allouh, B.W. Rosser, Y. Rinkevich, R. Reshef, I. Rozenboim, M. Wleklinski-Lee, and Z. Yablonka-Reuveni. 2004. Pattern of Pax7 expression during myogenesis in the posthatch chicken establishes a model for satellite cell differentiation and renewal. *Dev. Dyn.* 231:489–502.

Hughes, S.M., M. Cho, I. Karsch-Mizrachi, M. Travis, L. Silberstein, L.A. Leinwand, and H.M. Blau. 1993. Three slow myosin heavy chains sequentially expressed in developing mammalian skeletal muscle. *Dev. Biol.* 158:183–199.

Kassar-Duchossoy, L., E. Giacone, B. Gayraud-Morel, A. Jory, D. Gomes, and S. Tajbakhsh. 2005. Pax3/Pax7 mark a novel population of primitive myogenic cells during development. *Genes Dev.* 19:1426–1431.

Khan, J., M.L. Bittner, L.H. Saal, U. Teichmann, D.O. Azorsa, G.C. Goooden, W.J. Pavan, J.M. Trent, and P.S. Meltzer. 1999. cDNA microarrays detect activation of a myogenic transcription program by the PAX3-FKHR fusion oncogene. *Proc. Natl. Acad. Sci. USA.* 96:13264–13269.

LaBarge, M.A., and H.M. Blau. 2002. Biological progression from adult bone marrow to mononucleate muscle stem cell to multinucleate muscle fiber in response to injury. *Cell.* 111:589–601.

Mansouri, A., A. Stoykova, M. Torres, and P. Gruss. 1996. Dysgenesis of cephalic neural crest derivatives in *Pax7*$^{-/-}$ mutant mice. *Development.* 122:831–838.

Megeney, L.A., B. Kablar, K. Garrett, J.E. Anderson, and M.A. Rudnicki. 1996. MyoD is required for myogenic stem cell function in adult skeletal muscle. *Genes Dev.* 10:1173–1183.

Montarras, D., J. Morgan, C. Collins, F. Relaix, S. Zaffran, A. Cumano, T. Partridge, and M. Buckingham. 2005. Direct isolation of satellite cells for skeletal muscle regeneration. *Science.* 309:2064–2067.

Olguin, H.C., and B.B. Olwin. 2004. Pax-7 up-regulation inhibits myogenesis and cell cycle progression in satellite cells: a potential mechanism for self-renewal. *Dev. Biol.* 275:375–388.

Oustanina, S., G. Hause, and T. Braun. 2004. Pax7 directs postnatal renewal and propagation of myogenic satellite cells but not their specification. *EMBO J.* 23:3430–3439.

Parker, M.H., P. Seale, and M.A. Rudnicki. 2003. Looking back to the embryo: transcriptional networks in adult myogenesis. *Nat Rev. Genet.* 4:497–507.

Polesskaya, A., P. Seale, and M.A. Rudnicki. 2003. Wnt signaling induces the myogenic specification of resident CD45+ adult stem cells during muscle regeneration. *Cell.* 113:841–852.

Qu-Petersen, Z., B. Deasy, R. Jankowski, M. Ikezawa, J. Cummins, R. Pruchnic, J. Mytinger, B. Cao, C. Gates, A. Wernig, and J. Huard. 2002. Identification of a novel population of muscle stem cells in mice: potential for muscle regeneration. *J. Cell Biol.* 157:851–864.

Relaix, F., D. Rocancourt, A. Mansouri, and M. Buckingham. 2004. Divergent functions of murine Pax3 and Pax7 in limb muscle development. *Genes Dev.* 18:1088–1105.

Relaix, F., D. Rocancourt, A. Mansouri, and M. Buckingham. 2005. A Pax3/Pax7-dependent population of skeletal muscle progenitor cells. *Nature.* 435:948–953.

Seale, P., L.A. Sabourin, A. Girgis-Gabardo, A. Mansouri, P. Gruss, and M.A. Rudnicki. 2000. Pax7 is required for the specification of myogenic satellite cells. *Cell.* 102:777–786.

Seale, P., J. Ishibashi, A. Scime, and M.A. Rudnicki. 2004. Pax7 is necessary and sufficient for the myogenic specification of CD45$^+$:Sca1$^+$ stem cells from injured muscle. *PLoS Biol.* 2:E130.

Tajbakhsh, S., D. Rocancourt, G. Cossu, and M. Buckingham. 1997. Redefining the genetic hierarchies controlling skeletal myogenesis: Pax-3 and Myf-5 act upstream of MyoD. *Cell.* 89:127–138.

Torrente, Y., J.P. Tremblay, F. Pisati, M. Belicchi, B. Rossi, M. Sironi, F. Fortunato, M. El Fahime, M.G. D'Angelo, N.J. Caron, et al. 2001. Intraarterial injection of muscle-derived CD34$^+$Sca-1$^+$ stem cells restores dystrophin in *mdx* mice. *J. Cell Biol.* 152:335–348.

Wallace, V.A., and M.C. Raff. 1999. A role for Sonic hedgehog in axon-to-astrocyte signalling in the rodent optic nerve. *Development.* 126:2901–2909.

Zammit, P.S., J.P. Golding, Y. Nagata, V. Hudon, T.A. Partridge, and J.R. Beauchamp. 2004. Muscle satellite cells adopt divergent fates: a mechanism for self-renewal? *J. Cell Biol.* 166:347–357.